BORON ARSENIDE AND BORON PHOSPHIDE FOR HIGH TEMPERATURE AND LUMINESCENT DEVICES

Final Technical Report

Covering the Period July 1, 1969 to August 31, 1975

(NASA-CR-145404) BORON ARSENIDE AND BORON PHOSPHIDE FOR HIGH TEMPERATURE AND LUMINESCENT DEVICES Final Technical Report, 1 Jul. 1969 - 31 Aug. 1975 (Southern Methodist Univ.) 351 p HC $10.00 CSCL 07D G3/25

N76-10285

Unclas 39464

Prepared under NASA Grant NGL 44-007-042

by

Ting L. Chu, Principal Investigator
Southern Methodist University
Dallas, Texas 75275

for

Langley Research Center
National Aeronautics and Space Administration
Hampton, Virginia 23665

September, 1975

CONTENTS

LIST OF ILLUSTRATIONS

ABSTRACT

The objectives of this research program are (1) to investigate the crystal growth of boron arsenide and boron phosphide in the form of bulk crystals and epitaxial layers on suitable substrates, (2) to characterize the physical, chemical, and electrical properties of the crystals and epitaxial layers, and (3) to produce p-n junctions for device applications.

Bulk crystals of boron arsenide have been prepared by the chemical transport technique, and their carrier concentration and Hall mobility were measured. The growth of boron arsenide crystals from high temperature solutions was attempted without success. Boron arsenide layers were deposited on silicon substrates by the pyrolysis of a diborane-arsine mixture, and optical measurements implied that boron arsenide is a direct gap material with a room temperature gap of about 1.45 eV. No major efforts were directed to the fabrication of boron arsenide devices because of its irreversible decomposition at temperatures above 900° C.

Bulk crystals of boron phosphide have been prepared by chemical transport and solution growth techniques. The transport of polycrystalline boron phosphide at 1270-1290° C by bromine or iodine in the presence of a temperature gradient has produced p-type crystals with carrier concentrations on the order of 10^{18} cm^{-3}. The recrystallization of polycrystalline boron phosphide from a nickel phosphide solution was more successful for the growth of large boron phosphide crystals suitable for device

fabrication. The grown crystals were mostly in the form of platelets. Silicon and beryllium were used as n- and p-type dopants, respectively.

Epitaxial layers of boron phosphide were deposited on the basal plane of silicon carbide and solution-grown boron phosphide substrates at 1050-1150° C by the thermal reduction of a boron tribromide-phosphorus trichloride mixture. The structural and electrical properties of these layers were investigated.

Techniques required for the fabrication of boron phosphide devices such as junction shaping, diffusion, contact formation, etc., were investigated. The electrolytic etching technique was developed for the etching and polishing of p-type boron phosphide and for the delineation of mesa-type p-n junctions. Alloying techniques were developed for the formation of low-resistance ohmic contacts to boron phosphide.

Four types of boron phosphide devices were fabricated: metal-insulator-boron phosphide structures, Schottky barriers, boron phosphide-silicon carbide heterojunctions, and p-n homojunctions. Easily visible red electroluminescence was observed from both epitaxial and solution grown p-n junctions.

Significant progress has been made in the development of boron arsenide and boron phosphide technology during this research program.

I. Introduction

This is the Final Technical Report of a research program on the preparation and application of boron arsenide (BAs) and boron phosphide (BP) for high temperature and luminescent devices sponsored by the Langley Research Center of the National Aeronautics and Space Administration, Hampton, Virginia. The objectives of this program were (1) to investigate the crystal growth of boron arsenide and boron phosphide in the form of bulk crystals and epitaxial layers on suitable substrates, (2) to characterize the physical, chemical, and electrical properties of the crystals and epitaxial layers, and (3) to produce p-n junctions for device applications.

Boron arsenide and boron phosphide, with energy gaps of 1.46 and 2.0 eV, respectively,[1,2,3] are not well-known semiconductors. Because of the relatively large energy gaps, their devices should be capable of operation at much higher temperatures than silicon devices. In addition, both materials may be useful in electroluminescent devices[4]; boron phosphide, in particular, should emit visible radiation. Until recently, very little information concerning these applications was available, due to difficulties encountered in the preparation of single crystals and epitaxial layers of controlled chemical and structural perfection. During this research program, solutions to many of the basic problems relevant to the use of boron arsenide and boron phosphide were obtained.

The earliest information concerning the preparation and crystal structure of boron arsenide appeared in 1958.[5] Polycrystalline boron arsenide was prepared by direct union of the elements in evacuated, sealed, silica tubes at 800° C. Boron arsenide crystallizes in the zinc blende structure with a lattice parameter a = 4.777 Å, as deduced from x-ray powder diffraction data. Subsequently, the direct combination of arsenic and boron was used by several authors for the preparation of amorphous and polycrystalline boron arsenide.[1,6,7] The synthesis may be carried out in a single temperature or two-temperature furnace. In either case, two products were obtained depending on the temperature and arsenic pressure. At 800 to 900° C and arsenic pressure greater than one atmosphere, cubic monarsenide was produced. At 1000-1100° C and arsenic pressures less than one atmosphere, a subarsenide, B_6As, with an orthorhombic structure was produced. The monarsenide is stable up to 920° C and undergoes irreversible decomposition to the subarsenide at higher temperatures. The optical energy gap of microcrystalline boron arsenide was determined to be 1.46 eV.[1] Small single crystals of boron arsenide, with dimensions less than 0.25 mm, were obtained by chemical vapor transport with halogens as transporting agents.[8] Evacuated quartz ampoules, 5" long and 1" in diameter, containing polycrystalline boron arsenide and iodine were placed in tube furnaces using the inherent gradient of the furnaces to produce the vapor transport. The product transported through a temperature

gradient from 850° to 400° C was shown by x-ray analysis to be principally boron arsenide. No additional work has been reported on the preparation of boron arsenide crystals.

Boron phosphide has been known for many years; however, its composition and structure were not established until 1957.[9] Crystalline boron phosphide has a zinc-blende structure with a lattice parameter a = 4.55 Å. Amorphous and polycrystalline boron phosphide have been prepared by several techniques,[2,5,6,7,9,10,11] including the direct combination of the elements in sealed tubes at 900-1100° C, the pyrolysis of the addition compound of boron trichloride and phosphorus pentachloride, the reaction of boron halide and zinc phosphide, and the reaction of boron trichloride and phosphine. At elevated temperatures (1100° C or higher) and reduced pressures (about 1 mm), the monophosphide decomposes to a subphosphide, B_6P. Both the monophosphide and subphosphide are chemically inert toward boiling acids and alkalis. Prior to this program, small single crystals of boron phosphide had been grown from high temperature solutions,[2,12,13] by chemical vapor transport,[8,14] and by high pressure synthesis.[15] Two types of solution growth processes were investigated: recrystallization of polycrystalline boron phosphide in metal solvents, and precipitation from metal-boron-phosphorus melts. Neither solution technique consistently produced crystals larger than a few millimeters in any dimension. Chemical vapor transport and high pressure synthesis did not

yield crystals larger than a few tenths of a millimeter. During the course of this program, a few additional reports were published by other workers on the synthesis of boron phosphide by solution growth,[16] by chemical transport,[17] and by high pressure synthesis.[18,19] With one exception, crystals with dimensions less than 1 mm were reported. In one case,[16] crystals with one dimension up to 5 mm were claimed, but only one poorly formed crystal was shown.

With regard to the growth of epitaxial layers of boron arsenide and boron phosphide, very little information has been published. Expitaxial growth of layers of boron arsenide has not been reported, although a subarsenide ($B_{13}As_2$) was deposited on silicon substrates.[20] The growth of crystalline boron phosphide layers on silicon substrates has been reported.[17,21] Highly strained layers up to about 30 μm in thickners were obtained; small pieces were isolated for measurements by the removal of the silicon substrate. The layers contained silicon from the substrate, and, in addition, phosphorus from the deposited layer diffused into the silicon substrate during deposition. No mention of any attempts to make p-n junctions or other devices with the boron phosphide layers was made.

During the research program discussed here, significant progress was made in the development of boron arsenide and boron phosphide technology. Major emphasis was given to boron phosphide since it has a larger energy gap than boron arsenide. Techniques

to reproducibly grow large crystals and high quality epitaxial layers were developed. The properties of these crystals and layers were determined. In addition, techniques such as selective etching and ohmic contact technology were developed for device fabrication. Boron phosphide devices including Schottky barriers, metal-insulator-semiconductor (MIS) junctions, and p-n electroluminescent junctions were fabricated. These results are summarized in the following section of the report.

II. Technical Discussion

The basic technical approach selected for this program was essentially the growth of bulk crystals and the subsequent use of chemical vapor deposition techniques to grow epitaxial layers of controlled properties onto the bulk crystals. Extensive investigations were carried out in the preparation of crystals and epitaxial layers and in the development of other device fabrication techniques.

II.A. Growth and Properties of Bulk Crystals

Since the fabrication of most semiconductor devices with optimum properties requires single crystalline material of controlled chemical and structural perfection, a major emphasis was given to the development of crystal growth techniques for boron arsenide and boron phosphide. Since both materials decompose at temperatures considerably below their melting points, chemical vapor transport and solution growth were chosen as the crystal growth methods to be evaluated.

II.A.1. Boron Arsenide Crystals

II.A.1.a. Preparation of Polycrystalline Boron Arsenide

Polycrystalline material is required as the source material for closed tube chemical transport and for recrystallization from a solution. The preparation of polycrystalline boron arsenide was carried out in fused silica ampules by the reaction of a boron iodide, probably the monoiodide BI, with arsenic. For a 2.5 cm ID and 30 cm long ampule, optimum results were obtained

with 1 g of boron, 8 g of arsenic, and 0.25 g of iodine in the tube. The ampule was positioned in a furnace such that the boron was at 870° C at one end of the tube, and the arsenic was at 670° C at the other end. Although higher temperatures, in general, increase reaction rates, the irreversible decomposition of boron arsenide to the subarsenide near 900° C[1] limited the reaction temperature which could be used. In one week, about 50% of the boron reacted, and boron arsenide, identified by its x-ray powder pattern,[5] was found near the center of the reaction ampule. This material could be directly used as source material for the crystal growth experiments.

II.A.1.b. Boron Arsenide Crystal Growth by Chemical Transport

Chemical transport is one of the techniques available to grow crystals of materials which decompose at temperatures below the melting point.[22] In this technique, the polycrystalline material and a transport agent, which reacts reversibly with the material, are sealed into an ampule. The source material is positioned at one end of the sealed tube. The ampule is located in a furnace with the appropriate temperature gradient to transport the polycrystalline material, by reaction with the transport agent, to the other end, where single crystals can nucleate and grow. The basic parameters of this technique are the source temperature, the direction and magnitude of the temperature gradient, and the transport agent concentration.

Similar to the other III-V compounds, boron arsenide reacts reversibly with the halogens, and thus the halogens can be

used to transport boron arsenide. In general, the equilibrium constants of these reactions decrease with decreasing temperature, so that transport occurs from a high temperature source to regions of lower temperature. To carry out the crystal growth of boron arsenide by chemical transport, polycrystalline boron arsenide and a transport agent were sealed in fused silica tubes 2.5 cm ID and 15 to 25 cm long. The reaction tube was heated in a two temperature zone furnace. Boron arsenide was located at one end of the tube which was in the higher temperature zone; this zone was maintained at 875° C to prevent the irreversible decomposition of boron arsenide. The nucleation and growth of boron arsenide took place on the wall of the tube in the lower temperature zone. Many experiments were carried out to optimize the transport process. The transport rate was extremely slow when bromine or iodine alone was used as the transport agent, and chlorine produced no transport of boron arsenide. The addition of arsenic to the growth ampule greatly increased the transport rate, and an iodine-arsenic mixture was found to be the optimum transport agent for boron arsenide. The largest crystals were obtained with iodine and arsenic pressures in the ampules of 1.5 atm and 3 atm, respectively, and with a temperature gradient of 30° C along the length of the tube. With a two week reaction time, single crystals with dimensions up to 2 mm were obtained. Larger crystals, although occasionally found, could not be consistently grown even with longer reaction times.

The structural properties of boron arsenide crystals grown by the transport technique were studied by optical microscopy and X-ray diffraction techniques. Other than well-formed facets, the as-grown surfaces exhibited no structural features when examined with an optical microscope. Attempts were made to reveal structural defects in boron arsenide crystals by chemical etching. However, boron arsenide was found to be inert toward common etchants, such as bromine, nitric acid-hydrofluoric acid mixture, nitric acid-sulfuric acid mixtures, aqueous and molten alkalis, etc. Boron arsenide was etched slowly by boiling aqua regia and was etched rapidly by a molten mixture of sodium hydroxide and sodium peroxide. A small crystal with well-developed faces was etched with aqua regia, and the three-fold symmetry shown by the resulting linear etch figures suggests that this crystal is cubic with faces of {111} orientation. The faces of other small crystals have also been identified as of {111} orientation by X-ray Laue back reflection techniques. The lattice parameter of the boron arsenide crystals was determined by x-ray techniques to be 4.78 Å, which is in agreement with the value previously reported.[4]

The boron monarsenide crystals obtained by the transport technique were in the form of truncated pyramids. This geometry is not suitable for Hall measurement, but the electrical conductance of boron monarsenide crystals was measured in the temperature range from 77° K to 900° K. Ohmic contact to two faces

of the crystals was made by vacuum evaporation of aluminum or gold and subsequent annealing near 450° C. The crystals were p-type as determined by a thermoelectric probe. Figure 1 shows typical conductance data from a boron arsenide crystal. At temperatures below about 500° K the electrical conductance is essentially independent of temperature, due presumably to the low ionization energy of the impurities. At temperatures above 500° K, the slope of the plot corresponds to an activation energy of approximately 0.5 eV. The formation of a liquid alloy at the contacts prevented measurements at high enough temperatures to confirm the previously reported energy gap of boron arsenide.

II.A.1.c. Boron Arsenide Crystal Growth from Solution

Because of the limited success, in terms of crystal size, of the chemical transport process for the growth of boron arsenide crystals, attempts were made to grow boron arsenide from high temperature solutions. Experiments to recrystallize boron arsenide near 900° C were carried out with nickel arsenide (NiAs), copper arsenide (Cu_3As), and palladium arsenide (Pd_5As_2) as solvents. Mixtures of polycrystalline boron arsenide with one of the solvents were sealed in evacuated ampules and heated at 880° C for a few days. In all of the experiments, the boron arsenide recovered from the tubes had the same appearance and particle size as the starting material. Thus, boron arsenide is insoluble in the three arsenic compounds near 900° C. Another experiment was carried out in an attempt to precipitate boron

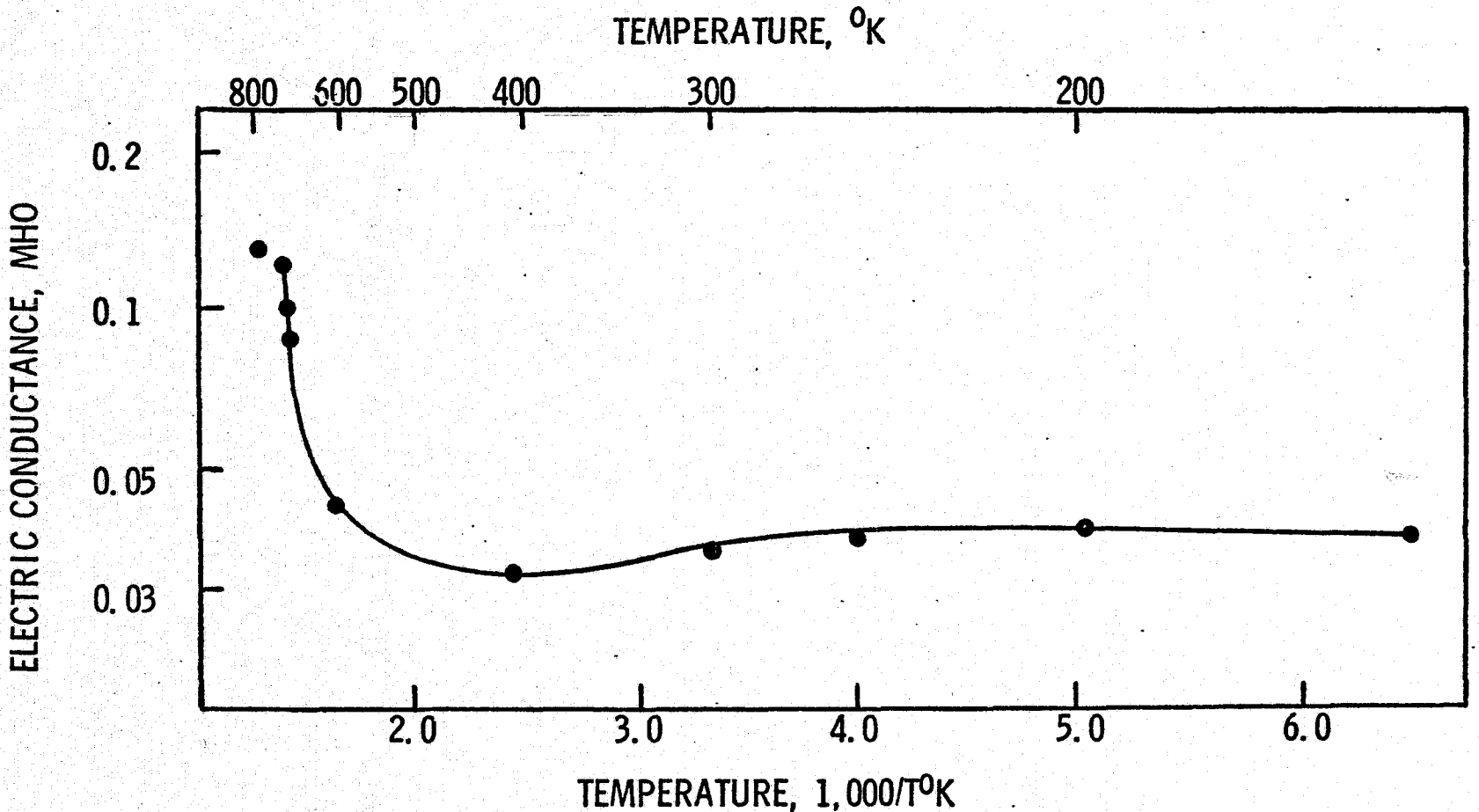

Fig. 1 Electrical conductance of a transported boron arsenide crystal as a function of temperature.

(15)

arsenide crystals. A mixture of boron and nickel was heated at 1120° C and saturated with arsenic at 1 atm pressure. After this mixture was slowly cooled, the resulting ingot was etched to dissolve the nickel arsenide. The residue was found by x-ray techniques to be a mixture of boron arsenide and boron subarsenide. It was concluded, therefore, that the solution growth is not a promising technique for the preparation of boron arsenide crystals.

II.A.2. Boron Phosphide Crystals

II.A.2.a. Preparation of Polycrystalline Boron Phosphide

Polycrystalline boron phosphide needed for the crystal growth investigations was conveniently produced by chemical vapor deposition. Initially, four possible reactions were considered to be potentially useful: the thermal decomposition of a mixture of diborane and phosphine, the reaction of boron tribromide and phosphine, the reaction of diborane with phosphorus trichloride, or the thermal reduction of a boron tribromide-phosphorus trichloride mixture. These chemical reactions may be written as:

$$B_2H_6(g) + 2PH_3(g) \rightarrow 2BP(s) + 6H_2(g) \quad (1)$$

$$BBr_3(g) + PH_3(g) \rightarrow BP(s) + 3HBr(g) \quad (2)$$

$$B_2H_6(g) + PCl_3(g) \rightarrow 2BP(s) + 6HCl(g) \quad (3)$$

$$BBr_3(g) + PCl_3(g) + 3H_2(g) \rightarrow BP(s) + 3HCl(g) + 3HBr(g) \quad (4)$$

Deposition experiments utilizing these reactions were carried out in the apparatus shown schematically in Fig. 2. Boron tribromide and phosphorus trichloride were introduced into

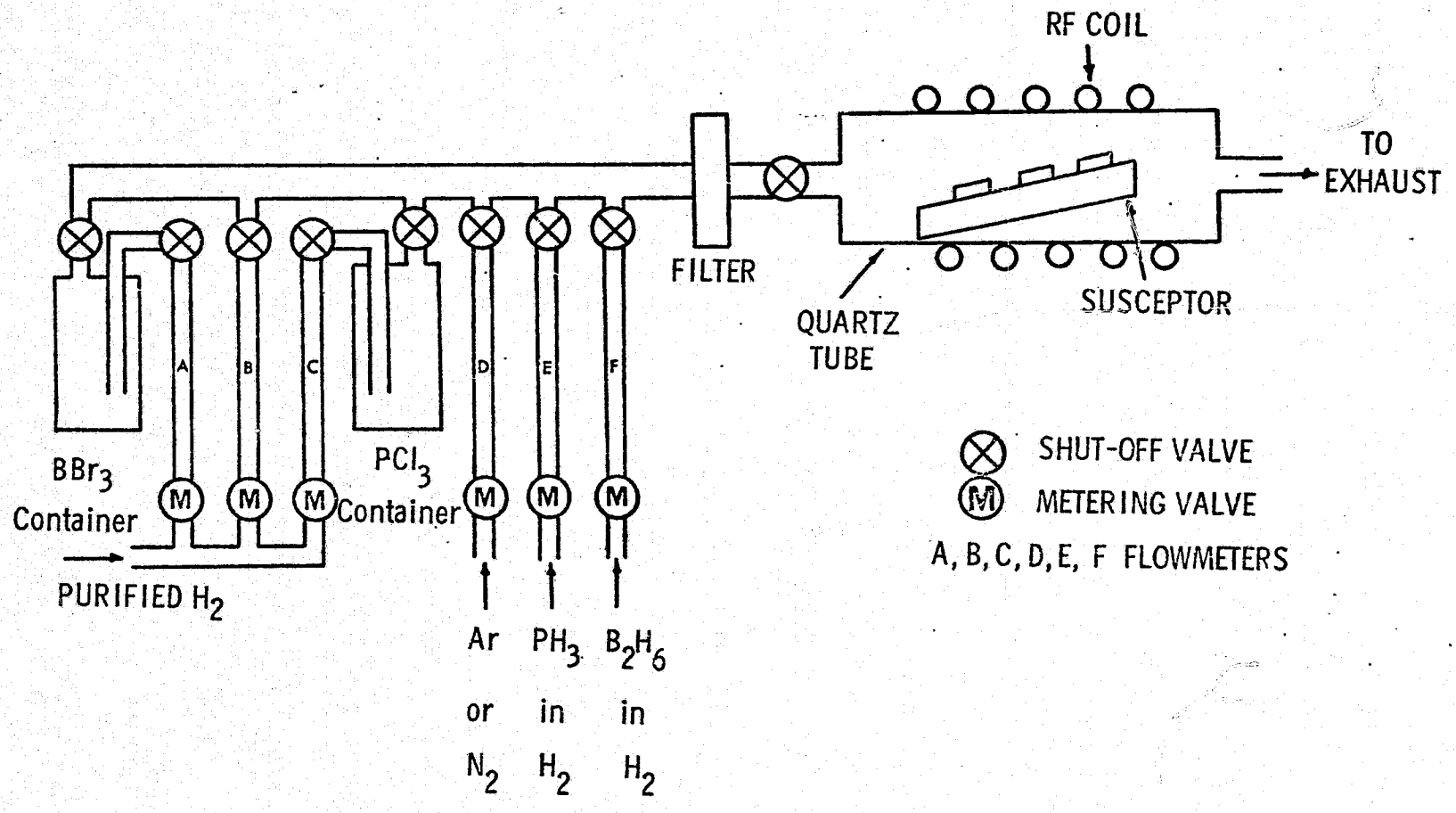

Fig. 2 Schematic diagram of the apparatus for the deposition of boron phosphide by the thermal reduction of halide mixtures.

the reaction tube by bubbling hydrogen through the respective containers held at a constant temperature. The other reactants were obtained as mixtures with hydrogen. The major component in all of the reactant systems was hydrogen which was purified by diffusion through a palladium-silver alloy.

Initial deposition experiments to evaluate the four possible reactions were carried out with silicon and fused silica substrates supported on a graphite susceptor. It was determined that reactions (2) and (3) are not suitable for the preparation of boron phosphide, due to a reaction near room temperature to produce a white solid, presumably a complex compound of the reactants. Reaction (1) is a suitable process to prepare boron phosphide, but a growth rate of only 15 μm/hr was obtained. Reaction (4) deposited boron phosphide at a rate of 60 μm/hr, and it is therefore the most suitable reaction for the production of large quantities of boron phosphide. Subsequent preparation of boron phosphide was carried out with reaction (4) in a fused silica reaction tube, 22 mm ID and 29 mm OD, heated by a resistance furnace to a maximum temperature of 1100° C. Typically, the flow rates of hydrogen, boron tribromide, and phosphorus trichloride were 8×10^{-2}, 1.5×10^{-3}, and 3×10^{-3} moles/min, respectively. The excess of phosphorus trichloride was used to minimize any decomposition of the deposited material. In this system, boron phosphide deposited on the portion of the reaction tube wall which was in a temperature region from about 950° C to

1100° C. About 30 g of boron phosphide was obtained with an eight hour reaction time. The x-ray powder technique showed the reaction product to be only boron phosphide.

II.A.2.b. Boron Phosphide Crystal Growth by Chemical Vapor Deposition

During the initial depositions to evaluate the thermal reduction of boron tribromide-phosphorus trichloride mixtures for the preparation of polycrystalline boron phosphide, rod-shaped, orange-red crystals were occasionally found on the susceptor. With the use of low H_2/BBr_3 molar ratios, crystals up to 5 mm in length were obtained. X-ray measurements showed that the crystals were boron phosphide, and that the long growth axis of the crystals was along a <111> direction.

Some of the electrical properties of these rod-like boron phosphide crystals were determined. Thermoelectric probe measurements indicated that the crystals were p-type. To determine the electrical resistivity, evaporated aluminum was deposited onto the ends of the crystals, and the crystals were annealed. The room temperature resistivity was, typically, about 20 ohm-cm, as determined from the sample resistance and geometry. A high temperature activation energy of about 0.88 eV was also measured. No further work was carried out with crystals grown by the chemical vapor deposition process, since the geometry is not suitable for substrates for device fabrication.

II.A.2.c. Boron Phosphide Crystal Growth by Chemical Transport[23]

Boron phosphide reacts reversibly with halogens and boron

trihalides as illustrated by these reactions:

$$4BP(s) + 6X_2(g) \rightleftarrows 4BX_3(g) + P_4(g) \quad (5)$$

$$4BP(s) + 2BX_3(g) \rightleftarrows 6BX_3(g) + P_4(g) \quad (6)$$

Where X is, for example, chlorine, bromine or iodine. Consequently, the halogens or the boron trihalides should transport boron phosphide in a temperature gradient, probably via the formation of a boron monohalide:

$$4BP(s) + 2X_2(g) \rightleftarrows 4BX(g) + 2P_4(g) \quad (7)$$

$$4BP(s) + 2BX_3(g) \rightleftarrows 6BX(g) + P_4(g) \quad (8)$$

To carry out the transport process, polycrystalline boron phosphide, phosphorus, and a transport agent were introduced into a thick-wall fused silica ampule. The reaction tube was attached to a vacuum manifold, cooled with liquid nitrogen, evacuated to less than 10^{-5} Torr, and sealed. Furnaces with two independently controlled temperature zones were used for the transport experiments. The polycrystalline source material located at one end of the tube was in the higher temperature zone, and the transported boron phosphide deposited on the wall of the tube in the lower temperature zone. The excess phosphorus in the ampules increased the transport rate and suppressed the decomposition of boron phosphide in the high temperature experiments. The transport agents investigated for the transport of boron phosphide included bromine, iodine, and phosphorus trichloride. Other parameters whose effects were studied include the transport agent pressure, the excess phosphorus pressure, the source temperature, the temperature gradient, and the condition of the silica ampule wall.

An initial series of transport experiments was carried out with source temperatures near and below 1150° C; conventional resistance heated furnaces can be used up to this temperature. Fused silica ampules 25 mm ID and 15 to 25 cm long were used. No transport of boron phosphide was observed with the source temperature below 1000° C. Subsequent experiments were therefore carried out with source temperatures in the range from 1100 to 1150° C. Many experiments were carried out to evaluate the effect of the other system parameters. Temperature gradients from 20° to 100° C were used. The different transport agents were used at various pressures, and the effect of the phosphorus pressure was also evaluated. In all cases, the transport rate was very slow, and the grown crystals had dimensions on the order of a few tenths of a millimeter after a three week reaction time. It was concluded that the transport rate was limited by the thermodynamics of the reactions, and that higher temperatures are needed for effective transport of boron phosphide.

To carry out the chemical transport of boron phosphide at temperatures up to about 1300° C, two zone furnaces with silicon carbide heating elements were constructed. The transport tubes used in these furnaces had a 10 mm ID, 16 mm OD, and a 12 cm length. A series of 45 detailed experiments was carried out with source temperatures from 1190° C to 1290° C and with 0.5 g of polycrystalline boron phosphide as the source material. The largest crystals were obtained with the highest source temperatures. It was determined that a phosphorus pressure of 3 atm

and a transport agent pressure of 1 atm are optimum. Phosphorus trichloride was found to be the fastest transport agent. With a temperature gradient of 4° C across the ampoules, essentially all of the boron phosphide was transported in 5 - 7 days; however, the transported material consisted of loosely bound aggregates of small crystals. The use of iodine or bromine as a transport agent produced better results. Using iodine as a transport agent and a temperature gradient of 15 - 20° C, the source material was transported in 7 - 10 days to yield orange - red crystals. The transported crystals were in the form of tightly bound aggregates about 5 mm in diameter and 1 - 2 mm thickness and in the form of polyhedrons measuring 1 - 2 mm on each side. Similar crystals were obtained with bromine as the transport agent with a 5°C temperature gradient.

In the technique described above for the crystal growth of boron phosphide, nucleation takes place on the wall of the reaction tube. Two types of crystals were obtained: aggregates consisting of from three to six single crystals, and isolated single crystal polyhedrons such as shown in Fig. 3. It was concluded that control over the nucleation process was necessary. Four techniques were investigated to control nucleation. Firstly, the deposition region of the reaction tube was flame worked to remove surface irregularities. Several experiments were carried out with flame-worked tubes using bromine as a transport agent and a 5° C gradient along the tube. In about one-half of the

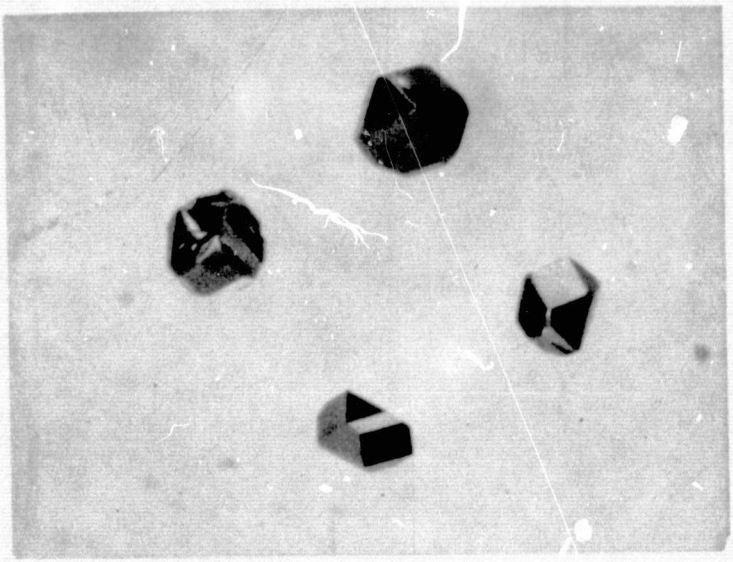

Fig. 3 Boron phosphide crystals obtained by the chemical transport technique.

experiments, no nucleation occurred on the wall of the reaction tube after ten days; a considerable number of crystallites would have formed if the wall of the reaction tube were not flame-treated. In the other half of the experiments, only one aggregate consisting of tightly bound single crystals up to 2 mm was formed at the tip of the reaction tube. These experiments indicate that flameworking of fused silica tube is a critical factor to achieve control of nucleation in the closed tube transport process. The other three techniques investigated for nucleation control were directed toward elimination of the aggregate structure of the deposited boron phosphide. A programmed temperature gradient technique was used in several experiments. A small gradient, 5° - 7° C, was used during the first few days to limit the formation of nuclei. The temperature of the deposition zone was then reduced about 5° C every two days until a final gradient of 30° C was established. Crystalline aggregates were obtained from these experiments. A third attempt to control nucleation was made by a reduction in the diameter of the transport ampule in the deposition zone. The deposition end of the ampule was made from 3 mm ID x 9 mm OD fused silica tubing attached to the 10 mm ID x 16 mm OD ampule. Single crystals with dimensions up to 2 mm grew in this narrow end of the ampule, but larger clusters tended to grow just outside the small diameter region. A fourth attempt to influence the nucleation of boron phosphide was made by the introduction of a seed into the growth ampule in the deposition zone. Improved results

were, however, not obtained.

The boron phosphide crystals obtained in this work, because of the use of higher temperatures and the control of random nucleation, are considerably larger than the transported crystals reported in the literature. They have well-formed faces, in contrast to the dendritic crystals of comparable size obtained by Grindberg et. al.[14] The hardness of the boron phosphide crystals was measured by the diamond pyramid hardness test. A square base diamond pyramid was forced into the specimen using a 1 kg load, and the diagonals of the impression were measured. The hardness of boron phosphide was calculated to be approximately 2450 kg mm^{-2} as compared with 2970 for silicon carbide determined under the same conditions.

The transported boron phosphide crystals are chemically inert in aqueous acids and alkalis. Molten potassium hydroxide or a molten mixture of 75% sodium hydroxide and 25% sodium peroxide at 380° C may be used as a preferential etchant to reveal defects in the boron phosphide crystals. The only non-preferential etchant appears to be a mixture of hydrogen and hydrogen chloride near 1000° C.

All of the transported boron phosphide crystals are p-type, as determined by the thermoelectric probe technique and by the direction of point-contact rectification. The electrical conductivity of transported boron phosphide crystals was measured over a wide temperature range. The crystals were first mechanically polished to yield two flat parallel faces by using 1 μm

alumina abrasives and were thoroughly cleaned for the application of ohmic contacts. Indium was found to be a suitable material to make ohmic contacts to the transported boron phosphide. After applying indium to the flat faces, the specimen was annealed in an argon atmosphere at 500° C for 1 hr. The dc current-voltage characteristics of a number of transported crystals were measured in the temperature range from 77° K to 350° K. A typical plot of the logarithm of the conductance versus reciprocal temperature is shown in Fig. 4. Two linear regions may be distinguished in the plot. Neglecting the temperature dependence of carrier mobility, the slopes of these two regions indicate the presence of two impurity states with activation energies of 0.009 and 0.052 eV, respectively. The room temperature resistivity of this crystal is approximately 0.55 ohm-cm. The room temperature carrier concentration in transported boron phosphide crystals was estimated from Schottky barrier measurements, described later, to be on the order of 10^{18} cm^{-3}.

Extensive investigation of the chemical transport technique for the growth of boron phosphide crystals was carried out during this program. Although crystals large enough to use as substrates for device work could be grown, the process was very slow. As a consequence, another crystal growth technique, solution growth, was investigated.

II.A.2.d. Boron Phosphide Crystal Growth by Precipitation[24]

The solution growth technique has been successfully applied

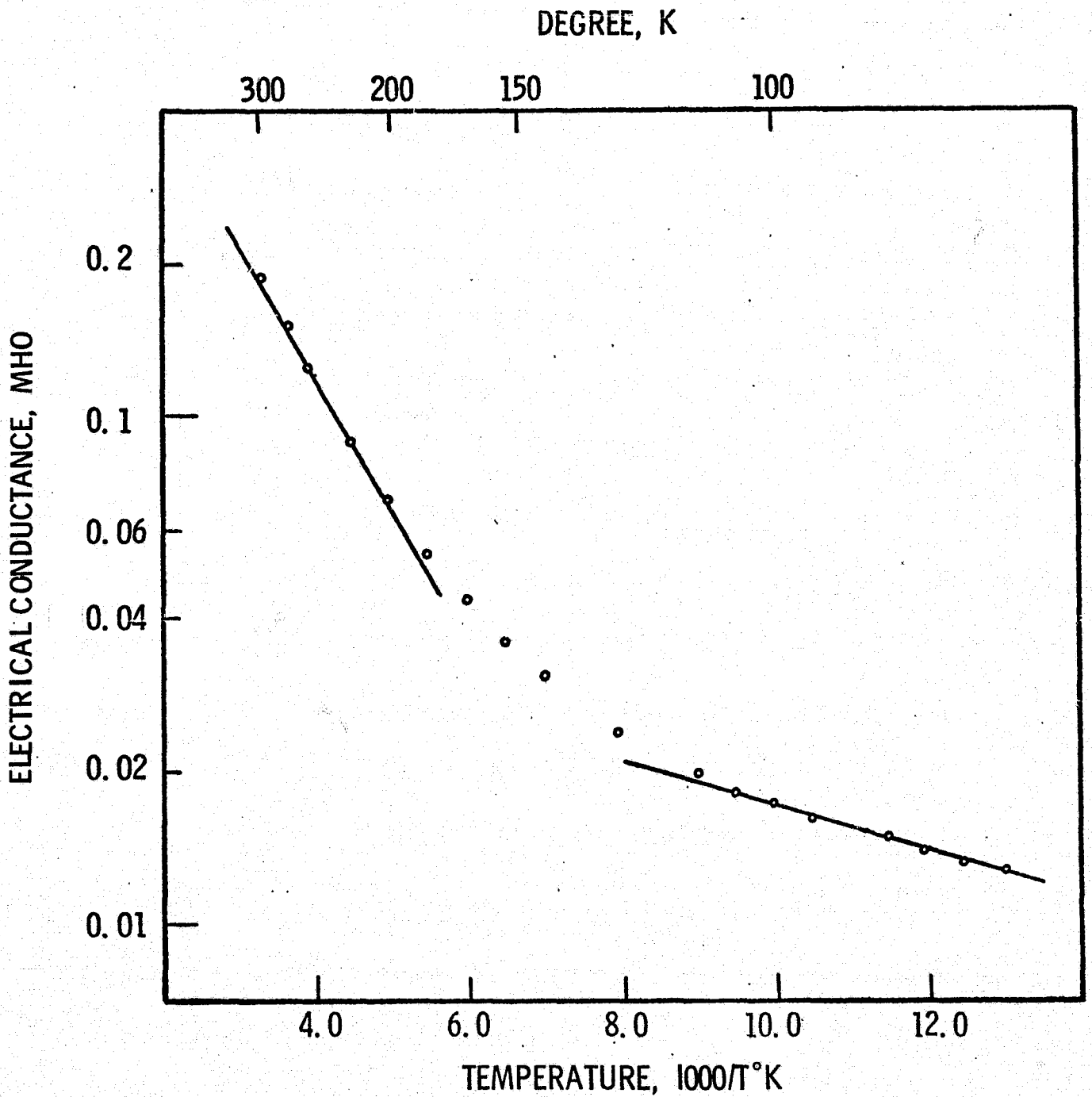

Fig. 4 Electrical conductance of a transported boron phosphide crystal as a function of temperature.

to the growth of boron phosphide crystals, and it was found to be more useful than chemical transport for the growth of large crystals suitable for device fabrications. An extensive investigation of the two basic solution growth techniques, recrystallization and precipitation, was made, and the results are summarized below.

The precipitation of boron phosphide from solution by the addition of phosphorus to a boron-metal melt with subsequent cooling of the melt was the first solution growth technique investigated. These experiments were carried out in the apparatus shown schematically in Fig. 5. A boron-metal ingot was first prepared by melting weighed quantities of the two materials in an alumina boat in a hydrogen atmosphere. The ingot and the boat fit into a cylindrical graphite susceptor, which itself fit into a fused silica spacer. This assembly was placed into a 50 mm ID silica tube with phosphorus, and the tube was evacuated to about 10^{-5} mm and sealed. Experiments were carried out by radio frequency heating of the susceptor and resistance heating of one end of the tube to control the phosphorus pressure.

The important process parameters, including the metal solvent, the concentration of boron in the solution, the temperature of the solution, the phosphorus pressure over the solution, the reaction time, and the cooling conditions were studied in a number of experiments.

Several metals, such as copper, iron nickel, and platinum, are possible solvent-formers for the solution growth of boron

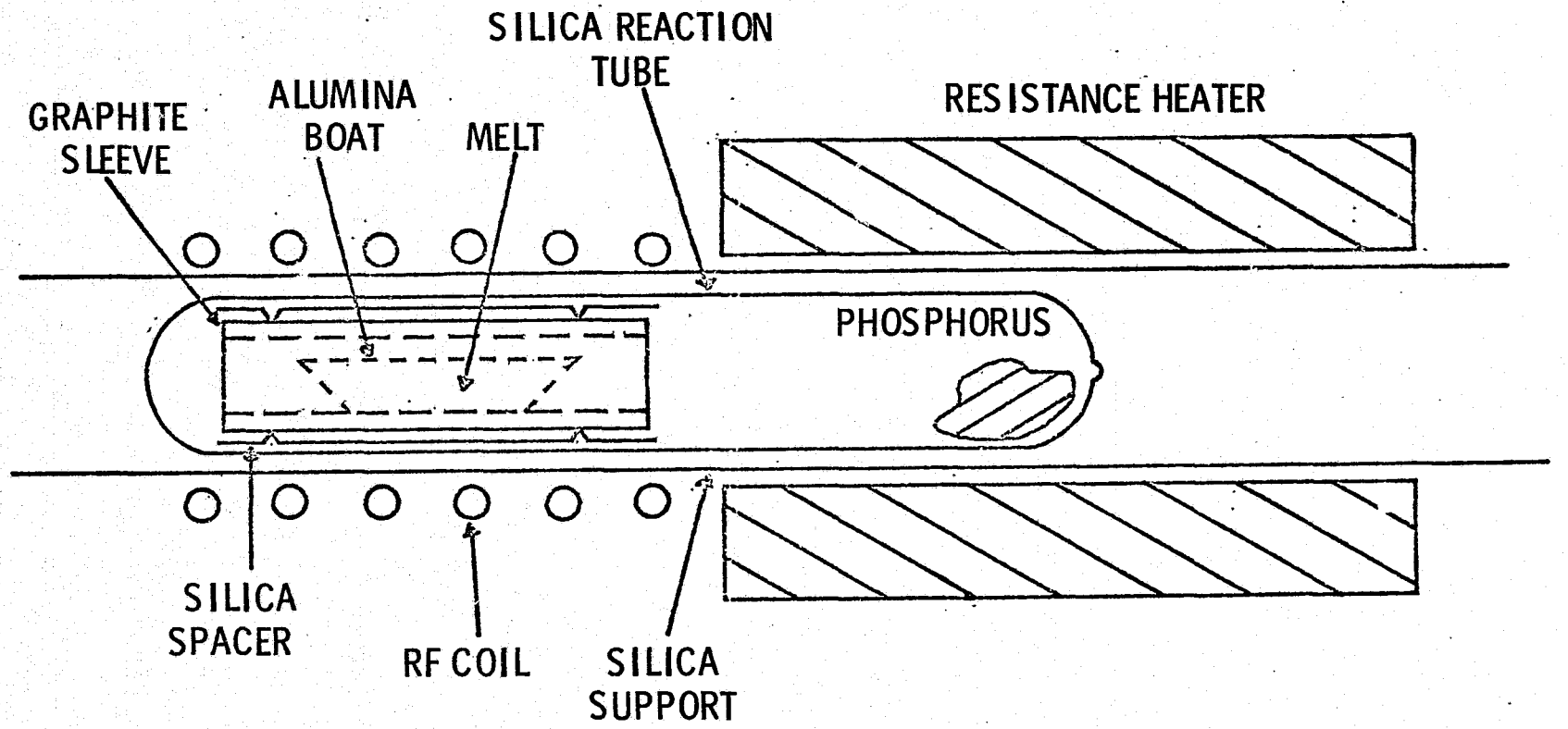

Fig. 5 Schematic diagram of the apparatus for the solution growth of boron phosphide.

(27)

phosphide, and copper and nickel phosphides appeared to be the most useful ones. To determine the conditions for the growth of boron phosphide crystals from solutions, solubility estimates for boron phosphide in nickel and copper phosphides were determined over a wide temperature range. Polycrystalline nickel phosphide and copper phosphide were first prepared. Since the nickel-phosphorus system is extremely complicated,[25] with as many as ten compounds, nickel phosphide was made in the same apparatus shown in Fig. 5 and under the same conditions used for the crystal growth experiments. In essence, molten nickel was heated in a phosphorus vapor atmosphere; the resulting ingot was found to be mostly $Ni_{12}P_5$. In the case of the copper-phosphorus system, there are only two compounds: Cu_3P and CuP_2. Both were synthesized by the reaction of copper and phosphorus in sealed tubes. Copper located at one end of the tube was heated at 1150° C, and the other end of the tube was heated to produce a phosphorus pressure of about 1 to 2 atm. Depending upon the Cu/P molar ratio in the ampule, either Cu_3P or CuP_2 was prepared.

To estimate the solubility of boron phosphide in nickel phosphide, a pulverized mixture of the two materials with excess phosphorus was heated and allowed to react in a sealed tube. The resulting ingot was then treated with acid to dissolve all components except boron phosphide. The recovered material, in general, consisted of undissolved boron phosphide and boron phosphide crystals. The initial amount of

boron phosphide was never recovered due to the complexity of the nickel-boron-phosphorus system. The weight per cent of boron phosphide dissolved in and recrystallized from nickel phosphide at various temperatures is shown in Fig. 6. Similar experiments were carried out with the two copper phosphides. Boron phosphide was found to be insoluble in CuP_2 in the temperature range of interest. Boron phosphide is soluble in Cu_3P; however, its solubility is lower than in $Ni_{12}P_5$. At 1220° C, for example, only 0.64% by weight of the initial boron phosphide recrystallized in a Cu_3P solution. From the data in Fig. 6, the boron-nickel alloy used for crystal growth at 1325° C should contain 2.3% (weight) boron so that, after saturating with phosphorus, the resulting solution of boron phosphide in nickel phosphide would be slightly undersaturated.

From the crystal growth experiments, it was concluded that both copper and nickel are suitable for the growth of boron phosphide crystals. Nickel was more extensively investigated, and crystals, such as shown in Fig. 7, with dimensions up to 3 mm were obtained. The crystal size was not strongly dependent on the initial boron concentration in the solution for boron concentrations less than 10%. A solution temperature of 1325° C was found to be suitable. A phosphorus pressure of 2 - 3 atm was found to be optimum; lower pressure resulted in the formation of boron subphosphide B_6P, and higher pressures created such strong convection currents in the reaction tube

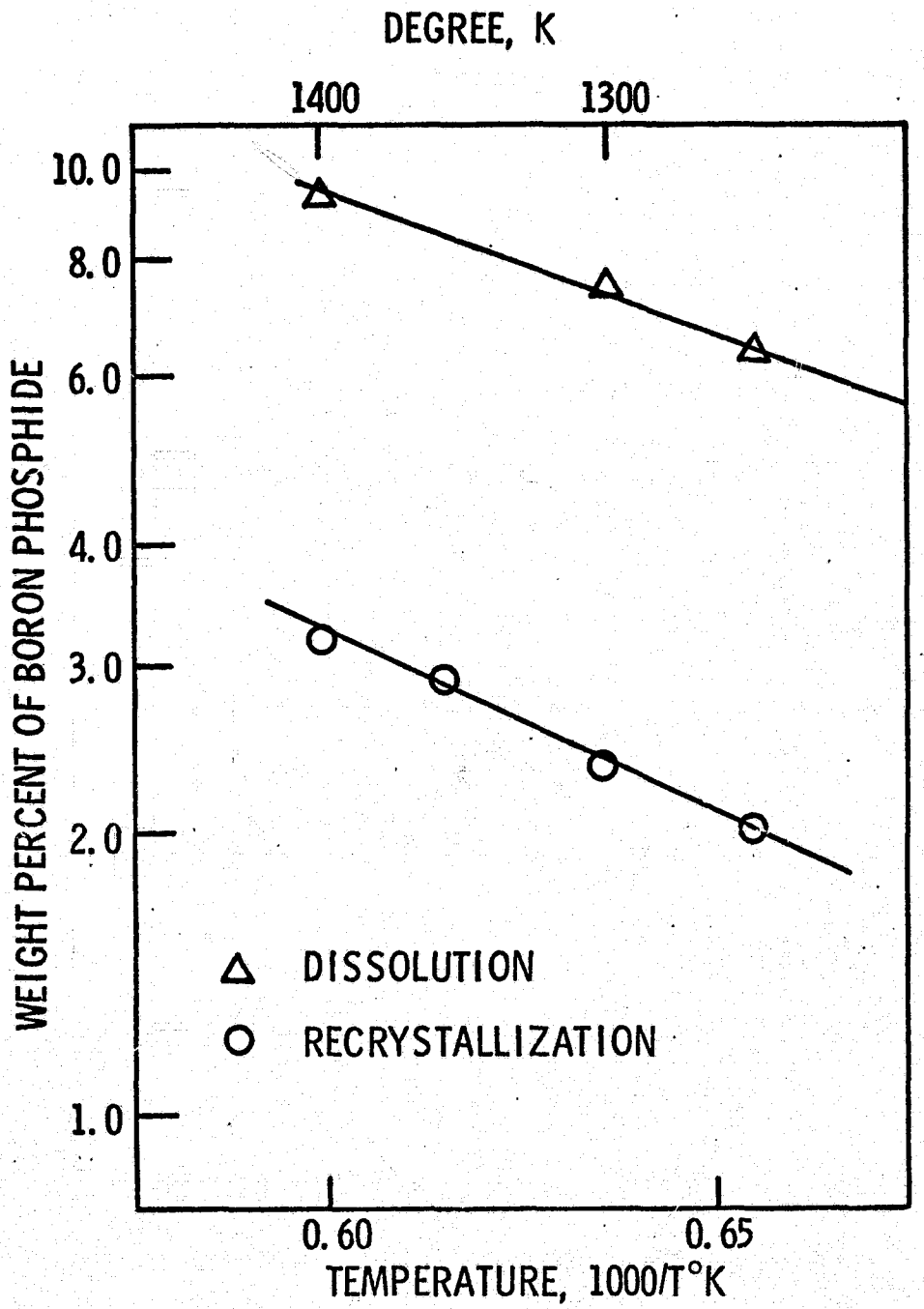

Fig. 6 The dissolution and recrystallization of boron phosphide as a function of temperature using nickel phosphide as a solvent.

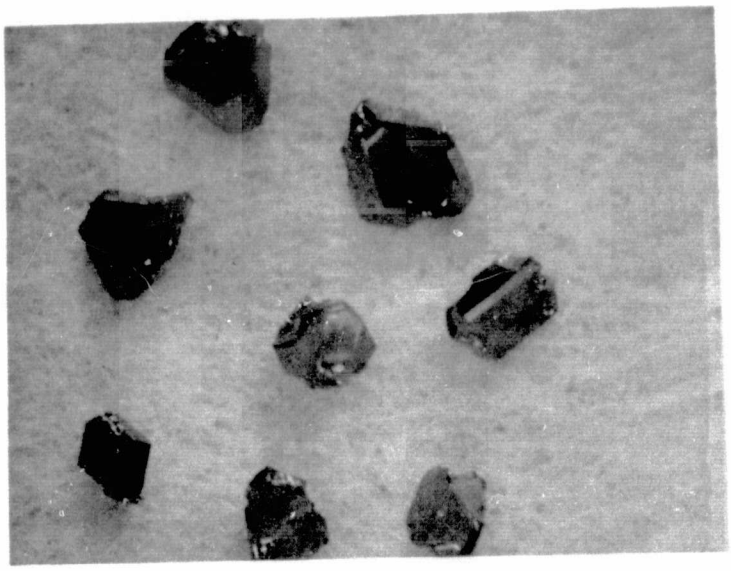

Fig. 7 Boron phosphide crystals grown from a nickel phosphide solution.

that the phosphorus pressure could not be controlled. The resulting crystal size was not strongly dependent upon the reaction time; a minimum of 4 hrs was required, however. Various cooling conditions were also studied. Crystal size increased as the cooling rate was decreased to about 10° C/hr; no further increase of crystal size was found with slower rates. A few experiments were also done by slowly pulling the reaction tube out of the radio frequency coil, but the results were inferior to the slow cooling of the entire solution. The properties of the boron phosphide crystals grown by precipitation were very similar to the properties of the crystals grown by recrystallization, and the results are given below.

II.A.2.e. Boron Phosphide Crystal Growth by Recrystallization[24,26]

Recrystallization of polycrystalline boron phosphide from nickel phosphide solutions was found to produce larger crystals than the precipitation method, and the recrystallization technique was, therefore, extensively investigated. In the recrystallization technique, a small temperature gradient was maintained across a saturated solution of boron phosphide in a metal phosphide with polycrystalline boron phosphide in the high temperature region. Due to the higher solubility at higher temperatures, a concentration gradient is set up across the solution, and consequently, transport of boron phosphide from the polycrystalline source to the lower temperature region occurs. In the lower temperature zone, boron phosphide will grow as crystalline material.

Recrystallization experiments were carried out to evaluate the effects of a number of parameters, including the metal phosphide solvent, the temperature conditions, and the system arrangement. High temperature experiments were done in sealed ampules with graphite crucibles heated by radio frequency induction. Low temperature growth experiments were done directly in sealed silica ampules in resistance heated furnaces. Excess phosphorus was used in all cases to avoid the formation of boron subphosphide.

The solvents evaluated for the recrystallization process were copper phosphide (Cu_3P) and a number of nickel phosphides. With copper phosphide as the solvent, most of the silica ampules cracked upon cooling, and since copper phosphide did not produce crystals larger than one of the nickel phosphides, major emphasis was given to the use of nickel phosphide. The composition of the nickel phosphide, which has not been previously investigated in boron phosphide crystal growth experiments, was found to be important in the recrystallization process. As mentioned above, the nickel-phosphorus system is very complicated.[24] Therefore, a variety of conditions, similar to those used for the crystal growth experiments, were used to synthesize nickel phosphide. Temperatures in the range from 1200° C to 1400° C and phosphorus pressures from about one to five atm were used. The predominant compound formed in many of these experiments was Ni_2P as determined by x-ray data; the material solidified as needle-like crystals which are typical of this compound.[25] In one case,

Ni_7P_3 was obtained. Some of the ingots obtained were phase mixtures of Ni_2P and other more phosphorus-rich nickel phosphides. A detailed analysis of the phase mixtures was not carried out, but NiP was probably the most phosphorus-rich compound formed. Since Ni_2P has a wide homogeneity range, it is also likely that there was excess phosphorus in the ingots.

All of the crystal growth experiments which produced large single crystals of boron phosphide used only Ni_2P as the solvent. The use of Ni_7P_3 produced only small crystals, and the phase mixtures of Ni_2P with other nickel phosphides produced no crystals. Ni_2P was conveniently made by the reaction of phosphorus vapor with nickel in sealed ampules near 1250° C. Also commercial nickel phosphide (Puratek, Norwood, Ohio), reported to be 99.9% Ni_2P, as the solvent produced equally good crystals if excess phosphorus over that amount used with the laboratory grown Ni_2P was added to the ampule. This indicates that the laboratory synthesized Ni_2P did contain excess dissolved phosphorus.

The investigation of the thermal conditions for the growth of boron phosphide showed that temperatures near 1200° C produce the largest crystals. Best results were obtained with polycrystalline source material at about 1220° C on the top of the solution with about a 20° C temperature gradient in the solution. Recrystallized boron phosphide was

found near the bottom of the growth ampule. With a three to four week growth time, boron phosphide crystals in the form of platelets and sometimes polyhedrons were obtained. The main faces of the platelets were up to 20 mm^2 in area, and the thickness of the platelets was up to about 1.5 mm. The polyhedrons had maximum dimensions of 5 mm x 4 mm x 3 mm. Platelets predominated in these experiments.

In an effort to improve the size of boron phosphide crystals, the accelerated container rotation technique[26,27,28,29] was adapted to the solution growth process discussed above. In the accelerated container technique, the growth container is rotated about its axis with acceleration and deacceleration. This type of movement leads to very effective mixing within the liquid. To apply the accelerated container technique, the ampules were connected to a drive mechanism such that they could be rotated about the axis of the furnace. The maximum rotation rate was adjustable up to 120 rpm, the acceleration was adjustable in the range of $\pm 0.4\pi$ rad/sec^2, and the time period was variable in the range from a few sec to one min.

The boron phosphide crystals grown with the accelerated container rotation technique were larger, had fewer voids, and had better developed faces than those obtained from a stationary container. The experiments with the accelerated container produced boron phosphide crystals with dimensions on the faces up to 8 mm, and some of the crystals are shown in Fig. 8. The size of the crystals obtained from the accelerated container was not

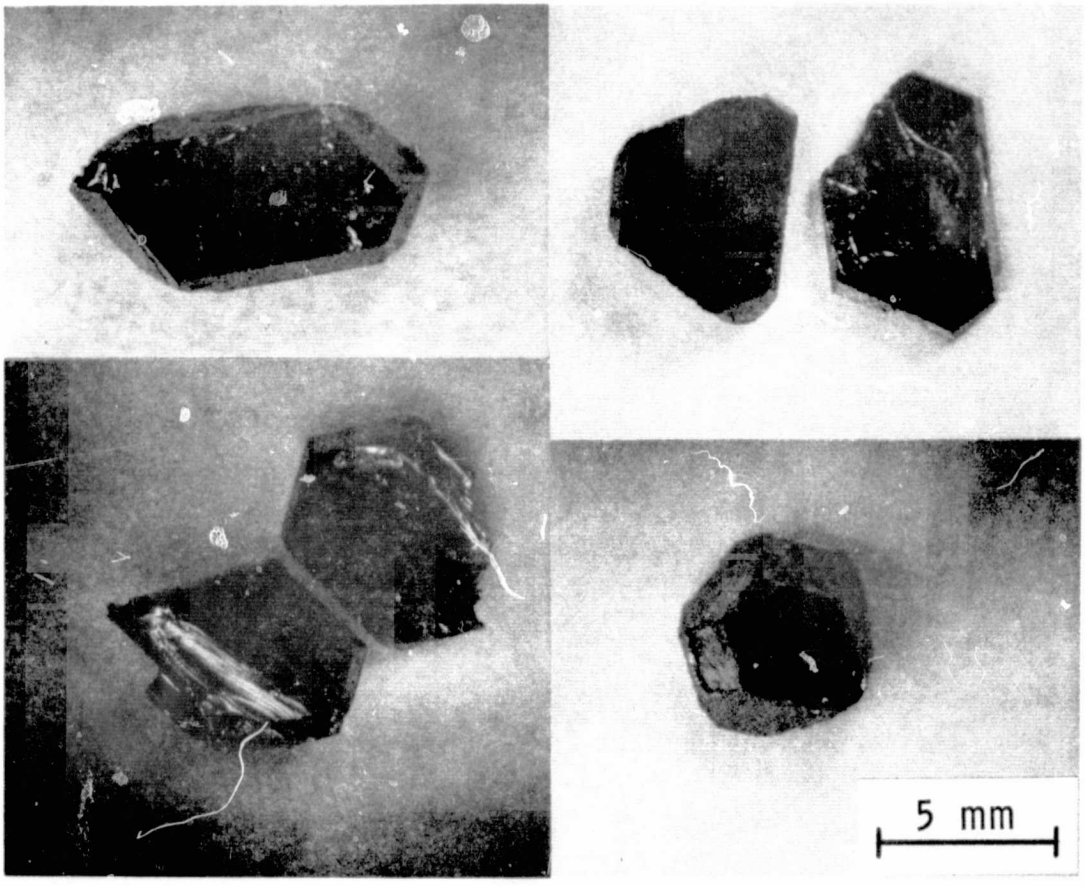

Fig. 8 Boron phosphide crystals grown by recrystallization near 1200° C from a nickel phosphide solution with accelerated container rotation.

sensitive to the exact rotation conditions. A one min time period and a maximum rotation rate in the range from 40 rpm to 70 rpm produced the best results. Two different cycles of rotation were used with similar results: a simple sawtooth rpm versus time cycle with rotation in both directions and a truncated sawtooth rpm versus time cycle with rotation in both directions. These results demonstrate the usefulness of accelerated crucible rotation for the preparation of boron phosphide crystals.

Boron phosphide crystals obtained from the recrystallization experiments were usually in the form of thin platelets, but polyhedrons were also obtained. The platelets had {111}-type main faces and grew by the twin plane reentrant edge mechanism[30] in which twinning about {111} planes occurs. Without the formation of twins, the growth of large crystals is not favored since the growing crystal would tend to facet with the slow growth {111} planes. Figure 9 is a photomicrograph which shows twin plane intersections with a polished and etched boron phosphide surface. Typically, the platelets had one main face flat and smooth and the other main face rough. The two faces could also be distinguished by chemical etching in a 3:1 molten mixture of sodium hydroxide and sodium peroxide at 400 to 500° C. Dislocation etch pits were observed on the smooth face and not on the other. If the etching behavior of boron phosphide is similar to that of other III-V compound

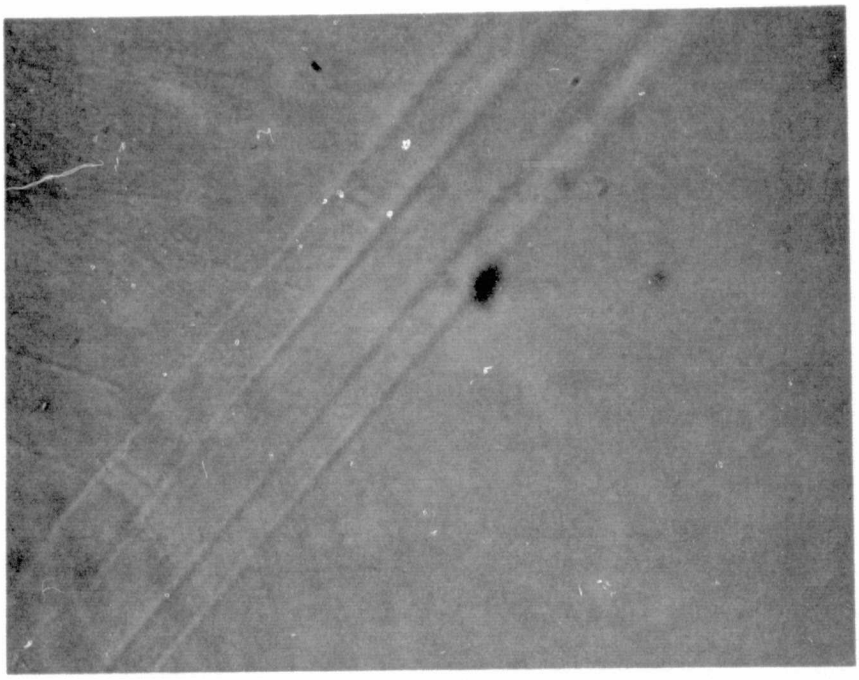

Fig. 9 Angle-lapped and chemically etched surface of a boron phosphide platelet showing the presence of twins.

semiconductors, then the face which developed dislocation etch pits on the boron phosphide crystals is the boron face.

The majority of the large boron phosphide crystals contained both p-type and n-type regions. Typically, the faces were n-type, and a central core was p-type. This inhomogeneous distribution of impurities is probably a result of two factors: a higher segregation coefficient for p-type impurities than for n-type impurities so that p-type impurities are depleted from the solution and a continuous supply of silicon, which as discussed below is an n-type impurity in boron phosphide, going into the solution from the ampule. A convenient technique to observe the n-type and p-type regions in these crystals is electrolytic etching, which is discussed in Section II.C.1. P-n junction electroluminescence was observed in some of the crystals with built-in junctions, and the emission characteristics are discussed in a later section.

A number of experiments were carried out in an effort to produce crystals with a more uniform distribution of impurities. In these experiments, the elements zinc, magnesium, beryllium, sulfur, selenium, tellurium, and silicon were investigated as dopants for boron phosphide. Beryllium, magnesium, and zinc were expected to be p-type dopants in boron phosphide. These materials were added to the solution in the growth ampules both as the elements and as the phosphides: Zn_3P_2, Be_3P_2, and Mg_3P_2. The addition of zinc to the solution did not appear to affect the electrical properties of the crystals. However, both beryllium

and magnesium were found to produce mostly p-type boron phosphide, although n-type regions were sometimes found in the crystals. Beryllium doping produced p-type crystals more consistently. Among the expected n-type dopants investigated, only tellurium tended to produce n-type crystals; some crystals with p-type and n-type regions were also obtained with tellurium doping. The addition of sulfur and selenium to the growth ampules did not noticeably affect the electrical properties of the crystals. The best n-type dopant, however, was silicon, and only n-type boron phosphide was obtained from growth experiments with silicon as the intentionally added impurity. The limited success of the doping experiments is probably due to the use of an element which is not a constituent of the grown crystals in the solution and to the presence of impurities in the nickel phosphide solvent.

The results discussed in this section represent significant progress in the crystal growth technology associated with the preparation of boron phosphide. Large crystals were obtained reproducibly, and some success was achieved with intentional doping experiments. The crystals are suitable for use as substrates for epitaxial growth to produce boron phosphide devices.

II.B. Preparation and Properties of Thin Layers

The deposition of thin semiconducting layers is a major device fabrication technology since layers with well defined and controlled properties can be grown. Amorphorus and single crystalline layers can be deposited. The growth of crystalline layers

on a substrate of the same material as the deposited material is referred to as homoepitaxy; crystalline growth on a foreign substrate is known as heteroepitaxy. Both processes were investigated during this program, and the results are discussed below.

II.B.1. Boron Arsenide Layers

The deposition of boron arsenide layers with various reactant systems and substrates was investigated. Because of the instability of boron arsenide at high temperatures, only the pyrolysis of a mixture of diborane and arsine was found to be suitable for the deposition of boron arsenide. The overall reaction is:

$$B_2H_6(g) + 2AsH_3(g) \rightarrow 2BAs(s) + 6H_2(g) \qquad (9)$$

Other reactant systems required higher temperatures such that boron arsenide is unstable. Depositions were done in the apparatus shown schematically in Fig. 2; the fused silica reaction tube was water-cooled to minimize any reaction in the gas phase.

In addition to boron arsenide, sodium fluoride, silicon carbide, and silicon were investigated as substrates for the deposition of boron arsenide. Sodium fluoride, which crystallizes in the face-centered cubic structure with a lattice parameter a = 4.62 Å, was chosen since its lattice parameter is close to that of boron arsenide, 4.777 Å. The basal plane of silicon carbide, with its three-fold symmetry and lattice spacing of 3.08 Å, could be used to deposit boron arsenide of {111} orientation, since the interatomic distance in boron arsenide is

3.38 Å. Silicon was also used as a substrate to investigate the boron arsenide-silicon system, although epitaxial growth was not expected.

The silicon carbide substrates were supported on a boron arsenide coated graphite susceptor. Before deposition the substrates were heated in hydrogen at about 1000° C. The deposition of crystalline boron arsenide could be achieved with 0.01% diborane and 0.06% arsine in hydrogen. A growth rate of about 10 μm/hr was obtained. The temperature of the substrate was critical to the growth of crystalline boron arsenide. Epitaxial growth, as determined by reflection electron diffraction patterns, was obtained near 820° C. However, at 800° C or at 850° C, polycrystalline deposits were obtained. It was not established if the epitaxial growth was continuous over the entire substrate or if islands of single crystalline material with perhaps slightly different orientations were obtained.

The deposition of boron arsenide on sodium fluoride was investigated with conditions similar to those used for silicon carbide substrates. The substrates were of a {111} orientation and were etched in deionized water. In all of the deposition experiments, the deposited layer cracked off from the substrate during cooling, due to a large difference between thermal expansion coefficients. The problem could not be eliminated even with very slow cooling rates.

The homoepitaxial growth of boron arsenide by the thermal decomposition of a diborane-arsine mixture was investigated.

Boron arsenide crystals obtained by the transport technique were used as substrates, and they were etched in-situ at 850° C by using a hydrogen-hydrogen chloride mixture. The deposition was carried out at a substrate temperature near 850° C with hydrogen containing 0.01% diborane and 0.06% arsine at a flow rate of 20 1/min. The as-grown surface exhibited triangular growth pyramids indicating that the deposit was epitaxial with respect to the substrate. The number of homoepitaxial growth experiments was limited, however, by the supply of boron arsenide crystals of suitable size.

The deposition of boron arsenide on silicon substrates was also studied to explore the applications of boron arsenide in silicon devices. The thermal decomposition of the hydride mixture was again used for the deposition process. The silicon substrates were 0.01 ohm-cm p-type with main faces of {111} orientation and were chemically polished with a nitric acid-hydrofluoric acid mixture. Prior to the deposition process, the substrates were heated in hydrogen at 1000° C to remove the oxide on the surface. The deposited boron arsenide layers were up to 10 μm thick and highly adherent to the silicon substrates. The boron arsenide layers deposited on silicon substrates were found to be amorphous from reflection electron diffraction examinations. The layers were inert to acids and alkalis.

Due to the chemical inertness of boron arsenide, the silicon substrate could be readily etched from the boron arsenide - silicon structures by a mixture of nitric acid and hydrofluoric acid.

The resulting layer was found to transmit dark red light. A specimen which was a few microns thick was placed between two quartz plates, and its absorption spectrum was measured with a Perkin=Elmer (model E-1) monochromator. The results are shown in Fig. 10 where the adsorption coefficient-thickness product (αd) is plotted versus photon energy. The intercept of the square or square root of the optical absorption coefficient versus energy plot on the energy axis has been used for the determination of the energy gap in semiconductors. For direct photon transitions, the plot of the square of absorption coefficient versus photon energy gives a straight line, and for indirect transitions, the square root of absorption coefficient is a linear function of photon energy. Figure 11 shows the data from Fig. 10 plotted both as $(\alpha d)^2$ and as $(\alpha d)^{1/2}$. The intercept of the $(\alpha d)^2$ versus E plot is about 1.45 eV, and the intercept of the $(\alpha d)^{1/2}$ versus E plot is 0.65 eV. The former value is in agreement with the reported optical band gap of boron arsenide, 1.47 eV. Therefore, boron arsenide is presumably a direct band gap material and should be useful for the fabrication of optoelectronic devices.

II.B.2. Boron Phosphide Layers[31]

The deposition of boron phosphide layers was extensively investigated during this program. Techniques were developed to deposit boron phosphide layers on solution-grown boron phosphide crystals and on other substrates such as silicon

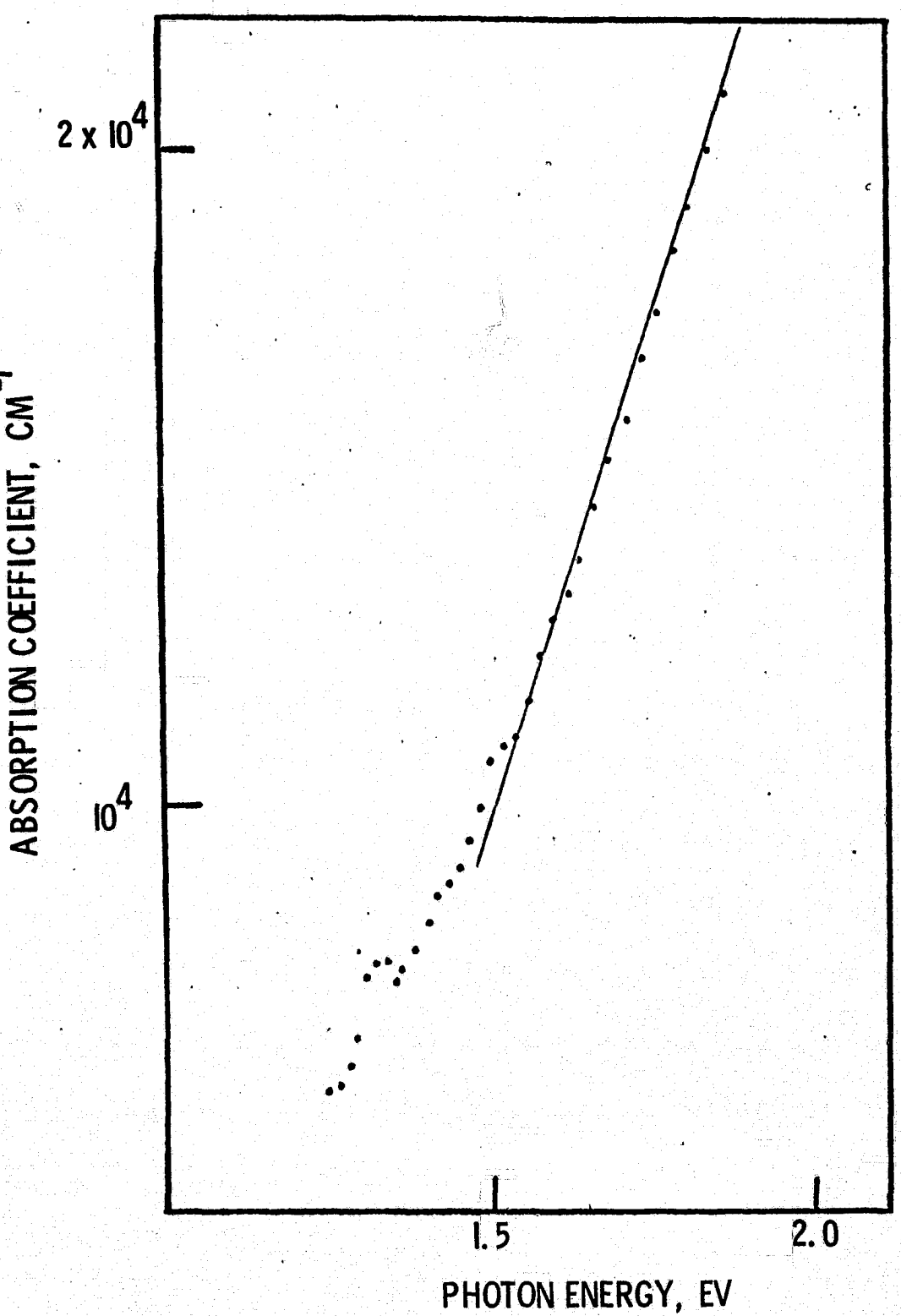

Fig. 10 A plot of the absorption coefficient versus photon energy for amorphous boron arsenide.

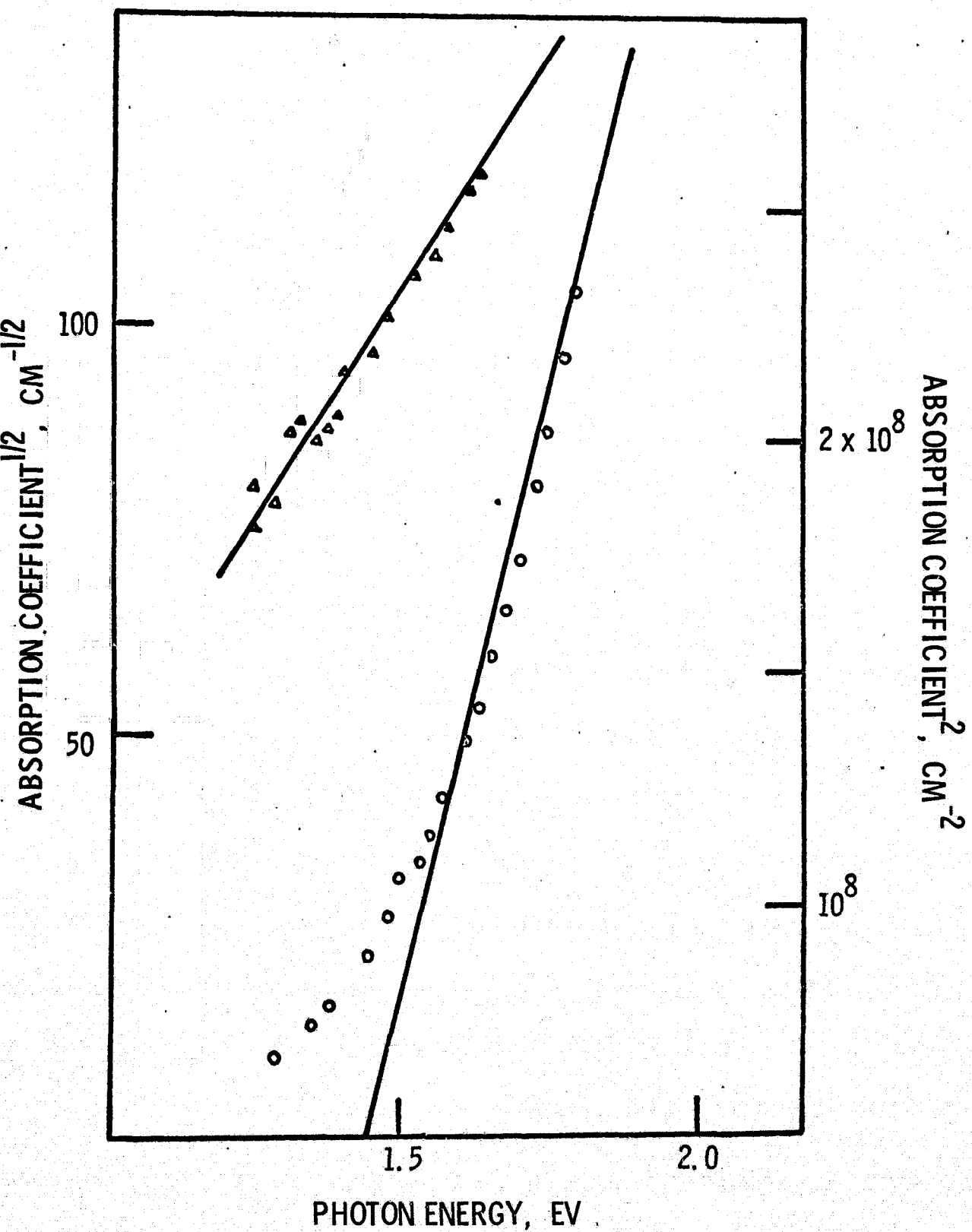

Fig. 11 Optical absorption data of a boron arsenide layer. The circles and triangles represent respectively the square and the square root of the absorption coefficient.

carbide and silicon. During the early part of this work, silicon carbide substrates were used in efforts to determine the best reactant system for the deposition of boron phosphide. Two reactions were considered:

$$B_2H_6(g) + 2PH_3(g) \rightarrow 2BP(s) + 6H_2(g) \quad (10)$$

$$BBr_3(g) + PC\ell_3(g) + 3H_2(g) \rightarrow BP(s) + 3HC\ell(g) + 3HBr(g) \quad (11)$$

It was concluded that the deposition of single crystalline material required the use of reaction (11), becuase of the high temperature thermal instability of the hydrides in reaction (10). Boron phosphide layers could be deposited from the hydrides at temperatures up to about 850° C, but due to the low temperature, the layers only exhibited preferred orientations. At higher substrate temperatures, gas phase reactions, even in water cooled reaction tubes, interfered with the oriented growth on the substrate. The thermal reduction of halides is, therefore, the preferred reactant system for the epitaxial deposition of boron phosphide layers.

Adherent and continuous layers of boron phosphide were deposited on silicon carbide substrates in the temperature range 850°-1150° C under a variety of conditions. The most important factors determining the crystallinity of the deposit were found to be the substrate temperature and the polarity of the substrate surface; boron phosphide layers deposited on the silicon face at high substrate temperatures have always exhibited the best structural perfection. Figure 12 shows an early stage of the boron phosphide growth on the silicon face of a silicon carbide substrate at 1150° C. This growth consists of isolated, oriented,

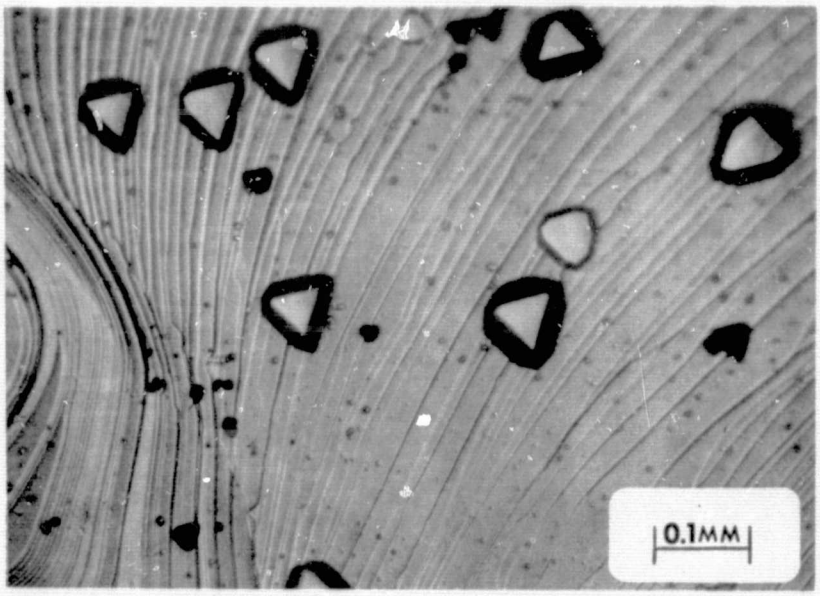

Fig. 12 Oriented boron phosphide crystallites deposited on the silicon face of a hexagonal silicon carbide substrate.

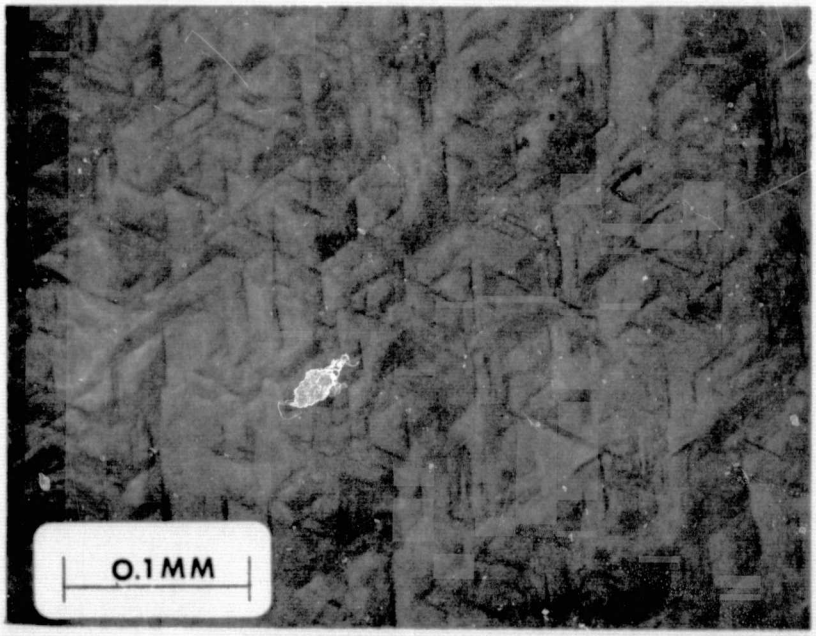

Fig. 13 As-grown surface of a boron phosphide layer of approximately 40 μm thickness deposited on the silicon face of a hexagonal silicon carbide substrate.

triangular crystallites, and the sides of the triangular growth are parallel to the edges of the substrates, i.e., the <010> direction of silicon carbide. The surface of the crystallites is of a {111} orientation as indicated by their symmetry. Furthermore, the triangular crystallites are of opposite orientations, indicating the presence of two equivalent {111} orientations related by a twofold rotation normal to the surface. The equivalent orientations result from the different stacking possibilities at the substrate deposit interface.

The grown surface of continuous boron phosphide layers also exhibits structural features. An example is given in Fig. 13 where the as-grown surface of a boron phosphide layer approximately 40 μm thick deposited on the silicon face is shown. This deposition was carried out at 1050° C using hydrogen, boron tribromide, and phosphorus trichloride at flow rates of 7×10^{-2}, 4×10^{-4}, and 4×10^{-3} mol/min, respectively, and the average deposition rate was 40 μm/hr. In addition to the triangular growth, the surface shows a number of linear figures at 60° or 120° to each other which sometimes intersect to form triangles or partial triangles. These figures are presumably stacking fault traces resulting from the coalescence of the initial crystallites. The geometry of the figures suggests that the entire grown layer is single crystalline and is epitaxial with respect to the substrate. The epitaxial relation is: BP(111) || SiC(001) and BP<1$\bar{1}$0> || SiC<010>. This relation was confirmed by reflection electron diffraction examinations.

The boron phosphide layers deposited on the silicon face of silicon carbide substrates at lower temperatures were also examined in detail by reflection electron diffraction. When the substrate temperature was decreased to 950° C or below, the deposit became completely polycrystalline. Upon examination by optical microscopy, the grown surface of the low temperature layers showed no geometrical features. The boron phosphide layers deposited on the carbon face of silicon carbide substrates were also found to be polycrystalline in most cases, although those deposited at higher temperatures exhibited some preferred orientation.

Epitaxial boron phosphide layers deposited on the silicon carbide substrates by the thermal reduction process without intentional doping are p type. The resistivity and carrier concentration of a typical specimen deposited at 1150° C, determined by the Hall measurements, are 0.2 ohm-cm and 10^{19} cm^{-3}, respectively, at 300° K and are 1 ohm-cm and 2×10^{17} cm^{-3}, respectively, at 200° K.

The electrical conductance of an epitaxial boron phosphide layer was measured in the temperature range 300° - 1070° K, and the results are shown in Fig. 14. Since the temperature dependence of the carrier mobility is very much smaller than that of the carrier concentration in the temperature range under consideration, the ionization energy of deep-lying impurities may be estimated from the slopes of the various regions of the plot in Fig. 14. Ionization energies estimated in this manner are

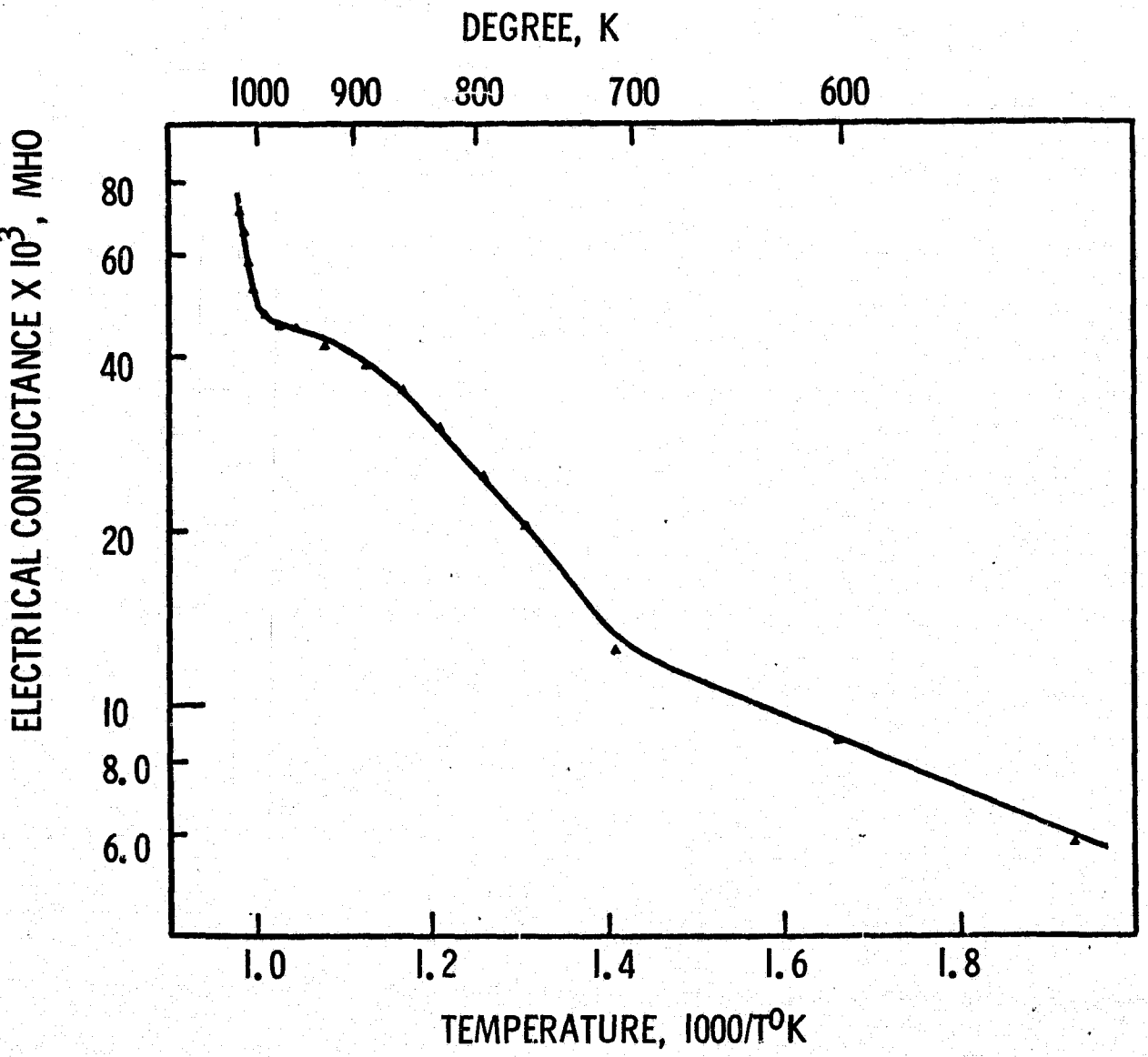

Fig. 14 Electrical conductance of an epitaxial boron phosphide layer as a function of temperature.

0.22 ± 0.04 and 0.66 ± 0.06 eV. At temperatures above 1000° K intrinsic ionization dominates, and the energy gap of boron phosphide was determined to be 1.95 ± 0,1 eV, in agreement with the energy gap from optical measurements.

Boron phosphide crystals from closed tube transport and platelets obtained from solution growth were used as substrates for the deposition of boron phosphide. Epitaxial layers on boron phosphide were found to have much better structural perfection than those deposited on silicon carbide substrates. The epitaxial deposition of boron phosphide on boron phosphide substrates was carried out by the thermal reduction of a boron tribromide-phosphorus trichloride mixture in hydrogen in a manner similar to deposition on silicon carbide. When transported boron phosphide crystals were used as substrates, they were first mechanically lapped and polished with alumina abrasives to yield two flat parallel faces. Solution grown platelets were most often used without surface preparation since one face of the solution grown crystals was usually very smooth. Major emphasis was given to the use of the solution grown crystals, since much larger crystals in larger quantity were available.

To carry out the epitaxial growth process, the boron phosphide substrates were positioned on a coated graphite susceptor in the reaction tube shown schematically in Fig. 2. A coating was necessary to minimize outgassing of impurities from the graphite. The best coating material was boron phosphide itself,

but this coating was always etched by the hydrogen chloride generated during the deposition. Consequently, the susceptor had to be recoated after each deposition. After evaluation of a variety of coatings, the following triple layer system was determined to be satisfactory: silicon carbide-silicon dioxide-silicon nitride.

Just before deposition, the substrates were briefly etched in-situ with phosphorus trichloride in hydrogen to remove a few micrometers of material. The vapor etch was done at 1075° C, which was also the deposition temperature. To start the deposition, boron tribromide was slowly introduced into the reactor. A key factor in the achievement of smooth featureless epitaxial layers is the very slow addition of boron tribromide over a five min period. Epitaxial boron phosphide on boron phosphide substrates can be deposited with growth rates from about 10 to 50 μm/hr. The best layers, which are smooth and featureless, were obtained with slow growth rates from 10 to 20 μm/hr. Typical deposition flow rates of hydrogen, boron tribromide, and phosphorus trichloride were 0.125, 1.44×10^{-4}, and 1.95×10^{-3} moles/min, respectively.

The electrical properties of the deposited layers were investigated, and intentional doping was used to control the properties of the layers. The conductivity type of the deposited boron phosphide was sensitive to the impurity content of the substrates, and this indicates that autodoping from the substrate occured, due most likely to the presence of hydrogen

chloride. For p-type and high resistivity n-type substrates, the deposited boron phosphide was p-type, as were layers deposited on silicon carbide. Intentional doping with hydrogen selenide could be used, therefore, to control the resistivity and to produce n-type layers. For heavily doped n-type substrates, which were often obtained from the solution growth process, only n-type layers could be grown unless certain preliminary steps were done. To produce p-type boron phosphide layers on n^+-substrates, the back of the substrates had to be covered either with a layer of deposited boron phosphide or silicon nitride. As a consequence, the resistivity control of boron phosphide layers on n^+-substrates was very difficult. Spreading resistance measurements on deposited boron phosphide layers indicated that the resistivity could be varied within a three order of magnitude range. The epitaxial growth techniques described here were used to prepare boron phosphide junction devices, and the results are discussed in Section II.D.

II.C. Device Fabrication Technology

To effectively utilize boron phosphide in devices, several techniques associated with the device fabrication were investigated. A new etching technique was developed, and the formation of ohmic contacts was achieved. Some new results in the area of dielectric film technology were also obtained.

II.C.1. Electrolytic Etching of Boron Phosphide[32]

Etching and polishing techniques are important processes for the study of semiconductors and for semiconductor device

fabrication. For elemental semiconductors and some of the compound semiconductors, convenient chemical etchants are available for surface preparation and for certain types of selective etching. In the case of boron phosphide, however, the only known etchants are fused alkalis near 400° C and hydrogen chloride near 1100° C. The former etchant attacks boron phosphide very nonuniformly, and for the latter etchant, the decomposition of material at 1100° C is a problem. As a consequence, electrolytic etching of boron phosphide was investigated during this program, and it was found to be the most useful etching technique for boron phosphide. Techniques were developed to polish and to selectively etch boron phosphide.

A schematic of the electrolytic cell used for the etching and polishing of boron phosphide is shown in Fig. 15. The current density-potential relationships were determined, and the crystal-electrolyte potential difference was measured relative to a calomel reference electrode. Measurements were made both in the dark and with illumination. The solution was continuously agitated by nitrogen bubbled into the electrolyte near the anode. A uniform removal of material without undercutting of etching masks was obtained with the boron phosphide platelets near the axis of a cylinderical molybdenum cathode, as shown in Fig. 15. A simple parallel plane electrode configuration was used for some of the basic measurements. The electrolytes investigated were aqueous solutions of common alkalis and acids, and a few chemical etchants previously used for other III-V semiconductors.

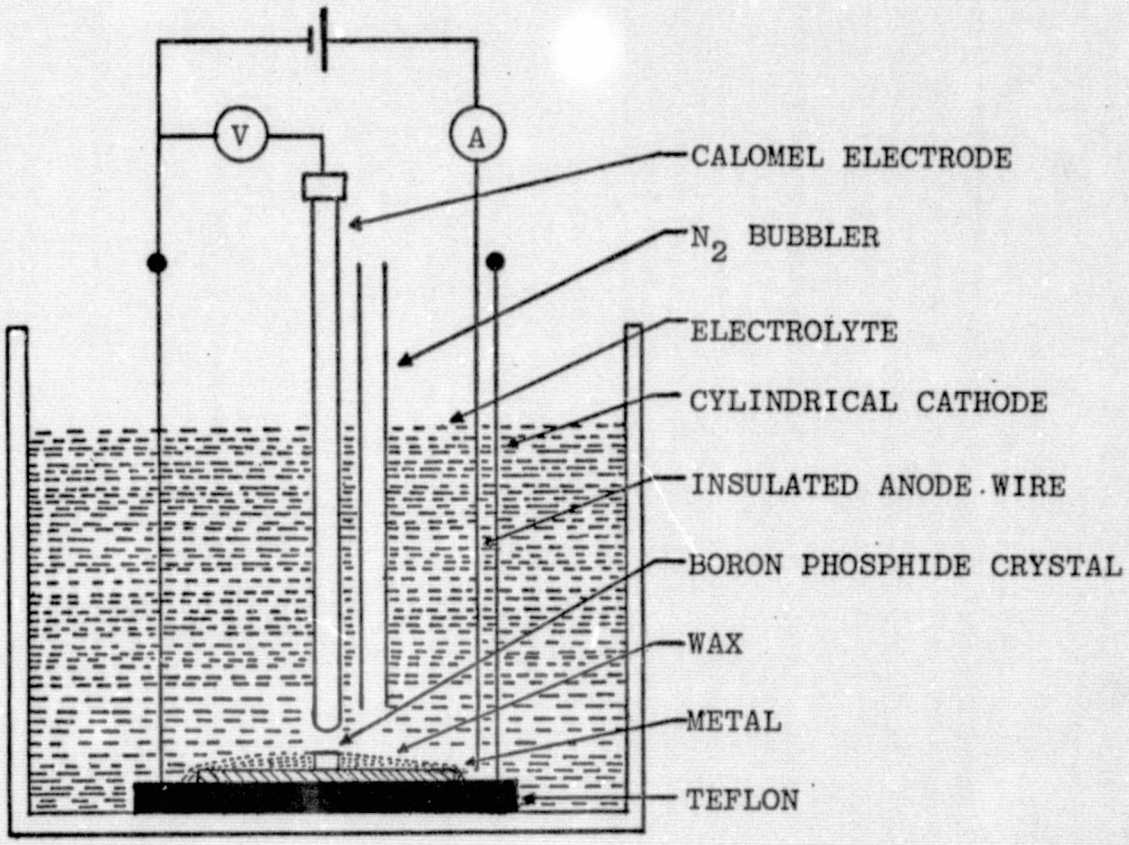

Fig. 15 Schematic of the electrolytic cell used for measurements and etching.

Prior to electrolytic etching, rough faces of the boron phosphide platelets were polished with 0.3 μm alumina abrasive, and as-grown smooth faces were etched without mechanical polishing. Ohmic contact to the back side of the boron phosphide crystals was made by electroless nickel plating, which is described in the next section. To control small area geometries for device fabrication, materials such as silicon dioxide and silicon monoxide were used to mask regions of the crystals.

Typical current density-potential relationships and rest potential values for p-type and n-type boron phosphide crystals in a 10% sodium hydroxide solution at room temperature in the dark are shown in Fig. 16. As expected, current saturation was observed in all of the experiments with n-type boron phosphide crystals. The p-type material was readily dissolved, and it drew much larger currents than n-type material. At low anode potentials, the $(\bar{1}\bar{1}\bar{1})$ face of both n-type and p-type boron phosphide drew larger current densities at a particular electrode potential than did the (111) face. At anode potentials higher than about 1 V, the difference between the currents drawn by the (111) faces and the $(\bar{1}\bar{1}\bar{1})$ faces is very small.

The rest potentials of n-type and p-type boron phosphide were measured in a number of electrolytes in addition to sodium hydroxide, and the rest potential for n-type crystals was always more negative than the rest potential for p-type crystals. A similar relationship was reported for gallium phosphide rest potentials.[33] For both n-type and p-type boron phosphide, the

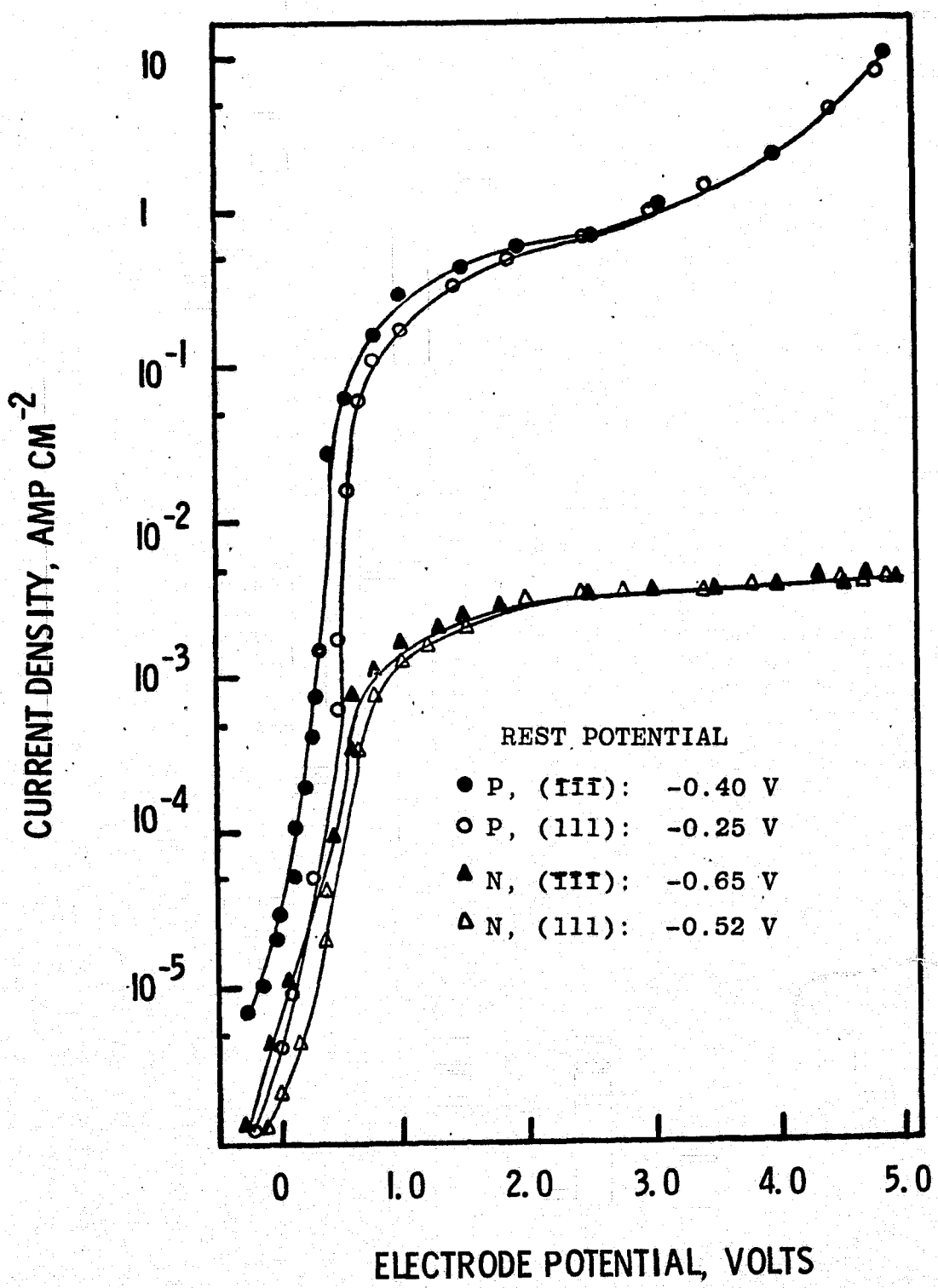

Fig.16 Current density vs. electrode potential for (111) and ($\bar{1}\bar{1}\bar{1}$) faces of n-type and p-type boron phoshide in a 10% NaOH solution in the dark.

rest potential was more positive for the (111) face. This polarity effect has also been observed for a number of other III-V compound semiconductors, and the group III element face was reported to have a more positive rest potential.[33,34,35] This observation agrees, therefore, with the tentative assignment, discussed in Section II.A.2.e., of the smooth face of the crystals to the boron face.

The following observations were made specifically from the etching of p-type boron phosphide. Twin lines and other gross crystallographic defects were revealed with current densities of 0.01 A/cm^2 or lower. For current densities between 0.01 A/cm^2 and about 0.2 A/cm^2, etch pits formed on the faces. At larger current densities, above about 0.5 A/cm^2, the (111) and ($\bar{1}\bar{1}\bar{1}$) faces had different etching characteristics. On the (111) face, a film tended to form; this film was, however, easily removed. The texture of the etched (111) face was rough as shown in Fig. 17A. On the ($\bar{1}\bar{1}\bar{1}$) face, however, there was no evidence of film formation, and a smooth, mirror-like surface shown in Fig. 17B was produced. These observations are very similar to the results reported for gallium phosphide;[32] at high current densities, the gallium face developed a rough texture and the phosphorus face became smooth. A few experiments were also carried out with other electrolytes, and the etching characteristics of p-type boron phosphide in potassium hydroxide solutions and common acids were found to be similar to the

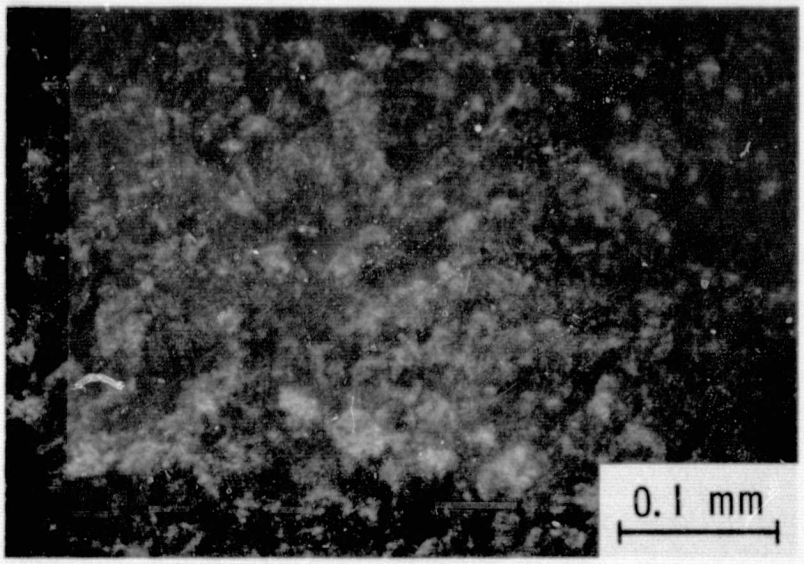

(A)

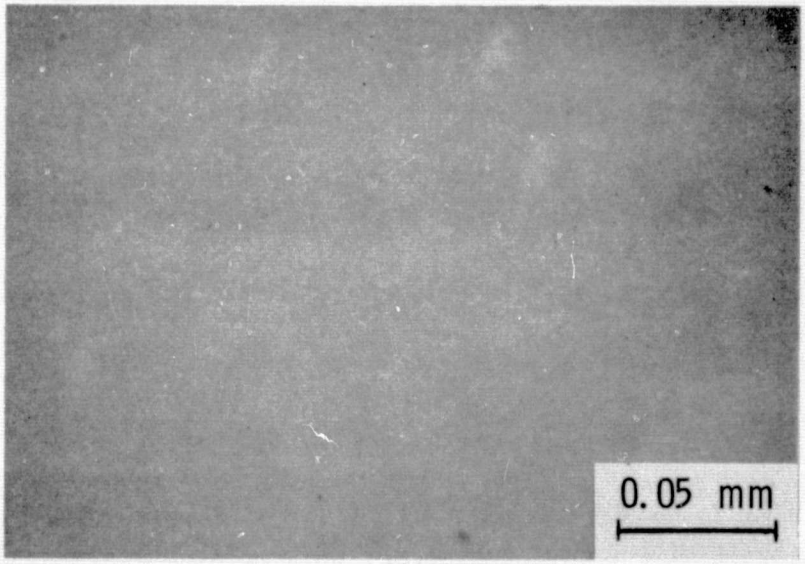

(B)

Fig. 17 Electrolytically etched surfaces of p-type boron phosphide with a current density of 0.5 A/cm^2.

(A): (111) face, (B): ($\bar{1}\bar{1}\bar{1}$) face.

characteristics obtained with the use of sodium hydroxide solutions.

In contrast to the etching of p-type boron phosphide, the etching of n-type boron phosphide was complicated by the formation of surface films at current densities higher than about 10^{-3} A/cm^2. At this current density, a film was visibly observed with a 15 min. etching period; with higher current densities, the film grew faster. The film could not be completely removed from the surface of the crystal even with ultrasonic agitation during etching, and the film was not soluble in hot alkali mixtures. X-ray measurements indicated that the films were predominantly boron phosphate (BPO_4).

With current densities above 1 A/cm^2 through n-type boron phosphide, a porous, brittle, fiber-like film formed on the surface. Reflection electron diffraction examination showed that these films were monocrystalline boron phosphide of (111) orientation. It was concluded, therefore, that anodic disintegration of n-type boron phosphide at high current densities occurred preferentially in <111> directions, and a surface layer which is a skeleton of the original crystal remained. Similar results were obtained from an etching study of gallium arsenide.

Various approaches were investigated to improve the etching characteristics of n-type boron phosphide. A variety of electrolytes in addition to sodium hydroxide were used without success; an insoluable film formed in all cases. The effect

of illumination on the etching of n-type boron phosphide was also investigated. A 650 watt incandescent lamp with a color temperature of 3400° K was used as the light source, so that a significant portion of the lamp output had an energy greater than the band gap of boron phosphide. A negative shift of about 0.2 V or more of the rest potentials was observed with illumination, but very little difference in the cell currents was found. Consequently, the anodic dissolution behavior was not significantly affected by the illumination. N-type boron phosphide was successfully etched without film formation only under one condition: the n-type material exposed to the electrolyte was one side of a shallow, forward biased p-n junction. This observation supports the well-known fact that a supply of holes is required for electrolytic etching.

It can be seen from Fig. 16 that the current density at, for example, 3 volts is about 300 times higher for p-type boron phosphide than for n-type material. This current density ratio corresponds approximately to the etch rate ratio between p-type and n-type boron phosphide, and suggests the possibility of selective removal of p-type material from boron phosphide p-n structures. The preferential etching of p-type material was initially investigated with a number of solution grown boron phosphide crystals with built-in p-n junctions on a crystal face. Selective removal of p-type boron phosphide was obtained with current densities between 0.1 A/cm^2 and 10 A/cm^2. To prevent the formation of a surface film on the n-type regions,

either very low current densities with a long etching time or very high currents for a very short time were used. Figure 18 shows one solution grown crystal which was selectively etched; the p-type region developed a mirror-like finish, and no removal of n-type material was observed. With low current densities and short etching times, electrolytic etching was also used to delineate thin epitaxially grown p-n junctions in boron phosphide.

Since electrolytic etching is selective, it can be used to produce mesa junction structures in boron phosphide. Mesa diodes were formed with both homoepitaxially and heteroepitaxially grown junctions. P-type layers of boron phosphide on n-type solution grown boron phosphide crystals and both n-type and p-type boron phosphide layers on hexagonal silicon carbide platelets were grown by the thermal reduction of a boron tribromide-phosphorus trichloride mixture. To isolate the mesas, either silicon dioxide or silicon monoxide was used to define the mesa pattern, and the exposed boron phosphide was electrolytically removed. In the preparation of the boron phosphide-silicon carbide heterojunctions, a sharp decrease in the current indicated the complete removal of the boron phosphide layer exposed to the electrolyte. At that stage, the electrolyte was replaced by a 1 N solution of hydrofluoric acid, and a slight anodic etching of the silicon carbide was carried out. This latter step improved the characteristics of the mesa junctions. The removal of n-type boron phosphide on silicon carbide required mechanical means to occasionally remove

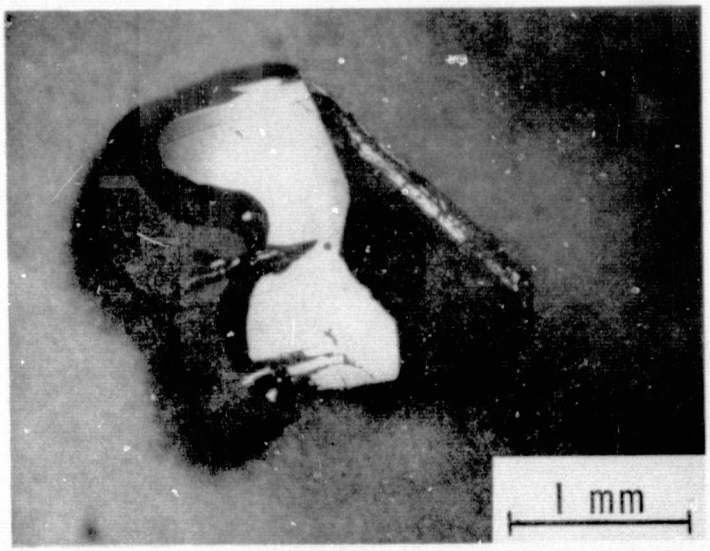

(A)

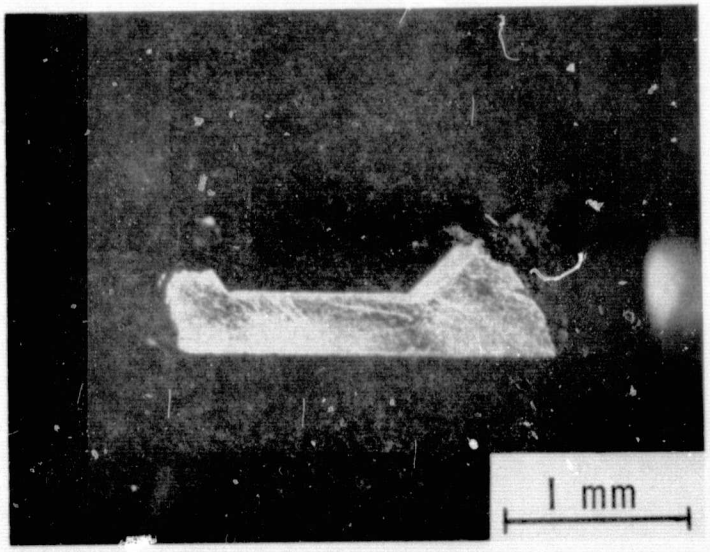

(B)

Fig. 18 Photomicrographs of an electrolytically etched boron phosphide crystal which has both n-type and p-type regions. Etching was done with 10 A/cm^2 for 10 sec.

(A): top view, (B): cross sectional view.

a surface film near the edge of the mesa. Figure 19 shows photomicrographs of two mesa junctions fabricated by anodic dissolution of boron phosphide. Figure 19A shows a homojunction made by selective removal of a portion of a p-type epitaxial layer on an n-type substrate, and Fig. 19B shows an n-type boron phosphide mesa on p-type silicon carbide. These devices have rectifying characteristics, and easily visible, red, p-n junction electroluminescence, discussed in Section II.D.4., was observed.

II.C.2. Diffusion into Boron Phosphide

During this program, a brief investigation was made to determine if impurities could be diffused into boron phosphide. Experiments were done in sealed tubes with added phosphorus at temperatures up to 1250° C. Prior to the diffusion experiments, the spreading resistance and type of the crystals were measured. The elements used for the diffusion experiments were germanium, silicon, and zinc. No change in the electrical properties of the surface of boron phosphide crystals was ever found. This indicates that successful diffusion into boron phosphide would require much higher temperatures.

II.C.3. Ohmic Contacts to Boron Phosphide

The formation of low resistance ohmic contacts is an essential technique in the development of devices from new semiconductor materials. Theoretically, it is advantageous (1) to use contacting materials of high work function on p-type and of low work function on n-type semiconductors, and (2) to create a region of high carrier concentration under the contact through

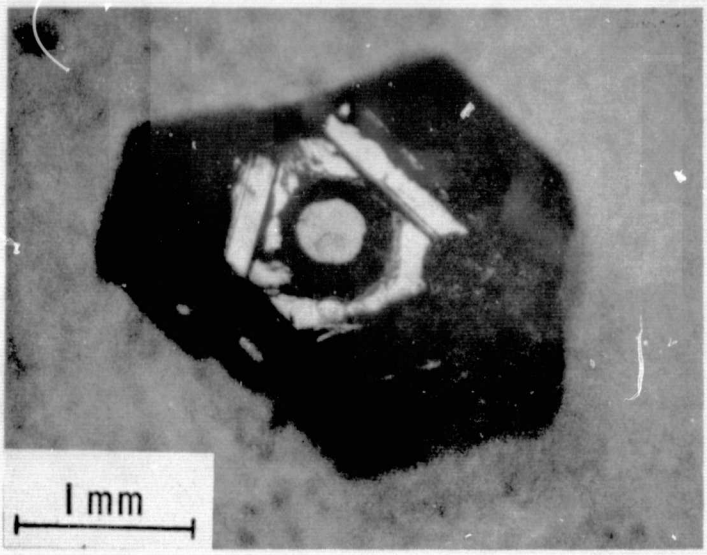

(A)

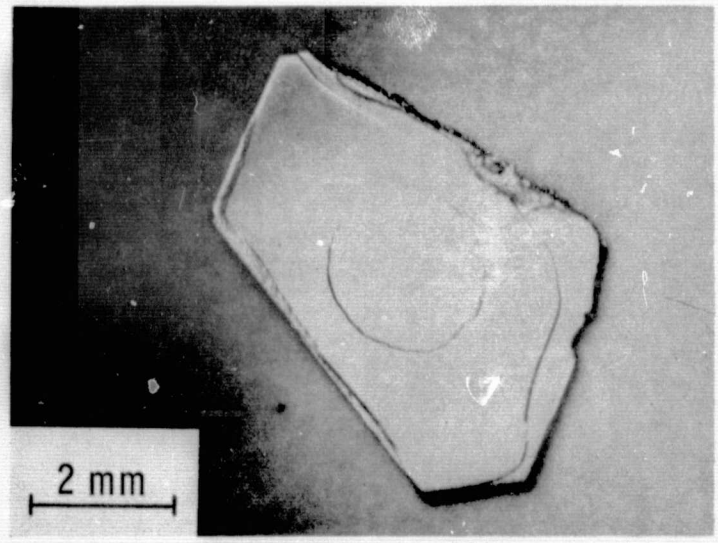

(B)

Fig. 19 Two mesa structures fabricated by electrolytic etching: (A) boron phosphide p-n homojunction and (B) boron phosphide-silicon carbide heterojunction.

alloying or in-diffusion of a suitable dopant provided by the contacting material. In practice, it is difficult to satisfy these conditions. For example, at temperatures high enough to affect alloying or impurity in-diffusion, boron phosphide decomposes. In this work, a number of materials were investigated under various heat treatment conditions to yield low resistance ohmic contacts to boron phosphide. The results are summarized in Table I. The carrier concentraions in boron phosphide crystals was approximately 10^{18} cm^{-3}. All the metals or their alloys were deposited on boron phosphide by evaporation under a pressure of 10^{-6} Torr or lower with the exception of nickel. The electroless plating was used for the deposition of nickel, and indium was also applied by soldering in addition to evaporation. Annealing was carried out in a hydrogen atmosphere from 600° to 850° C for 5 min to 1 hr. though occasionally the annealing was carried out at 950° C for a few minutes. The current-voltage characteristics of these contacts were then determined on a curve tracer.

For n-type solution grown crystals, aluminum and indium contacts remained non-ohmic even after annealing up to 750° C for 1 hr. Electroless nickel was found to form low resistance, ohmic contacts to all but lightly doped n-type boron phosphide crystals. The plating was carried out at 90° to 100° C using Nicklex (Transene Company, Inc., Danvers, Mass.) plating solution. Lapping of boron phosphide crystals with 600 grit silicon carbide abrasive facilitated the plating process and improved the adhesion of nickel deposit to the crystal. The electroless

Table I

Contact Resistance of Different Materials to Boron Phosphide

Conductivity Type of BP	Contact Material	Contact Resistance (ohm-cm^2) After Heat Treatment				
		As Deposited	600°C	750°C	850°C	950°C
N	Al	N-O	N-O	N-O	--	--
N	In	N-O	N-O	--	--	--
N	Ag	N-O	N-O	N-O	N-O	N-O
N	Ag-Ge	N-O	N-O	N-O	N-O	--
N	Ag-Sn	N-O	N-O	N-O	N-O	--
N	Ag-Si	N-O	N-O	N-O	N-O	--
N	Au	N-O	--	--	Ohmic	--
N	Au-Si(1-5%)	N-O	--	--	$\sim 10^{-2}$	--
N	Au-Sn	N-O	--	--	$\sim 10^{-2}$	--
N	Au-Ge-Ni	N-O	--	--	--	--
N	Au-Ge	N-O	--	--	Ohmic	--
N	Electroless Ni	N-O	--	--	$\sim 10^{-2}$	--
P	Au-Be(1%)	N-O	--	--	$\sim 10^{-2}$	--
P	In	N-O	--	--	Ohmic	--
P	Al	N-O	--	--	Ohmic	--

N-O = Non-ohmic

plating of lightly doped boron phosphide with nickel was very difficult and was facilitated considerably by rinsing boron phosphide platlets in palladium chloride solution, deionized water, stannous chloride solution, and deionized water successively before plating. Annealing temperatures of 850° to 900° C produced ohmic contacts of specific contact resistance on the order of 10^{-2} ohm-cm^2.

In the fabrication of small area devices, evaporated contacts are preferred, and gold, silver, and a number of their alloys were investigated. Gold-germanium-nickel and gold-silicon have produced low resistance ohmic contacts to n-type boron phosphide, and gold-beryllium has formed low resistance ohmic contacts to p-type material. On heavily doped boron phosphide crystals, evaporated gold contacts were found to be ohmic after annealing in all cases.

II.C.4. Dielectric Film Technology

The production of dielectric films is a key process in silicon technology. For this reason, the suitability of boron phosphide and boron arsenide to function as dielectric films on silicon was investigated during this program. Because of their energy gaps, the intrinsic resistivity of boron phosphide and boron arsenide should be high. One other material, aluminum nitride, was also studied.

As discussed in Section II.B.1., smooth adherent films of boron arsenide could be deposited on (111) silicon substrates. Since the films were amorphous, they were investigated as

dielectrics in metal-boron arsenide-silicon structures. Devices were made by vacuum evaporation of small diameter aluminum or gold electrodes onto the boron arsenide. Individual samples were mounted in sealed headers so that characteristics could be measured.

To study the electrical conduction mechanisms in boron arsenide, the current-voltage characteristics of metal-boron arsenide-silicon structures were measured over a wide temperature range. Typical results are shown in Fig. 20, where the current-voltage relations are plotted on logarithmic scales. In general, at low bias levels, the slope is unity, which describes an ohmic region. As the bias is increased, the slope of the log I versus log V plot increases to two, and with higher bias, larger values of the slope occur. At low bias levels, the room temperature resistivity of amorphous boron arsenide is approximately 10^6 ohm-cm. The ohmic behavior at low bias levels could be due to electronic conduction, which typically has activation energies less than 1 eV, or to ionic conduction, which has activation energies of several electron volts. Figure 21 shows a plot of the logarithm of the conductance versus the reciprocal temperature taken from Fig. 20 at 0.1 volt. The slope of this plot yields an activation energy of 0.26 eV indicating that electronic conduction prevails. The region with a slope of two in the log I versus log V plot corresponds to space-charge-limited current. The higher slope region represents trap filled limited conduction, which occurs

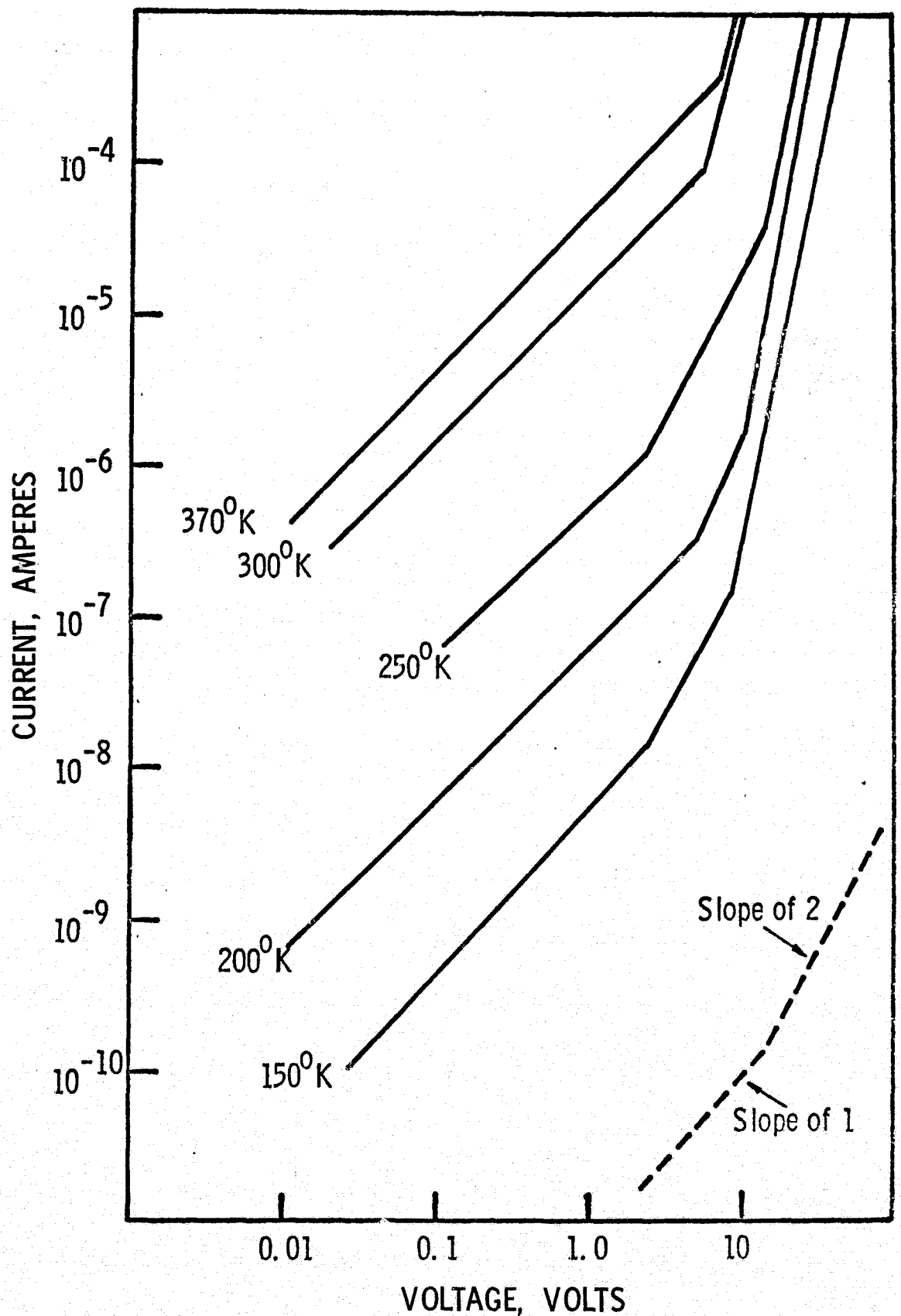

Fig. 20 Typical current-voltage characteristics of an aluminum-boron arsenide-silicon structure with a boron arsenide film of 1 μm thickness.

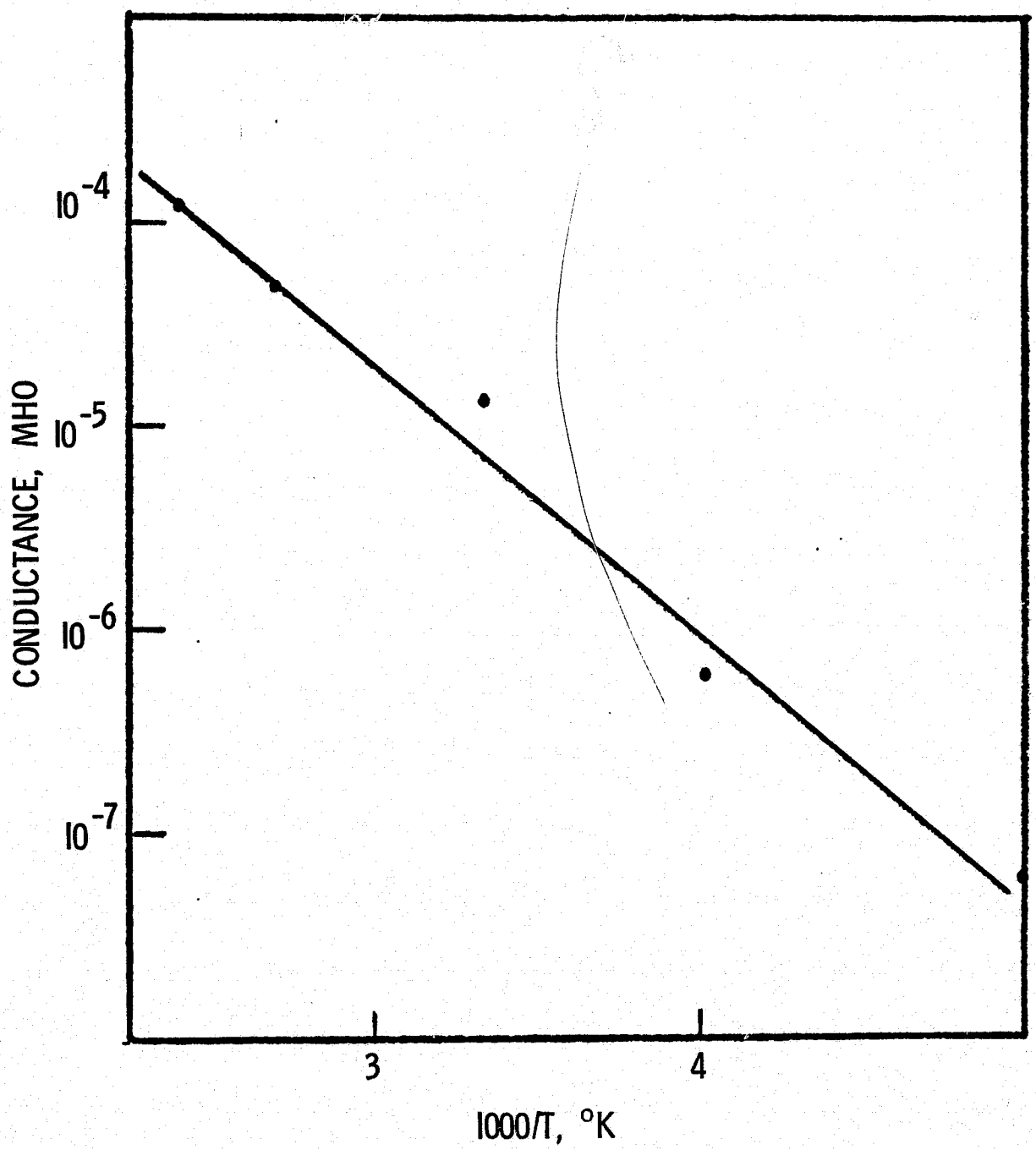

Fig. 21 Conductance at 0.1 V versus reciprocal temperature from Fig. 20 for a boron arsenide layer.

when all of the traps in a dielectric are filled by injected carriers.[36] Since the traps cannot accomodate additional charge, a sharp increase in current occurs. To further characterize the metal-boron arsenide-silicon structures, attempts were made to measure capacitance-voltage characteristics. However, the relatively large conductance of the boron arsenide resulted in large leakage currents, and reproducible data were not obtained.

Boron phosphide was also investigated as a dielectric in aluminum-boron phosphide-silicon devices. Amorphorus boron phosphide was deposited on (111) oriented silicon by the hydride decomposition reaction (10). Current-voltage characteristics similar to those obtained from the metal-boron arsenide-silicon structures were obtained from the aluminum-boron phosphide-silicon structures. As expected from the relative values of the band gaps, the conductance of the boron phosphide devices was lower, by one to two orders of magnitude, than the boron arsenide devices.

One other material, aluminum nitride, was characterized as a dielectric material on silicon during this program.[37] The pyrolysis of an aluminum trichloride-ammonia complex, $A\ell Cl_3 \cdot 3NH_3$, was used to deposit very fine grain, uniform, highly adherent aluminum nitride layers on (111) oriented silicon substrates. The crystal structure of the layers was determined basically by the deposition temperature, and grain sizes, which were measured by transmission electron microscopy to be 100 Å to 2200 Å. The

layers had a density very close to the reported bulk density for aluminum nitride. The Becke line method was used to measure the refractive index of the deposited layers, and a value 1.991 ± 0.003 was found. The dielectric constant of the layers was somewhat dependent upon the deposition temperature; for deposition temperatures from 800° C to 1000° C; the dielectric constant was 11.5 ± 0.2, and for a 1100° C deposition, the value was 8.1 ± 0.3. The as-deposited dielectric constant was not affected by later high temperature heating to 1100° C, which indicates the stability of the aluminum nitride layers. The layers were also found to be effective diffusion masks for boron and phosphorus diffusions, and the layers can be etched to produce patterns with standard photolithographic techniques. These properties indicate that aluminum nitride has potential as a dielectric in solid state devices.

II.D. Boron Phosphide Device Fabrication

The ultimate goal of this program was the fabrication and evaluation of devices. Since it was concluded that a useful supply of boron arsenide material was not easily obtainable, major emphasis was given to device fabrication from boron phosphide. The larger energy gap of boron phosphide also indicates that it would be a more useful material than boron arsenide. Four types of boron phosphide devices were made during this program: metal-insulator-semiconductor structures, heterojunctions with silicon carbide, Schottky barriers, and p-n homojunctions. The characteristics, including electroluminescent emission, of these devices

are discussed below.

II.D.1. Metal-Insulator-Semiconductor Structures

Because of the importance of metal-insulator-semiconductor (MIS) devices, work was done to evaluate the use of boron phosphide as the semiconductor in MIS structures. Devices were made both on solution grown crystals and on epitaxial layers of boron phosphide.

The nature of the insulator-semiconductor interface often determines the characteristics of MIS devices. For this reason, a number of techniques were evaluated to prepare the insulating layer on boron phosphide. The oxidation and nitrification of boron phosphide were investigated. Boron phosphide was found to be readily oxidized in an oxygen atmosphere at 800° C or higher. However, the resulting product, which was a mixture of boron phosphate (BPO_4) and boron oxide (B_2O_3), was not adherent to the boron phosphide substrate. Oxidation at lower temperatures produced boron phosphate films with pinholes. The nitrification of boron phosphide was investigated by heating the crystals in ammonia for several hours. At temperature below 925° C, no appreciable reaction was observed. As the temperature was increased to about 1000° C, a discontinuous film of boron nitride was produced. Since neither film produced by the oxidation or nitrification technique appeared to be suitable as a dielectric on boron phosphide, deposited layers of silicon dioxide and silicon nitride were investigated.

Silicon nitride and silicon nitride-silicon dioxide double layers were used as dielectrics in the fabrication of boron phosphide MIS structures. The oxide and nitride were deposited by the oxidation and ammonolysis of silane, respectively. A number of experiments were carried out to determine the conditions and the rate of deposition of silicon dioxide and silicon nitride on boron phosphide. For silicon dioxide, a deposition temperature of 550° C was found to be convenient, and the deposition rate was 360 Å/min. For silicon nitride, a deposition temperature of 850° C was used, and the deposition rate was 190 Å/min. The silicon dioxide and silicon nitride films were transparent and were adherent to boron phosphide. When observed through the high power metallurgical microscope, the films showed no pinholes. The electrical resistivity of a typical 1500 Å thick silicon nitride film was on the order of 10^{10} ohm-cm and the dielectric strength was about 10^{6} v/cm.

Several approaches were investigated for the fabrication of boron phosphide MIS structures. In one approach, silicon nitride films from 1000 to 2000 Å in thickness were deposited on a mechanically polished face of either n-type solution grown crystals or homoepitaxial boron phosphide. After the deposition of silicon nitride, the back of the boron phosphide substrate was lapped to remove unwanted silicon nitride. An ohmic contact was made on the back of the boron phosphide. Aluminum gate

electrodes of 0.25 mm diameter were then deposited onto the silicon nitride by vacuum evaporation to complete the fabrication process.

The MIS devices were evaluated from their capacitance-voltage characteristics measured with a Boonton 75 C bridge. These measurements were made under a dc bias upon which was superimposed a small ac signal with a frequency of 0.4MHz. Typical characteristics of an MIS structure with n-type boron phosphide are shown in Fig. 22. The positive flat-band voltage indicates the existence of a negative charge in the silicon nitride near the silicon nitride-boron phosphide interface. Because of the negative charge in the nitride, an inversion layer is formed at the entire n-type boron phosphide surface for a positive gate voltage. Since the insulating layer extends over an area greater than the metal electrode, the inversion layer consists of two parts: an intrinsic portion directly beneath the metal region and an extrinsic portion in the area covered only by the insulator. The two parts are coupled to form a distributive R-C network, which consists of the lateral resistance of the inversion region and the depletion capacitance. The distribtued R-C network beyond the gate can be considered a low pass filter, and because of the high charge density in the insulator, this extrinsic portion of the inversion layer will dominate the device characteristic. Therefore, as frequency increases, the ac propagates a shorter distance away from the

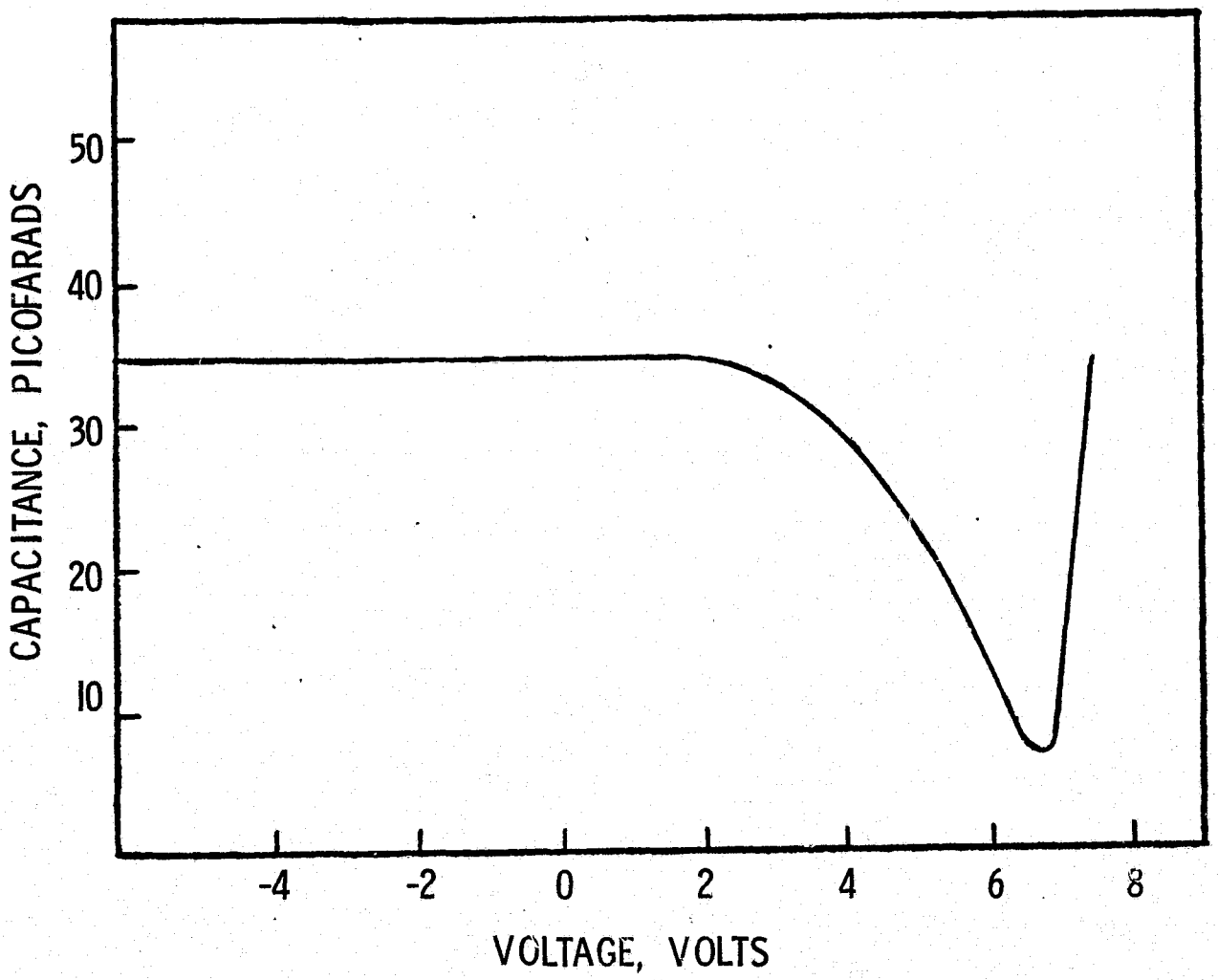

Fig. 22 Capacitance-voltage relation of an aluminum-silicon nitride-boron phosphide structure at 400 kHz.

gate before dying out. Both the external conductance and external capacitance will then be smaller, and measured capacitance will become bias independent at a value less than insulator capacitance. At high enough frequency, depending upon lateral resistance and boron phosphide resistivity, hardly any ac propagates into the distributed network. At this cut off frequency, the overall capacitance of the insulator is in series with the depletion capacitance for all values of bias at which the boron phosphide under the gate is inverted. As a consequence of these effects due to the high charge density near the insulator-semiconductor interface, the capacitance-voltage characteristics of these devices appears to be a low frequency characteristic.

To minimize the impurity concentration at the silicon nitride-boron phosphide interface, another fabrication procedure, which involved the sequential deposition of the semiconductor and the insulator in the same reaction tube, was investigated. Devices were made by the deposition of a high resistivity n-type epitaxial boron phosphide layer onto a boron phosphide substrate followed immediately by the deposition of a 2000 Å thick silicon nitride layer. Vacuum evaporation was again used to deposit 0.25 mm diameter aluminum gate electrodes. The capacitance-voltage relationship of a typical boron phosphide MIS structure made as just described is shown in Fig. 23. Although some charge is still present near the silicon nitride-boron phosphide interface, the quantity of the charge has been

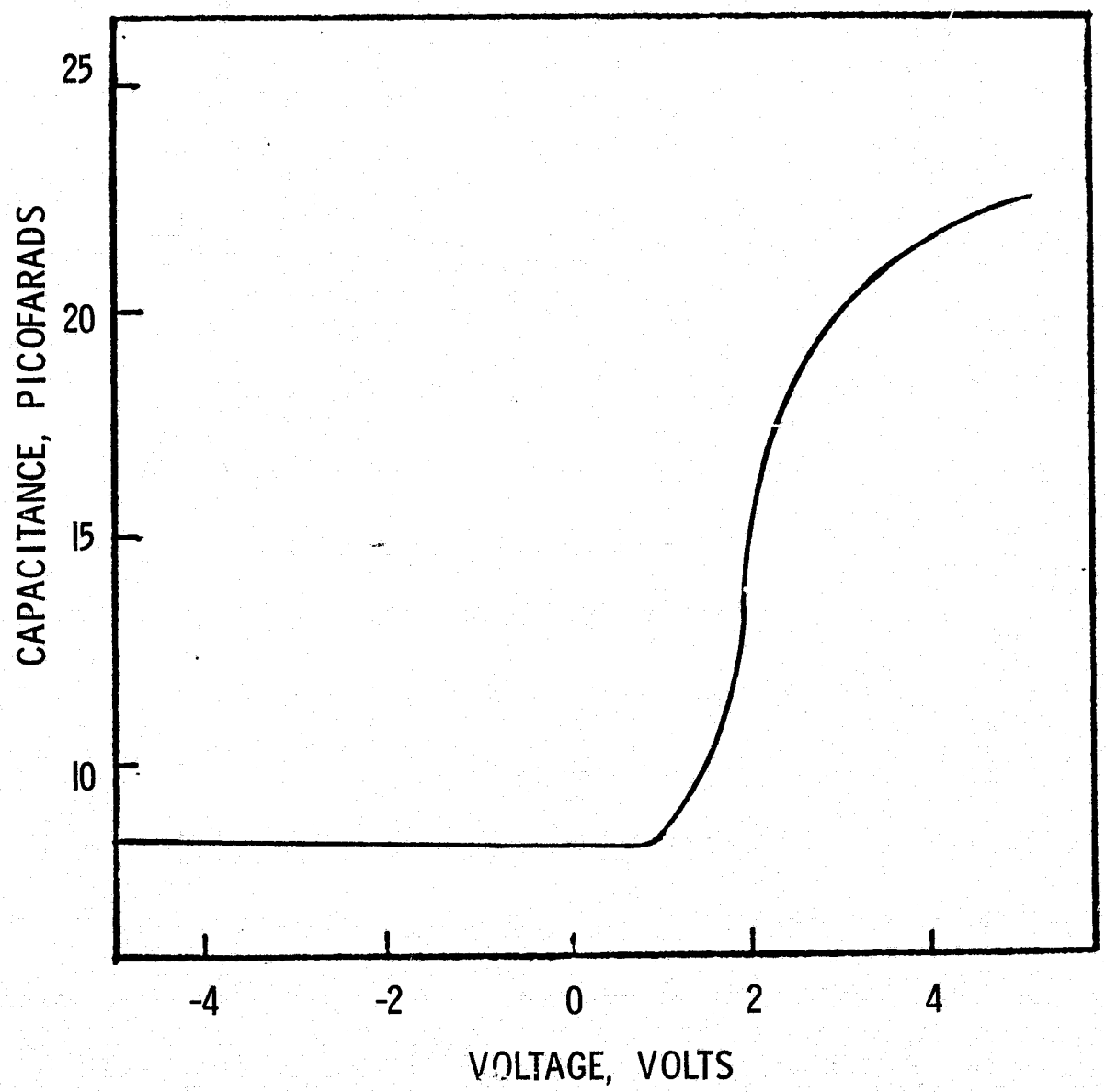

Fig. 23 Capacitance-voltage relation of an aluminum-silicon nitride-boron phosphide structure at 400 KHz.

reduced compared with the device whose characteristics are given in Fig. 22. The characteristic of Fig. 23 is typical of high frequency MIS device behavior. Similar device characteristics were obtained with the use of a silicon dioxide-silicon nitride double layer insulator in boron phosphide MIS devices.

II.D.2. Schottky Barrier Devices

The fabrication of boron phosphide Schottky barrier diodes requires the formation of ohmic and Schottky contacts on the opposite faces of a boron monophosphide crystal or platelet. The use of gold and aluminum as Schottky contacts were investigated. The resulting diodes were characterized by current-voltage and capacitance-voltage measurements.

The ohmic contact was first made to the back face of a boron phosphide platelet using the technique described in Section II.C.3. The platelet was thoroughly cleaned and heated in the vacuum evaporator to remove the adsorbed water vapor. The Schottky contacts in the form of 0.01" diameter dots were evaporated to the front face of the platelet at 120-130° C through a metal mask.

Capacitance-voltage measurements on Schottky diodes were made with a Boonton Model 75 C bridge, and the capacitance was measured as a function of bias voltage. The current-voltage measurements were made using a regulated power supply, a digital voltmeter, and an electrometer.

Figure 24 shows the capacitance-voltage relation of an aluminum Schottky contact on an n-type solution grown boron phosphide crystal. A relative straight line was obtained from the $\frac{1}{C^2}$ versus V plot, and the intercept at the voltage axis indicated that the diffusion potential is about 0.75 V. The dopant concentration calculated from the slope of the plot was about 9.4×10^{17} cm^{-3}. The current-voltage characteristics of a gold Schottky contact on an n-type solution grown boron phosphide crystal is shown in Fig. 25. The parameter "n" in the diode equation calculated from the slope of this plot is approximately 3.4. At voltages higher than about 0.8 V, the series resistance of the device dominates. The relative large "n" value is due presumably to the presence of an interfacial layer. The reverse breakdown voltage of most diodes was about ten volts. In general, the current-voltage characteristics appear to be dominated by surface leakage, and efficient passivation is necessary for meaningful results.

II.D.3. Silicon Carbide-Boron Phosphide Heterojunctions

The fabrication and characterization of silicon carbide-boron phosphide heterojunctions are discussed in this section. Junctions between semiconductors with different energy gaps have a number of potential applications, such as majority carrier rectifier, high speed band-pass photodetector, and other photovoltaic devices. Many of these applications utilize the fact that the larger energy gap semiconductor in a heterojunction is transparent to radiation which is generated or

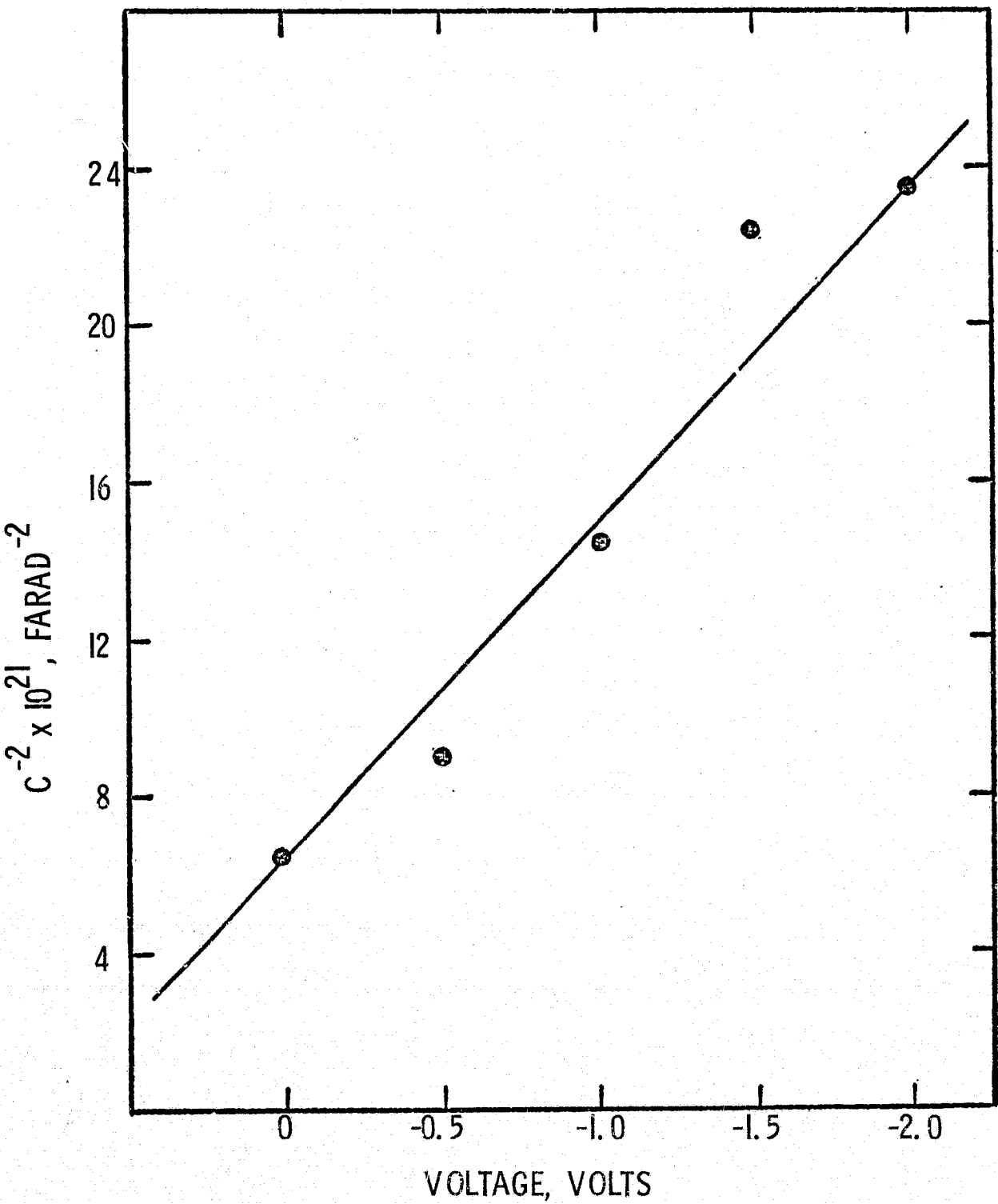

Fig. 24 Capacitance-voltage characteristics of an Aℓ-(n) BP Schottky diode.

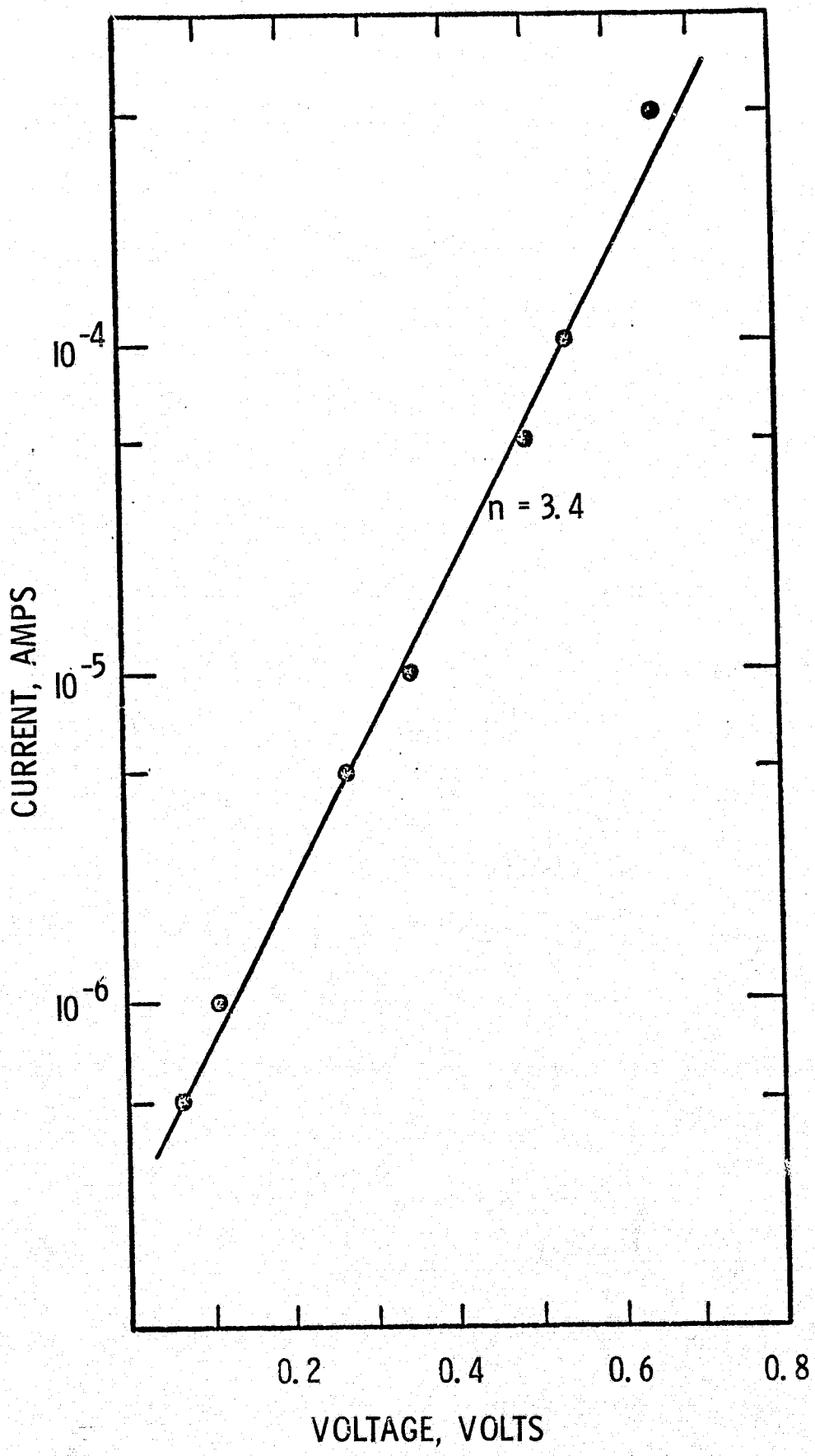

Fig. 25 Current-voltage characteristics of a Au-(n) BP Schottky diode.

absorbed in the other material. In practice, heterojunction devices suffer from one major limitation: a high density of states within the band gap at the junction interface. These interface states can act as trapping centers, and they severely limit the realization of the promise of heterojunction devices. These interface states are due, in large part, to the lattice parameter and thermal expansion coefficient mismatch between the two materials of the device. Both types of mismatch will produce a strained lattice and dislocations. In addition, interface states can result from impurity incorporation during the fabrication process.

The fabrication of the silicon carbide-boron phosphide heterojunctions was based upon the epitaxial deposition process discussed in Section II.B.2. P-type boron phosphide layers were grown on the n-type silicon carbide to form the heterojunction. After removal of the deposit on the back of the substrate, ohmic contacts were made to both sides of the junction by sequential plating of palladium and nickel. Contact resistance was reduced by an anneal near 850° C for 1 hour in a hydrogen or argon atmosphere. Mesa-type junctions were then made by the electrolytic etching technique discussed in Section II.C.1.

Current-voltage characteristics of the heterojunctions were measured. Preliminary data were taken from the characteristic on a diode curve tracer. Diodes with poor reverse characteristics were often improved by additional electrolytic

etching. When additional etching did not improve the diode reverse characteristics, the diode was transferred to a probe station for point by point measurements. Figures 26 and 27 show, respectively, the forward and reverse current-voltage characteristics of a (n) silicon carbide-(p) boron phosphide junction. The forward current is proportional to exp(qV/nkT) with n = 1.9. At voltages higher than 0.7 V, the series resistance of the device limited the forward current. The reverse current increases exponentially with voltage up to -4 V. Below -4 V, the current increases slowly with voltage. These characteristics are to be expected according to the model of a heterojunction proposed by Dolega.[38] In this model, the presence of a thin layer with an extremely small carrier life time at the interface between the two semiconductors is considered to be typical of p-n heterojunctions. In practice, therefore, the p-n heterojunction may behave more like two metal-semiconductor contacts in series. If the impurity concentrations in the two sides of the junction are widely different, practically all of the voltage drop occurs on the side with the lower impurity concentration. This corresponds to a single Schottky barrier, and the value of n should be one. If the impurity concentrations on the two sides are comparable, a voltage drop occurs on both sides of the junction, and in theory n should be two. Another feature of the Dolega model is the prediction of an exponential increase followed by a

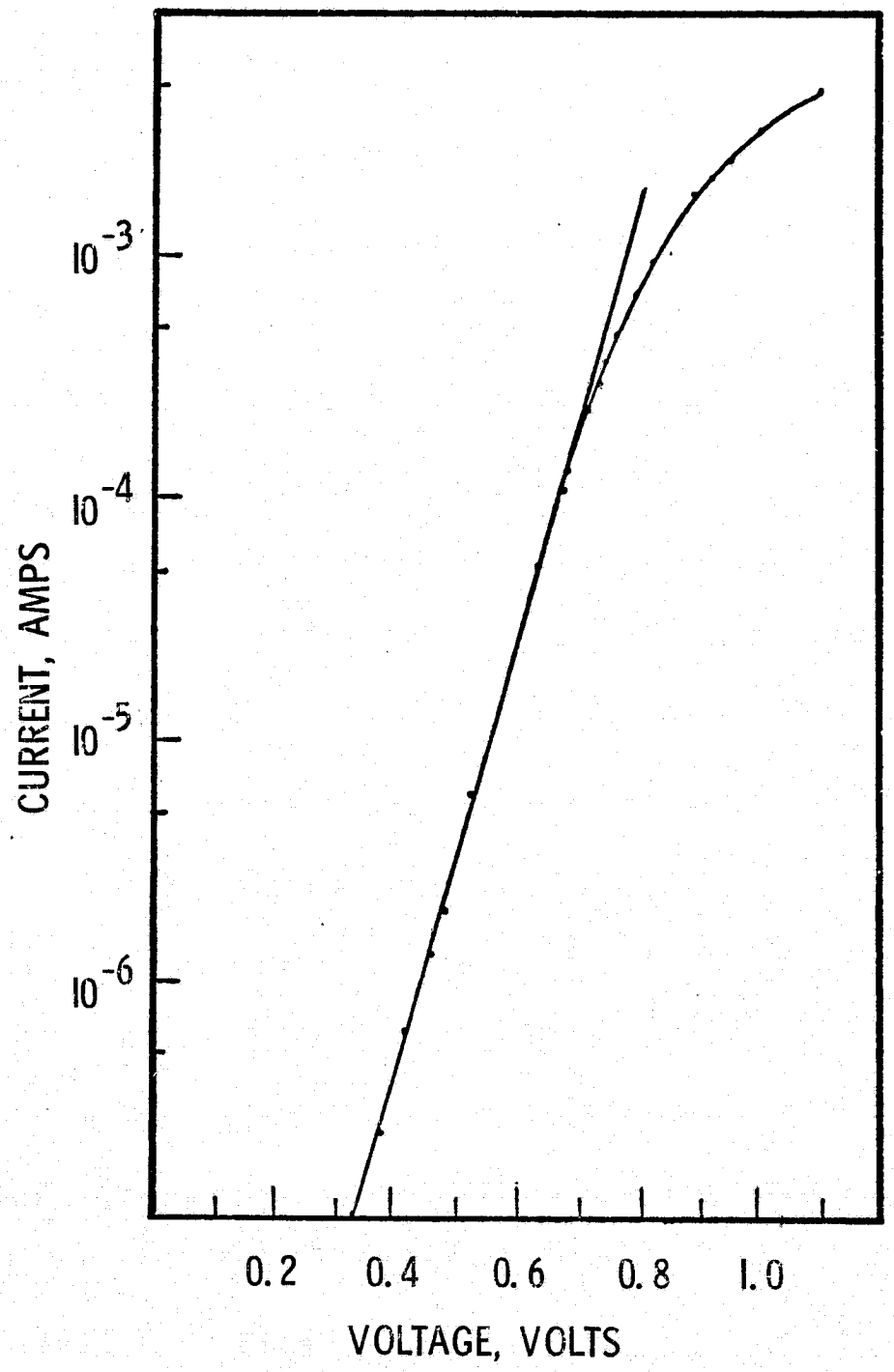

Fig. 26 Forward characteristics of a (n) silicon carbide-(p) boron phosphide heterojunction.

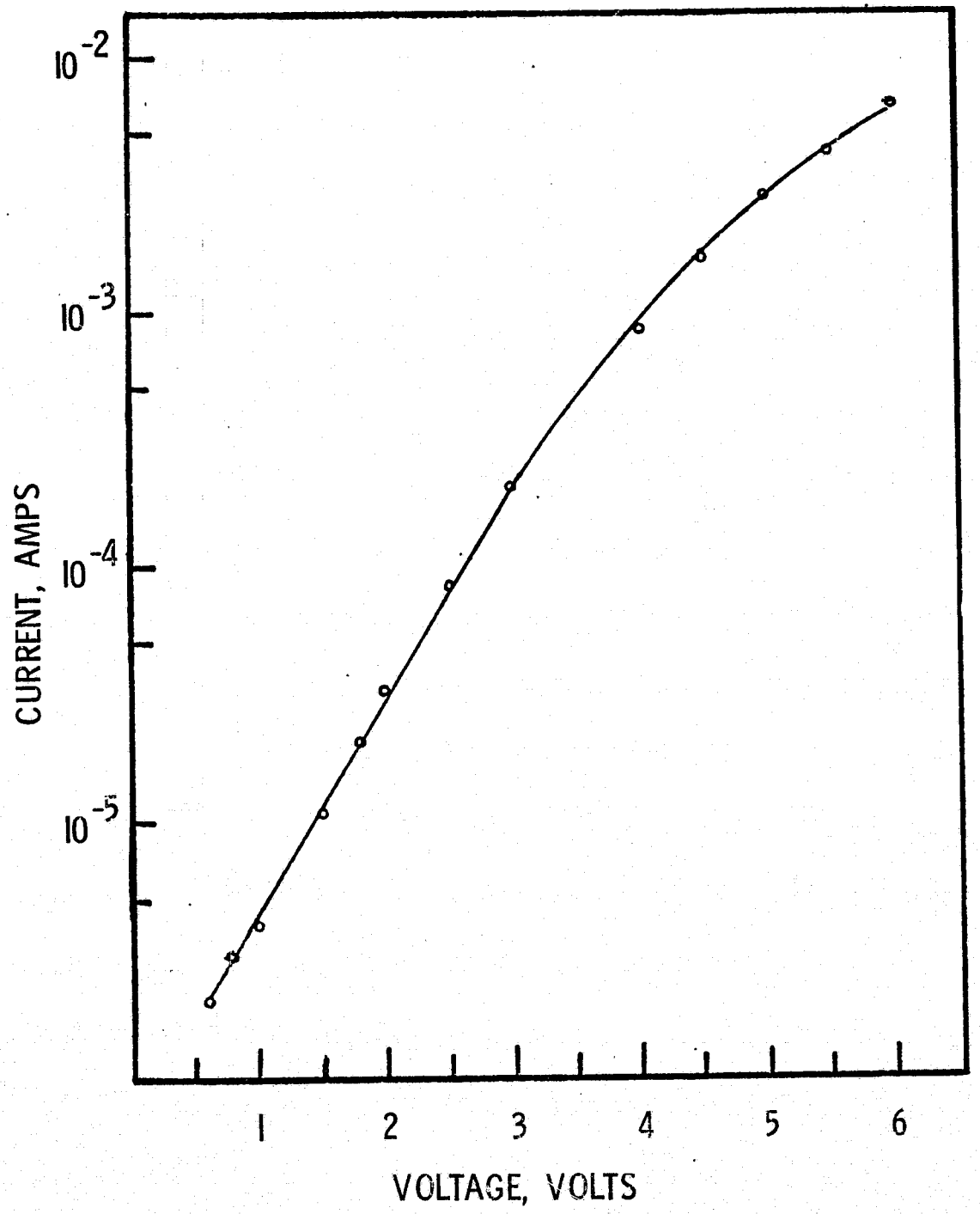

Fig. 27 Reverse characteristics of a (n) silicon carbide-(p) boron phosphide heterojunction.

linear increase in the reverse current as the reverse bias is increased. The characteristic of Fig. 27 suggests this type of behavior.

Capacitance-voltage measurements were also taken on (n) silicon carbide-(p) boron phosphide heterojunction diodes. Figure 28 shows the relationship between the inverse capacitance squared and voltage for the diode described above. The linear relation between C^{-2} versus V indicates the abrupt nature of the junction. The voltage intercept in the case of heterodiodes may be a function of the impurity profile in either or both of the semiconducting materials. For a p-n heterojunction with the more heavily doped semiconductor on the n-side, for example, most of the depletion region would be in the p-side semiconductor and the voltage intercept would indicate the energy gap of the p-side semiconductor. The voltage intercept of about 2.6 V in Fig. 28, which is intermediate between the band gaps of silicon carbide and boron phosphide, suggests that both sides of the silicon carbide-boron phosphide heterojunctions have comparable impurity concentrations. The voltage intercept can also be interpreted as the potential barrier resulting from two Schottky diodes in series.

II.D.4. Boron Phosphide P-N Electroluminescent Homojunctions

Boron phosphide p-n junction structures were prepared by the epitaxial growth of boron phosphide using thermal reduction of a boron tribromide-phosphorus trichloride mixture with hydrogen on solution grown boron phosphide platelets. Mesa diodes

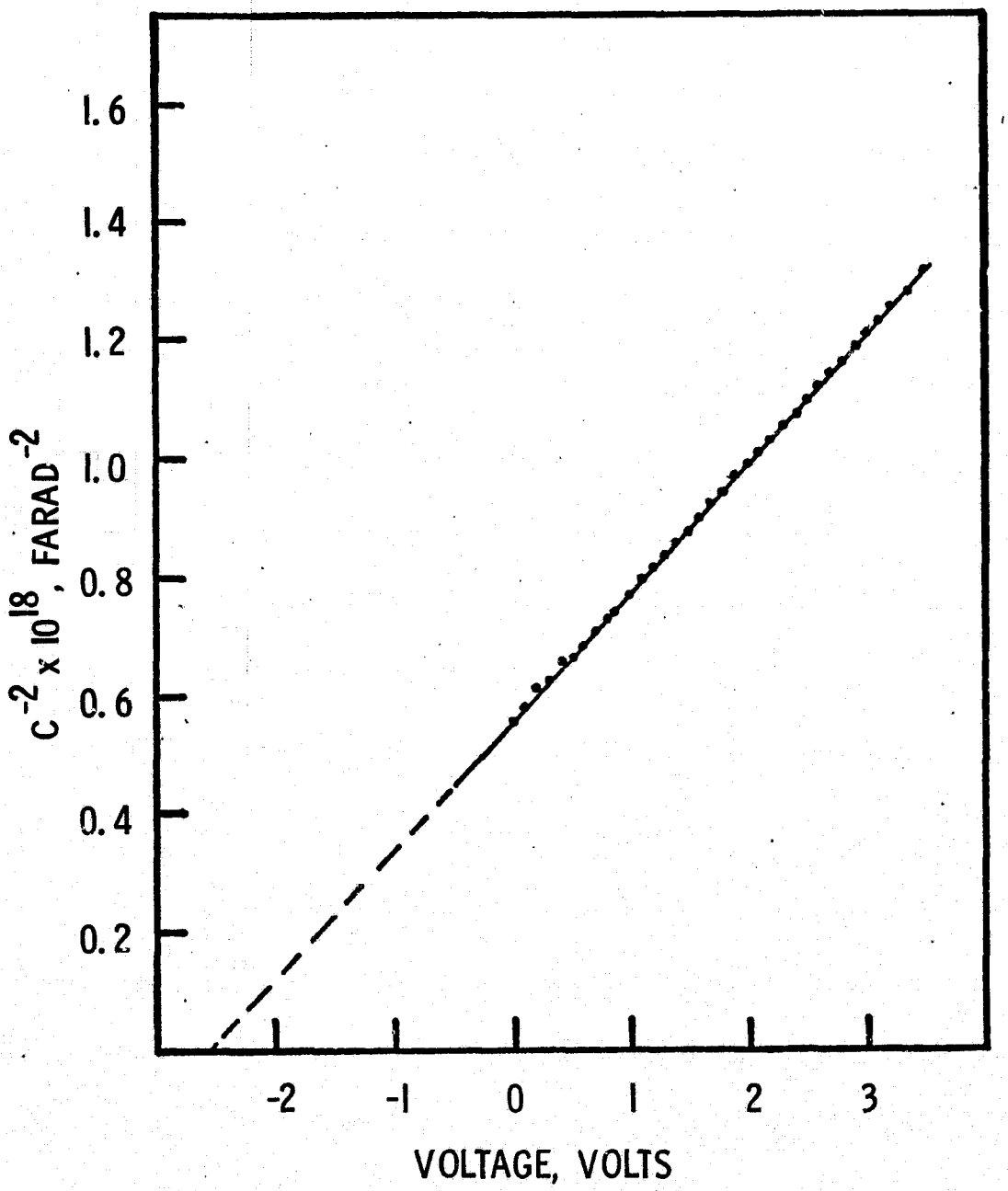

Fig. 28 Capacitance-voltage characteristics of an (n) silicon carbide-(p) boron phosphide heterojunction.

were isolated by electrolytic etching or by laser scribing. Figures 29A and 29B show, respectively, an array of laser scribed boron phosphide diodes and the typical current-voltage characteristics. Built-in p-n junctions in solution grown boron phosphide crystals were also isolated by electrolytic etching. Gold or gold-silicon contacts were evaporated onto the n-type region and gold-beryllium contacts were evaporated on the p-type region. After evaporation, the contacts were annealed in hydrogen at 850° C to reduce the contact resistance. The fabricated boron phosphide diodes were mounted on a TO-18 header with a single component silver epoxy. The mounted diodes were generally encapsulated in Hysol LED epoxy before making measurements.

Figure 30 shows the current-voltage characteristics of an unpassivated epitaxial boron phosphide diode fabricated on an n-type solution grown substrate. The slow rise of current with voltage in the forward direction is due to the high series resistance of the device. The reverse breakdown voltage was higher than 20 volts. The excessive leakage current was reduced by passivation.

The current-voltage and capacitance-voltage characteristics of a built-in p-n junction in a solution grown boron phosphide crystal are shown in Fig. 31 and 32, respectively. Over a small range of voltage, the n value is approximately 2 at 300° K and 3.4 at 77° K. This is due to the carrier recombination in the space charge region. A linear relationship between C^{-2} and V

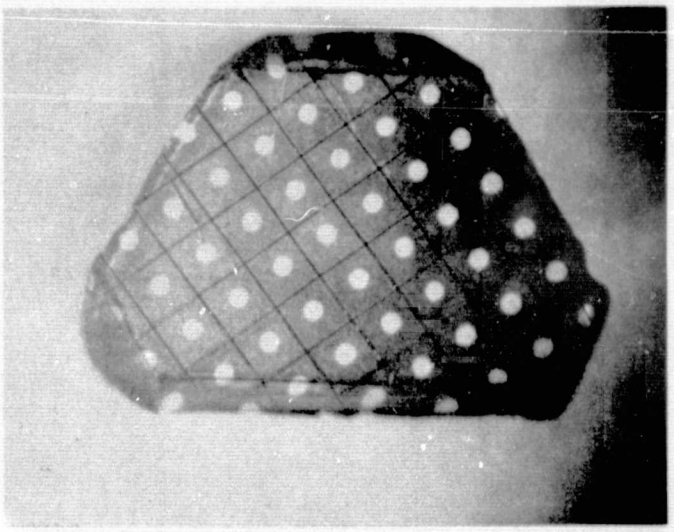

(A)

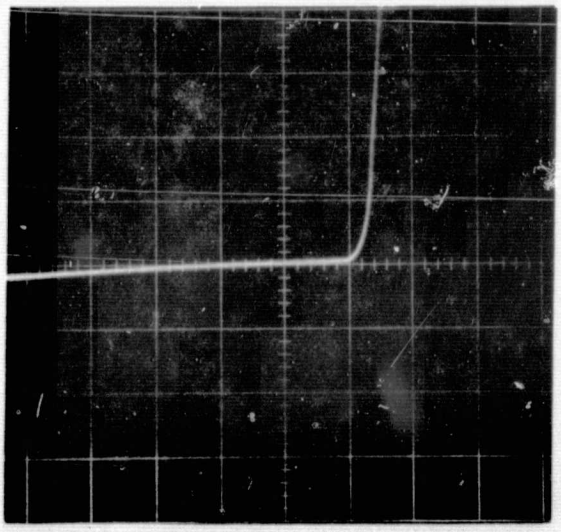

(B)

Fig. 29 (A) An array of laser scribed boron phosphide p-n junction diodes. (B) Current-voltage characteristics of a laser scribed diode (Horizontal: 2 V/div., Vertical: 1 mA/div.).

C.2

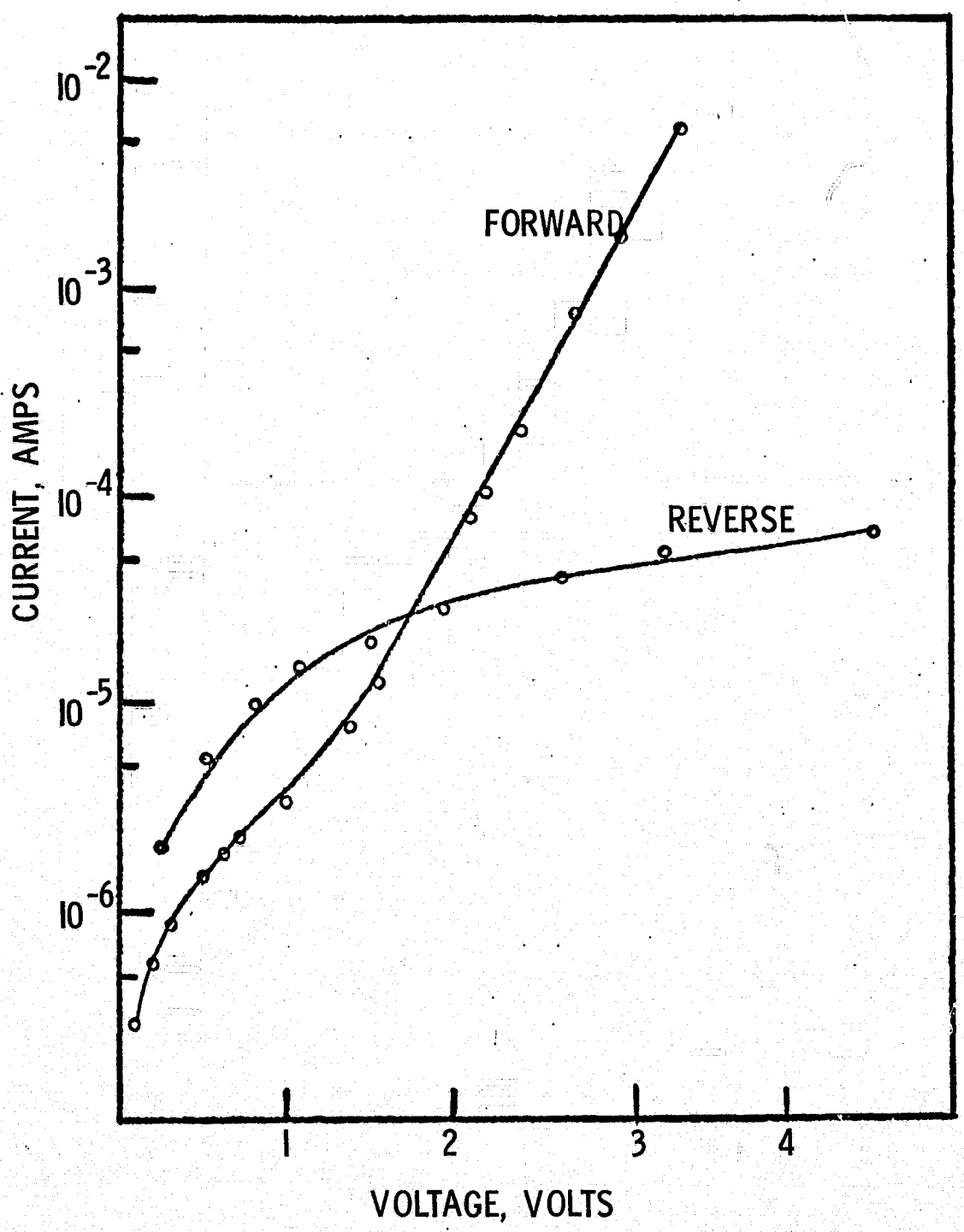

Fig. 30 Current-voltage characteristics of an epitaxial boron phosphide p-n junction.

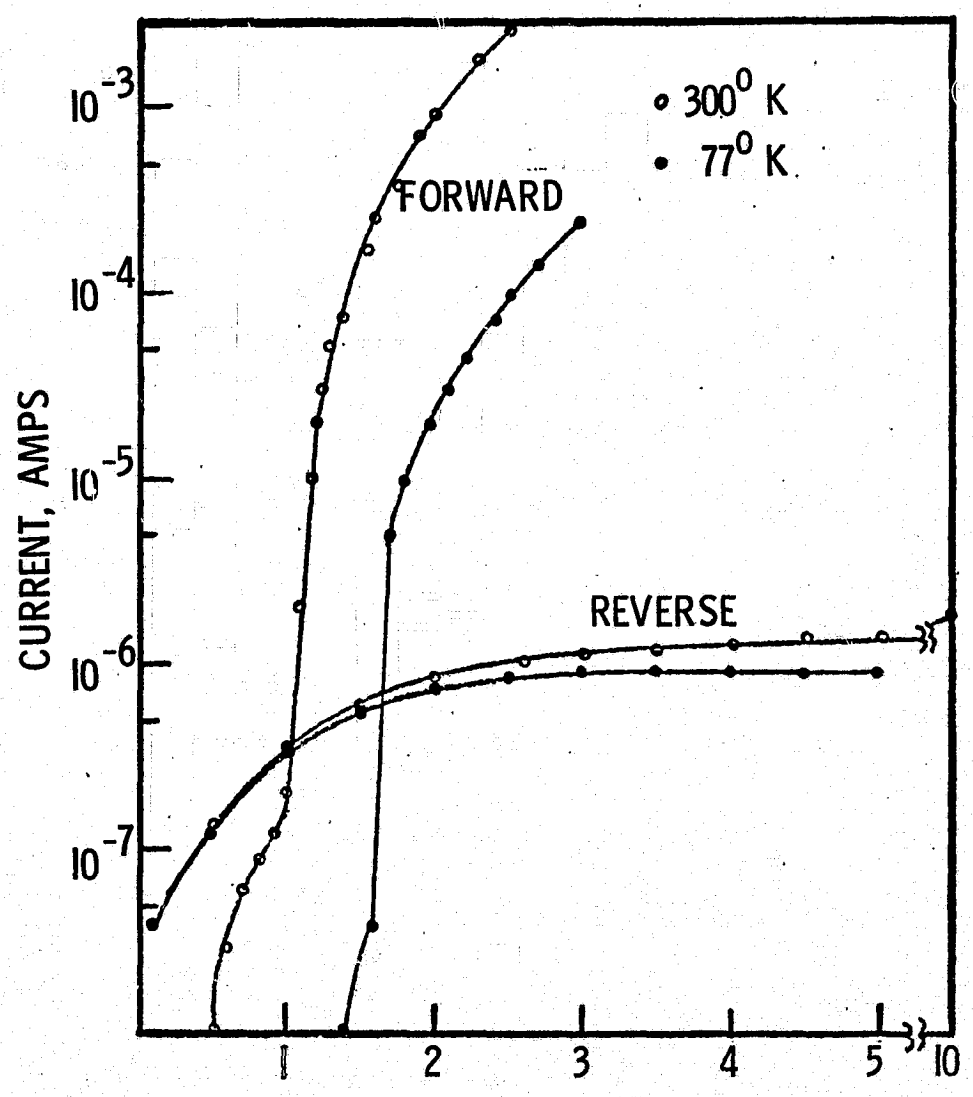

Fig. 31 Current-voltage characteristics of a solution grown p-n junction (approximate junction area: 0.05 cm^2).

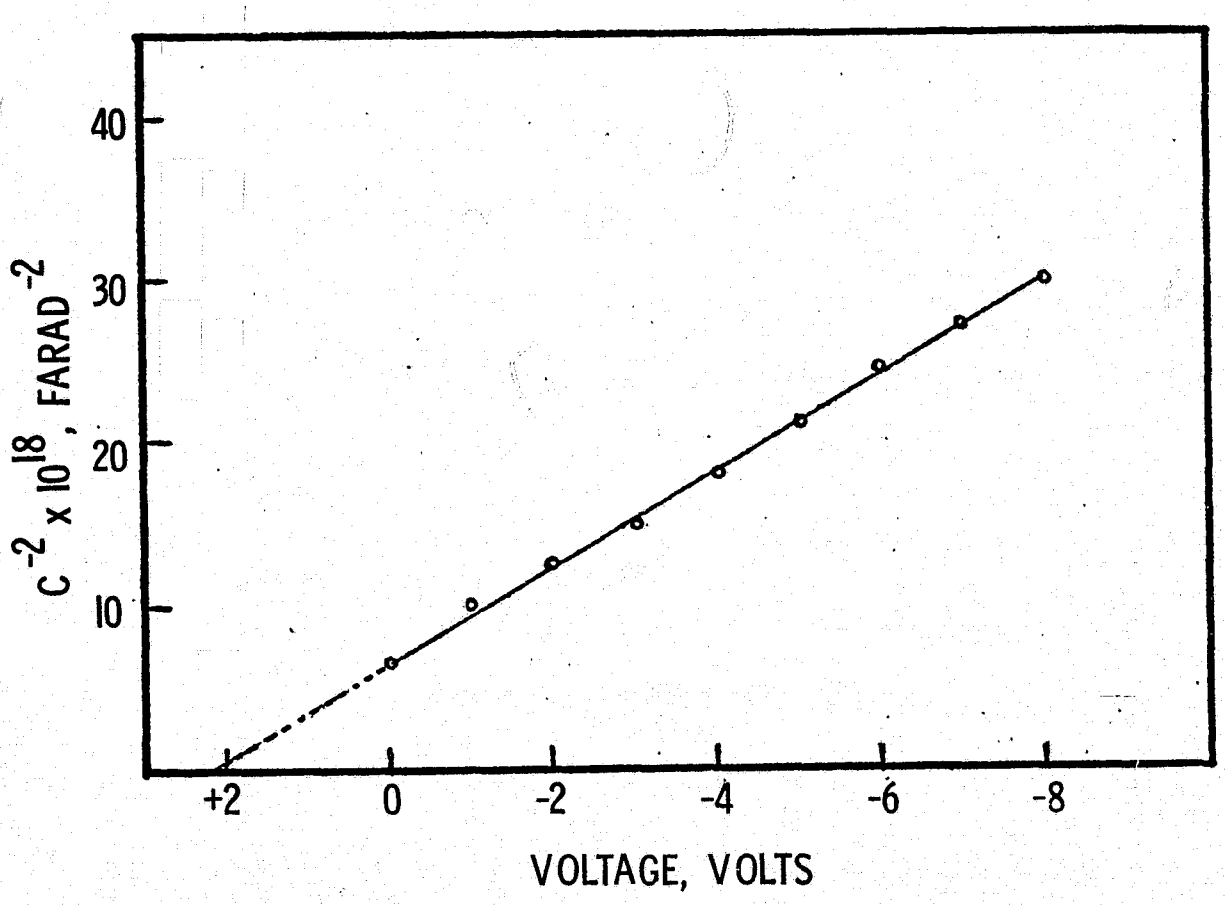

Fig. 32 Capacitance-voltage characteristics of a solution-grown p-n junction (approximate junction area: 5×10^{-2} cm^2).

indicates the abrupt nature of the junction. The voltage intercept is about 2.1 V, slightly greater than the energy gap of boron phosphide. This is attributed to the presence of p-i-n structure in place of a simple p-n junction. The carrier concentration calculated from the slope of C^{-2} versus V relation is approximately 10^{18} cm^{-3}.

The electroluminescence from boron phosphide p-n junctions and point-contact diodes was studied under dc and pulsed conditions. For spectral measurements, the diode emission was focused on the entrance slit of a Perkin-Elmer model E-1 monochromator. The detector was a RCA 7102 photomultiplier tube (with S-1 characteristics). The emission from solution grown diodes was visible in room light and appeared to originate from n-type region. Also, electroluminescence was observed when the diode was under forward or reverse bias, although the brightness level was much higher under reverse bias. Figure 33 shows the spectral emission of a solution grown phosphide p-n junction under reverse bias. The spectrum consists of bands associated with transitions between impurity states. The spectrum extends into near infra red (about 1.5 cV). The electroluminescence from epitaxial p-n junctions had similar spectral distribution as, but of less intensity than, the solution grown diodes.

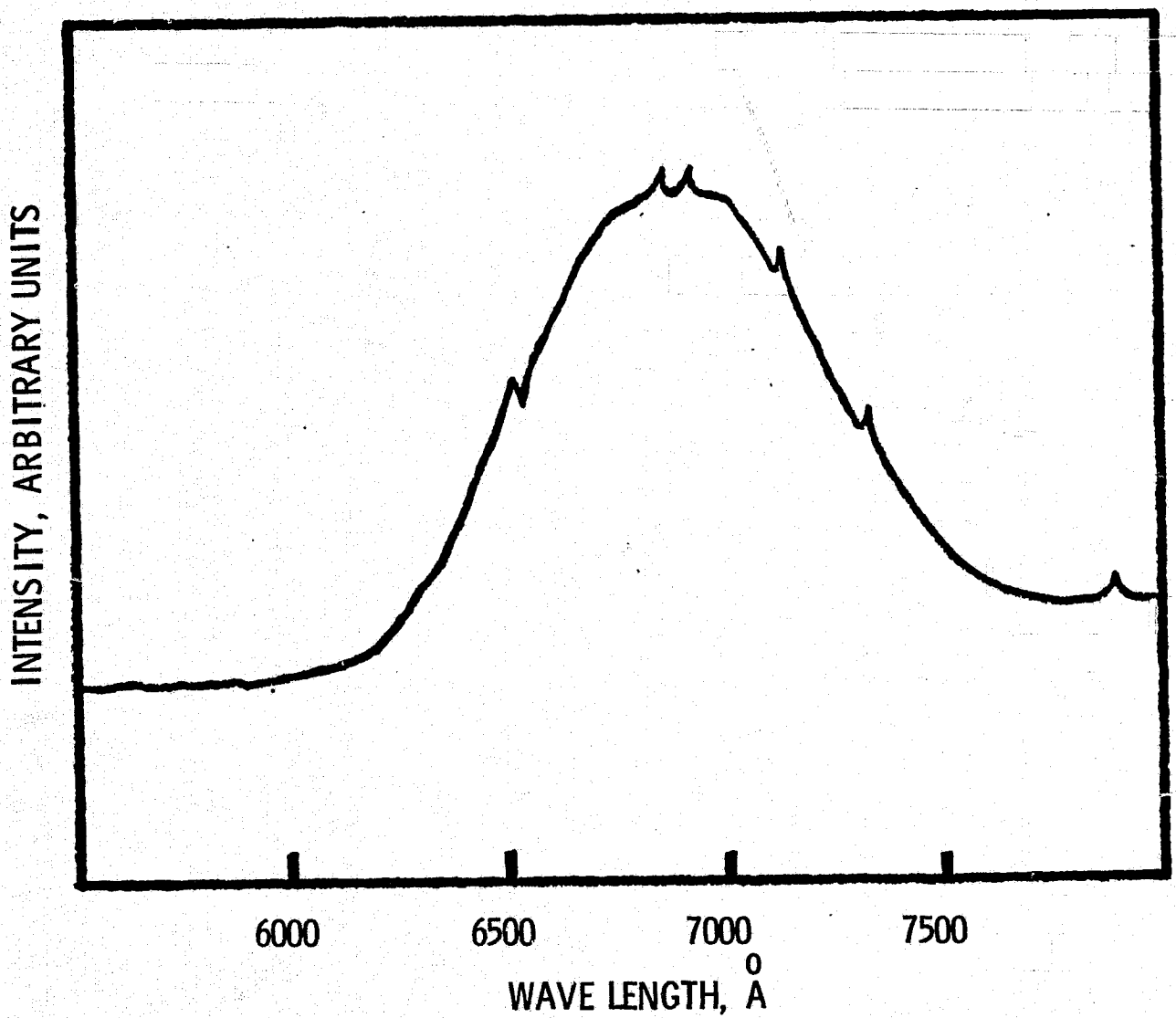

Fig. 33 Electroluminescent spectrum from a boron phosphide p-n junction.

III. Summary and Conclusions

Boron arsenide and boron phosphide with energy gaps of 1.46 and 2.0 eV, respectively, are not well-known semiconductors. In this work, extensive investigations have been carried out concerning the crystal growth, characterization, and device fabrication of these compounds.

Boron arsenide decomposes irreversibly at temperatures above 900° C, thus limiting the temperature of the crystal growth process. Single crystals of boron arsenide have been prepared by the chemical transport of polycrystalline boron arsenide in the presence of a temperature gradient. The transported crystals are p-type and have a resistivity of approximately 0.01 ohm-cm in the temperature range 77-500° K. The hole concentration and Hall mobility, essentially independent of temperature in the range 77-300° K, have been estimated to be in the range of 10^{18}-$10^{19} cm^{-3}$ and 100-400 $cm^2 V^{-1} sec^{-1}$, respectively. The crystal growth of boron arsenide from high temperature solutions has also been attempted without success because of the low solubility of boron arsenide in nickel arsenide, copper arsenide, and palladium arsenide at 900° C or below. No major efforts were directed to the fabrication of boron arsenide devices because of the small size of available boron arsenide crystals and its thermal instability.

Thin layers of boron arsenide have been deposited on several substrates at 800-850° C by the thermal decomposition of a diborane-arsine mixture in a hydrogen atmosphere. Boron arsenide

deposited on silicon substrates of {111} orientation were amorphous. Optical absorption measurements implied that boron arsenide is a direct gap material with a room temperature energy gap of about 1.45 eV. The current-voltage characteristics of metal-boron arsenide-silicon structures have indicated that the current-controlling mechanism is similar to that of an insulator containing traps of uniform energy.

Single crystals of boron phosphide have been grown by the chemical transport and solution growth techniques using polycrystalline starting material. The transport of polycrystalline boron phosphide by iodine and bromine in a closed tube was studied in detail, including source temperature, temperature gradient, and surface condition of the reaction tube. At a source temperature of 1270-1290° C, single crystals of boron phosphide were obtained in the form of polyhedra of several millimeters size with well-defined faces. The transported crystals were p-type with a room temperature resistivity of approximately 0.5 ohm-cm. Resistivity measurements in the temperature range 77-350° K indicated the presence of two impurity states with activation energies of approximately 0.009 and 0.052 eV, respectively.

The solution growth technique was more successful than the transport technique for the growth of large boron phosphide crystals suitable for device fabrication. Two approaches were investigated: (1) the addition of phosphorus to a boron-nickel or boron-copper melt, and (2) the recrystallization of boron phosphide from a nickel phosphide or copper phosphide solution

in a temperature gradient. The solubility of boron phosphide in nickel phosphide was found to be higher than that in copper phosphide, and the temperature gradient recrystallization of boron phosphide from nickel phosphide solution at 1200-1220° C was found to produce large crystals than the addition of phosphorus to a boron-nickel melt. The solution grown crystals were mostly in the form of platelets up to 20 mm^2 in area; they had main faces of {111} orientation and were formed by the twin-plane re-entrant edge mechanism. They were usually n-type with a room-temperature resistivity of about 0.5 ohm-cm and a carrier concentration of about 10^{18} cm^{-3}. The size and perfection of solution-grown boron phosphide crystals were improved by the accelerated container rotation technique which provides very effective mixing within the solution. The crystals contained both p-type and n-type regions; the faces were usually n-type, and a central core was p-type. The addition of silicon to the boron phosphide-nickel phosphide solution produced only n-type boron phosphide, and the addition of beryllium produced p-type crystals.

The deposition of boron phosphide layers on silicon carbide platelets, {111} oriented silicon substrates, and boron phosphide crystals was investigated extensively by using the thermal reduction of a boron tribromide-phosphorus trichloride mixture. Boron phosphide layers deposited on the silicon face of silicon carbide substrates at 1050-1150° C were single crystalline and epitaxial with respect to the substrate. Without intentional doping, the

epitaxial layers were p-type with a room temperature carrier concentration of about 10^{19} cm^{-3}. Resistivity measurements in the temperature range 300-1000° K indicated the presence of two impurity levels with activation energies of approximately 0.22 and 0.66 eV, respectively. Boron phosphide layers deposited on vapor-and solution-grown crystals had much better structural perfection than those deposited on silicon carbide substrates. The electrical resistivity of n-type epitaxial boron phsophide layers was controlled by using hydrogen selenide as a dopant.

Several techniques associated with the fabrication of boron phosphide devices such as junction shaping, diffusion, and contact formation have been investigated. Because of the chemical inertness of boron phosphide at room temperature, electrolytic etching is the most useful etching technique for boron phosphide and has been studied in detail using various electrolytes. A technique was developed to etch and polish p-type boron phosphide; however, an insoluble film tended to form on the surface of n-type material, and material removal was very slow. The large difference in the etch rates of p-type and n-type boron phosphide has allowed selected removal of material and delineation of mesa-type p-n junctions. The diffusion of several n- and p-type dopants into boron phosphide was investigated at temperatures up to 1250° C, and no change in the electrical properties of the surface of boron phosphide crystals was ever observed. Among the large number of metals and alloys investigated, electroless nickel was found to form low resistance ohmic contacts to all but lightly-

doped n-type boron phosphide crystals. Evaporated gold-germanium and gold-silicon have produced low resistance ohmic contacts to n-type boron phosphide, and gold-beryllinum has formed low resistance ohmic contacts to p-type material.

Four types of boron phosphide devices were fabricated: metal-insulator-boron phosphide structures, Schottky barriers, boron phosphide-silicon carbide heterojunctions, and p-n homojunctions. The metal-silicon nitride-boron phosphide structures are characterized by the presence of negative charges in the semiconductor-dielectric interface. The current-voltage characteristics of (n) silicon carbide-(p) boron phosphide heterojunction structures have been found to deviate considerably from p-n homojunction structures and indicate a high recombination rate at the interface. Epitaxial boron phosphide p-n junctions and built-in p-n junctions in solution grown boron phosphide crystals were isolated by electrolytic etching. The current-voltage and capacitance-voltage characteristics of these diodes have been investigated. Easily visible electroluminescence has been observed from these junctions.

IV. References

1. S. K. Ku, "Preparation and Properties of Boron Arsenides and Boron Arsenide - Gallium Arsenide Mixed Crystals," J. Electrochem. Soc., 113, 813 (1966).

2. C. C. Wang, M. Cardona, and A. G.Fischer, "Preparation, Optical Properties, and Band Structure of Boron Phosphide," RCA Rev., 25, 159 (1964).

3. R. J. Archer, R. Y. Koyama, E. E. Loebner, and R. C. Lucas, "Optical Absorption, Electroluminescence, and the Band Gap of BP," Phys. Rev. Lett., 12, 538 (1964).

4. T. L. Chu and R. K. Smeltzer, "Epitaxial Growth of III-V Compounds for Electroluminescent Light Sources," IEEE Trans. Parts, Hybrids, and Packaging, PHP-9, 208 (1973).

5. J. A. Perri, S. LaPlaca, and B. Post, "New Group III-Group V Compounds: BP and BAs," Acta Cryst., 11, 310 (1958).

6. F. V. Williams and R. A. Ruehrwein, "The Preparation and Properties of Boron Phosphides and Arsenides," J. Amer. Chem. Soc., 82, 1330 (1960).

7. P. E. Grayson, J. T. Buford, and A. F. Armington, "Pressure Synthesis of Boron Phosphide and Boron Arsenide," Electrochem. Tech., 3, 338 (1965).

8. A. F. Armington, "Vapor Transport of Boron, Boron Phosphide, and Boron Arsenide," J. Crystal Growth, 1, 47 (1967).

9. P. Popper and T. A. Ingles, "Boron Phosphide, A III-V Compound of zinc-Blende Structure," Nature, 179, 1075 (1957).

10. K. Vickery, "Synthesis of Boron Phosphide and Nitride," Nature, 184, 268 (1959).

11. J. L. Peret, "Preparation and Properties of Boron Phosphide," J. Amer. Cer. Soc., 47, 44 (1964).

12. B. Stone and D. Hill, "Semiconducting Properties of Cubic Boron Phosphide," Phys. Rev. Lett., 4, 282 (1960).

13. B. V. Baranov, V. D. Prochukhan, and N. A. Goryunova, "Production of Course-Crystalline Boron Phosphide from Solution in a Melt with Cu_3P," Izv. Akad. Nauk SSSR, Neorgan. Materialy, 3, 1691 (1967) {English translation p. 1477}.

14. Ya. Kh. Grinberg, Z. S. Medvedva, A. A. Eliseev, and E. G. Zhukov, "Production of Boron Phosphide Single Crystals From Vapor," Soviet Physics - Doklady, 10, 6 (1965).

15. T. Niemyski, S. Mierzejewska-Appenheimer, and J. Majewski, "High-Pressure Crystallization of Boron Phosphide from Liquid Phosphorus," in "Crystal Growth," ed. H. S. Peiser (Peragamon, Oxford, 1967) p.585.

16. M. Iwani, N. Fujita, and K. Kawabe, "Preparation of BP Single Crystals from B-Ni-P Solution," Jap. J. Appl. Phys., 10, 1746 (1971).

17. T. Nishinaga, H. Ogawa, H. Watanabe, and T. Arizumi, "Vapor Growth of Boron Monophosphide Using Open and Closed Tube Processes," J. Crystal Growth, 13/14, 346 (1972).

18. K. P. Ananthanarayanan, C. Mohanty, and P. J. Gielisse, "Synthesis of Single Crystal Boron Phosphide," J. Crystal Growth, 20, 63 (1973).

19. T. Kobayshi, K. Susa, S. Taniguchi, "Synthesis of BP Under High Pressures," Mat. Res. Bull., 9, 625 (1974).

20. M. Hirayama and K. Shohno, "Hetero-Epitaxial Growth of Lower Boron Arsenide on Si Substrate Using AsH_3-B_2H_6-H_2 System," Jap. J. Appl. Phys., 12, 1960 (1973).

21. M. Takigawa, M. Hirayama, and K. Shohno, "Hetero-Epitaxial Growth of BP on Si Substrate Using B_2H_6-PH_3-H_2 System," Jap. J. Appl. Phys., 13, 411 (1974).

22. H. Schafer, Chemical Transport Reactions, Academic Press, New York, 1964.

23. T. L. Chu, J. M. Jackson, and R. K. Smeltzer, "The Growth of Boron Monophosphide Crystals by Chemical Transport," J. Crystal Growth, 15, 254 (1972).

24. T. L. Chu, J. M. Jackson, and R. K. Smeltzer, "The Crystal Growth of Boron Monophosphide from Metal Phosphide Solutions," J. Electrochem. Soc., 120, 802 (1973).

25. E. Larsson, "An X-ray Investigation of the Ni-P System and the Crystal Structures of NiP and NiP_2," Arkiv för Kemi, 23, 335 (1965).

26. T. L. Chu, M. Gill, and R. K. Smeltzer, "Growth of Boron Monophosphide Crystals with the Accelerated Container Rotation Technique," J. Crystal Growth, submitted for publication.

27. H. J. Scheel and E. O. Schulz-DuBois, "Flux Growth of Large Crystals by Accelerated Crucible-Rotation Technique," J. Crystal Growth, 8, 304 (1971).

28. H. J. Scheel, "Accelerated Crucible Rotation: A Novel Stirring Technique in High-Temperature Solution Growth," J. Crystal Growth, 13/14, 560 (1972).

29. W. Tolksdorf and F. Welz, "The Effect of Local Cooling and Accelerated Crucible Rotation on the Quality of Garnet Crystals," J. Crystal Growth, 13/14, 566 (1972).

30. J. W. Faust and H. F. John, "The Growth of Semiconductor Crystals from Solution Using the Twin-Plane Reentrant-Edge Mechanism," J. Phys. Chem. Solids, 25, 1407 (1964).

31. T. L. Chu, J. M. Jackson, A. E. Hyslop, and S. C. Chu, "Crystals and Epitaxial Layers of Boron Phosphide," J. Appl. Phys., 42, 420 (1971).

32. T. L. Chu and M. Gill, "Electrolytic Etching of Boron Phosphide," J. Electrochem. Soc., submitted for publication.

33. R. L. Meek and N. E. Schumaker, "Anodic Dissolution and Selective Etching of Gallium Phosphide," J. Electrochem. Soc., 119, 1148 (1972).

34. H. C. Gatos and M. C. Lavine, "Characteristics of the {111} Surfaces of the III-V Intermetallic Compounds," J. Electrochem. Soc., 107, 427 (1960).

35. M. E. Straumanis, J. P. Krumme, and W. J. James, "Current Density Anodic Potential Curves of Single Crystal GaAs at Low Currents in KOH," J. Electrochem. Soc., 115, 1050 (1968).

36. M. A. Lampert and P. Mark, Current Injection in Solids, Academic Press, New York, 1970, pp. 72-77.

37. T. L. Chu and R. W. Kelm, "The Preparation and Properties of Aluminum Nitride Films," J. Electrochem. Soc., 122, 995 (1975).

38. U. Dolega, "Theorie des pn-Kontaktes zwischen Halbleitern mit verschiedenen Kristallgittern," Z. Naturforsch., 18, 653 (1963).

Appendix A. Research Contributors

Dr. Ting L. Chu, Professor and Principal Investigator
Dr. Shirley S. Chu, Associate Professor
Dr. Ronald K. Smeltzer, Research Associate
Dr. Adin E. Hyslop, former graduate student
Dr. Jay M. Jackson, former graduate student
Dr. Reynold K. Kelm, Jr., former graduate student
Dr. Manzur Gill, former graduate student
Mr. Henry B. Morris, former graduate student

APPENDIX B

"Crystals and Epitaxial Layers of Boron Phosphide" T. L. Chu, J. M. Jackson, A. E. Hyslop, and S. C. Chu, J. Appl. Phys., 42, 420-424 (1971).

Reprinted from:

JOURNAL OF APPLIED PHYSICS VOLUME 42, NUMBER 1 JANUARY 1971

Crystals and Epitaxial Layers of Boron Phosphide*

T. L. CHU, J. M. JACKSON, A. E. HYSLOP, AND S. C. CHU

Electronic Sciences Center, Southern Methodist University, Dallas, Texas 75222

(Received 12 August 1970)

The thermal decomposition of diborane–phosphine mixtures in a hydrogen atmosphere and the thermal reduction of boron tribromide–phosphorus trichloride mixtures with hydrogen have been used for the deposition of boron phosphide on the basal plane of hexagonal silicon carbide substrates. In the thermal decomposition process, the substrate must be maintained at temperatures below 900°C to minimize the contribution of gas-phase reactions, and the boron phosphide layers showed only preferred orientations. The thermal reduction process was carried out over a wide temperature range, and the boron phosphide layers deposited on the silicon face of silicon carbide substrates at 1050°–1150°C were found, by optical microscopy and reflection electron diffraction examinations, to be single crystalline and epitaxial with respect to the substrate. Epitaxial boron phosphide layers prepared by the halide reduction reaction without intentional doping are p type with a room-temperature carrier concentration of approximately 10^{19} cm^{-3}. Resistivity measurements in the temperature range 300°–1000°K indicated the presence of two impurity states with activation energies of approximately 0.22 and 0.66 eV, respectively. Needle-shaped boron phosphide crystals have also been obtained by the halide reduction reaction. They are single crystals with the elongated axis along a ⟨111⟩ direction and are p type with a room-temperature resistivity of approximately 20 Ω cm.

I. INTRODUCTION

Boron forms two phosphides: a cubic monophosphide (BP) with an energy gap of 2.0 eV [1,2] and a rhombohedral subphosphide (B_6P) with an energy gap of 3.3 eV.[3] The monophosphide, referred to as boron phosphide hereinafter, decomposes into the subphosphide at high temperatures (1100°C) and reduced pressures (about 1 mm).[4]

Because of its high melting point and thermal instability, boron phosphide crystals have been grown only by solution growth and chemical transport techniques. Recrystallization from nickel or iron solutions at 1300°–1500°C under a phosphorus pressure has produced orange–red crystals of boron phosphide up to several millimeters in size.[2] These crystals, containing about 0.01% solvent as the major impurity, were p type with a room-temperature carrier concentration of 10^{18} cm^{-3} and a room-temperature mobility of 500 cm^2/V sec. Boron phosphide crystals produced by the chemical transport technique were considerably smaller, and their properties have not been characterized.[5,6]

In recent years, chemical vapor growth techniques have been used successfully for the crystal growth of several refractory III–V compounds such as gallium arsenide, aluminum arsenide, gallium–aluminum arsenide, etc. These techniques have the advantages that the crystal growth can be achieved at relatively low temperatures and that the composition of the reactant mixture can be varied over a wide range. In this work, chemical reactions between gaseous boron and phosphorus compounds have been used for the growth of boron phosphide single crystals. To control the nucleation and growth processes, the basal plane of hexagonal silicon carbide platelets was also used as the substrate. Hexagonal silicon carbide appears to be the most suitable substrate available from considerations of chemical inertness, crystal symmetry, and lattice parameters. The basal plane of silicon carbide has three-fold symmetry and a lattice parameter of 3.08 Å, which is very similar to the interatomic distance in the {111} plane of boron phosphide, 3.21 Å (the lattice parameter of boron phosphide is 4.55 Å).

Several chemical reactions between gaseous boron and phosphorus compounds are thermochemically feasible for the deposition of boron phosphide. The thermal decomposition of a diborane–phosphine mixture in a hydrogen atmosphere and the thermal reduction of a boron tribromide–phosphorus trichloride mixture with hydrogen were used in this work. The thermal decomposition reaction takes place readily at relatively low temperatures, and boron phosphide layers deposited on silicon carbide substrates at 850°C were found to show only preferred orientations. The thermal reduction process requires higher substrate temperatures, and boron phosphide layers deposited on the silicon face of hexagonal silicon carbide at 1050°–1150°C were found to be single crystalline and epitaxial with respect to the substrate.

Needle-shaped single crystals of boron phosphide have also been prepared by the thermal reduction technique. The preparation processes and the properties of the grown material are discussed in this paper.

II. EXPERIMENTAL

The deposition of boron phosphide was carried out in a gas-flow system by the thermal decomposition of diborane–phosphine mixtures in a hydrogen atmosphere and the thermal reduction of boron tribromide–phosphorus trichloride mixtures with hydrogen. One major difference between these two reactions is the magnitude of their free energy changes. The hydrides are thermodynamically unstable at room temperature

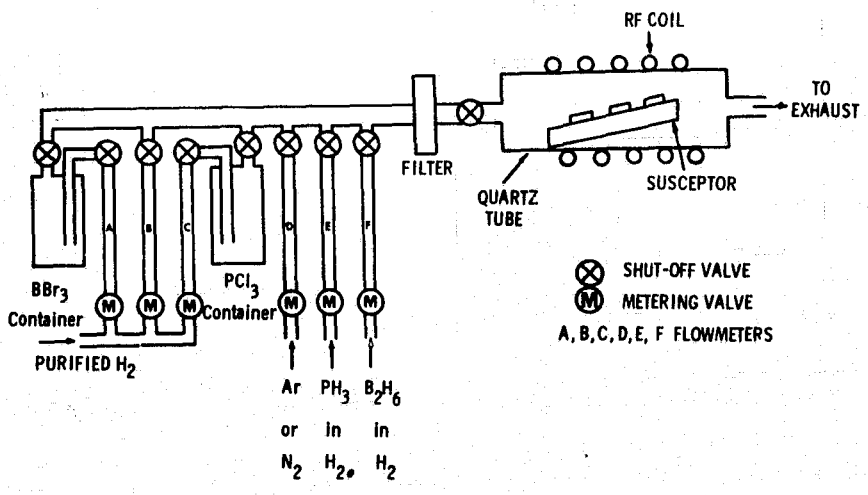

FIG. 1. Schematic diagram of the apparatus for the deposition of boron phosphide.

and decompose rapidly at 500°C and above. This thermal instability tends to promote homogenous nucleation by pyrolysis in the gas phase, and the solid boron compound thus formed will interfere with the oriented growth. Although the gas-phase nucleation can be suppressed by using a low partial pressure of hydrides in the reactant, a high gas-flow velocity over the substrate surface, and a water-cooled reaction tube, these conditions are not effective at relatively high substrate temperatures, 900°C for example. The halides are thermally more stable than the hydrides, and higher substrate temperatures may be used in the thermal reduction process with essentially no gas-phase reactions. At high substrate temperatures, however, a phosphorus pressure equal to or greater than the vapor pressure of boron phosphide must be present over the substrate surface to maintain the stoichiometry of the deposit.

Hydrogen used in the deposition process was purified by diffusion through a palladium–silver alloy. Diborane and phosphine were purchased in the form of hydrogen–hydride mixtures, each containing about 5% of the hydride. Boron tribromide and phosphorus trichloride were of the reagent grade. The hexagonal silicon carbide substrates, obtained through the courtesy of Dr. R. B. Campbell of Westinghouse Astronuclear Laboratories, Large, Penn., were in the form of thin platelets with main faces parallel to the basal plane. At one main face, the silicon carbide structure terminates in silicon atoms triply bonded to the matrix, and at the other, the structure terminates in triply bonded carbon atoms. The polarity of the substrate surface was distinguished by etching with a molten 3:1 sodium hydroxide–sodium peroxide mixture; the face remaining smooth being the silicon face and the rough face being the carbon face.[7]

The apparatus used for the deposition of boron phosphide is shown schematically in Fig. 1. The flow of various gases was directed by using appropriate valves and measured with flowmeters. The boron tribromide and phosphorus trichloride containers were maintained in a constant temperature bath, and the halides were vaporized by using hydrogen as a carrier gas. The reactant mixture of the desired composition was passed through a filter into a fused silica reaction tube. The reaction tube for the halides reaction was of 25-mm i.d., and that for the hydride reaction was of 55-mm i.d., and was water cooled to minimize the gas-phase reactions. In the reaction tube, the silicon carbide substrates were supported on a boron phosphide-coated graphite susceptor, and the susceptor was heated externally by an rf generator.

The deposition of boron phosphide by the hydride reaction was carried out at substrate temperatures below 900°C so that gas-phase reactions were negligible. The flow rate of hydrogen was 20 liter/min, and the reactant contained up to 0.05% of diborane and phosphine. The deposition of boron phosphide by the halide reaction was carried out in the temperature range 850°–1150°C. A relatively low flow rate of hydrogen, 1.7 liter/min, was used so that a phosphorus pressure of a few millimeters could be readily maintained over the substrate surface when desired. The flow rates of boron and phosphorus halides were varied over a wide range.

The thickness of boron phosphide layers on a silicon carbide substrate was determined by direct measurement of the fractured cross section of the specimen with an optical microscope. The structural properties of the deposited material were determined by optical microscopy, reflection electron diffraction, and x-ray diffraction techniques.

The Ohmic contacts on boron phosphide were made by the evaporation of aluminum or gold, followed by annealing in argon at 600°C (for aluminum contacts) or 800°C (for gold contacts) for about 15 min. To

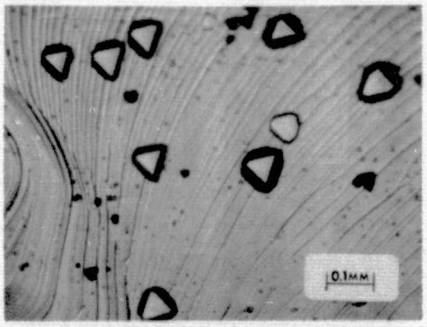

FIG. 2. Oriented boron phosphide crystallites deposited on the silicon face of a hexagonal silicon carbide substrate.

measure the electrical resistivity, the specimen was mounted on a ceramic disk by using Saureisen cement, and the metal contacts were connected to the lead wires by using an ultrasonic bonder or by using a tungsten pressure contact.

III. RESULTS AND DISCUSSION

A. The Epitaxial Growth of Boron Phosphide

The deposition of boron phosphide by the thermal reduction of a boron tribromide–phosphorus trichloride mixture will be discussed first. This deposition reaction is chemically reversible. Since an excess of phosphorus trichloride was used in the deposition process to minimize the decomposition of boron phosphide, the deposition rate of boron phosphide at a given temperature depended strongly on the concentration of boron tribromide in the reactant mixture. For example, when the flow rates of hydrogen, boron tribromide, and phosphorus trichloride were 7×10^{-2}, 8×10^{-4}, and 5×10^{-3} mol/min, respectively, the deposition rate of boron phosphide at 1150°C was negligible. By increasing the flow rate of boron tribromide to 10^{-3} mol/min, boron phosphide was deposited at an average rate of 80 μ/h. The reversibility of the halide reduction reaction is believed to be advantageous in that the surface atoms at desirable sites can be removed preferentially by the reverse reaction, thereby reducing the concentration of defects in the deposit.

Adherent and continuous layers of boron phosphide were deposited on silicon carbide substrates in the temperature range 850°–1150°C under a variety of conditions. The most important factors determining the crystallinity of the deposit were found to be the substrate temperature and the polarity of the substrate surface; boron phosphide layers deposited on the silicon face at high substrate temperatures have always exhibited the best structural perfection. Figure 2 shows an early stage of the boron phosphide growth on the silicon face of a silicon carbide substrate at 1150°C. This growth consists of isolated, oriented, triangular crystallites, and the sides of the triangular growth are parallel to the edges of the substrates, i.e., the $\langle 010\rangle$ direction of silicon carbide. The surface of the crystallites is of a $\{111\}$ orientation as indicated by their symmetry. Furthermore, the triangular crystallites are of opposite orientations, indicating the presence of two equivalent $\{111\}$ orientations related by a twofold rotation normal to the surface. The equivalent orientations result from the different stacking possibilities at the substrate–deposit interface.

The grown surface of continuous boron phosphide layers also exhibits structural features. An example is given in Fig. 3 where the as-grown surface of a boron phosphide layer of approximately 40-μ thickness deposited on the silicon face is shown. This deposition was carried out at 1050°C using hydrogen, boron tribromide, and phosphorus trichloride at flow rates of 7×10^{-2}, 4×10^{-4}, and 4×10^{-3} mol/min, respectively, and the average deposition rate was 40 μ/h. In addition to the triangular growth, the surface shows a number of linear figures at 60° or 120° to each other which sometimes intersect to form triangles or partial triangles. These figures are presumably stacking fault traces resulting from the coalescence of the initial crystallites. The geometry of the figures suggests that the entire grown layer is single crystalline and is epitaxial with respect to the substrate. The epitaxial relation is: $BP(111) \parallel SiC(001)$ and $BP\langle 1\bar{1}0\rangle \parallel SiC\langle 010\rangle$. This relation was confirmed by reflection electron diffraction examinations. A typical diffraction pattern is shown in Fig. 4. The electron beam was incident in the $[11\bar{2}]$ direction of the specimen, and the observed pattern indicated that the [111] direction of the boron phosphide layer is perpendicular to the substrate plane.

The boron phosphide layers deposited on the silicon face of the substrate at lower temperatures were also examined in detail by reflection electron diffraction. When the substrate temperature was decreased to 950°C or below, the deposit became essentially polycrystalline. The grown surface also exhibited no

FIG. 3. As-grown surface of a boron phosphide layer of approximately 40-μ thickness deposited on the silicon face of a hexagonal silicon carbide substrate.

geometrical features when examined with an optical microscope. The boron phosphide layers deposited on the carbon face of silicon carbide substrates were found to be polycrystalline in most cases, although those deposited at higher temperatures exhibited some preferred orientations.

When the halide reduction reaction was used for the epitaxial growth process, boron phosphide was also found to deposit on the backside of the silicon carbide substrate. This was due to the transport of boron phosphide from the susceptor to the backside of the substrate by hydrogen halide, the by-product of the thermal reduction reaction. Boron phosphide layers up to 50 μ in thickness have been transported in this manner, and those transferred to the silicon face of the substrate at temperature above 950°C have been found to be single crystalline and epitaxial with respect to the substrate by optical microscopy and reflection electron diffraction examinations. The pyrolysis of a diborane–phosphine mixture has also produced adherent and continuous layers of boron phosphide on silicon carbide substrates at temperatures up to 900°C. When hydrogen containing 0.01% diborane and 0.04% phosphine was used at a flow rate of 0.89 mol/min, the deposition rate of boron phosphide on the silicon carbide substrate at 850°C was 8–10 μ/h. In most cases, the deposit exhibited shiny and smooth surfaces, and no structural features were observed when examined with an optical microscope. However, electron diffraction examinations indicated that the deposit was generally polycrystalline and in a few cases, exhibited some preferred orientations (Fig. 5). The lack of single crystallinity is presumably related to the relatively low temperature used in the growth process.

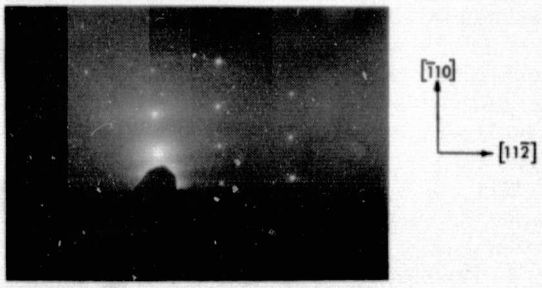

FIG. 4. Reflection electron diffraction pattern of an epitaxial boron phosphide layer deposited on the silicon face of a hexagonal silicon carbide substrate by the thermal reduction of halide mixtures.

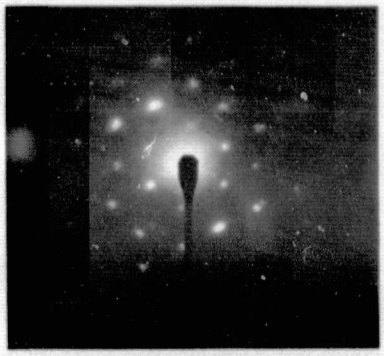

FIG. 5. Reflection electron diffraction pattern of a boron phosphide layer deposited on the silicon face of a hexagonal silicon carbide substrate by the pyrolysis of hydride mixtures.

B. Electrical Properties of Epitaxial Boron Phosphide

Epitaxial boron phosphide layers deposited on the silicon carbide substrates by the thermal reduction process without intentional doping are p type. The resistivity and carrier concentration of a typical specimen deposited at 1150°C, determined by the Hall measurements, are 0.2 Ω cm and 10^{19} cm^{-3}, respectively, at 300°K and are 1 Ω cm and 2×10^{17} cm^{-3}, respectively, at 200°K.

The electrical conductance of an epitaxial boron phosphide layer was measured in the temperature range 300°–1070°K, and the results are shown in Fig. 6. Since the temperature dependence of the carrier mobility is very much smaller than that of the carrier concentration in the temperature range under consideration, the ionization energy of deep-lying impurities may be estimated from the slopes of the various regions of the plot in Fig. 6. Ionization energies estimated in this manner are 0.22±0.04 and 0.66±0.06 eV. At temperatures above 1000°K intrinsic ionization dominates, and the energy gap of boron phosphide was determined to be 1.95±0.1 eV, in agreement with the energy gap from optical measurements.[1]

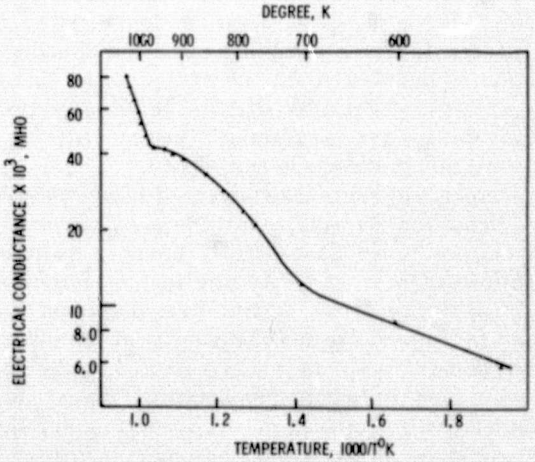

FIG. 6. Electrical conductance of an epitaxial boron phosphide layer as a function of temperature.

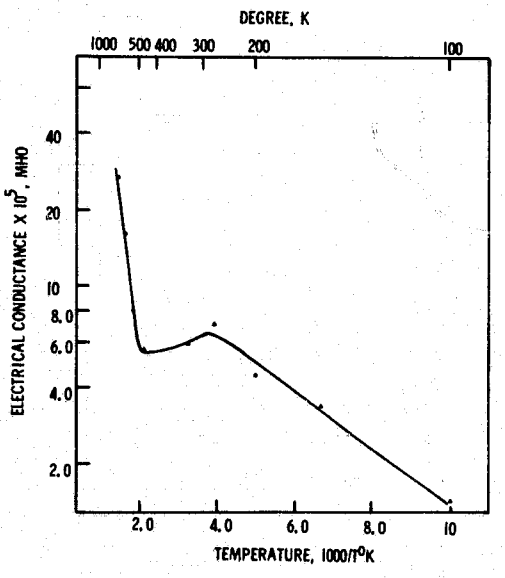

FIG. 7. Electrical conductance of a needle-shaped boron phosphide crystal as a function of temperature

C. Boron Phosphide Crystals

During the epitaxial growth of boron phosphide by the thermal reduction of boron tribromide–phosphorus trichloride mixtures, orange-red needle-shaped boron phosphide crystals were occasionally deposited on the susceptor surface. These crystals were of triangular cross section, with each side approximately 0.2-mm wide, and were up to 5-mm long. The structural properties of these crystals were examined by single-crystal x-ray methods using Cu$K\alpha$ radiation. The oscillation photograph obtained by oscillating the crystal about the elongated axis indicated that the interlayer spacing is 7.88 Å, three times the d_{111} spacing in boron phosphide, and that the elongated axis is a ⟨111⟩ direction. The Weissenberg photograph taken with the crystal rotating about the same axis further confirmed that the needle-shaped crystals are single-crystalline boron phosphide.

The vapor grown boron phosphide crystals without intentional doping are also p type with a room temperature resistivity of approximately 20 Ω cm. The electrical conductance of a typical crystal grown at 1050°C is shown in Fig. 7. Two impurity states are apparent. The shallow state has an activation energy of several hundredths of an electron volt and is responsible for the room-temperature conductivity. The other state has an activation energy of 0.60±0.06 eV, which has also been observed in epitaxial boron phosphide. Further work concerning the impurities in vapor grown boron phosphide is underway and will be discussed in a subsequent publication.

IV. SUMMARY

Adherent boron phosphide layers have been deposited on the basal plane of hexagonal silicon carbide substrates by the thermal reduction of the halide mixtures and the thermal decomposition of the hydride mixtures. The substrate temperature and the polarity of the substrate surface are the most important factors determining the crystallinity of the deposit. Boron phosphide layers deposited on the silicon face of the substrate at 1050°–1150°C by the thermal reduction process have been found to be single crystalline and epitaxial with respect to the substrate. These layers are p type and have an impurity concentration of approximately 10^{19} cm^{-3} at room temperature.

Needle-shaped single crystals of boron phosphide have also been grown by the thermal reduction reaction. These crystals are also p type and contain at least two acceptor impurities.

* This research was supported by the National Aeronautics and Space Administration under Grant NGL 44-007-042.

[1] R. J. Archer, R. Y. Koyama, E. E. Loebner, and R. C. Lucas, Phys. Rev. Lett. **12**, 538 (1964).
[2] C. C. Wang, M. Cardova, and A. G. Fischer, RCA Rev. **25**, 159 (1964).
[3] R. A. Burmeister and P. E. Greene, Bull. Amer. Phys. Soc. **10**, 1184 (1965).
[4] F. V. Williams and R. A. Ruehrwein, J. Amer. Chem. Soc. **82**, 1330 (1960).
[5] A. F. Armington, J. Cryst. Growth **1**, 47 (1967).
[6] A. A. Eliseev and E. G. Zhukov, Sov. Phys. Dokl. **10**, 6 (1965).
[7] K. Brack, J. Appl. Phys. **36**, 3560 (1965).

APPENDIX C

"The Growth of Boron Monophosphide Crystals by Chemical Transport," T. L. Chu, J. M. Jackson, and R. K. Smeltzer, J. Crystal Growth, 15, 254-258 (1972).

Reprinted from:
Journal of Crystal Growth **15** (1972) 254–258 © *North-Holland Publishing Co.*
Printed in the Netherlands

THE GROWTH OF BORON MONOPHOSPHIDE CRYSTALS BY CHEMICAL TRANSPORT*

T. L. CHU, J. M. JACKSON and R. K. SMELTZER

Electronic Sciences Center, Southern Methodist University, Dallas, Texas 75222, U.S.A.

Received 21 April 1972; revised manuscript received 8 May 1972

The crystal growth of boron phosphide, BP, has been investigated by using the closed-tube chemical transport of polycrystalline material, prepared by the hydrogen reduction of a boron tribromide–phosphorus trichloride mixture. Experimental parameters including the nature of the transport agent, source temperature, temperature gradient, and surface condition of the reaction tube, were studied. Using iodine or bromine as a transport agent and a source temperature of 1270–1290 °C, single crystals of boron phosphide, identified by the X-ray diffraction method, were obtained in the form of polyhedra with well-defined faces. Molten potassium hydroxide or a molten mixture of sodium hydroxide–sodium peroxide were used as an etchant to reveal structure defects in boron phosphide crystals. The transported boron phosphide crystals were p-type with a room temperature resistivity of approximately 0.5 ohm-cm. Resistivity measurements in the temperature range 77–350 °K indicated the presence of two impurity states with activation energies of approximately 0.009 and 0.052 eV, respectively. In spite of the high impurity concentrations, the transported crystals are suitable as substrates for the epitaxial growth of boron phosphide.

1. Introduction

Boron monophosphide (BP, boron phosphide hereafter), a semiconductor with an energy gap of 2 eV, has been under study during the past decade because of its potential for high temperature and luminescent devices[1–10]). However, its high melting point (about 3000 °C) and appreciable dissociation pressure at high temperatures (about 24 Torr at 1300 °C) have prohibited the use of melt-grown techniques for the preparation of boron phosphide crystals. On the other hand, lower temperature techniques such as the flux growth from a nickel phosphide solution[5,6]) and the chemical vapor transport in a halide or sulfide atmosphere[8,9]) have been used. The flux growth technique has had moderate success; however, the transport process has produced only very small crystals.

The crystal growth of boron phosphide by the chemical transport technique is based on the reversible reaction between boron phosphide with group VI or group VII elements. The equilibrium of these reactions varies with temperature in such a manner that boron phosphide is transported from a high temperature source to lower temperature regions in a closed-tube. By controlling the nucleation and growth of the transported boron phosphide on the wall of the reaction tube, single crystals can be obtained. The important parameters affecting the quality of the transported crystals include the source temperature, the temperature gradient along the reaction tube, the nature and pressure of the transport agent, and the surface condition in the deposition region of the reaction tube. These parameters have not been studied in detail, and the available information is mainly in the form of preliminary results. The transport process reported thus far was carried out in the temperature range 800–1200 °C[8,9]), and the crystals grown were very small, 0.25–0.3 mm in size.

In the present work, the crystal growth of boron phosphide by the closed-tube chemical transport technique has been studied with emphasis on increasing the transport rate and controlling the formation of initial nuclei. Phosphorus trichloride, bromine, and iodine were used as transport agents. The experimental procedures and results are summarized in this paper.

* This research was supported by the Langley Research Center of the National Aeronautics and Space Administration under Grant NGL 44-007-042.

2. Experimental results and discussion

2.1. Polycrystalline boron phosphide

The polycrystalline boron phosphide source material for the transport process was prepared by the thermal

reduction of a boron tribromide–phosphorus trichloride mixture with hydrogen in a gas flow system. Hydrogen used in the reaction was purified by diffusion through a palladium–silver alloy. Boron tribromide and phosphorus trichloride were purified by fractional distillation using a Pyrex column, and they were introduced into the reaction tube by using hydrogen as a carrier gas. To maintain a constant composition of the reactant mixture, boron tribromide and phosphorus trichloride containers were immersed in a constant temperature bath. A fused silica tube of 25 mm ID, heated in a tube furnace at about 1100 °C, was used as the reaction tube for the deposition of boron phosphide. The typical flow rates of hydrogen, boron tribromide, and phosphorus trichloride were 8×10^{-2}, 1.5×10^{-3}, and 3×10^{-3} moles/min, respectively. An excess of phosphorus trichloride was used to maintain the stoichiometry of the deposit; the excess phosphorus will not condense on the wall of the reaction tube because of its high temperature. The deposition rate was approximately 2 g/hr. The deposit was analyzed by the X-ray powder technique, and the diffraction data were in good agreement with those reported for boron phosphide[2]). The thermoelectric probe measurement indicated that the as-deposited boron phosphide was usually of n-type conductivity.

2.2. Chemical transport of boron phosphide

The growth of boron phosphide crystals by the chemical transport technique was carried out with bromine, iodine, and phosphorus trichloride as transport agents. To carry out the transport process, polycrystalline boron phosphide, phosphorus, and a transport agent were introduced into a thick-wall fused silica tube; phosphorus was used to suppress the decomposition of boron phosphide at high temperatures. The reaction tube was attached to a vacuum manifold, cooled with liquid nitrogen, evacuated to less than 10^{-5} Torr, and sealed. A furnace with two independently-controlled temperature zones was used for the transport reaction. The polycrystalline source material located at one end of the tube was in the higher temperature zone, and the transported boron phosphide deposited on the wall of the tube in the lower temperature zone.

The temperature gradient used in the chemical transport crystal growth process should be as small as possible so that the entire system approaches equilibrium. At small temperature gradients, 25 °C for example, no transport was observed when the temperature of the boron phosphide source was below 1000 °C. Initial experiments were therefore carried out with the source temperature in the range 1000–1150 °C, and the transport rate was found to be determined mainly by the temperature gradient and the pressure of the transport agent. When bromine, iodine, or phosphorus trichloride at 1–2 atm was used as the transport agent, no appreciable transport was observed after several days at a gradient of 25 °C or smaller. When the gradient was increased to 50–75 °C, the transport rate was found to be very slow in all cases. Also, many small crystals, a fraction of a millimeter in size, were deposited on the wall of the reaction tube after 2–3 weeks of reaction time. The low transport rate could be related to the thermodynamics of the transport reaction. The transport takes place via the formation of boron monohalide according to the reaction.

$$4\,BP(s)+2\,BX_3(g) = 6\,BX(g)+P_4(g), \quad X = Cl, Br, \text{ or } I. \tag{1}$$

Although no accurate thermochemical data on boron phosphide are available, qualitative information on reaction (1) can be obtained by considering the transport of boron by boron halides according to the following reaction:

$$2\,B(s)+BX_3(g) = 3\,BX(g), \quad X = Cl, Br, \text{ or } I. \tag{2}$$

The equilibrium constants of reaction (2) in the temperature range 1200–1600 °K, calculated from the standard free energy of formation of boron halides[11]), are summarized in table 1. The equilibrium constant of this reaction, though very small, increases rapidly with increasing temperature, and the transport of boron by boron trihalides becomes more favorable at

Table 1

Equilibrium constants of the reaction between B and BX

Temperature (° K)	X = Cl	X = Br	X = I
1200	2.95×10^{-19}	1.05×10^{-22}	4.42×10^{-20}
1300	1.59×10^{-16}	1.04×10^{-19}	2.71×10^{-17}
1400	3.41×10^{-14}	3.79×10^{-17}	6.53×10^{-15}
1500	3.54×10^{-12}	6.21×10^{-15}	7.51×10^{-13}
1600	2.0×10^{-10}	5.3×10^{-13}	4.7×10^{-11}

higher temperatures. Since boron phosphide has a negative free energy of formation, the equilibrium constants of reaction (1) are smaller than those of reaction (2). Therefore, the transport of boron phosphide must be carried out at as high temperatures as practical, within the capabilities of fused silica, to achieve a reasonable transport rate. The use of higher temperature also limits the formation of initial nuclei, thus favoring the growth of larger crystals.

A series of detailed transport experiments with the source temperature in the range 1270–1290 °C was carried out in fused silica tubes of 10 mm ID, 16 mm OD, and 12 cm long heated in globar furnaces. About 0.5 g of polycrystalline boron phosphide was used in each experiment. A phosphorus pressure of 3 atm and a transport agent pressure of 1 atm were found to be optimum for the transport process. These experimental conditions were used to compare the effects of transport agents. Phosphorus trichloride was found to be the fastest transport agent. With a temperature gradient of 4 °C across the ampoules, essentially all of the boron phosphide was transported in 5–7 days; however, the transported material consisted of loosely bound aggregates of small crystals. The use of iodine or bromine as a transport agent has produced better results. Using iodine as a transport agent and a temperature gradient of 15–20 °C, the source material was transported in 7–10 days to yield orange-red crystals. The transported crystals were in the form of discs of about 5 mm diameter and 1–2 mm thickness and in the form of polyhedrons measuring 1–2 mm on each side. Optical microscope examinations indicated that the discs consist of several single crystal grains and that the polyhedrons appear to be single crystalline. Fig. 1 shows a photograph of several polyhedrons. Their faces are predominately triangular and rectangular. Single-crystal X-ray oscillation and Weissenberg methods indicated that the polyhedrons are single crystalline and that the rectangular face is of a {110} orientation. Similar crystals were obtained by using bromine as a transport agent with a 5 °C gradient.

In the technique described above for the crystal growth of boron phosphide, the nucleation takes place on the wall of the reaction tube, and the surface condition of the wall plays an important role in the nucleation process. The commercial fused silica tube frequently has surface irregularities on the inside wall,

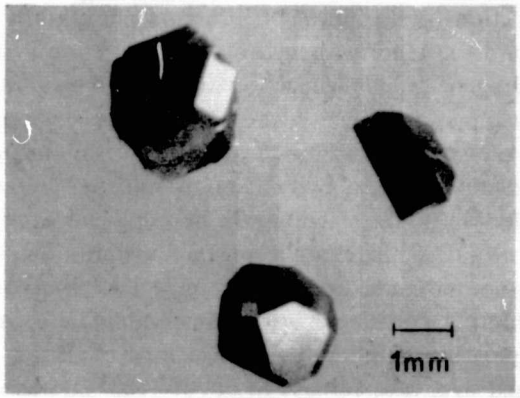

Fig. 1. Boron phosphide crystals obtained by the chemical transport technique.

thus promoting the formation of random nuclei. The resulting crystals are therefore small, and the growth process is not reproducible. To control the nucleation process, the deposition region of the reaction tube was flame-worked to remove any surface irregularities. Several experiments were carried out with flame-worked tubes using bromine as a transport agent and a 5 °C gradient along the tube. In about one-half of the experiments, no nucleation occurred on the wall of the reaction tube after ten days; a considerable number of crystallites would have formed if the wall of the reaction tube were not flame-treated. In the other half of the experiments, only one aggregate consisting of tightly bound single crystals up to 2 mm was formed at the tip of the reaction tube. These experiments indicate that flameworking of fused silica tube is a critical factor to achieve the control of nucleation in the closed tube transport process.

2.3. Properties of transported boron phosphide crystals

The boron phosphide crystals obtained in this work, because of the use of higher temperatures and the control of random nucleation, are considerably larger than the transported crystals reported in the literature. They have well-formed faces, in contrast to the dendritic crystals of comparable size obtained by Grindberg et al.[8])

The transported boron phosphide crystals are p-type, as determined by the thermoelectric probe technique and by the direction of point-contact rectification. The hardness of the boron phosphide crystals was measured by the diamond pyramid hardness test. A

square base diamond pyramid was forced into the specimen using a 1 kg load, and the diagonals of the impression were measured. The hardness of boron phosphide was calculated to be approximately 2450 kg mm^{-2} as compared with 2970 for silicon carbide determined under the same conditions.

The transported boron phosphide crystals are chemically inert, insoluble in aqueous acids and alkalis. At high temperature, 1000 °C for example, boron phosphide crystals may be etched non-preferentially by a mixture of hydrogen and hydrogen chloride. Molten potassium hydroxide or a molten mixture of 75% sodium hydroxide and 25% sodium peroxide at 380 °C may be used as a preferential etchant to reveal defects in boron phosphide crystals. Fig. 2 shows the etch

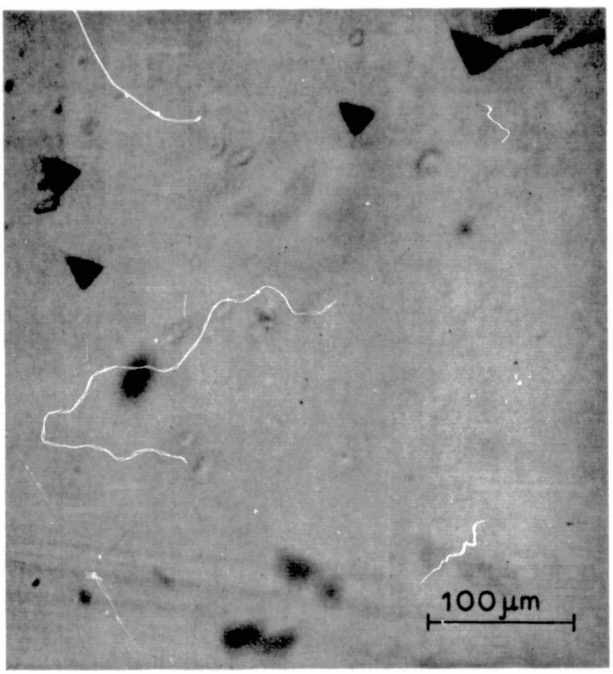

Fig. 2. Etch figures showing dislocations in a transported boron phosphide crystal (molten KOH etch, 8 min).

figures on a rectangular face of a boron phosphide crystal after the as-grown surface was etched in molten potassium hydroxide for 8 min. The isosceles triangular figures are dislocation pits, and the geometry of these pits also confirms the {110} orientation of the rectangular face of the crystal. The $(111)_A$ and $(111)_B$ faces also exhibit different etching behavior in a molten mixture of sodium hydroxide and sodium peroxide.

The electrical conductivity of transported boron phosphide crystals was measured over a wide temperature range. The crystals were mechanically polished to yield two flat parallel faces by using 1 µm alumina abrasives and were thoroughly cleaned for the application of ohmic contacts. Indium was selected as the contact material on the basis of its ability to wet boron phosphide. The cleanliness of the metal and the crystal surface was found to be very important for obtaining good wetting. After applying indium to the flat faces, the specimen was annealed in an argon atmosphere at various temperatures. The annealing of the specimen at 500 °C for 1 h was found to be satisfactory for producing low resistance ohmic contacts to transported boron phosphide crystals. The dc current–voltage characteristics of a number of transported crystals were measured in the temperature range 77–350 °K. A typical plot of logarithm conductance versus reciprocal temperature is shown in fig. 3. The room temperature resistivity of this crystal is approximately 0.55 ohm-cm. Two linear regions may be distinguished in the plot of fig. 3. Neglecting the temperature dependence of carrier mobility, the slopes of these two regions indicate the presence of two impurity states with activation energies of 0.009 and 0.052 eV, respectively.

The room temperature carrier concentration in transported boron phosphide crystals was estimated

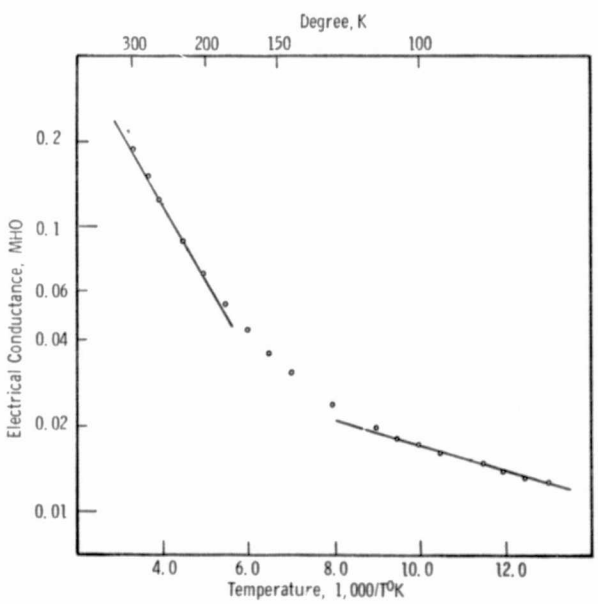

Fig. 3. Electrical conductance of a transported boron phosphide crystal as a function of temperature.

from Schottky barrier measurements to be of the order of 10^{18} cm^{-3}. Thus, the transported crystals are not useful directly for device purposes. However, they are suitable as substrates for the epitaxial growth of boron phosphide, and the dopant concentration in the epitaxial layer can be better controlled. Both n- and p-type epitaxial boron phosphide layers as well as p–n junctions have been prepared by the thermal reduction of a boron tribromide–phosphorus trichloride mixture with hydrogen using the transported crystals as substrates. These results will be discussed in a subsequent communication.

3. Summary

Single crystals of boron phosphide have been prepared by the closed-tube chemical transport technique. Best results were obtained by using iodine or bromine as a transport agent in a flame-worked reaction tube, a source temperature of 1270–1290 °C, and a small temperature gradient. The use of a flame-worked tube and high source temperature has resulted in larger and better quality crystals than previously reported. Structural defects in boron phosphide crystals can be revealed by using molten potassium hydroxide or a molten mixture of sodium hydroxide and sodium peroxide as an etchant. The transported crystals are p-type and have a room temperature resistivity of about 0.5 ohm-cm. Resistivity measurements in the temperature range 77–350 °K indicated the presence of two impurity states with activiation energies of approximately 0.009 and 0.052 eV, respectively. The transported crystals have been successfully used as substrates for the epitaxial growth of boron phosphide.

Acknowledgment

The authors wish to thank Dr. Shirley S. Chu for her assistance in the X-ray diffraction work reported here.

References

1) P. Popper and T. A. Ingles, Nature **179** (1957) 1075.
2) J. A. Perri, S. LaPlaca and B. Post, Acta Cryst. **11** (1958) 310.
3) K. Vickery, Nature **184** (1959) 268.
4) F. V. Williams and R. A. Ruehrwein, J. Am. Chem. Soc. **82** (1960) 1330.
5) B. Stone and D. Hill, Phys. Rev. Letters **4** (1960) 282.
6) C. C. Wang, M. Cardona and A. G. Fischer, RCA Rev. **25** (1964) 159.
7) R. J. Archer, R. Y. Koyana, E. E. Loebner and R. C. Lucas, Phys. Rev. Letters **12** (1964) 538.
8) Ya. Kh. Grinberg, Z. S. Medvedeva, A. A. Eliseev and F. G. Zhukov, Soviet Phys.-Dokl. **10** (1965) 6.
9) A. F. Armington, J. Crystal Growth **1** (1967) 47.
10) T. L. Chu, J. M. Jackson, A. E. Hyslop and S. C. Chu, J. Appl. Phys. **42** (1971) 420.
11) *JANAF Interim Thermochemical Tables* (Dow Chemical Company, Midland, Michigan, 1965).

APPENDIX D

"The Crystal Growth of Boron Monophosphide from Metal Phosphide Solutions," T. L. Chu, J. M. Jackson, and R. K. Smeltzer, J. Electrochem. Soc., 120, 802-806 (1973).

The Crystal Growth of Boron Monophosphide from Metal Phosphide Solutions

T. L. Chu,* J. M. Jackson, and R. K. Smeltzer*

Electronic Sciences Center, Southern Methodist University, Dallas, Texas 75222

Reprinted from JOURNAL OF THE ELECTROCHEMICAL SOCIETY
Vol. 120, No. 6, June 1973
Printed in U.S.A.

The Crystal Growth of Boron Monophosphide from Metal Phosphide Solutions

T. L. Chu,* J. M. Jackson, and R. K. Smeltzer*

Electronic Sciences Center, Southern Methodist University, Dallas, Texas 75222

ABSTRACT

The crystal growth of boron phosphide, BP, has been investigated using two approaches: (*i*) the addition of phosphorus to a boron-nickel or boron-copper melt, and (*ii*) the recrystallization of boron phosphide from a nickel phosphide or copper phosphide solution in a temperature gradient. To determine the optimum conditions for the growth processes, the solubility of boron phosphide in nickel phosphide ($Ni_{12}P_5$) and copper subphosphide (Cu_3P) was determined over a wide temperature range. The solubility of boron phosphide in nickel phosphide was found to be higher than that in copper phosphide. Boron phosphide crystals of about 3-mm size were obtained by the addition of phosphorus to a boron-nickel or boron-copper melt at 1300°C or above, followed by slow cooling. The temperature gradient recrystallization of boron phosphide from nickel phosphide at 1200°C has produced larger crystals. The solution-grown crystals were in the form of hoppers and platelets with platelets dominating. The platelets had main faces of {111} orientation and were formed by the twin-plane re-entrant-edge mechanism. The solution-grown crystals are usually n-type with a room temperature resistivity of about 0.5 ohm-cm and a dopant concentration of about 10^{18} cm^{-3}. They have been used successfully as substrates for the epitaxial growth of boron phosphide.

Boron monophosphide (BP, referred to as boron phosphide hereafter) crystallizes in the zincblende structure and has an indirect energy gap of about 2 eV (1). Because of its relatively large energy gap, this material has potential applications for high-temperature devices and for visible light-emitting devices. However, these devices have not been developed because of the difficulties involved in the growth of single crystals of boron phosphide of controlled chemical and structural perfection. Conventional melt-growth techniques are not feasible for the crystal growth of boron phosphide because of its high melting point (3000°C) and its dissociation into boron subphosphide (B_6P) at temperatures considerably below the melting point (2). Boron phosphide crystals have been grown from metal phosphide solutions and by the chemical transport technique under conditions where its thermal dissociation is negligible.

The growth of boron phosphide crystals from metal phosphide solutions has been briefly reported in several investigations (1, 3-5); however, no information concerning the effects of various process parameters is available. In the present work, the process parameters in the solution growth of boron phosphide have been extensively studied with the objective of producing

* Electrochemical Society Active Member.

Key words: boron phosphide, crystal growth, nickel phosphide, semiconductors, twin planes.

larger crystals suitable as substrates for the epitaxial growth of boron phosphide (6); the epitaxial growth technique is believed to be the most promising approach for the preparation of boron phosphide device structures, since the concentration and distribution of dopants in the epitaxial layer can be reproducibly controlled. Copper and nickel phosphides were used as solvents, and the growth process was carried out by the addition of phosphorus to a boron-metal melt and by the recrystallization of boron phosphide from a metal phosphide solution in the presence of a temperature gradient. The experimental procedures and results are summarized below.

Solubility of Boron Phosphide in Metal Phosphides

The most important parameter in the solution-growth process is the choice of a suitable solvent. The solvent must either be essentially insoluble in boron phosphide, or it must be electrically inactive if it has significant solubility.

Several metals, such as copper, iron, nickel, and platinum, are possible solvent-formers for the solution growth of boron phosphide, and copper and nickel phosphides appear to be the most useful ones on the basis of the available information. An examination of binary phase diagrams (7-9) reveals the following relations: (*i*) boron is soluble in copper and nickel over a wide temperature range: nickel forms four borides (Ni_2B, Ni_3B_2, NiB, and Ni_2B_3) and copper forms no borides, (*ii*) nickel forms at least eight phosphides: Ni_3P, Ni_5P_2, $Ni_{12}P_5$, Ni_2P, Ni_5P_4, NiP, NiP_2, and NiP_3, and the first four phosphides have melting points below 1200°C, and (*iii*) copper forms two phosphides: Cu_3P and CuP_2 (10). Thus, the B-Cu-P system is relatively simple, and the use of nickel phosphide for the solution growth of boron phosphide may involve rather complicated mixtures.

To determine the conditions for the growth of boron phosphide crystals from solutions, the solubilities of boron phosphide in nickel and copper phosphides were determined over a wide temperature range. Polycrystalline boron phosphide, nickel phosphide, and copper phosphide were first prepared as follows.

Boron phosphide was prepared by the thermal reduction of a boron tribromide-phosphorus trichloride mixture with hydrogen in a gas flow system. A mixture of hydrogen, boron tribromide, and phosphorus trichloride, at flow rates of 8×10^{-2}, 1.5×10^{-3}, and 3×10^{-3} moles/min, respectively, was introduced into a fused silica tube heated at about 1100°C in a resistance-heated furnace. The reaction took place on the wall of the silica tube, depositing boron phosphide. The excess of phosphorus trichloride in the reactant prevented any phosphorus deficiency in the deposit. The deposit was confirmed to be boron phosphide by the x-ray Debye-Scherrer technique. Approximately 30g of boron phosphide was formed during an 8-hr period.

Nickel phosphide was synthesized by the reaction of phosphorus vapor with nickel under conditions similar to those used for the solution growth of boron phosphide, and a schematic diagram of the apparatus is shown in Fig. 1. An alumina boat containing a nickel ingot was fitted into a cylindrical graphite sleeve of 1 in. ID and 1¼ in. OD, which was used as a susceptor for rf heating. The susceptor was positioned in a fused silica spacer so that the graphite contacted the spacer only at four points. This assembly and an excess of red phosphorus were placed in a fused silica tube of 50 mm ID and 55 mm OD which was evacuated to less than 10^{-5} Torr and sealed. The reaction tube was about 45 cm long after sealing. The end of the tube containing the susceptor and phosphorus was heated to sublime all phosphorus to the other end of the tube. The susceptor was heated at the desired temperature, 1200°-1400°C, with an rf generator, and a resistance heater surrounding a major portion of the reaction tube was used to maintain the phosphorus pressure in

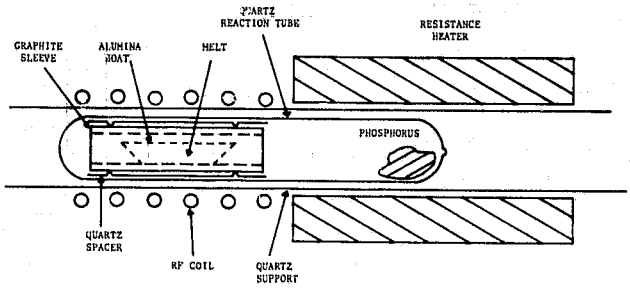

Fig. 1. Schematic diagram of the apparatus used for the synthesis of nickel phosphide and the solution growth of boron phosphide.

the tube at about 2 atm. The nickel appeared to be saturated with phosphorus after several hours; however, the reaction time was usually 24 hr or longer to assure saturation. The x-ray Debye-Scherrer pattern of the resulting product was identical with that of $Ni_{12}P_5$ (11). Nickel phosphides with higher phosphorus content were not obtained.

Copper phosphide was synthesized by the reaction of phosphorus vapor with copper in a closed tube. Weighed amounts of copper and red phosphorus were placed in a fused silica tube, evacuated to less than 10^{-5} Torr, and sealed. The reaction tube was then placed in a two-temperature zone furnace. Copper located at one end of the tube was heated at 1150°C, and the temperature of the other zone was maintained to yield a phosphorus pressure of about 1 atm. Depending on the Cu/P molar ratio in the reactants, Cu_3P or CuP_2, identified by their x-ray Debye-Scherrer patterns (10, 12), were obtained.

To determine the solubility of boron phosphide, a pulverized mixture of 1.0g boron phosphide, 0.04g red phosphorus, and 10.0g nickel phosphide ($Ni_{12}P_5$) was sealed in an evacuated fused silica tube of 10 mm ID and 16 mm OD; phosphorus was used to suppress the decomposition of boron phosphide at high temperatures. The boron phosphide was sieved through a 74μ screen so that the amount of recrystallized material, which would have considerably larger particle size, could be easily determined. The silica tube was fitted into a cylindrical graphite susceptor. The susceptor was sealed into a second silica tube containing about 0.2 atm of argon (the argon pressure was used to suppress the expansion of the inner tube at high temperatures), and the susceptor was at least 1 cm from the tube wall so that the susceptor could be heated to high temperatures. The graphite susceptor was then heated with an rf generator at the desired temperature, 1200°-1400°C for 5-24 hr. The content of the reaction tube was treated with a nitric acid-hydrofluoric acid mixture to dissolve all species except boron phosphide. Whenever recrystallization had occurred, the residual boron phosphide was found to contain small orange-red crystals in addition to the original powder material, and the crystals were separated by sieving the mixture through a 74μ screen. The recovered powder material was undissolved boron phosphide, and the collected crystalline material was recrystallized boron phosphide. In all cases, boron phosphide was not completely recovered due presumably to the complexity of the Ni-B-P system. At 1300°C, for example, 0.75g of boron phosphide dissolved in 10g of nickel phosphide, whereas only 0.23g recrystallized from the solution. The weights per cent of boron phosphide dissolved in, and recrystallized from, nickel phosphide at various temperatures is shown in Fig. 2. It is seen that it has a significant solubility in nickel phosphide at 1200°C, even though this temperature is just above the melting point of nickel phosphide.

The melting point of copper subphosphide, Cu_3P, is 1022°C. The solubility of boron phosphide in copper subphosphide was determined at 1150° and 1220° in a manner similar to that described above. Boron phosphide was found to be essentially insoluble in copper

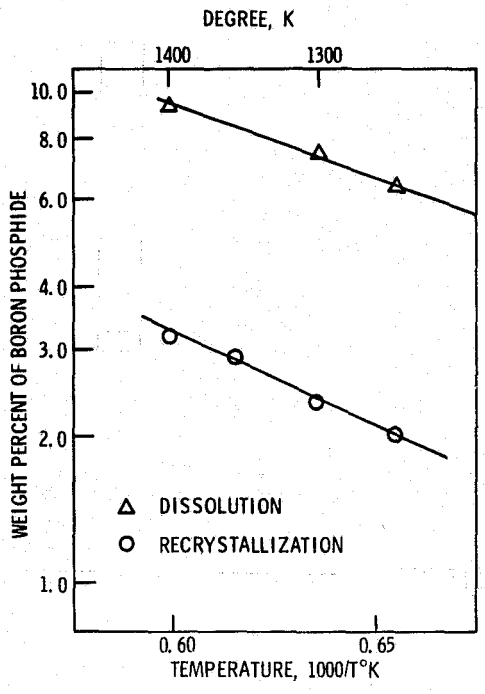

Fig. 2. Dissolution and recrystallization of boron phosphide as a function of temperature using nickel phosphide as a solvent.

subphosphide at 1150°C. When the experiment was carried out at 1220°C for 48 hr, about 85% of the boron phosphide was recovered, and 0.64% (weight) of the initial boron phosphide recrystallized. Thus, boron phosphide is less soluble in copper subphosphide than in nickel phosphide. Also, boron phosphide was found to be insoluble in copper diphosphide, CuP_2, at temperatures up to 1200°C.

Growth of Boron Phosphide Crystals by the Addition of Phosphorus to a Boron-Metal Melt

The slow cooling of a phosphorus-saturated solution of boron in nickel was used for the growth of boron phosphide crystals. The apparatus is the same as that used for the preparation of nickel phosphide shown in Fig. 1. A boron-nickel ingot was prepared by melting weighed quantities of boron and nickel in an alumina boat in a hydrogen atmosphere. Typically, 40g of nickel was used, and the melt was maintained at 1400°C for at least 1 hr to form a homogeneous mixture. The resulting ingot was then sealed in the reaction tube in a manner as shown in Fig. 1. After maintaining a phosphorus pressure over the melt at a predetermined temperature, boron and nickel were converted into the corresponding phosphides. The solution was slowly cooled, and the resulting material was treated with nitric acid to isolate the boron phosphide crystals.

The important process parameters including the phosphorus pressure over the solution, the initial concentration of boron in solution, the temperature of the solution, the reaction time, and the cooling rate, were studied in a number of experiments. A phosphorus pressure of 2-3 atm was found to be optimum; lower pressure resulted in the formation of boron subphosphide B_6P, and higher pressures created such strong convection currents in the reaction tube that the phosphorus pressure could not be controlled. The concentration of boron in nickel was first selected on the basis of the data shown in Fig. 2. The boron-nickel alloy used for crystal growth at 1325°C should contain 2.3% (weight) boron so that, after saturating with phosphorus, the resulting solution of boron phosphide in nickel phosphide would be slightly undersaturated. The solution was maintained at 1325°C for 4 hr and then cooled at a rate of 10°C/hr to about 1150°C. The boron phosphide crystals obtained in this manner were up to 3 mm in size, and the yield was about 50% on the basis of the amount of boron used. Several changes in the process parameters were then made. Higher temperatures did not noticeably change the size distribution or yield of the crystals; however, crystals were smaller on the average at temperatures below 1300°C. The use of higher concentrations of boron in nickel, up to 10%, also did not change significantly the size of boron phosphide crystals. By maintaining the solution at high temperatures under the phosphorus pressure over extended periods, the yield of boron phosphide crystals was slightly increased, but the results were no better in other aspects. Also, no improvements in crystal size were obtained with cooling rates of less than 10°C/hr. Experiments were also carried out by slowly pulling the reaction tube out of the rf coil, and the results were inferior to the slow cooling of the entire solution. To eliminate the possibility that particulate matter from the graphite susceptor had induced excessive nucleation in solution, one experiment was carried out using a molybdenum susceptor and produced very similar results.

A series of experiments was carried out using the addition of phosphorus to a boron-copper melt. Although the solubility of boron in copper is less than that in nickel, the effects of the alloy composition, temperature, reaction time, and cooling rate on the size distribution of crystals were essentially the same as the use of a boron-nickel melt.

Growth of Boron Phosphide Crystals by Recrystallization from Metal Phosphide Solutions

The addition of phosphorus to a boron-nickel or boron-copper melt requires a reaction temperature of at least 1300°C for obtaining boron phosphide crystals of reasonable size. Lower temperature techniques are preferable, and the temperature dependence of the solubility of boron phosphide in metal phosphides was utilized for the crystal growth of boron phosphide by the temperature gradient recrystallization technique. In this technique, a small temperature gradient is maintained across a saturated solution of boron phosphide in a metal phosphide with a polycrystalline boron phosphide source in the higher temperature region. A concentration gradient is thus set up across the solution, and this gradient results in the transport of boron phosphide from the polycrystalline source to the lower temperature region in the solution. The nucleation process in this region can be controlled to yield relatively large crystals.

The recrystallization experiments were carried out in vertical fused silica tubes using a resistance-heated furnace for recrystallization temperatures up to 1200°C and rf heating for higher temperatures. Since the density of boron phosphide is considerably lower than that of metal phosphide solutions, the top of the reaction tube was in the highest temperature region in the majority of the experiments. In a typical high-temperature experiment, 1.5g of polycrystalline boron phosphide and 35g of copper subphosphide were placed in a graphite cylinder of 1 in. ID and 3 in. in height. The crucible was supported by a fused-silica holder and sealed in a fused-silica tube with sufficient phosphorus to yield 2 or 3 atm pressure during recrystallization. The graphite crucible was heated with an rf generator. The top of the solution was maintained at about 1300°C and the bottom was a few degrees cooler. The crucible was slowly cooled after one day, and the resulting boron phosphide was completely recrystallized with crystals up to 2 mm in size. These results were not significantly improved by using nickel phosphide as the solvent or by using a silica liner in the graphite crucible. The relatively small size of boron phosphide crystals obtained in these experiments are presumably due to the high recrystallization rate resulting from the difficulty of controlling a small temperature gradient with rf heating.

The recrystallization experiments at lower temperatures have produced crystals superior to the high-temperature experiments. The best results were obtained with nickel phosphide solutions. In a typical experiment, 0.5g of boron phosphide, 15g of nickel phosphide, and 0.08g of phosphorus were placed in a fused silica tube of 10 mm ID × 16 mm OD, which was evacuated and sealed. The tube was held in a vertical furnace so that the top of the solution was at the highest temperature, 1200°C, and a 5°C gradient existed across the solution. After three weeks, boron phosphide crystals, mostly in the form of platelets up to 4 mm in size, were obtained. At 1150°C or below, no measurable recrystallization was observed after two weeks. Thus, among the techniques investigated in this work, the temperature gradient recrystallization of boron phosphide from nickel phosphide at 1200°C appears to be best suited for the growth of boron phosphide crystals.

Properties of Solution-Grown Boron Phosphide Crystals

Boron phosphide crystals obtained in this work were in the form of hoppers and platelets, with platelets dominating among crystals grown by the recrystallization technique. They are chemically inert, insoluble in aqueous acids and alkalis. Molten potassium hydroxide or a molten mixture of 3:1 sodium hydroxide-sodium peroxide was used as a preferential etchant to reveal structural defects in boron phosphide crystals.

The platelets are usually in the six-sided form, intermediate between a regular hexagon and an equilateral triangle. Figure 3 shows several boron phosphide platelets obtained by the recrystallization technique. The platelets usually have one smooth main face, and the x-ray Laue back-reflection technique indicated that the main face is of {111} orientation. The platelets are also characterized by a twinned structure with twinning taking place about {111} planes. Figure 4 shows the angle-lapped and chemically etched surface of a boron phosphide platelet; the parallel lines are grooves and are the intersections of the twin planes with the angle-lapped surface. In this case, the twin planes are 2-4μ apart. Twinning has been shown to be essential for the growth of the platelets (13). Since the {111} faces are the slowest growing, a stable octahedral structure bounded by these planes would be formed without twinning, and additional growth onto this structure would be difficult because of the high energy of nucleation on the {111} faces. In the twinned structure, however, intersection of the twins forms re-entrant grooves on alternating edges in three of the six equivalent <211> directions that lie in the plane of the twins. The twins intersect at ridges on the other three edges. The grooves provide locations for multiple attachment of new atoms so the energy of nucleation is lowered and growth can ensue preferentially in those directions.

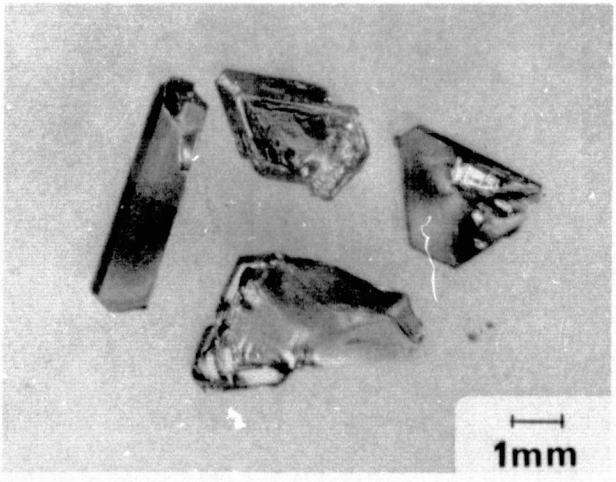

Fig. 3. Typical boron phosphide platelets grown by recrystallization from a nickel phosphide solution at 1200°C.

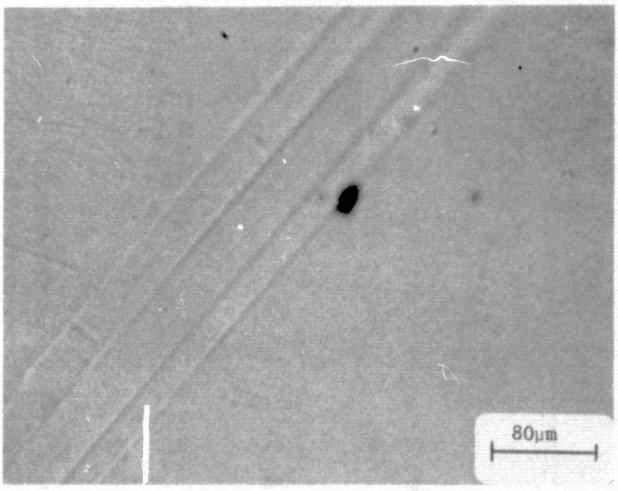

Fig. 4. Angle-lapped and chemically etched surface of a boron phosphide platelet showing the presence of twins.

The hopper-faced boron phosphide crystals were frequently obtained from solutions with a high boron concentration. The crystals consist of separate but often interleaved {111} platelets grown out at different levels from intersecting faces. Edges are favored growth sites in this structure. Although the presence of hopper crystals indicates that many of the solutions were too concentrated, the size and shape of the well-formed twinned crystals did not vary with the presence or absence of the hopper type.

The solution-grown boron phosphide crystals exhibit both n- and p-type conductivity with the n-type predominant. Their electrical conductivities have been measured in the temperature range 77°-500°K. Ohmic contacts were obtained by evaporating indium onto the surface of the crystal followed by annealing at 500°C. A typical conductance-temperature relation of an n-type crystal is shown in Fig. 5. An activation energy of about 0.13 eV dominates in the temperature range 200°-500°K; however, the conductivity is controlled by shallow levels which could not be determined from the data here. Typical resistivities are 0.5 ohm-cm at room temperature and 50 ohm-cm at 77°K.

The room-temperature carrier concentration in solution-grown boron phosphide crystals was estimated from Schottky barrier measurements. Gold dots of 0.01-in. diameter evaporated onto the surface of the crystal were used as the barrier. Capacitance-voltage data from a number of samples has yielded net donor concentrations on the order of 10^{18} cm^{-3}.

The solution-grown boron phosphide crystals are not directly useful for device purposes because the dopant concentration and distribution in these crystals cannot be readily controlled. However, they are ideal as substrates for the epitaxial growth of boron phosphide. Both n- and p-type epitaxial layers with controlled dopant concentration have been deposited on the solution grown crystals by the thermal reduction of a boron tribromide-phosphorus trichloride mixture with hydrogen. The properties of these epitaxial layers will be discussed in another publication.

Summary and Conclusions

Single crystals of boron phosphide have been prepared from metal phosphide solutions by two techniques: (i) the addition of phosphorus to a boron-nickel or boron-copper melt at 1300°C followed by slow cooling of the resulting solution, and (ii) the recrystallization of boron phosphide from a nickel phosphide or copper phosphide solution at 1200°C in a temperature gradient. The solution-grown crystals are in the form of hoppers and platelets with platelets domi-

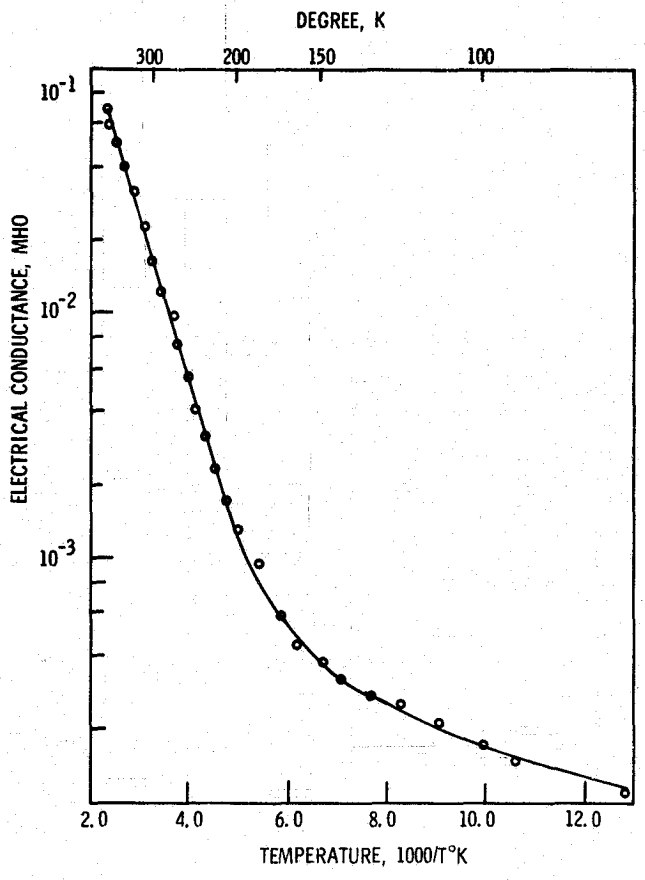

Fig. 5. Electrical conductance of a solution-grown boron phosphide crystal as a function of temperature.

nating. The twin-plane re-entrant-edge mechanism is responsible for the formation of platelets The solution-grown crystals have a dopant concentration on the order of 10^{18} cm^{-3} and are not useful directly for device purposes. They have been used successfully as substrates for the epitaxial growth of boron phosphide.

Acknowledgment

This research was supported by the Langley Research Center of the National Aeronautics and Space Administration under Grant NGL 44-007-042.

Manuscript submitted July 5, 1972; revised manuscript received Dec. 19, 1972. This was Paper 53 presented at the Houston, Texas, Meeting of the Society, May 7-11, 1972.

Any discussion of this paper will appear in a Discussion Section to be published in the December 1973 JOURNAL.

REFERENCES

1. C. C. Wang, M. Cardona, and A. G. Fischer, *RCA Rev.*, **25**, 159 (1964).
2. F. V. Williams and R. A. Ruehrwein, *J. Am. Chem. Soc.*, **82**, 1330 (1960).
3. B. Stone and D. Hill, *Phys. Rev. Letters*, **4**, 282 (1960).
4. B. V. Baranov, V. D. Proclukhan, and N. A. Goryunova, *Izv. Akad. Nauk SSSR, Neorgan. Materialy*, **3**, 1691 (1967) [English translation, p. 1477].
5. M. Iwami, N. Fujita, and K. Kawabe, *Jap. J. Appl. Phys.*, **10**, 1746 (1971).
6. T. L. Chu, J. M. Jackson, A. E. Hyslop, and S. C. Chu, *J. Appl. Phys.*, **42**, 420 (1971).
7. M. Hansen, "Constitution of Binary Alloys," McGraw-Hill Book Co., New York (1958).
8. F. A. Shunk, "Constitution of Binary Alloys, Second Supplement," McGraw-Hill Book Co., New York (1969).
9. E. Larsson, *Arkiv Kemi*, **23**, 335 (1965).
10. O. Olofsson, *Acta Chem. Scand.*, **19**, 229 (1965).
11. S. Rundqvist and E. Larson, *ibid.*, **13**, 551 (1959).
12. H. Haraldsen, *Z. Anorg. Chem.*, **240**, 337 (1939).
13. J. W. Faust, Jr. and H. F. John, *J. Phys. Chem. Solids*, **25**, 1407 (1964).

APPENDIX E

"Epitaxial Growth of III-V Compounds for Electroluminescent Light Sources," T. L. Chu and R. K. Smeltzer, IEEE Trans. Parts, Hybrids, and Packaging, PHP-9, 208-215 (1973).

Epitaxial Growth of III-V Compounds for Electroluminescent Light Sources

TING L. CHU and R. K. SMELTZER

Abstract—**During the past decade, semiconductor junction electroluminescence has evolved from a laboratory phenomenon to a manufacturing technology. This success can be attributed to the extensive research in the preparation and characterization of III-V compounds. Materials emitting radiation in various regions of the visible spectrum are now available.**

The epitaxial growth techniques used in the fabrication of III-V compound electroluminescent devices are reviewed. Both vapor and liquid phase epitaxial techniques are discussed, including the applications of these techniques to well established materials as well as newer materials. The state of the art of light-emitting devices fabricated from members of the III-V compounds and their solid solutions is also reviewed.

Introduction

During the past decade, junction electroluminescence, the emission of radiation from a semiconductor p-n junction under forward bias, has evolved from a laboratory phenomenon to a manufacturing technology. Electroluminescent junction devices, commonly known as light-emitting diodes, fabricated from several III-V compounds are now produced at reasonable costs and are used extensively as incoherent light sources. They have replaced gas discharge or filamentary indicators and displays in many applications and have potential applications for optical coupling, communication links, data transmission, etc. Light-emitting diodes have a number of advantages over other light sources: very fast response time, low voltage and power requirements, long life and high reliability, nearly monochromatic radiation output, small size and light weight, and compatibility with integrated circuitry. The efficiencies of light-emitting diodes have been continually improved and costs drastically reduced during the few years since they became commercially available. Continued efforts in these areas are expected to lead to increased utilization of light-emitting diodes in new applications and new products.

The success of junction electroluminescent technology can be attributed to the extensive research and development in the preparation and characterization of III-V compounds and their solid solutions. The present technology of III-V compounds is considerably more advanced than that of other electroluminescent materials, such as silicon carbide and II-VI compounds. Silicon carbide, though it emits radiation in the visible region, cannot be readily prepared in the form of single crystals with a controlled concentration of dopants because of the high processing temperature, about 2500°C, required. Several II-VI compounds have band gaps suitable for visible light emission; however, they can only be prepared in the form of n- or p-type crystals, and p-n junctions cannot be formed. On the other hand, several III-V compounds have been manufactured in the form of single crystals with controlled concentration and distribution of dopants, and only these compounds are useful for economical electroluminescent junction devices at present.

The band gaps of the III-V semiconductors are in the range from 0.18 to 3.3 eV, corresponding to radiation with wavelengths in the range of 69 000-3700 Å. (Boron and aluminum nitrides, with band gaps of approximately 10 and 6 eV, respectively, are considered as insulators.) These data are summarized in Fig. 1. The wavelength of the emitted radiation may also be tailored by using a ternary compound, i.e., a solid solution of two III-V compounds with one element in common. For example, gallium arsenide, a direct gap material, and gallium phosphide, an indirect gap material, form a continuous series of solid solutions, and the wavelength of the luminescence may be varied continuously from 8680 to 5540 Å according to the composition of the solid solution. The efficiency of the conversion of electrical energy to optical energy can be measured in terms of external quantum efficiency (ratio of external photon current to electron current) and internal quantum efficiency (ratio of internal photon current to electron current). The external quantum efficiency (the most often measured quantity) could be considerably lower than the internal quantum efficiency because of optical losses in extracting the emitted radiation from the semiconductor. At the present state of the art, the external efficiency of visible light-emitting diodes is up to about 7% at room temperature, although the internal efficiency could exceed 50%. The quantum efficiency is not the only important criterion for visible light-emitting diodes. The brightness is

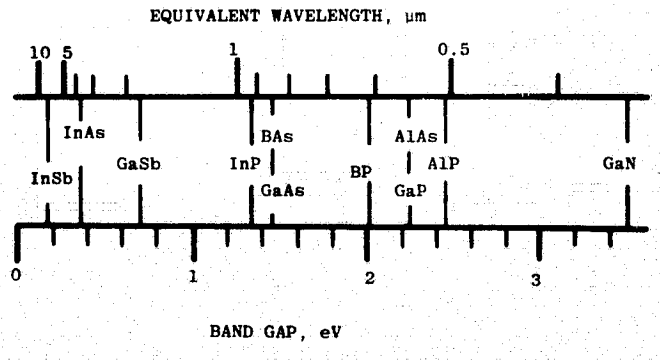

Fig. 1. Room temperature band gap and equivalent wavelength of III-V compound semiconductors.

Manuscript received July 16, 1973; revised August 4, 1973. This work was supported by the NASA Langley Research Center under Grant NGL 44-007-042.

T. L. Chu is with the Institute of Technology, Southern Methodist University, Dallas, Tex. 75275.

R. K. Smeltzer is with the Semiconductor Research and Development Laboratory, Texas Instruments, Inc., Dallas, Tex. 75222.

used as a measure of the visual response to the radiation emitted from the diode surface and is proportional to the external quantum efficiency of the diode and to the sensitivity of the eye. Brightness in excess of 1000 footlamberts is readily available in commercial devices at normal current densities of 10 A/cm^2.

The III-V electroluminescent junction devices have been fabricated by diffusion and epitaxial growth techniques, with the latter dominating. The main objective of this paper is to review the epitaxial growth of III-V compounds and their solid solutions and the current status of their devices. The theory of junction electroluminescence is also briefly discussed. For a comprehensive discussion of light-emitting diodes, the reader is referred to a recent publication by Bergh and Dean [1].

II. Basic Theory of Junction Electroluminescence

At present, the p-n junction formed by selected members of III-V compounds is the most efficient electroluminescent device. The emission characteristics are determined by the band gap and band structure of the semiconductor and the nature and concentration of dopants in the junction region. The light emission from a p-n junction consists of two steps: the injection of minority carriers across the junction, and the radiative recombination of excess carriers.

Minority carrier injection is a relatively simple process. Fig. 2(a) shows the energy band diagram of a p-n junction at equilibrium, where a built-in voltage prevents the diffusion of electrons and holes across the junction. The magnitude of the built-in voltage is determined mainly by the carrier concentrations in both sides of the junction and the energy gap of the semiconductor. When both the n- and p-regions are heavily doped, the built-in voltage approaches the band gap. Under forward bias, Fig. 2(b), the built-in voltage is lowered, and the flow of holes and electrons across the junction is enhanced. This injection results in an increase in the minority carrier concentrations above their equilibrium values. These excess carriers must recombine with the majority carriers near the junction to restore the equilibrium condition. This recombination can occur via radiative and nonradiative processes. In general, more injected carriers recombine nonradiatively than radiatively due mainly to the presence of recombination centers associated with chemical and structural defects, such as impurity precipitates and dislocations.

The concept of radiative recombination is therefore essential for the understanding of junction electroluminescence. In a semiconductor with impurity states, the recombination can take place directly across the band gap or as impurity-induced recombination due to the localization of charge carriers (Fig. 3). In the latter case, at least one type of carrier must be captured at a luminescent center before recombination can occur, and only shallow centers are useful since recombination at deep levels will be either at infrared energies or will be nonradiative. It is evident that band-to-band recombination is much more important for direct gap semiconductors than for indirect gap materials. In indirect gap semiconductors, band-to-band recombination requires the absorption or emission of a phonon to conserve momentum. Electron-hole recombination has a much lower probability in this three particle process. Recombinations in direct and indirect gap semiconductors are discussed in the following paragraphs in more detail using gallium arsenide and gallium phosphide as examples.

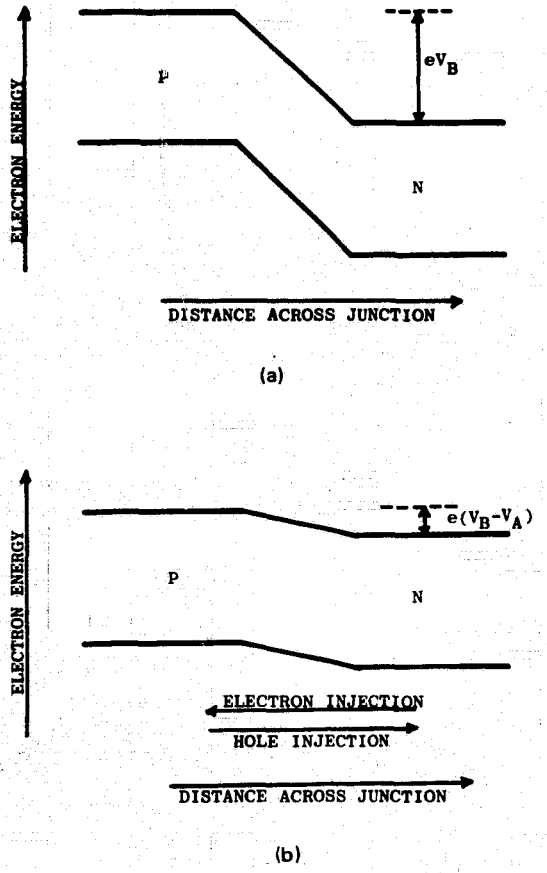

Fig. 2. (a) Energy band structure of a semiconductor p-n junction in thermal equilibrium (upper). (b) Energy band structure of a semiconductor p-n junction under forward bias (lower). V_B is the built-in potential, and V_A is the applied bias.

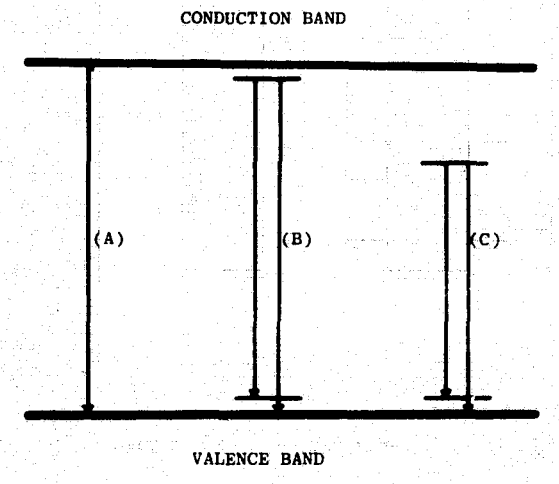

Fig. 3. Some radiative recombination processes in semiconductors: (*A*) interband transition; (*B*) transitions involving shallow impurity states, and (*C*) transitions involving a deep impurity state.

A. Recombination in Direct Band Gap Semiconductors

The fundamental luminescent mechanism in direct gap semiconductors, such as gallium arsenide, is the interband recombination. However, due to the high doping density required for efficient electroluminescent junctions, the impurity levels are broadened into band tails. At carrier concentrations higher than about $10^{18}cm^{-3}$, the band tailing has been shown to shift the emission peak to higher energy for n-type gallium arsenide and to lower energy for p-type materials [2]. This phenomenon is a result of the much higher density of states in the valence band tail than in the conduction band tail due to the larger hole effective mass. Consequently, donor levels of higher energy partially fill the conduction band, and most of the electrons are at energy levels in excess of the band gap from the valence band. Conversely, as the acceptor concentration is increased, more states are available within the tail because of the large hole mass, and the recombination shifts to lower energies.

Self-absorption is a severe limitation to the external efficiency of direct gap electroluminescent junctions because of the high absorption coefficient of the semiconductor for radiation with energy near the band gap. Analogous to the emission spectrum, the absorption peak shifts to higher energies in n-type gallium arsenide and to lower energies in p-type gallium arsenide [3]. A reduction in self-absorption effects in gallium arsenide has been achieved by closely compensating the n- and p-regions with an amphoteric dopant such as silicon [4], [5]. In these compensated junctions, the emission shifts to lower energies where the absorption coefficient is smaller.

The same basic recombination phenomena occur in direct gap ternary compounds, such as gallium arsenide phosphide containing less than 44 Mole percent of gallium phosphide, except that for compounds with compositions near the direct-indirect gap transition, the energy of the indirect band minima is not far separated from that of the direct band minima. The relative population in the two conduction bands will then be determined by the effective masses and the energy separation. A significant electron population in the indirect band minima will limit the internal efficiency.

B. Recombination in Indirect Band Gap Semiconductors

Radiative recombination in indirect gap semiconductors takes place predominantly via impurity states. The mechanism responsible for the green and red emitting gallium phosphide diodes is associated with isoelectronic traps. The isoelectronic substitution of nitrogen for phosphorus in the crystal lattice is responsible for the green electroluminescence [6], [7]. A shallow electron trap about 8 meV below the conduction band is created by the nitrogen substitution because of the differences between the electronic configuration and nuclear charge of nitrogen and phosphorus atoms. After trapping an electron, the negative nitrogen center binds a hole by columbic attraction, and the electron and hole radiatively decay as an exciton [8]. The substitution of an isolectronic complex such as a Zn-O or Cd-O pair in adjacent lattice sites in gallium phosphide is responsible for the red electroluminescence [9], [10]. The Zn-O pair creates a deep trap about 0.4 eV below the conduction band which is not associated with zinc or oxygen alone. Bound exciton recombination at the Zn-O trap or the electron transition from the Zn-O pair level to the zinc acceptor level can take place. These two mechanisms have slightly different energies at the emission peak [11].

An important asset of the indirect band gap semiconductors over the direct gap materials is the reduced absorption near the band edge. For example, the absorption coefficient in gallium phosphide containing Zn-O pairs has been shown to be relatively small over the entire red emission range [3].

III. Epitaxial Growth of III-V Compounds for Electroluminescent Junctions

The III-V compounds most suited for the fabrication of light-emitting diodes include gallium arsenide, gallium phosphide, gallium arsenide phosphide, and gallium aluminum arsenide. These materials are refractory, possess appreciable vapor pressures at high temperatures, and their melts are chemically reactive (for example, gallium arsenide melts at 1237°C and has a decomposition pressure of approximately 1 atm at its melting point). Thus, melt-growth techniques cannot readily produce single crystals of III-V compounds of sufficient perfection and purity for device purposes. Although electroluminescent junctions have been prepared from melt-grown crystals by diffusion, epitaxial growth from vapor and liquid phases is now widely used for the production of high efficiency light-emitting diodes. Epitaxial growth techniques have the following distinct advantages: 1) III-V compounds can be prepared at temperatures below their decomposition temperatures, and 2) the thickness of the grown layer and the impurity concentration and distribution in the layer can be accurately controlled. The epitaxial layers deposited on melt-grown crystals have better chemical and structural perfection than melt-grown crystals and are more suitable for the active regions of a device.

Epitaxial growth by chemical reaction of gaseous reactants on substrate surfaces (usually referred to as vapor phase epitaxy) is the most versatile technique for the preparation of thin layers of semiconductors [12]. The chemical reaction must be predominately heterogeneous and take place on the substrate surface. In contrast, volume reaction results in the formation of atomic or molecular clusters of random orientation in the space surrounding the substrate, and the deposition of these clusters on the substrate will produce nonoriented growth. Furthermore, the by-products of the reaction must be volatile at the processing temperature to insure high purity of the deposit. Vapor phase epitaxial growth is usually carried out in a gas-flow system so that the dopant concentration and distribution can be readily controlled by programming the composition of the reactant mixture. Several types of chemical reactions have been used for the epitaxial growth of III-V compounds. For example, epitaxial layers of gallium arsenide have been prepared by the following three reactions.

1) Hydrogen chloride, gallium, and arsenic according to the following sequence [13]:

$$2\,Ga\,(\ell) + 2HCl\,(g) \rightarrow 2\,GaCl\,(g) + H_2\,(g)$$
$$6\,GaCl\,(g) + As_4\,(g) \rightarrow 4\,GaAs\,(s) + 2\,GaCl_3\,(g).$$

2) Arsenic trichloride, hydrogen, and gallium according to the following sequence [14]:

$$4\,AsCl_3(g) + 6H_2(g) \rightarrow 12\,HCl(g) + As_4(g)$$
$$2\,Ga(\ell) + 2\,HCl(g) \rightarrow 2\,GaCl(g) + H_2(g)$$
$$6\,GaCl(g) + As_4(g) \rightarrow 4\,GaAs(s) + 2\,GaCl_3(g).$$

3) Hydrogen chloride, gallium, and arsine according to the following sequence [15]:

$$2\,Ga(\ell) + 2\,HCl(g) \rightarrow 2\,GaCl(g) + H_2(g)$$
$$GaCl(g) + AsH_3(g) \rightarrow GaAs(s) + HCl(g) + H_2(g).$$

Similar reactions have been used for the epitaxial growth of other compounds, including gallium phosphide and indium arsenide. The most important parameters affecting the chemical and structural perfection of the grown layer are the surface preparation of the substrate, the substrate temperature, and the composition and flow rate of the reactant mixture. The *in-situ* etching of the substrate just prior to the growth process is commonly used to provide a clean and damage-free surface.

Epitaxial layers of III-V compounds have also been grown from solution, usually referred to as liquid-phase epitaxy. For example, gallium arsenide is soluble in gallium, and its solubility increases with increasing temperature. Thus, during the slow cooling of a saturated solution of gallium arsenide in gallium in the presence of a substrate crystal, the solution becomes supersaturated, and nucleation and growth will take place on the substrate producing an epitaxial layer. This process involves three steps: 1) the diffusion of solute to the crystal-solution interface, 2) the deposition of solute on the growing interface, and 3) the dissipation of the heat of crystallization. Since step 1) or 2) is usually rate-determining, the growth rates are low, on the order of 1 μm/min. Several techniques have been developed to bring the substrate into contact with the solution. In the tilting technique [16], the substrate is initially held against the bottom at the upper end of a tilted boat, and the saturated solution is prepared at the lower end. Growth is accomplished by tilting the boat back to the horizontal position followed by the cooling of the solution. Growth can be stopped by tilting the boat again. Multilayer structures have been produced by the sliding boat technique [17]. In this technique, the substrate is fixed and solutions of various compositions are slid successively over the substrate at a predetermined temperature for various time intervals. The liquid phase epitaxial growth technique is less efficient as a manufacturing technique than the vapor phase technique. In the case of ternary compounds, different segregation coefficients of the constituents will lead to variations in the composition of the layer along the growth direction.

The current state of the art of several important materials is discussed in the following sections.

A. Gallium Arsenide

Gallium arsenide with a direct gap of 1.47 eV at room temperature is a very efficient infrared emitter. Considerable efforts have been made to convert the infrared radiation to visible light by coating gallium arsenide diodes with phosphors [18]-[21]. The phosphor conversion mechanism involves a two-step excitation of rare earth ions in a fluoride host crystal; an ion is excited to the desired emitting state by consecutive absorption of two photons of lower energy. At present, efficiencies of red and green gallium arsenide-phosphor diodes are not competitive with visible light-emitting p-n junction devices; however, the blue gallium arsenide-phosphor diodes have the highest efficiency for blue emission.

High-efficiency gallium arsenide light-emitting diodes are fabricated from silicon-doped gallium arsenide produced by liquid phase epitaxial growth. Vapor grown gallium arsenide, in spite of the much more extensive investigations, is less efficient for light-emitting devices, due presumably to the presence of high concentrations of chemical and structural defects. These defects (which reduce radiation recombination efficiency) are minimized by carrying out the epitaxial growth of gallium arsenide from gallium solutions [22], [23]. Liquid phase epitaxial growth is particularly significant in that n- and p-type gallium arsenide can be produced by controlling the growth temperature using silicon as the amphoteric dopant [24], [25]; a highly compensated n-type region followed by a highly compensated p-type region is produced during recrystallization. The amphoteric behavior of silicon in gallium arsenide has not been satisfactorily explained, since local mode infrared absorption measurements indicate that, although silicon on gallium sites is the primary donor in n-type gallium arsenide, silicon on arsenic sites is not the major acceptor in p-type material [26]. Self-absorption in gallium arsenide is also reduced by doping with silicon. The highest external efficiency reported for a silicon-doped gallium arsenide diode at room temperature is 32%, obtained by using a high index of refraction glass dome [27]. The wavelength of the emission peak (which is important for the operation of phosphors for conversion to visible light) was varied from about 9200 to 10 000 Å by varying the silicon concentration. However, the internal absorption was still the major limitation to the efficiency.

The amphoteric effects of germanium and tin in gallium arsenide have also been studied using liquid-phase epitaxial growth [28]. Although epitaxial layers of good perfection were grown, only p-type material was obtained by doping with germanium and n-type material was obtained by using tin as a dopant.

B. Zinc-Oxygen Pair Doped Gallium Phosphide

Gallium phosphide doped with Zn-O pairs, though not the most popular red emitter at present, has the highest external quantum efficiency compared with that of other electroluminescent junctions, such as gallium arsenide phosphide. One major limitation to the more widespread use of gallium phosphide light-emitting diodes is the high cost of materials. Bulk crystals of gallium phosphide required as substrates for the epitaxial growth process are expensive. In addition, only liquid phase epitaxial growth, which is less amenable to manufacturing than vapor growth, is currently capable of yielding usable diodes.

The first work which demonstrated the potential of gallium phosphide junction electroluminescence was carried out by liquid phase epitaxial growth using the tilting technique [29].

N-type epitaxial gallium phosphide layers were deposited from a tellurium-doped solution onto gallium phosphide substrates grown from a zinc- and oxygen-doped solution; the solution saturated with gallium phosphide at 1140°C was cooled to 700°C in 40 min. The diodes had an external efficiency of 0.075% over a broad band centered at about 7000 Å at room temperature. The efficiency of the diodes was shown to be a strong function of the tellurium concentration in the solution [30]. The annealing of epitaxial diodes at 400°-725°C for 16 hours has been shown to improve the efficiency to almost 2% [31]. Since the light emission occurs predominately in the p-region, higher efficiencies have been obtained in diodes fabricated by the epitaxial growth of p-type layers on n-type solution-grown gallium phosphide substrates. However, the p-type dopants, zinc and gallium oxide, are volatile from solution (gallium oxide reacts with gallium to form a volatile suboxide), and more complex closed systems were sometimes used for the epitaxial growth process. The earlier devices had efficiencies of up to 1% [32]-[34]. An increase in efficiency to 1.4% was achieved by using double epitaxial layers, i.e., the liquid phase epitaxial growth of an n-layer on n-type substrates followed by the growth of a p-layer in an open system, and efficiencies as high as 3.4% were obtained by compensating the p-type layer with tellurium [35]. By carrying out the growth of double epitaxial layers in a closed tube and using optimized dopant concentrations and annealing during growth, higher efficiencies, 7%, were achieved [36]. The net donor and acceptor concentration profiles were found to be graded throughout the double epitaxial layer structures. Most recently, efficiencies up to 8% have been reported for double-epitaxial layers grown on Czochralski substrates in a semi-sealed system [37].

One current limitation of the zinc-oxygen pair doped gallium phosphide electroluminescent junction is that the wide-band emission peaks near the edge of the visible spectrum so that much of the radiated power is in the infrared. For equal radiated power, gallium arsenide phosphide diodes appear much brighter. However, gallium phosphide diodes emit much more power than gallium arsenide phosphide diodes for the same input power, so that the two materials have about equal brightness when operated at their suggested input currents.

C. Nitrogen-Doped Gallium Phosphide

Because of the spectral response of the eye, green-emitting diodes are of particular interest, and high luminous efficiencies can be obtained with low power and low quantum efficiencies. Several techniques have been used to produce green emission from gallium phosphide diodes. The first efficient green-emitting gallium phosphide diodes were found in the internal built-in p-n junctions resulting from nonuniform distribution of donor and acceptor atoms during the growth of gallium phosphide platelets from a gallium solution doped with a shallow donor (sulfur, selenium, or tellurium) and a shallow acceptor, zinc [38]. Later devices were made by liquid-phase epitaxial growth using zinc and sulfur as dopants [39], [40]. Vapor phase epitaxial growth has also been used in conjunction with zinc diffusion to produce green-emitting gallium phosphide junction devices [41]. The external quantum efficiencies of these early devices were typically 0.02%. It should be noted, however, that an external efficiency of 0.01% in the green is visually equivalent to one of about 1% in the red.

The highest efficiencies in green-emitting gallium phosphide diodes were achieved with nitrogen-doped layers prepared by liquid phase epitaxial growth. Both single and double epitaxial layers deposited on solution grown and Czochralski substrates in an open system have been evaluated [42], [43]. A pulsed external quantum efficiency of 0.6% was measured from nitrogen- and zinc-doped p-type layers epitaxially deposited on solution grown n-type gallium phosphide followed by annealing. Double epitaxial layers grown on Czochralski substrates yielded lower efficiencies, about 0.1% under dc operation. The internal efficiency of these devices was found to increase with increasing concentration of nitrogen in both sides of the p-n junction; however, the high nitrogen concentrations lead to enhanced self-absorbtion. Thus, much improved devices could be made by using high nitrogen concentration only in the junction region.

Since the luminous efficiency of zinc-oxygen pair doped gallium phosphide diodes is similar to that of nitrogen-doped diodes, the possibility of producing hues between red and green exists. By introducing nitrogen into n-layers grown onto zinc- and oxygen-doped substrates, the hue could be controlled at a given current by adjusting the doping levels or by varying the diode current for a given dopant profile [44].

D. Gallium Arsenide Phosphide

At present, gallium arsenide phosphide deposited on gallium arsenide substrates is the most suitable material for the mass production of red and amber light-emitting diodes [45], [46]. At room temperature, the change from a direct to an indirect transition occurs at the composition $GaAs_{0.56}P_{0.44}$, corresponding to an energy gap of 1.9 eV. The extensive use of gallium arsenide phosphide diodes is due mainly to the relatively low cost of the vapor phase epitaxial growth process which is used exclusively for their fabrication. The vapor phase epitaxial growth technique permits the grading of composition in the gallium arsenide phosphide layer to reduce the effects of lattice mismatch between the gallium arsenide substrate and the epitaxial layer. The liquid-phase technique, though used widely in the fabrication of gallium arsenide and gallium phosphide light-emitting diodes, has not been successful for the epitaxial growth of gallium arsenide phosphide on gallium arsenide substrates [47].

Several reactions can be used for the deposition of gallium arsenide phosphide. Most of the current work utilizes the reaction of gallium, hydrogen chloride, arsine, and phosphine in a hydrogen atmosphere in a gas flow system [15]. The composition of the epitaxial layer can be adjusted by controlling the AsH_3/PH_3 molar ratio in the reactant mixture. Also, the concentration of dopants in the layer can be readily changed.

Compositional grading is necessary to produce efficient gallium arsenide phosphide diodes since there is a 1.44% difference in lattice parameters between gallium arsenide and $GaAs_{0.6}P_{0.4}$, which is the composition for high luminous

efficiency. There have been extensive studies of dislocations due to this lattice mismatch [46], [48]-[51]. It is well established that the gradual grading of the composition of the epitaxial layer improves the structural perfection.

The use of zinc diffusion into vapor grown n-type epitaxial gallium arsenide phosphide has produced the highest efficiency red-emitting gallium arsenide phosphide diode [52]. The external quantum efficiency of diodes over the entire compositional range of gallium arsenide phosphide has been measured for different donor concentrations. As the phosphorus content increases, the diode efficiency decreases, and the luminous efficiency increases. The maximum brightness occurs at the composition $GaAs_{0.6}P_{0.4}$ which has an external quantum efficiency of 0.2%. The maximum external quantum efficiency obtained in gallium arsenide phosphide diodes was 0.6%.

Recently, zinc diffused gallium arsenide phosphide diodes have been fabricated with nitrogen doping on the n-side of the junction [53], [54]. For $GaAs_{0.6}P_{0.4}$, the emission peak shifts further towards the red. However, for gallium arsenide phosphide in the indirect gap composition range, higher quantum efficiencies were found, and higher brightness was achieved for orange, yellow, and green emissions.

E. Gallium Aluminum Arsenide

Aluminum arsenide with an indirect band gap of 2.2 eV has been investigated as an electroluminescent material; however, light-emitting junctions formed by the diffusion of zinc into vapor grown epitaxial layers were found to have very low efficiencies [55]. The chemical reactivity of aluminum arsenide may also limit its applications. On the other hand, aluminum arsenide and gallium arsenide have very similar lattice parameters and form solid solutions over the entire composition range. The transition from direct to indirect energy band structure occurs at the composition $GaAl_{0.63}As_{0.37}$ corresponding to a band gap of 1.92 eV [56]. Thus, gallium arsenide is an ideal substrate for the epitaxial growth of gallium aluminum arsenide.

The first attempt to epitaxially grow gallium aluminum arsenide on gallium arsenide substrates was carried out by the closed-tube chemical transport technique [57]. The source material was a mixture of aluminum arsenide and gallium arsenide powder. Because of the difference in chemical reactivity of aluminum arsenide and gallium arsenide, the epitaxial layer was of different composition from the source material, and its aluminum content increased along the growth axis. P-n junction diodes were prepared from the vapor grown material by diffusion, and electroluminescence from these diodes was strongly influenced by deep-lying competitive recombination centers [58]. The perfection of gallium aluminum arsenide can be improved considerably by using liquid-phase epitaxial growth.

The first efficient gallium aluminum arsenide visible electroluminescent junction was produced by a modification of Nelson's technique [16], and the p-n junction was formed at a controllable distance from the substrate-epitaxial layer interface in a single-step cooling cycle by means of counter-doping the solution [59]. Room temperature external quantum efficiencies of up to 3.3% were measured on diodes with emission peaks at 1.70 eV. An important feature of the gallium-rich region of the Ga-Al-As system is the large distribution coefficient of aluminum between the solid and liquid phases [60] which, though it may appear to be a problem, has been used to advantage. During the epitaxial growth process, the rapid depletion of aluminum from the liquid phase produces a decreasing aluminum content in the grown layer [61]. The larger band gap in the first part of the grown layer shifts the absorption edge to higher energies, so that by removing the substrate, the self-absorption effect can be greatly reduced. The brightest diodes emitted at 1.83 eV with an external quantum efficiency of 0.8%. More recently, an external quantum efficiency of 4% at 6950 Å has been achieved by the diffusion of zinc into epitaxial gallium aluminum arsenide grown from the liquid phase [62]. Also, a liquid phase epitaxial technique with a decreasing growth rate has been reported to create an increasing aluminum concentration in the grown layer; however, visible emission did not occur in the diodes fabricated in this manner [63].

F. Other Materials

In addition to the compounds previously discussed, several other III-V compounds are attractive for electroluminescent diodes in the visible region. However, difficulties encountered in the crystal growth of these compounds have limited their applications at present.

Gallium nitride with a direct band gap of 3.5 eV has the potential for emission in the ultraviolet. The preparative techniques to date include the ammonolysis of gallium monochloride [64]-[66], the thermal decomposition of a gallium tribromide-ammonia complex [67], and liquid-phase epitaxial growth [68]. However, foreign substrates were used in all cases; neither the structure nor the electrical properties of the heteroepitaxial layers are adequate for devices. In particular, p-type gallium nitride has not been prepared, and high resistivity material resulting from the compensation of the normally low-resistivity n-type gallium nitride has been used for light-emitting junctions. Low-efficiency green, blue, yellow, and violet luminescence has been reported at the i-n interface [69]-[72].

Solid solutions of indium and gallium phosphides, with a direct band gap up to 2.2 eV at the composition $In_{0.2}Ga_{0.8}P$ [73], are potential materials for emission in the red, orange, and yellow regions of the spectrum. P-n junctions in indium gallium arsenide have been produced by zinc diffusion and liquid and vapor phase epitaxial growth techniques [74, [75]. However, no useful room-temperature efficiencies have been obtained. One major problem has been the lack of a suitable substrate on the basis of lattice parameters and thermal expansion coefficients. Gallium arsenide, which has been used as the substrate in all studies, is suitable only for the growth of indium phosphide-rich solid solutions with emissions in the infrared region.

Solid solutions of aluminum gallium phosphides and solid solutions of indium aluminum phosphide are also potential electroluminescent materials. The only aluminum gallium phosphide diodes reported had very low efficiencies [76]. Indium aluminum phosphide probably has the largest direct

band gap of all alloys under discussion; however, no electroluminescent diodes have been reported.

IV. Summary

Contemporary light-emitting diode technology has been reviewed with emphasis on the epitaxial growth techniques for junction formation and on the experimental efficiencies achieved. Economically, gallium arsenide phosphide light-emitting diodes are most widely used. Green light-emitting gallium phosphide devices are becoming increasingly popular as cost effective fabrication techniques are developed. The desire for efficient light emission of colors other than those currently available supplies sufficient impetus for the eventual solution of material problems encountered in the fabrication of light-emitting diodes from other III-V compounds.

References

[1] A. A. Bergh and P. J. Dean, "Light-Emitting Diodes," *Proc. IEEE*, vol. 60, pp. 156-223, 1972.

[2] D. A. Cusano, "Radiative Recombination from GaAs Directly Excited by Electron Beams," *Solid State Communications*, vol. 2, pp. 353-358, 1964.

[3] H. C. Casey and F. A. Trumbore, "Single Crystal Electroluminescent Materials," *Mat. Sci. Eng.*, vol. 6, pp. 69-109, 1970.

[4] G. Lucovsky, A. J. Varga, and R. F. Schwarz, "Edge Absorption and Photoluminescence in Closely Compensated GaAs," *Solid State Communications*, vol. 3, pp. 9-13, 1965.

[5] H. Rupprecht, J. M. Woodall, K. Konnerth, and D. G. Petit, "Efficient Electroluminescence from GaAs Diodes at 300°K," *App. Phys Lett.*, vol. 9, pp. 221-223, 1966.

[6] D. G. Thomas, J. J. Hopfield, and C. J. Frosch, "Isoelectronic Traps Due to Nitrogen in Gallium Phosphide," *Phys. Rev. Lett.*, vol. 15, pp. 857-860, 1965.

[7] D. G. Thomas and J. J. Hopfield, "Isoelectronic Traps Due to Nitrogen in Gallium Phosphide," *Phys. Rev.*, vol. 150, pp. 680-689, 1966.

[8] P. J. Dean, M. Gershenzon, and G. Kaminsky, "Green Electroluminescence from Gallium Phosphide Diodes Near Room Temperature," *J. Appl. Phys.*, vol. 38, pp. 5332-5342, 1967.

[9] T. N. Morgan, B. Welber, and R. N. Bhargava, "Optical Properties of Cd-O and Zn-O Complexes in GaP," *Phys. Rev.*, vol. 166, pp. 751-753, 1968.

[10] C. H. Henry, P. J. Dean, and J. D. Cuthbert, "New Red Pair Luminescence from GaP," *Phys. Rev.*, vol. 166, pp. 754-756, 1968.

[11] J. D. Cuthbert, C. H. Henry, and P. J. Dean, "Temperature-Dependent Radiative Recombination Mechanisms in GaP(Zn,O) and GaP(Cd,O)," *Phys. Rev.*, vol. 170, pp. 739-748, 1968.

[12] T. L. Chu and R. K. Smeltzer, "Recent Advances in the Chemical Vapor Growth of Electronic Materials," *J. Vac. Sci. Technol.*, vol. 10, pp. 1-10, (1973).

[13] S. W. Ing and H. T. Minden, "Open Tube Epitaxial Synthesis of GaAs and GaP," *J. Electrochem. Soc.*, vol. 109, pp. 995-997, 1962.

[14] J. R. Knight, D. Effer, and P. R. Evans, "The Preparation of High Purity Gallium Arsenide by Vapor Phase Epitaxial Growth," *Solid-State Electronics*, vol. 8, pp. 178-180, 1965.

[15] J. J. Tietzen and J. A. Amick, "The Preparation and Properties of Vapor-Deposited Epitaxial $GaAs_{1-x}P_x$ Using Arsine and Phosphine," *J. Electrochem. Soc.*, vol. 113, pp. 724-728, 1966.

[16] H. Nelson, "Epitaxial Growth from the Liquid State and Its Application to the Fabrication of Tunnel and Laser Diodes," *RCA Rev.*, vol. 24, pp. 603-615, 1963.

[17] M. B. Panish, I. Hayashi, and S. Sumski, "Double-Heterostructure Injection Lasers with Room-Temperature Threshold as Low as 2300 A/cm^2," *Appl. Phys. Lett.*, vol. 16, pp. 326-327, 1970.

[18] F. W. Ostermayer, "Preparation and Properties of Infrared to Visible Conversion Phosphors," *Met. Trans.*, vol. 2, pp. 747-755, 1971.

[19] S. V. Galginaitis, "The Use of Up-Converter Phosphors in Semiconductor Light-Emitting Devices and Displays," *Met. Trans.*, vol. 2, pp. 757-761, 1971.

[20] J. E. Geusic, F. W. Ostermayer, H. M. Marcos, L. G. Van Uitert, and J. P. van der Ziel, "Efficiency of Red, Green, and Blue Infrared to Visible Conversion Sources," *J. Appl. Phys.*, vol. 42, pp. 1958-1960, 1971.

[21] L. F. Johnson, H. J. Guggenheim, T. C. Rich, and F. W. Ostermayer, "Infrared to Visible Conversion by Rare-Earth Ions in Crystals," *J. Appl. Phys.*, vol. 43, pp. 1125-1137, 1972.

[22] C. S. Kang and P. E. Green, "Preparation and Properties of High Purity Epitaxial GaAs Grown from Ga Solution," *Appl. Phys. Lett.*, vol. 11, pp. 171-173, 1967.

[23] M. B. Panish, "Luminescence of Zinc-Doped Solution Grown GaAs: The Effect of Arsenic Pressure," *J. Phys. Chem. Solids*, vol. 29, pp. 409-410, 1968.

[24] H. Kressel, J. U. Dunse, H. Nelson, and F. Z. Hawrylo, "Luminescence in Silicon-Doped GaAs by Liquid-Phase Epitaxy," *J. Appl. Phys.*, vol. 39, pp. 2006-2011, 1968.

[25] M. B. Panish and S. Sumski, "Ga-As-Si: Phase Studies and Electrical Properties of Solution-Grown Si-Doped GaAs," *J. Appl. Phys.*, vol. 41, pp. 3195-3196, 1970.

[26] W. G. Spitzer and M. B. Panish, "Silicon-Doped Gallium Arsenide Grown from Gallium Solution: Silicon Site Distribution," *J. Appl. Phys.*, vol. 40, pp. 4200-4202, 1969.

[27] I. Ladany, "Electroluminescence Characteristics and Efficiency of GaAs: Si Diodes," *J. Appl. Phys.*, vol. 42, pp. 654-656, 1971.

[28] J. Vilms and J. P. Garrett, "The Growth and Properties of LPE GaAs," *Solid-State Electronics*, vol. 15, pp. 443-455, 1972.

[29] M. R. Lorenz and M. Pilkuhn, "Preparation and Properties of Solution-Grown Epitaxial p-n Junctions in GaP," *J. Appl. Phys.*, vol. 37, pp. 4094-4102, 1966.

[30] H. Kressel and I. Kadany, "The Effect of the Donor Concentration on the Optical Efficiency of Solution-Grown GaP Diodes," *Solid State Electronics*, vol. 11, pp. 647-652, 1968.

[31] R. A. Logan, H. G. White, and F. A. Trumbore, "P-N Junctions in GaP with External Electroluminescence Efficiency $\sim$ 2% at 25°C," *Appl. Phys. Lett.*, vol. 10, pp. 206-208, 1967.

[32] F. A. Trumbore, M. Kowalchik, and H. G. White, "Efficient Electroluminescence in GaP p-n Junctions Grown by Liquid-Phase Epitaxy on Vapor-Grown Substrates," *J. Appl. Phys.*, vol. 38, pp. 1987-1988, 1967.

[33] K. K. Shih, M. R. Lorenz, and L. M. Foster, "Preparation of Efficient Electroluminescent Diodes from p-on-n Liquid Phase Epitaxial Layers of GaP," *J. Appl. Phys.*, vol. 39, pp. 2747-2749, 1968.

[34] H. A. Allen and G. A. Henderson, "Efficient Red-Emitting p-n Junctions Formed in GaP by Solution Growth of Thick Layers of p-Type Material on Vapor-Grown n-Type Substrates," *J. Appl. Phys.*, vol. 39, pp. 2977-2978, 1968.

[35] I. Ladany, "Gallium Phosphide Double-Epitaxial Diodes," *J. Electrochem. Soc.*, vol. 116, pp. 993-996, 1969.

[36] R. H. Saul, J. Armstrong, and W. H. Hackett, Jr., "GaP Red Electroluminescent Diodes with an External Quantum Efficiency of 7%," *Appl. Phys. Lett.*, vol. 15, pp. 229-231, 1969.

[37] R. Solomon and D. DeFevere, "Epitaxial GaP by a Semi-Sealed Dip Process for High Efficiency Red LED's," *J. Electronic Mater.*, vol. 1, pp. 1-5, 1972.

[38] L. M. Foster, T. S. Plaskett, and J. E. Scardefield, "Formation of Built-In Light-Emitting Junctions in Solution-Grown GaP Containing Shallow Donors and Acceptors," *IBM J. Res. Dev.*, vol. 10, pp. 122-131, 1966.

[39] K. K. Shih, J. M. Woodall, S. E. Blum, and L. M. Foster, "Efficient Green Electroluminescence from GaP p-n Junctions Grown by Liquid-Phase Epitaxy," *J. Appl. Phys.*, vol. 39, pp. 2962-2963, 1968.

[40] K. K. Shih and G. D. Petit, "Properties of GaP Green-Light Emitting Diodes Grown by Liquid-Phase Epitaxy," *J. Appl. Phys.*, vol. 39, pp. 5025-5029, 1968.

[41] A. S. Epstein, "Room Temperature Green Electroluminescent Diodes Prepared from n-Type Vapor Grown Epitaxial Gallium Phosphide," *Solid State Electronics*, vol. 12, pp. 485-491, 1969.

[42] R. A. Logan, H. G. White, and W. Wiegmann, "Efficient Green Electroluminescence in Nitrogen-Doped GaP p-n Junctions," *Appl. Phys. Lett.*, vol. 13, pp. 139-141, 1968.

[43] R. A. Logan, H. G. White, and W. Wiegmann, "Efficient Green Electroluminescent Junctions in GaP," *Solid-State Electronics*, vol. 14, pp. 55-70, 1971.

[44] W. Rosenzweig, R. A. Logan, and W. Wiegmann, "Variable Hue GaP Diodes," *Solid-State Electronics*, vol. 14, pp. 655-660, 1971.

[45] J. W. Burd, "A Multi-Wafer Growth System for the Epitaxial Deposition of GaAs and $GaAs_{1-x}P_x$," *Trans. Met. Soc. AIME*, vol. 245, pp. 571-576, 1969.
[46] R. A. Burmeister, Jr., G. P. Pighini, and P. E. Greene, "Large Area Epitaxial Growth of $GaAs_{1-x}P_x$ for Display Applications," *Trans. Met Soc. AIME*, vol. 245, pp. 587-592, 1969.
[47] K. K. Shih, "Epitaxial Growth of $GaAs_xP_{1-x}$ from the Liquid Phase," *J. Electrochem. Soc.*, vol. 117, pp. 387-389, 1970.
[48] D. A. Grenning and A. H. Herzog, "Dislocations and Their Relation to Irregularities in Zinc-Diffused Gallium Arsenide Phosphide p-n Junctions," *J. Appl. Phys.*, vol. 39, pp. 2783-2790, 1968.
[49] G. B. Stringfellow and P. E. Greene, "Dislocations in $GaAs_{1-x}P_x$," *J. Appl. Phys.*, vol. 40, pp. 502-507, 1969.
[50] M. S. Abrahams, L. R. Weisberg, C. J. Buiocchi, and J. Blanc, "Dislocation Morphology in Graded Heterojunctions $GaAs_{1-x}P_x$," *J. Mat. Sci.*, vol. 4, pp. 223-235, 1969.
[51] C. E. E. Stewart, "Some Observations on the Dislocation Etching of $GaAs_{1-x}P_x$ Epitaxial Layers," *J. Crystal Growth*, vol. 8, pp. 269-275, 1971.
[52] A. H. Herzog, W. O. Groves, and M. G. Craford, "Electroluminescence of Diffused $GaAs_{1-x}P_x$ Diodes with Low Donor Concentrations," *J. App. Phys.*, vol. 40, pp. 1830-1838, 1969.
[53] W. O. Groves, A. H. Herzog, and M. G. Craford, "The Effect of Nitrogen Doping on $GaAs_{1-x}P_x$ Electroluminescent Diodes," *Appl. Phys. Lett.*, vol. 19, pp. 184-186, 1971.
[54] M. G. Craford, D. L. Kenne, W. O. Groves, and A. H. Herzog, "The Luminescent Properties of Nitrogen Doped Gallium Arsenide Phosphide Light-Emitting Diodes," *J. Electronic Mater.*, vol. 2, pp. 137-158, 1973.
[55] C. J. Nuese, A. G. Sigai, M. Ettenberg, J. J. Ganon, and S. L. Gilbert, "Preparation of Visible Light-Emitting p-n Junctions in AlAs," *Appl. Phys. Lett.*, vol. 17, pp. 90-92, 1970.
[56] H. C. Casey, Jr., and M. B. Panish, "Composition Dependence of the $Ga_{1-x}Al_xAs$ Direct and Indirect Energy Gaps," *J. Appl. Phys.*, vol. 40, pp. 4910-4912, 1969.
[57] J. F. Black and S. M. Ku, "Preparation and Properties of AlAs-GaAs Mixed Crystals," *J. Electrochem. Soc.*, vol. 113, pp. 249-254, 1966.
[58] S. M. Ku and J. K. Black, "Injection Electroluminescence in $Al_xGa_{1-x}As$ Diodes of Graded Energy Gap," *J. Appl. Phys.*, vol. 37, pp. 3733-3740, 1966.
[59] H. Rupprecht, J. M. Woodall, and G. D. Petit, "Efficient Electroluminescence at 300°K from $Ga_{1-x}Al_xAs$ p-n Junctions Grown by Liquid Phase Epitaxy," *Appl. Phys. Lett.*, vol. 11, pp. 81-83, 1967.
[60] M. B. Panish and S. Sumaki, "Ga-Al-As: Phase, Thermodynamic, and Optical Properties," *J. Phys. Chem. Solids*, vol. 30, pp. 129-137, 1969.
[61] J. M. Woodall, H. Rupprecht, and W. Reuter, "Liquid Phase Epitaxial Growth of $Ga_{1-x}Al_xAs$," *J. Electrochem. Soc.*, vol. 116, pp. 899-903, 1969.
[62] E. G. Dierschke, L. E. Stone, and R. W. Haisty, "Efficient Electroluminescence from Zinc-Diffused $Ga_{1-x}Al_xAs$ Diodes at 25°C," *Appl. Phys. Lett.*, vol. 19, pp.98-100, 1971.
[63] J. D. Taynai, R. H. Deitch, and C. J. Summers, "Luminescent Properties of AlGaAs Grown by Transient-Mode Liquid Epitaxy," *J. Electronic Mater.*, vol. 1, pp. 213-223, 1972.
[64] H. P. Maruska and J. J. Tietjen, "The Preparation and Properties of Vapor-Deposited Single-Crystalline GaN," *Appl. Phys. Lett.*, vol. 15, pp. 327-329, 1969.
[65] D. K. Wickenden, K. R. Faulkner, R. W. Brander, and B. J. Isherwood, "Growth of Epitaxial Layers of Gallium Nitride on Silicon Carbide and Corundum Substrates," *J. Crystal Growth*, vol. 9, pp. 158-164, 1971.
[66] M. Illegems, "Vapor Epitaxy of Gallium Nitride," *J. Crystal Growth*, vol. 13/14, pp. 360-364, 1972.
[67] T. L. Chu, "Gallium Nitride Films," *J. Electrochem. Soc.*, vol. 118, pp. 1200-1203, 1971.
[68] R. A. Logan and C. D. Thurmond, "Heterepitaxial Thermal Gradient Solution Growth of GaN," *J. Electrochem. Soc.*, vol. 119, pp. 1727-1735, 1972.
[69] J. I. Pankove, E. A. Miller, and J. E. Berkeyheiser, "GaN Electroluminescent Diodes," *RCA Rev.*, vol. 32, pp. 383-392, 1971.
[70] J. I. Pankove, E. A. Miller, and J. E. Berkeyheiser, "GaN Blue Light-Emitting Diodes," *J. Luminescence*, vol. 5, pp. 84-86, 1972.
[71] J. I. Pankove, E. A. Miller, and J. E. Berkeyheiser, "GaN Yellow Light-Emitting Diodes," *J. Luminescence*, vol. 6, pp. 54-60, 1973.
[72] H. P. Maruska, D. A. Stevenson, and J. I. Pankove, "Violet Luminescence of Mg-Doped GaN," *Appl. Phys. Lett.*, vol. 22, pp. 303-305, 1973.
[73] M. R. Lorenz, W. Reuter, W. P. Kumke, R. J. Chicotka, G. D. Petit, and J. M. Woodall, "Band Structure and Direct Transition Electroluminescence in the $In_{1-x}Ga_xP$ Alloys," *Appl. Phys. Lett.*, vol. 14, pp. 421-423, 1968.
[74] C. J. Nuese, D. Richman, and R. B. Clough, "The Preparation and Properties of Vapor-Grown $In_{1-x}Ga_xP$," *Met. Trans.*, vol. 2, pp. 789-794, 1971.
[75] B. W. Hakki, "Growth of $In_{1-x}Ga_xP$ p-n Junctions by Liquid Phase Epitaxy," *J. Electrochem. Soc.*, vol. 118, pp. 1469-1493, 1971.
[76] H. Kressel and I. Ladany, "Electroluminescence in $Al_xGa_{1-x}P$ Diodes Prepared by Liquid-Phase Epitaxy," *J. Appl. Phys.*, vol. 39, pp. 5339-5340, 1968.

Reprinted by permission from IEEE TRANSACTIONS ON PARTS, HYBRIDS, and PACKAGING
Vol. PHP-9, No. 4, December 1973, pp. 208-215

APPENDIX F

"The Preparation and Properties of Aluminum Nitride Films," T. L. Chu and R. W. Kelm, Jr., J. Electrochem. Soc., 122, 995-1000 (1975).

The Preparation and Properties of Aluminum Nitride Films

T. L. Chu* and R. W. Kelm, Jr.*

Institute of Technology, Southern Methodist University, Dallas, Texas 75275

ABSTRACT

Aluminum nitride films have been deposited on silicon substrates at 800°-1200°C by the pyrolysis of an aluminum trichloride-ammonia complex, $AlCl_3 \cdot 3NH_3$, in a gas flow system. The deposit was transparent, tightly adherent to the substrate, and was confirmed to be aluminum nitride by x-ray and electron diffraction techniques. The deposited aluminum nitride films were found to be polycrystalline with the crystallite size increasing with increasing temperature of deposition. Other properties of aluminum nitride films relevant to device applications, including density, refractive index, dissolution rate, dielectric constant, and masking ability, have been determined. These properties indicate that aluminum nitride films have potential as a dielectric in electronic devices.

Aluminum nitride is a refractory, large energy gap material [sublimation temperature 2400°C (1), energy gap 5.9-6.2 eV (2, 3)] and has chemical, physical, and electrical properties suitable for several applications in electronic devices. For example, its large energy gap, good thermal stability [equilibrium vapor pressure of nitrogen at 1500°C: 0.05 Torr (4)], and chemical inertness [stable in air at temperatures up to 700°C (5)] suggest that aluminum nitride is a good dielectric for active and passive components in semiconductor devices. Aluminum nitride, being a piezoelectric material with a high acoustic velocity, is also well suited for the fabrication of surface wave acoustic devices.

Aluminum nitride has been prepared by several techniques, such as the direct combination of the elements and chemical reactions of gaseous aluminum and nitrogen-containing compounds on substrate surfaces. The direct combination technique requires temperatures in excess of 1500°C (2, 5, 6) and is not suitable for device applications. On the other hand, aluminum nitride films have been deposited on the surfaces of refractory metals, insulators, and semiconductors at considerably lower temperatures by the reaction of aluminum trichloride with ammonia (1, 3, 7-12) and the reaction of trimethylaluminum with ammonia (13). Aluminum nitride films up to 5 μm in thickness have also been deposited on metallic substrates by diode reactive sputtering, and the dielectric properties of sputtered aluminum nitride films were found to be superior to those of bulk polycrystalline material (14). The chemical deposition technique appears to be more compatible with the current device technology; however, the utilization of aluminum nitride in semiconductor devices has not been explored.

In this work, aluminum nitride films have been deposited on single crystal silicon substrates by the pyrolysis of an aluminum trichloride-ammonia complex in a gas flow system. The properties of the deposited films, such as structure, composition, density, refractive index, dissolution rate, dielectric constant, masking ability, etc., have been determined. The experimental methods and results are discussed in this paper.

Preparation of Aluminum Nitride Films

The ammonolysis of aluminum trichloride is commonly used for the deposition of aluminum nitride films. Because of the hygroscopic nature of aluminum chloride, an aluminum trichloride-ammonia complex was used as the starting material. The complex was prepared by saturating reagent grade anhydrous aluminum trichloride in a fused silica reaction tube with anhydrous ammonia at room temperature. The resulting mass was heated at 350°C in an ammonia flow, and the complex sublimed yielding a white crystalline powder. The composition of the complex, determined by dissolving a weighed amount of the specimen in a known volume of 0.1*N* hydrochloric acid and titrating the excess acid with 0.1*N* sodium hydroxide, was $AlCl_3 \cdot 3NH_3$. This complex is considerably more stable in the laboratory ambient than aluminum trichloride. Its vapor pressure was determined from the extent of vaporization in a sealed silica tube after heating at a predetermined temperature for 24 hr. The vapor pressure data in the temperature range 500°-800°K are shown in Fig. 1; the complex has sufficient vapor pressure at temperatures below 300°C for utilization in the deposition of aluminum nitride. The heat of vaporization of the complex calculated from the slope of this plot was 11.8 ± 0.2 kcal/mole.

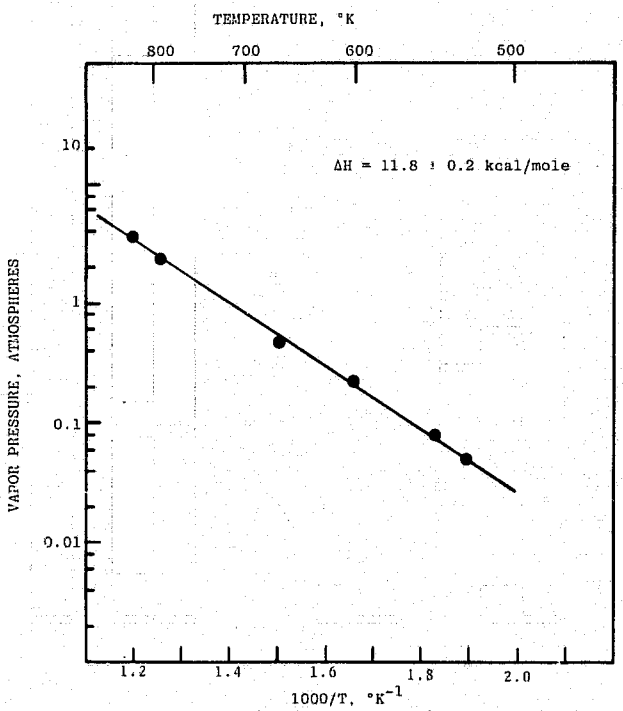

Fig. 1. Vapor pressure of aluminum trichloride-ammonia complex $AlCl_3 \cdot 3NH_3$.

* Electrochemical Society Active Member.

Key words: aluminum nitride, chemical deposition, electronic de-

The deposition of aluminum nitride by the pyrolysis of the aluminum trichloride-ammonia complex in a gas flow system was carried out using an apparatus shown schematically in Fig. 2. The diluent gases used in the deposition process were commercial hydrogen purified by diffusion through a palladium-silver alloy and Matheson anhydrous ammonia of better than 99.99% purity. The reaction tube was made of clear fused silica, 55 mm ID and 3 ft long. A fused silica boat containing the aluminum trichloride-ammonia complex was maintained at 250°C by using an external resistance heater, and hydrogen or a 6:1 hydrogen-ammonia mixture at a flow rate of 30 liters/min was used to carry the complex to the substrate surface. The silicon substrates with main faces of {111} orientation were n-type, 5-20 ohm-cm resistivity, and were mechanically polished and chemically etched in the usual manner. They were supported on a silicon carbide-coated graphite susceptor, and the susceptor was heated externally by an rf generator. Prior to the deposition of aluminum nitride, the substrates were heated at 1150°C in hydrogen for ½ hr to remove the oxide on the surface. In some experiments, the substrate surfaces were etched *in situ* at 1170°C with a hydrogen-hydrogen chloride mixture containing 2% hydrogen chloride. The deposition of aluminum nitride was carried out at substrate temperatures in the range of 800°-1200°C, and the deposition time was usually 15-45 min. The thickness of aluminum nitride films on silicon substrates was determined by removing part of the film and measuring the height of the step generated with a Sloan Dektak and Graphic Chart Recorder.

Under the conditions described above, the deposited films are transparent and tightly adherent to the substrate. The average deposition rates in the temperature range 800°-1200°C are shown in Fig. 3. The deposition rate decreased with increasing temperature from 160 Å/min at 800°C to 120 Å/min at 900°C and 90 Å/min at 1000°C. This decrease of deposition rate is due presumably to the increased contribution of gas phase nucleation at high temperatures. The gas phase nucleation becomes more pronounced at higher concentrations of the aluminum trichloride-ammonia complex in the reactant mixture. For example, films deposited at a rate of 750 Å/min at 900°C had a cloudy appearance as a result of the enhanced gas phase nucleation.

The films deposited in the temperature range 800°-1100°C were analyzed by the x-ray diffraction technique. Silicon substrates were removed from the specimens by etching with a nitric acid-hydrofluoric acid mixture, and the resulting material was pulverized and examined by the Debye-Scherrer technique using nickel-filtered CuKα radiation. The diffraction patterns were identical with those reported for aluminum nitride (15), thus confirming that the deposited films were aluminum nitride.

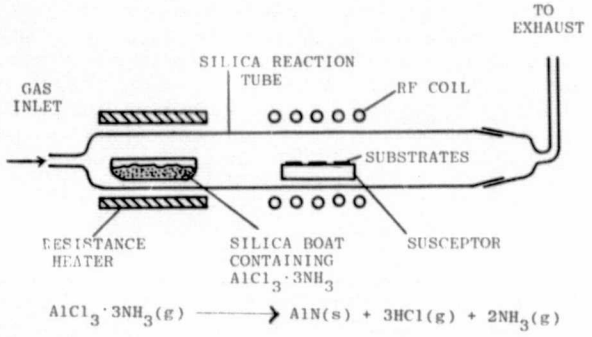

Fig. 2. Schematic of the apparatus used for the deposition of aluminum nitride films.

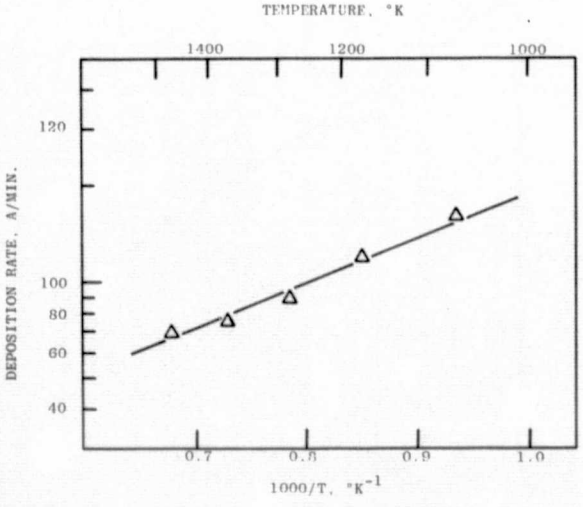

Fig. 3. Average deposition rate of aluminum nitride films as a function of temperature.

Properties of Aluminum Nitride Films

Structure.—Aluminum nitride films deposited on silicon substrates under proper conditions were uniform, transparent, and highly adherent to the substrate. They showed no structural features when examined with an optical microscope. Several films were investigated by transmission electron microscopy using a Hitachi Model 11BU electron microscope after removing the substrates with a nitric acid-hydrofluoric acid mixture. Figure 4 shows the micrographs of aluminum nitride films deposited in the temperature range 800°-1100°C. All films were polycrystalline, and the average linear dimensions of the crystallites increased with increasing deposition temperature. Typical dimensions of crystallites were 100, 200, 600, 1100, and 2200Å in films deposited at 800°, 900°, 1000°, 1100°, and 1200°C, respectively. This increase in crystallite size with temperature is to be expected. The diffraction patterns of aluminum nitride films deposited at various temperatures are shown in Fig. 5. The d-spacings measured from these patterns further confirm that all films are aluminum nitride. Figure 5

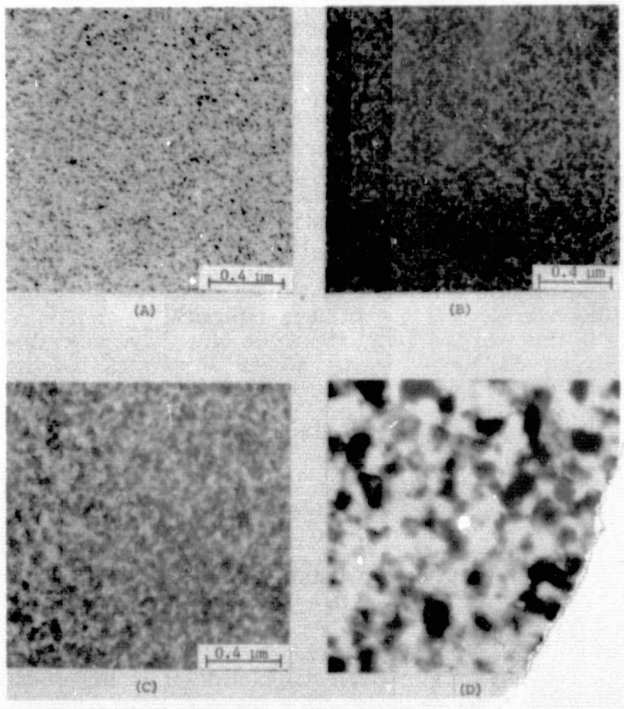

Fig. 4. Transmission electron micrographs of α' films deposited at (A) 800°C, (B) 900°C, (C) 1100°C.

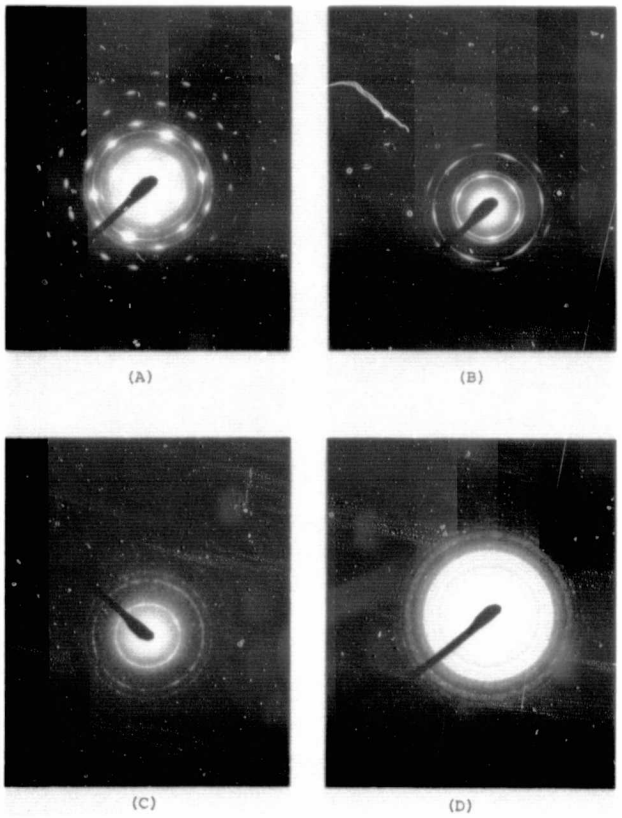

Fig. 5. Electron diffraction patterns of aluminum nitride films deposited at (A) 800°C, (B) 900°C, (C) 1100°C. and (D) 1200°C.

indicates that aluminum nitride films deposited at temperatures above 1000°K are polycrystalline and that preferred orientations are increasingly apparent with decreasing temperature of deposition. The single crystallinity of the substrates appears to have little or no effect on the structural properties of aluminum nitride since aluminum nitride films deposited on the surface of silicon dioxide were essentially the same as those on silicon substrates.

Density, refractive index, and optical absorption.—The density of aluminum nitride films deposited at various temperatures was determined by the floating equilibrium technique using a mixture of 1-bromo 2-iodo benzene and methylene iodide. The temperature of deposition was found to affect only slightly the density of aluminum nitride. Aluminum nitride films deposited at 800°, 900°, 1000°, and 1100°C have densities of 3.15, 3.18, 3.18, and 3.20 ± 0.01 g/cm^3, respectively, as compared with a reported value of 3.13 g/cm^3 (12) and the theoretical density of 3.26 g/cm^3.

The refractive index of aluminum nitride films deposited in the temperature range 800°-1200°C was determined by the Becke line method to be 1.991 ± 0.003, irrespective of the deposition temperature. A few samples were also measured by the ellipsometric technique; the results, though not as reproducible, were usually in good agreement with those by the Becke line method. However, refractive indices as high as 2.17 ± 0.05 have been reported for single crystalline aluminum nitride prepared by the direct reaction of aluminum with nitrogen (16).

The optical absorption spectra of aluminum nitride films deposited under various conditions were taken on a Beckman Model DK-2 spectrophotometer at room temperature. Typical results are shown in Fig. 6, where the thickness of the aluminum nitride film was 18 μm for curve A and 13 μm for curve B. The fundamental absorption edge for all specimens measured was found to be 5.9 ± 0.2 eV, in agreement with that observed by others (2). However, the films deposited at very high rates, 700 Å/min or higher irrespective of deposition temperature, exhibited an additional absorption band in the 3.0 to 3.2 μm region (curve A) while those deposited at low rates, 300 Å/min or lower, showed no absorption in this region (curve B). The absorption in the 3.0-3.2 μm region is presumably due to the N-H or Al-Cl bonds in aluminum nitride films deposited at high rates. As stated previously, the gas phase nucleation becomes pronounced at high deposition rates. The decomposition of the aluminum trichloride-ammonia complex in the gas phase may not proceed to completion, and the deposited material contained N-H or Al-Cl bonds. Thus, the use of low deposition rates is essential for obtaining good quality aluminum nitride films.

Dissolution behavior.—The deposited aluminum nitride films are soluble in phosphoric acid and sodium hydroxide solutions. To determine the dissolute rate of aluminum nitride films, a portion of the specimen was covered with Apiezon Q wax or photoresist, and the specimen was immersed in the etchant with constant agitation for various lengths of time. The dissolution rate was then determined by removing the protective coating and measuring the difference in the step heights using the Dektak system.

The dissolution rate of aluminum nitride films, deposited in the temperature range 800°-1200°C, in a 10% sodium hydroxide solution was determined in the

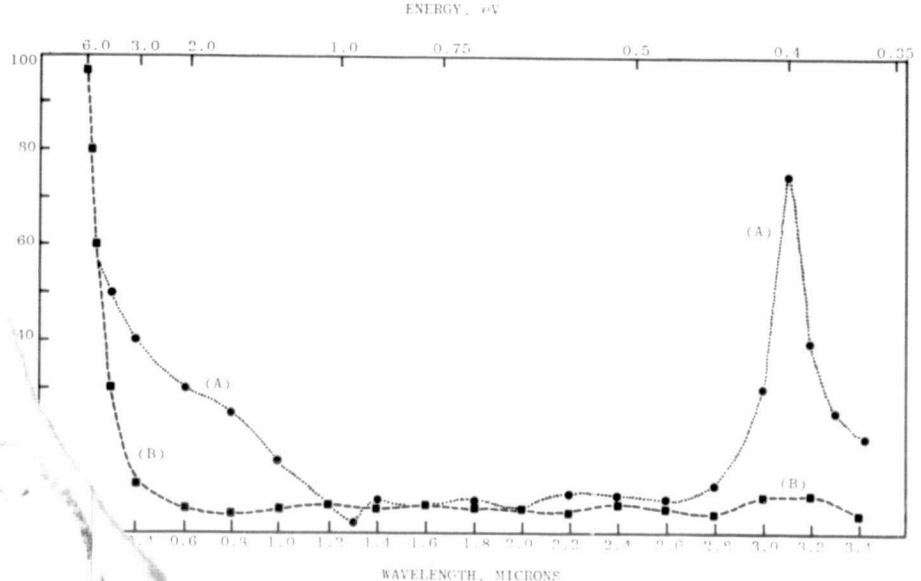

Fig. 6. Optical absorption spectra of aluminum nitride films deposited at a rate of about 700 Å/min (A) and at a rate of about 300 Å/min (B).

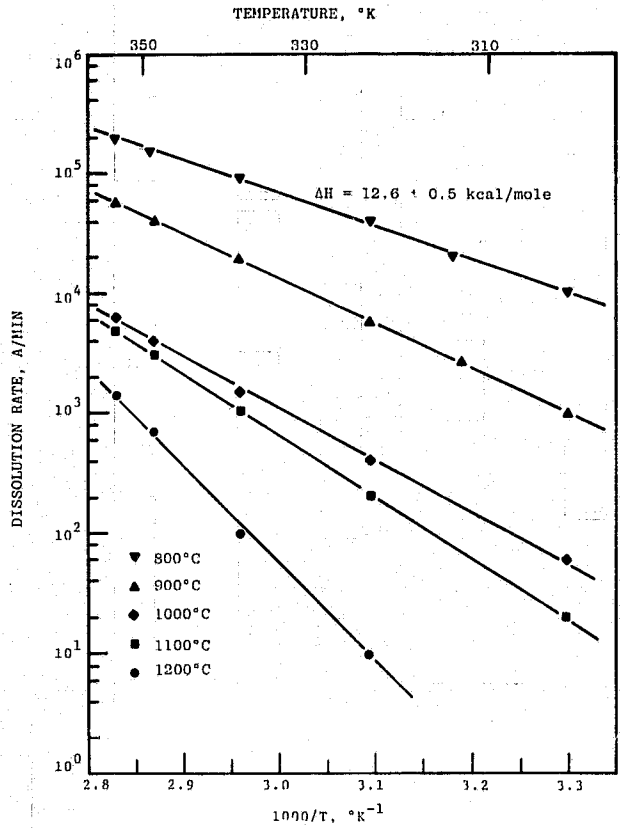

Fig. 7. Dissolution rate of aluminum nitride films, deposited in the temperature range 800°-1200°C, in 10% sodium hydroxide solution.

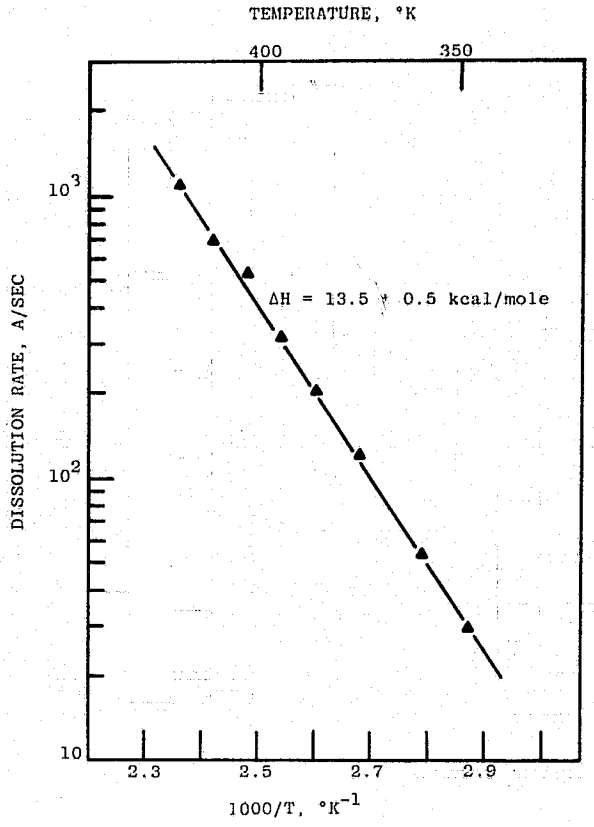

Fig. 8. Dissolution rate of aluminum nitride films deposited at 900°C in 85% phosphoric acid.

temperature range 30°-80°C. The results are shown in Fig. 7. At a given temperature, the dissolution rate of aluminum nitride films decreased with increasing deposition temperature, due presumably to the larger crystallites of aluminum nitride deposited at higher temperatures. Also, the dissolution rate of aluminum nitride films deposited at low temperatures was found to remain the same after annealing at higher temperatures, indicating negligible grain growth. The activation energy of dissolution for aluminum nitride films deposited at 800°C was found to be 12.6 ± 0.5 kcal/mole. The activation energy also increased with increasing deposition temperature. The relatively large activation energy indicates that the dissolution of aluminum nitride films is a surface-reaction controlled process.

The dissolution rate of aluminum nitride films deposited at 900°C was also determined using an 85% phosphoric acid solution. At temperatures up to 50°C, the dissolution rate of aluminum nitride was negligible. Figure 8 shows the dissolution rate in the temperature range 75°-150°C, and the activation energy of this dissolution was found to be 13.5 ± 0.5 kcal/mole, similar to the use of sodium hydroxide solution as an etchant.

Both sodium hydroxide and phosphoric acid solutions used in this work were found to produce clean and structureless surfaces, similar in appearance to the as-grown aluminum nitride films, when examined with an optical microscope.

Masking ability.—To explore the usefulness of aluminum nitride in silicon devices, its capabilities and limitations as masks against the diffusion of boron, phosphorus, aluminum, and gallium into silicon were investigated. Aluminum nitride films of 1000-1700Å thickness, deposited on silicon substrates at 900°C were used in the diffusion experiments. The substrates were n-type, 5-10 ohm-cm resistivity for the diffusion of boron, aluminum, and gallium, and were p-type, 10-20 ohm-cm for the diffusion of phosphorus. The aluminum nitride film was removed completely from circular areas (usually 500 μm diameter) of the specimen by photolithographic techniques using sodium hydroxide or phosphoric acid as an etchant. Sharp, well-defined edges were obtained with virtually no undercutting.

The boron diffusion was carried out by depositing boron oxide glass on the specimen surface at 970°C for 40 min from a boron nitride source followed by redistribution at 1300°C for 1 hr. In the phosphorus diffusion process, phosphorus oxide glass was deposited on the specimen surface at 1000°C for 30 min using phosphorus oxytrichloride as the source, and the redistribution was carried out at 1150°C for 1.5 hr. After the diffusion process, an unmasked region of the specimen was angle-lapped, and the aluminum nitride mask was removed by etching. The resistivity profile on the masked and unmasked regions of the main face and on the beveled surface was measured by the spreading resistance technique (17). The results for the boron diffusion into n-type silicon and the phosphorus diffusion into p-type silicon are shown in Fig. 9. The silicon under the aluminum nitride film was found to have the same conductivity type with essentially no change in resistivity, while p-n junctions were formed in unmasked regions. Thus, aluminum nitride films are successful for masking the diffusion of boron and phosphorus under the conditions used here.

Subsequent to the boron and phosphorus diffu process, the dissolution rate of the aluminum n masks in a 10% sodium hydroxide solution was sured. Aluminum nitride films with boron ox phosphorous oxide coatings showed no mea change in dissolution rate or appearance after at 1150°C for 1.5 hr, indicating the inertnes num nitride toward the dopant oxide. Ho the heat-treatment was carried out at after the deposition of boron oxide, rate of the nitride films decreased

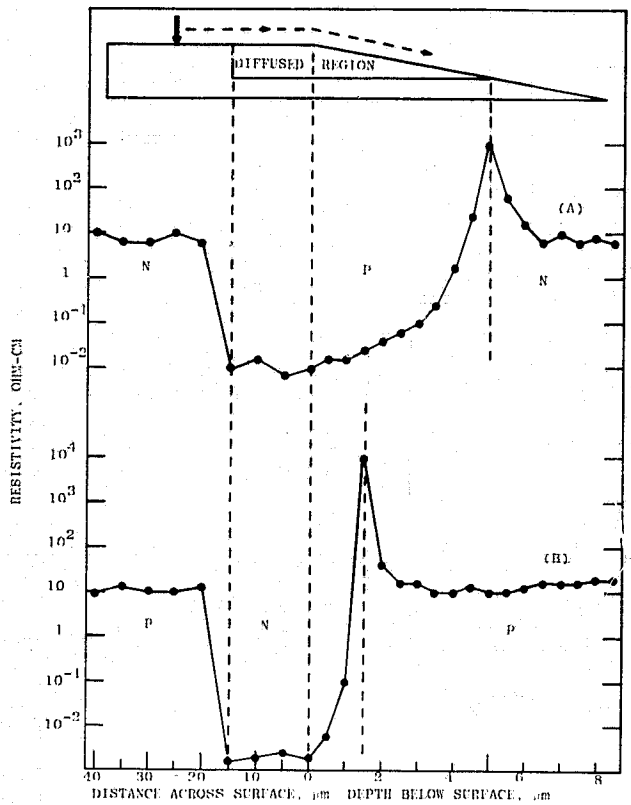

Fig. 9. Resistivity profiles in n-type (A) and p-type (B) silicon specimens after diffusion using aluminum nitride as a diffusion mask.

cating a reaction between aluminum nitride and boron oxide.

The aluminum and gallium diffusions were carried out at 1150°C for 1.5 hr in sealed fused silica tubes using the element as the source material. Aluminum nitride films failed to mask the diffusion of dopant in both cases. This is due presumably to the penetration of aluminum and gallium vapor through the grain boundaries in finely polycrystalline aluminum nitride films at high temperatures.

Dielectric properties.—The dielectric properties of aluminum nitride films were measured at room temperature using aluminum-aluminum nitride-silicon structures. Aluminum contacts of 2.5×10^{-2} cm diameter were deposited on aluminum nitride, and ohmic contacts were applied to the back surface of silicon substrates by electroless plating (18).

The dielectric strength of aluminum nitride films deposited in temperature range 800°-1000°C on low resistivity silicon substrates was measured at room temperature using d.c. and 400 kHz. The average dielectric strength of aluminum nitride was found to be 1.5×10^7 V/cm for films of 300-400Å thickness, independent of deposition temperature; it decreased to the apparent bulk value of approximately 10^7 V/cm for film thicknesses greater than about 1000Å. Aluminum nitride films deposited at 1100°C or above were found to have lower dielectric strength than those deposited at 800°-1000°C, due presumably to the inclusions in the films of the products of volume reaction where the decomposition of the aluminum trichloride-ammonia complex was not complete. The d-c dielectric strength of aluminum nitride films of 2000Å thickness prepared at 800°-1000°C was also measured at higher temperatures and was found to be approximately 10^7 V/cm at 30°C, 5×10^6 V/cm at 100°C, 2.5×10^6 V/cm at 200°C, 1.5×10^6 V/cm at 250°C, and 10^6 V/cm at 300°C.

Capacitance measurements were made on aluminum-aluminum nitride-silicon structures using a Boonton 75C Direct Capacitance Bridge operated at frequencies up to 0.5 MHz. The insulator capacitance was used to obtain the dielectric constant value. The dielectric constant of aluminum nitride films prepared at 800°, 900°, and 1000°C was found to be 11.5 ± 0.2, and that prepared at 1100°C was considerably lower, usually 8.1 ±0.3, as compared with 9.14 reported for the low-frequency dielectric constant of single crystalline aluminum nitride (19). Also, the dielectric constant of an aluminum nitride film prepared at 800°C was found to remain unchanged after heating at 1100°C in hydrogen for 1 hr, again indicating the structural stability of aluminum nitride. The dielectric constant of all aluminum nitride films prepared in the temperature range 800°-1100°C was found to be independent of frequency and temperature in the ranges 5-500 kHz and 100°-500°K, respectively.

It should be mentioned that the properties of aluminum nitride films discussed above are independent of the nature of the carrier gas, hydrogen or 6:1 hydrogen-ammonia mixture, used in the deposition process.

Summary and Conclusions

Aluminum nitride films have been deposited on silicon substrates at 800°-1200°C in a gas flow system by the thermal decomposition of an aluminum trichloride-ammonia complex, $AlCl_3 \cdot 3NH_3$. This complex was prepared by saturating aluminum trichloride with ammonia and purified by sublimation. The deposit was transparent, tightly adherent to the substrate and was verified by x-ray and electron diffraction techniques to be aluminum nitride. Transmission electron microscopy indicated that all aluminum nitride films were polycrystalline; the crystallite size increased with increasing temperature of deposition, and the preferred orientations became more apparent at lower deposition temperatures.

At deposition temperatures in the range of 800°-1000°C, the average density, refractive index, dielectric strength, and dielectric constant of aluminum nitride were found to be 3.18 g/cm^3, 1.99, 10^7 V/cm, and 11.5, respectively. Aluminum nitride films are soluble in sodium hydroxide and phosphoric acid solutions, and the standard photolithographic technique can be readily applied. Aluminum nitride films were found to be capable of masking against the diffusion of boron and phosphorus into silicon from the oxide sources. These properties indicate that aluminum nitride films have great potential as a dielectric in solid-state devices.

Acknowledgment

This research was supported by the Langley Research Center of the National Aeronautics and Space Administration under Grant NGL 44-007-042.

Manuscript submitted Feb. 6, 1974; revised manuscript received March 12, 1975.

Any discussion of this paper will appear in a Discussion Section to be published in the June 1976 JOURNAL. All discussions for the June 1976 Discussion Section should be submitted by Feb. 1, 1976.

REFERENCES

1. Th. Renner, *Z. Anorg. Allg. Chem.*, **298**, 22 (1959).
2. G. A. Cox, D. O. Cummins, K. Kawabe, and R. H. Tredgold, *J. Phys. Chem. Solids*, **28**, 543 (1967).
3. W. M. Yim, E. J. Stofko, P. J. Zanzucchi, J. I. Pankove, M. Ettenberg, and S. L. Gilbert, *J. Appl. Phys.*, **44**, 292 (1973).
4. D. L. Hildenbrand and W. F. Hall, *J. Phys. Chem.*, **67**, 888 (1963).
5. K. M. Taylor and C. Lenie, *This Journal*, **107**, 308 (1960).
6. G. A. Wolf, I. Adams, and J. W. Mellichamp, *Phys. Rev.*, **114**, 1262 (1959).
7. T. L. Chu, D. W. Ing, and A. J. Noreika, *Solid-State Electron.*, **10**, 1023 (1967).
8. A. M. Lejus, J. Thery, J. C. Giller, and R. Collongues, *Compt. Rend.*, **257**, 157 (1963).

9. A. J. Noreika and D. W. Ing, *J. Appl. Phys.*, **39**, 5578 (1968).
10. A. A. Pletyushkin and N. G. Slavina, *Neorg. Mater.*, **4**, 893 (1968).
11. M. D. Lyutaya, I. G. Chernysh, and Z. A. Yaremenko, *iibid.*, **5**, 1929 (1969).
12. D. W. Lewis, *This Journal*, **117**, 978 (1970).
13. H. M. Manasevit, F. M. Erdmann, and W. I. Simpson, *ibid.*, **118**, 1864 (1971).
14. A. J. Noreika, M. H. Francomb, and S. A. Zeitman, *J. Vacuum Sci. Technol.*, **6**, 194 (1969).
15. M. Stackelberg and K. F. Spiess, *Z. Phys. Chem.*, **A175**, 140 (1935).
16. J. Pastrnak and L. Roskovcova, *Phys. Status Solidi*, **14**, K5 (1966).
17. R. G. Mazur and D. H. Dickey, *This Journal*, **113**, 255 (1966).
18. M. V. Sullivan and J. H. Eigler, *ibid.*, **104**, 226 (1957).
19. A. T. Collins, E. C. Lightowlers, and P. J. Dean, *Phys. Rev.*, **158**, 833 (1967).

Reprinted from JOURNAL OF THE ELECTROCHEMICAL SOCIETY
Vol. 122, No. 7, July 1975
Printed in U.S.A.

APPENDIX G

"Electrolytic Etching of Boron Phosphide," T. L. Chu, M. Gill, and S. C. Chu, J. Electrochem. Soc., March, 1975.

ELECTROLYTIC ETCHING OF BORON PHOSPHIDE[†]

T. L. Chu,* M. Gill, and Shirley S. Chu
Institute of Technology
Southern Methodist University, Dallas, Texas 75275

ABSTRACT

The electrolytic etching of boron phosphide in various electrolytes was investigated. Conditions to polish p-type boron phosphide were determined, but an insoluble film tended to form on the surface of n-type material. For electrode potentials near and above 1 V, the removal of p-type material proceeded at a rate more than 100 times faster than the removal rate of n-type material. This difference in the etch rates allows selective removal of material, and mesa-type p-n homojunction and boron phosphide-silicon carbide heterojunction structures were fabricated.

[†]Supported by the Langley Research Center of the National Aeronautics and Space Administration under Grant NGL-44-007-042.

*Electrochemical Society Active Member

Key words: boron phosphide, electrolytic etching, electrolytic polishing, selective etching.

INTRODUCTION

Etching and polishing techniques are important processes for the study of semiconductors and for semiconductor device fabrication. For elemental semiconductors and some of the compound semiconductors, convenient chemical etchants are available for surface preparation and for certain types of selective etching. However, there are materials which are either inert to ordinary chemical etchants or are attacked very irregularly. In the case of boron phosphide, the only known etchants are fused alkalis at 400°-500°C and hydrogen chloride near 1100°C. The former etchant attacks boron phosphide very nonuniformly, and for the latter etchant, the decomposition of material at 1100°C is a problem. As a consequence, electrolytic etching may be the most useful etching technique for boron phosphide.

The purpose of this paper is to describe the experimental results obtained from an investigation of electrolytic etching of boron phosphide. Both p-type and n-type materials were studied, although more extensive data were obtained from p-type boron phosphide. The difference in the etching behavior of (111) and ($\bar{1}\bar{1}\bar{1}$) faces was investigated. Also, electrolytic etching was used as a selective etching process in the fabrication of junction devices.

EXPERIMENTAL

Electrolytic etching studies were carried out with both n-type and p-type boron phosphide platelets, which were grown by recrystallization from a nickel phosphide solution (1).

Boron phosphide crystals up to 7 mm x 4 mm x 3 mm have been obtained recently (2) by the accelerated container rotation technique (3,4). The main faces of the platelets have a (111) orientation; usually one face is smooth and the other face is rough. The two faces could also be distinguished by chemical etching in a 3:1 molten mixture of sodium hydroxide and sodium peroxide at 400 to 500°C. Dislocation etch pits were observed on the smooth face and not on the other. It is well established that the chemical etching of other III-V compound semiconductors produces etch pits on the group III face and not on the group V face (5). If the etching behavior of boron phosphide is similar to that of other III-V compound semiconductors, then the face which developed dislocation etch pits on the boron phosphide crystals is the boron, or the (111), face. The room temperature carrier concentration of the solution grown boron phosphide crystals, determined by measurements on Schottky barrier diodes, was on the order of 10^{18} cm^{-3} or above (6).

Prior to electrolytic etching, rough faces of the boron phosphide platelets were polished with 0.3 μm alumina abrasive, and as-grown smooth faces were etched without mechanical polishing. Ohmic contact to the back side of the boron phosphide crystals was made by electroless nickel plating followed by an annealing in hydrogen or argon at 800 to 850°C for one hour. For the etching process, Apiezon W wax was used as a mask so that only the desired region of the crystal surface was exposed to the

electrolyte. Silicon monoxide and silicon dioxide were also used for masking purposes and were found to be more reliable than Apiezon W wax for controlling small area geometries in the fabrication of mesa structures.

A schematic of the electrolytic cell used for the etching and polishing of boron phosphide is shown in Fig. 1. The current density-potential relationships were determined, and the crystal-electrolyte potential difference was measured relative to a calomel reference electrode. Measurements were made both in the dark and with illumination. The solution was continuously agitated by nitrogen bubbled into the electrolyte near the anode. A uniform removal of material without undercutting of etching masks was obtained with the boron phosphide platelets near the axis of a cylinderical molybdenum cathode, as shown in Fig. 1. A simple parallel plane electrode configuration was used for some of the basic measurements. The electrolytes investigated were aqueous solutions of common alkalis and acids, and a few chemical etchants previously used for other III-V semiconductors. With these techniques, mesa-type heteroepitaxial boron phosphide-silicon carbide junction and boron phosphide p-n junction structures were isolated.

RESULTS

Typical current density-potential relationships and rest potential values for p-type and n-type boron phosphide crystals in a 10% sodium hydroxide solution at room temperature in the dark are shown in Fig. 2. As expected, current saturation was observed in all of the experiments with n-type boron phosphide crystals. The p-type material was readily dissolved, and it

drew much larger currents than n-type material. At low anode potentials, the $(\bar{1}\bar{1}\bar{1})$ face of both n-type and p-type boron phosphide drew larger current densities at a particular electrode potential than did the (111) face. At anode potentials higher than about 1 V, the difference between the currents drawn by the (111) faces and the $(\bar{1}\bar{1}\bar{1})$ faces is very small.

The rest potentials of n-type and p-type boron phosphide were measured in a number of electrolytes in addition to sodium hydroxide, and the rest potential for n-type crystals was always more negative than the rest potential for p-type crystals. A similar relationship was reported for gallium phosphide rest potentials [7]. For both n-type and p-type boron phosphide, the rest potential was more positive for the (111) face. This polarity effect has also been observed for a number of other III-V compound semiconductors, and the group III element face was reported to have a more positive rest potential (5,7,8). This observation agrees, therefore, with the tentative assignment of the smooth (111) face of the crystals to the boron face.

The following observations were made specifically from the etching of p-type boron phosphide. Twin lines and other gross crystallographic defects were revealed with current densities of 0.01 A/cm^2 or lower. For current densities between 0.01 A/cm^2 and about 0.2 A/cm^2, etch pits formed on the faces. At larger current densities, above about 0.5 A/cm^2, the (111) and $(\bar{1}\bar{1}\bar{1})$ faces had different etching characteristics. On the

(111) face, a film tended to form; this film was, however, easily removed. The texture of the etched (111) face was rough as shown in Fig. 3A. On the ($\bar{1}\bar{1}\bar{1}$) face, however, there was no evidence of film formation, and a smooth, mirror-like surface finish shown in Fig. 3B was produced. These observations are very similar to the results reported for gallium phosphide (7); at high current densities, the gallium face developed a rough texture and the phosphorus face became smooth. A few experiments were also carried out with other electrolytes, and the etching characteristics of p-type boron phosphide in potassium hydroxide solutions and common acids were found to be similar to the characteristics obtained with the use of sodium hydroxide solutions.

In contrast to the etching of p-type boron phosphide, the etching of n-type boron phosphide was complicated by the formation of surface films at current densities higher than about 10^{-3} A/cm^2. At this current density, a film was observed with a 15 min. etching period; with higher current densities, the film grew faster. The film could not be completely removed from the surface of the crystal even with ultrasonic agitation during etching, and the film was not soluble in hot alkali mixtures. X-ray measurements indicated that the films were predominantly boron phosphate (BPO_4).

With current densities above 1 A/cm^2 through n-type boron phosphide, a porous, brittle, fiber-like film formed on the surface. Reflection electron diffraction examination showed that these films were monocrystalline boron phosphide of (111)

orientation. It was concluded, therefore, that anodic disintegration of n-type boron phosphide at high current densities occurred preferentially in <111> directions, and a surface layer which is a skeleton of the original crystal remained. Similar results were obtained from an etching study of gallium arsenide (9).

Various approaches were investigated to determine the conditions for the electrolytic polishing of n-type boron phosphide. A variety of electrolytes in addiiton to sodium hydroxide were used without success; an insoluable film formed in all cases. The effect of illumination on the etching of n-type boron phosphide was also investigated. A 650 watt incandescent lamp with a color temperature of 3400°K was used as the light source, so that a significant portion of the lamp output had an energy greater than the band gap of boron phosphide. A negative shift of about 0.2 V or more of the rest potentials was observed with illumination, but very little difference in the cell currents was found. Consequently, the anodic dissolution behavior was not significantly affected by the illumination. N-type boron phosphide was successfully etched without film formation only under one condition: the n-type material exposed to the electrolyte was one side of a shallow, forward biased p-n junction. This observation supports the well-known fact that a supply of holes is required for electrolytic etching (10,11).

SELECTIVE ETCHING

It can be seen from Fig. 2 that the current density at, for example, 3 volts is about 300 times higher for p-type boron

phosphide than for n-type material. This current density ratio corresponds approximately to the etch rate ratio between p-type and n-type boron phosphide, suggesting the possibility of selective removal of p-type material from boron phosphide p-n structures. The preferential etching of p-type material was initially investigated with a number of solution grown boron phosphide crystals with built-in p-n junctions on a crystal face. Selective removal of p-type boron phosphide was obtained with current densities between 0.1 A/cm^2 and 10 A/cm^2. To prevent the formation of a surface film on the n-type regions, either very low current densities with a long etching time or very high currents for a very short time were used. Figure 4 shows one solution grown crystal which was selectively etched; the p-type region developed a mirror-like finish, and no removal of n-type material was observed. With low current densities and short etching times, electrolytic etching was also used to delineate thin epitaxially grown p-n junctions in boron phosphide.

Since electrolytic etching is selective, it can be used to produce mesa junction structures in boron phosphide. Mesa diodes were formed with both homoepitaxially and heteroepitaxially grown junctions. Both n-type and p-type layers of boron phosphide were deposited on solution grown boron phosphide cyrstals and on hexagonal silicon carbide platelets by the thermal reduction of a boron tribromide-phosphorus trichloride mixture (12). To isolate the mesas, either silicon dioxide or silicon

monoxide was used to define the mesa pattern, and the exposed boron phosphide was electrolytically removed. In the preparation of the boron phosphide-silicon carbide heterojunctions, a sharp decrease in the current indicated the complete removal of the boron phosphide layer exposed to the electrolyte. At that stage, the electrolyte was replaced by a 1N solution of hydrofluoric acid, and a slight anodic etching of the silicon carbide was carried out. This latter step improved the characteristics of the mesa junctions. The removal of n-type boron phosphide on silicon carbide required mechanical means to occasionally remove a surface film near the edge of the mesa. Figure 5 shows photomicrographs of two mesa junctions fabricated by anodic dissolution of boron phosphide. Figure 5A shows a homojunction made by selective removal of a portion of an n-type epitaxial layer on a p-type substrate, and Fig. 5B shows a p-type boron phosphide mesa on n-type silicon carbide. These devices have rectifying characteristics, and easily visible, red, p-n junction electroluminescence was observed in some of the homojunction and heterojunction structures (13).

SUMMARY

Electrolytic etching of boron phosphide was investigated for device applications, since there is no suitable chemical etchant for this material. A technique was developed to etch and polish p-type boron phosphide. In contrast, an insoluable film tended to form on n-type boron phosphide, and material removal was very slow. Due to a large differential etch rate ratio between p-type and n-type material, boron phosphide p-n junction interfaces were delineated by electrolytic etching. Electrolytic

etching was also applied to the fabrication of mesa-type boron phosphide p-n junctions and boron phosphide-silicon carbide heterojunction structures. Because of the inert nature of boron phosphide, electrolytic etching is the most suitable means available to remove p-type material and to isolate mesa-type junctions.

ACKNOWLEDGMENT

The authors wish to thank Dr. R. K. Smeltzer for discussions and critical reading of the manuscript.

REFERENCES

1. T. L. Chu, J. M. Jackson and R. K. Smeltzer, This Journal, 120, 802 (1973).
2. T. L. Chu, M. Gill, and R. K. Smeltzer, J. Crystal Growth, submitted for publication.
3. H. J. Scheel and E. O. Schulz-DuBois, J. Crystal Growth, 8, 304 (1971).
4. H. J. Scheel, J. Crystal Growth, 13/14, 560 (1972).
5. H. C. Gatos and M. C. Lavine, This Journal, 107, 427, (1960).
6. H. B. Morris, M. S. Thesis, Southern Methodist University, Dallas, Texas (1973).
7. R. L. Meek and N. E. Schumaker, This Journal, 119, 1148 (1972).
8. M. E. Straumanis, J. P. Krumme and W. J. James, This Journal, 115, 1050 (1968).
9. J. P. Krumme and M. E. Straumanis, Trans. Met. Soc. AIME, 239, 395 (1967).
10. W. H. Brattain and C. G. B. Garrett, Bell Syst. Tech. J., 34, 129 (1955).
11. H. Gerischer in "Physical Chemistry" IXA, p. 523, H. Eyring, Editor, Academic Press, New York (1970).
12. T. L. Chu, J. M. Jackson, A. E. Hyslop, and S. C. Chu, J. Appl. Phys., 42, 420 (1971).
13. T. L. Chu and M. Gill, to be published.

FIGURE CAPTIONS

Figure 1 Schematic of the electrolytic cell used for measurements and etching.

Figure 2 Current density vs. electrode potential for (111) and ($\bar{1}\bar{1}\bar{1}$) faces of n-type and p-type boron phosphide in a 10% NaOH solution in the dark.

Figure 3 Electrolytically etched surfaces of p-type boron phosphide with a current density of 0.5 A/cm^2. (A): (111) face, (B): ($\bar{1}\bar{1}\bar{1}$) face.

Figure 4 Photomicrographs of an electrolytically etched boron phosphide crystal which has both n-type and p-type regions. Etching was done with 10 A/cm^2 for 10 sec. (A): top view, (B): cross sectional view.

Figure 5 Two mesa structures fabricated by electrolytic etching: (A) boron phosphide p-n homojunction and (B) boron phosphide-silicon carbide heterojunction.

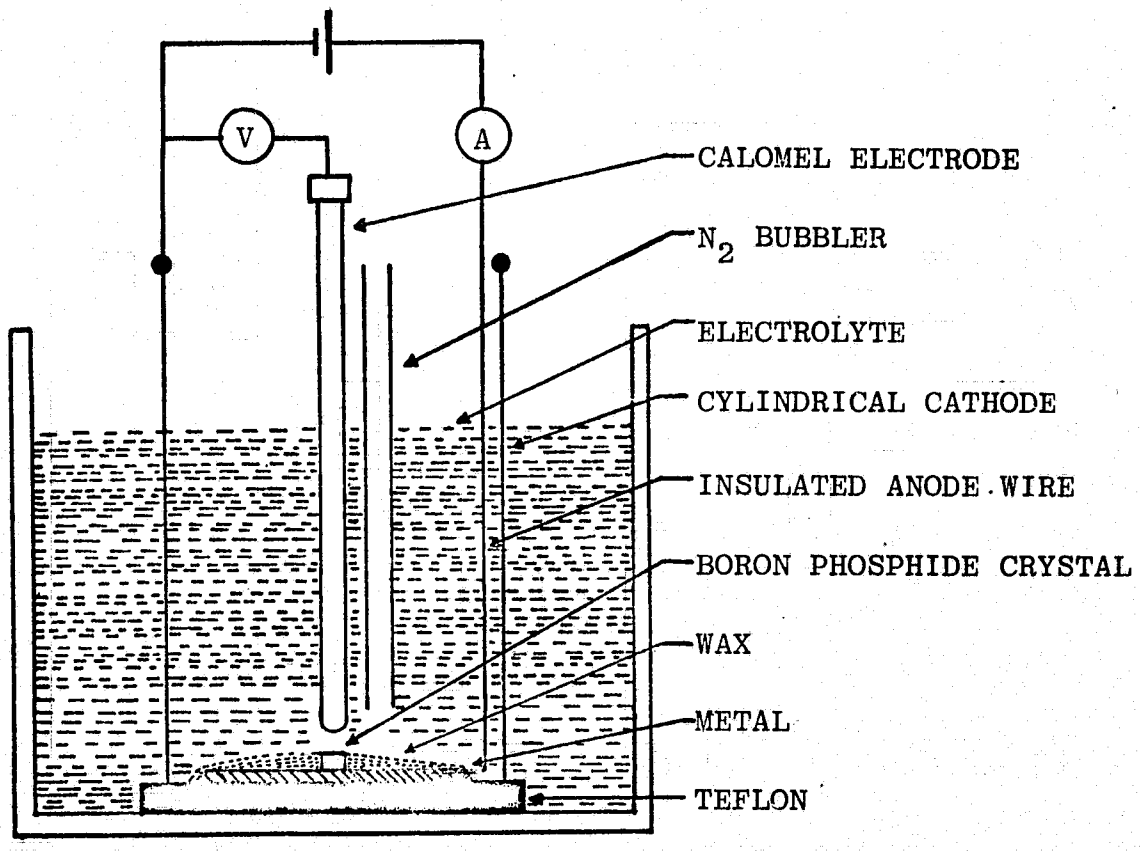

Fig. 1 Schematic of the electrolytic cell used for measurements and etching.

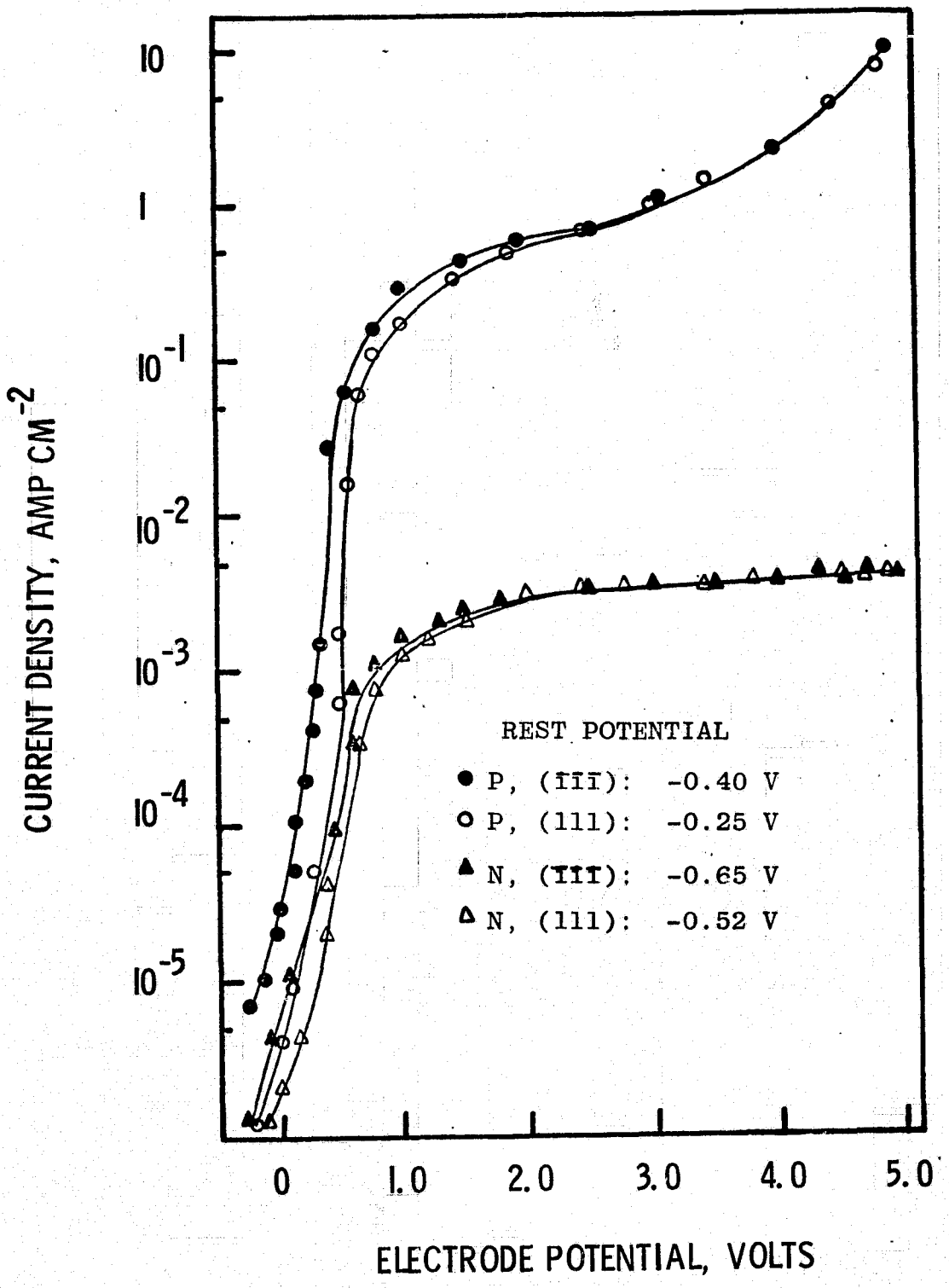

Fig. 2 Current density vs. electrode potential for (111) and (1̄1̄1̄) faces of n-type and p-type boron phoshide in a 10% NaOH solution in the dark.

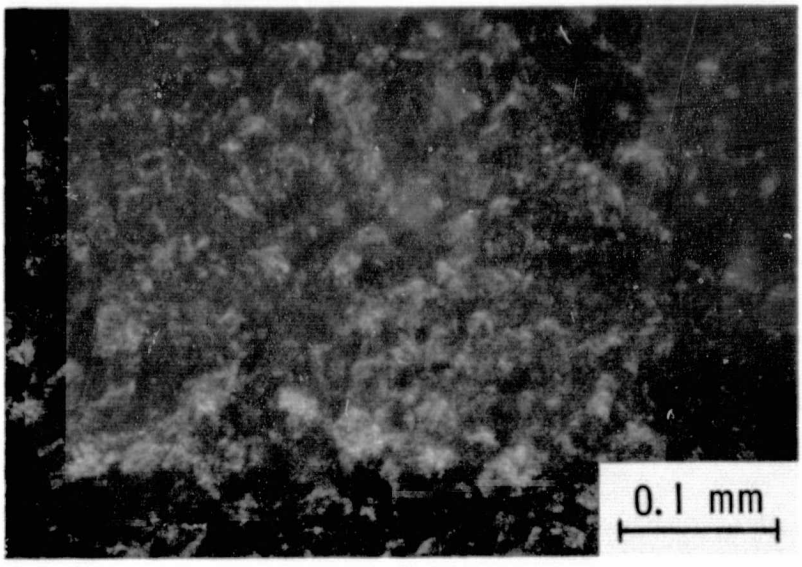

(A)

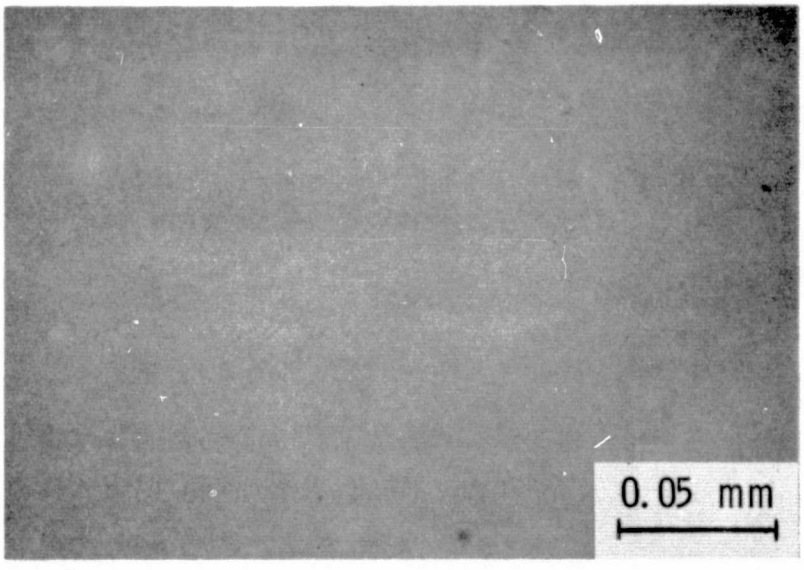

(B)

Fig. 3 Electrolytically etched surfaces of p-type boron phosphide with a current density of 0.5 A/cm^2.

(A): (111) face, (B): ($\bar{1}\bar{1}\bar{1}$) face.

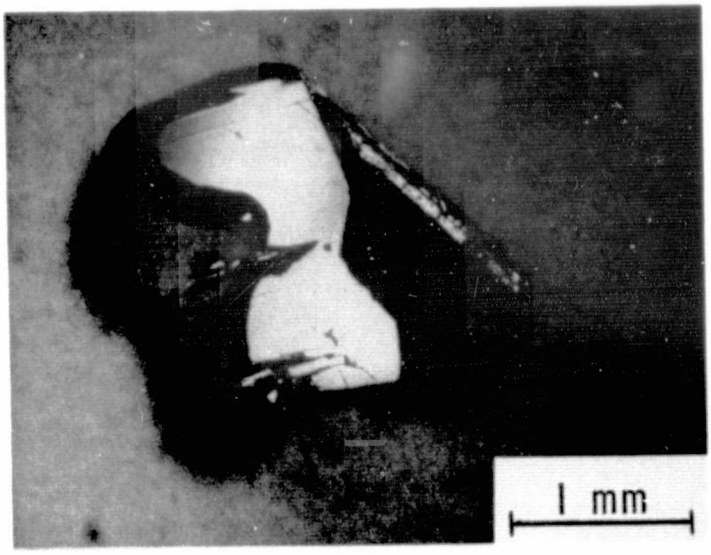

(A)

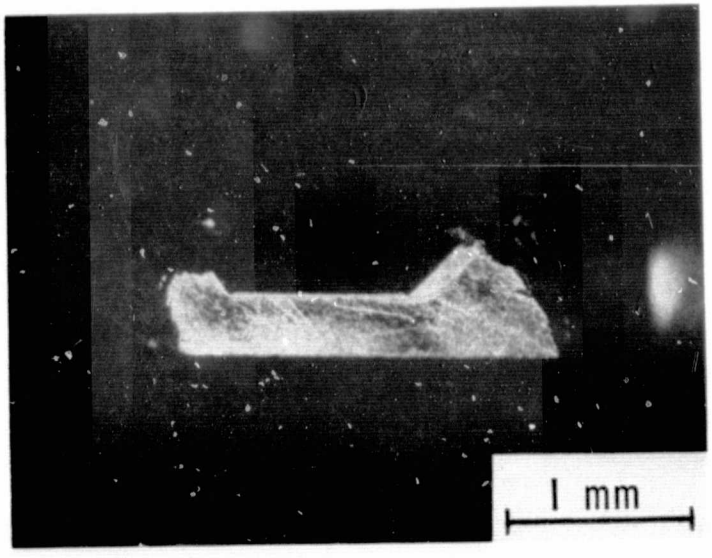

(B)

Fig. 4 Photomicrographs of an electrolytically etched boron phosphide crystal which has both n-type and p-type regions. Etching was done with 10 A/cm^2 for 10 sec.

(A): top view, (B): cross sectional view.

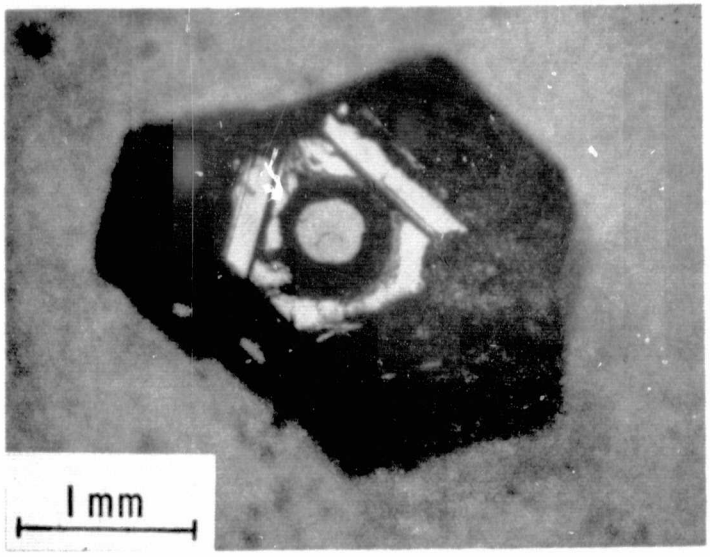

(A)

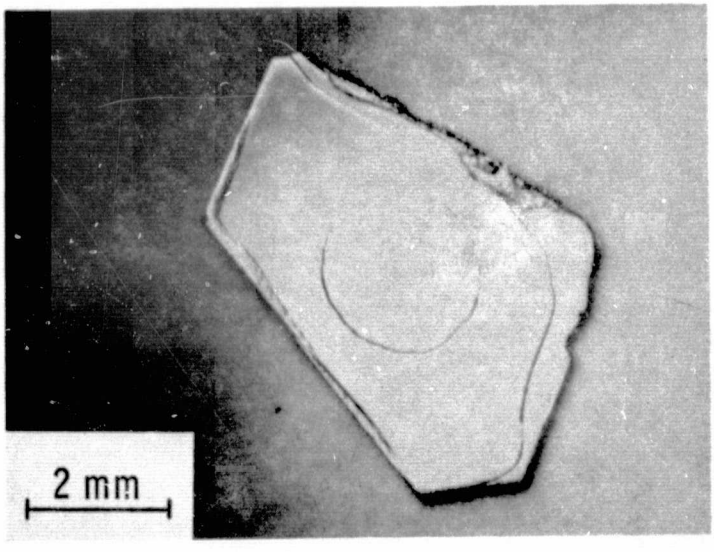

(B)

Fig. 5 Two mesa structures fabricated by electrolytic etching: (A) boron phosphide p-n homojunction and (B) boron phosphide-silicon carbide heterojunction.

APPENDIX H

"Growth of Boron Monophosphide Crystals with the Accelerated Container Rotation Technique," T. L. Chu, M. Gill, and R. K. Smeltzer, J. Crystal Growth, accepted for publication.

GROWTH OF BORON MONOPHOSPHIDE CRYSTALS WITH THE ACCELERATED CONTAINER ROTATION TECHNIQUE*

T. L. Chu, M. Gill, and R. K. Smeltzer
Institute of Technology
Southern Methodist University
Dallas, Texas 75275, U.S.A.

The recrystallization technique for the growth of boron phosphide from a nickel phosphide solution was extended to include accelerated container rotation. In comparison with crystals grown in a stationary container, larger crystals, with dimensions on the faces up to 8 mm, were obtained with the accelerated container technique. It was also established that the particular nickel phosphide used as the solvent for boron phosphide is important; optimum results were obtained with Ni_2P. The majority of the large boron phosphide crystals grown from solution contained both n-type and p-type regions, and easily visible, red p-n junction electroluminescence was observed. The addition of silicon to the nickel phosphide-boron phosphide solutions produced only n-type boron phosphide and the addition of beryllium produced p-type crystals. The crystals are suitable as substrates for epitaxial growth of boron phosphide and for electrolytic etching studies.

*Supported by the Langley Research Center of the National Aeronautics and Space Administration under Grant NGL 44-007-042.

1. Introduction

Boron monophosphide (BP, referred to as boron phosphide hereafter) is one of the III-V compound semiconductors with a large energy gap, approximately 2.0 eV[1,2]. The preparation of large single crystals of boron phosphide is, however, difficult. Its unknown high melting point, high dissociation pressure (about 1 mm at 1100°C), and decomposition into a subphosphide (B_6P) at elevated temperatures[3]) pose difficulties in the crystal growth of boron phosphide, especially by conventional melt growth techniques. Neither chemical transport[4,5]) nor high pressure synthesis[6,7,8]) have produced single crystals larger than about 2 mm in any one dimension. Boron phosphide crystals have been grown by recrystallization from solution [2,9,10]) and by precipitation from boron-nickel-phosphorus melts [10,11]). Crystals with one dimension up to about 4 mm have been obtained from these solutions.

In the work discussed here, the recrystallization technique for the preparation of boron phosphide was extended to include accelerated container rotation, which was reported to improve the crystal size and quality of aluminate and garnet crystals[12-14]). Various nickel phosphides were investigated as solvents for boron phosphide. In addition, the results of intentional doping experiments, which produced both n-type and p-type boron phosphide, are discussed. The experimental procedures and results are summarized below.

2. Crystal Growth of Boron Phosphide

2.1 Recrystallization in a Stationary Container

From previous work[10]) it was concluded that recrystallization from nickel phosphide near 1200°C is the most promising technique investigated to date to grow large crystals of boron phosphide. For this reason, a more detailed study of the parameters of this process was carried out. In the recrystallization technique, a small temperature gradient is maintained across a saturated solution of boron phosphide in nickel phosphide with a source of polycrystalline boron phosphide at the high temperature end of the solution. Due to the higher solubility at higher temperatures, a concentration gradient is set up across the solution, and consequently, transport of boron phosphide from the polycrystalline source to the lower temperature region occurs.

The recrystallization experiments were carried out in evacuated fused silica ampules located in a vertical resistance heated furnace. The ampules were 13 cm long, with a 15 mm ID and a 20 mm OD. A fused silica rod, which extended to a cooler part of the furnace, was attached to the bottom of the ampule as a heat sink. The ampules contained 30 to 35 grams of nickel phosphide, 1.0 to 2.0 grams of polycrystalline boron phosphide, and various amounts of phosphorus. The boron phosphide source material was at the top of the solution. The ampules were positioned in the furnace such that the furnace temperature near the top of the solution was typically 1220°C, and at the bottom of the solution, the furnace temperature was 1200°C. In the experi-

ments which produced boron phosphide crystals, the crystals were found in the lower half of the ampule near the ampule wall.

The composition of the nickel phosphide, which has not been previously investigated in boron phosphide crystal growth experiments, was found to be important in the recrystallization process. The nickel-phosphorus system itself is known to be extremely complicated, and as many as ten different nickel phosphides, some with very similar stoichiometries, have been reported[15]. Therefore, a variety of conditions were used to synthesize nickel phosphide during this investigation. The synthesis was done with temperatures and phosphorus pressures similar to those conditions required for the recrystallization of boron phosphide. That is, temperatures in the range from 1200°C to 1400°C and phosphorus pressures from about one to five atm were used. The predominant compound formed in many of these experiments was Ni_2P as determined by x-ray data; the material solidified as needle-like crystals which are typical of this compound[15]. In one case, Ni_7P_3 was obtained. Some of the ingots obtained were phase mixtures of Ni_2P and other more phosphorus-rich nickel phosphides. A detailed analysis of the phase mixtures was not carried out, but NiP was probably the most phosphorus-rich compound formed. Since Ni_2P has a wide homogeneity range, it is also likely that there was excess phosphorus in the ingots.

All of the crystal growth experiments which produced large single crystals of boron phosphide used only Ni_2P as the solvent. The use of Ni_7P_3 produced only small crystals, and the phase mixtures of Ni_2P with other nickel phosphides produced no crystals. Ni_2P was conveniently made by the reaction of phosphorus vapor with nickel in sealed ampules near 1250°C. Also commercial nickel phosphide (Puratek, Norwood, Ohio), reported to be 99.9% Ni_2P, as the solvent produced equally good crystals if excess phosphorus over that amount used with the laboratory grown Ni_2P was added to the ampule. This indicates that the laboratory synthesized Ni_2P did contain excess dissolved phosphorus.

The amount of excess phosphorus needed in the crystal growth ampules was also investigated. With the commercial nickel phosphide, typically about 2 g of phosphorus was used, and with the laboratory grown Ni_2P, about 0.5 g of phosphorus was used. Small variations of these amounts did not affect the results. With a three to four week growth time, boron phosphide crystals in the form of platelets and sometimes polyhedrons were obtained. The main faces of the platelets were up to 20 mm^2 in area, and the thickness of the platelets was up to about 1.5 mm. The polyhedrons had maximum dimensions of 5 mm x 4 mm x 3 mm. Platelets predominated in these experiments, and their morphology is discussed in the next section.

2.2 Recrystallization with the Accelerated Container Rotation Technique

The accelerated container technique is an effective technique to stir liquids, and this technique was adapted to the solution growth procedures discussed above. The ampules were connected to a drive mechanism such that they could be rotated about the axis of the furnace. The maximum rotation rate was adjustable up to 120 rpm, the acceleration was adjustable in the range of $\pm 0.4\pi$ rad/sec^2, and the time period was variable in the range from a few sec to one min.

The boron phosphide crystals grown with the accelerated container rotation technique were larger, had fewer voids, and had better developed faces than those obtained from a stationary container. The experiments with the accelerated container produced boron phosphide crystals with dimensions on the faces up to 8 mm, and some of the crystals are shown in Fig. 1. The size of the crystals obtained from the accelerated container was not sensitive to the exact rotation conditions. A one min time period and a maximum rotation rate in the range from 40 rpm to 70 rpm produced the best results. Two different cycles of rotation were used with similar results: a simple sawtooth rpm versus time cycle with rotation in both directions and a truncated sawtooth rpm versus time cycle with rotation in both directions. These results demonstrate the usefulness of accelerated crucible rotation for the preparation of boron phosphide crystals.

Boron phosphide crystals obtained from the recrystallization experiments were usually in the form of thin platelets, but

polyhedrons were also obtained. The platelets usually had one main face flat and smooth and the other main face rough. The platelets had (111)-type main faces, and as previously described [10]) grew by the twin plane reentrant edge mechanism[16]). For platelets which grew with both main faces smooth, etching in a 3:1 sodium hydroxide:sodium peroxide mixture was found to produce etch pits on the face which normally grew with a smooth surface; no structure was produced by this etchant on the normally rough face.

The majority of the large boron phosphide crystals contained both p-type and n-type regions. Typically the faces were n-type and a central core was p-type. This inhomogeneous distribution of impurities is probably a result of two factors: a higher segregation coefficient for p-type impurities than for n-type impurities so that p-type impurities are depleted from the solution and a continuous supply of silicon, which as discussed below is an n-type impurity in boron phosphide, going into the solution from the ampule. A convenient technique to observe the n-type and p-type regions in these crystals is electrolytic etching[17]). Since p-type material etches much faster than n-type material, exposed p-type boron phosphide will be removed rapidly from a crystal. Figure 2 shows a cross section from a boron phosphide crystal which had the p-type core exposed on one main face. P-type boron phosphide could also be electrolytically polished to a smooth finish.

P-n junction electroluminescence was also observed in some of the crystals with built-in junctions. Easily visible red

emission was seen from the n-type side of crystals whose p-type core has been partly etched away. The electroluminescent emission required a current density of about 10 A/cm^2 through the junctions.

3. Intentional Doping of Recrystallized Boron Phosphide

Since the boron phosphide crystals obtained from these growth experiments usually contained both p-type and n-type regions, a number of doping experiments were carried out in an effort to produce crystals with a more uniform distribution of impurities. In these experiments, the elements zinc, magnesium, beryllium, sulfur, selenium, tellurium, and silicon were investigated as dopants.

Beryllium, magnesium, and zinc were expected to be p-type dopants in boron phosphide. These materials were added to the solution in the growth ampules both as the elements and as the phosphides: Zn_3P_2, Be_3P_2, and Mg_3P_2. The addition of zinc to the solution did not appear to affect the electrical properties of the crystals. However, both beryllium and magnesium were found to produce mostly p-type boron phosphide, although n-type regions were sometimes found in the crystals. Beryllium doping produced p-type crystals more consistently.

Among the expected n-type dopants investigated, only tellurium tended to produce n-type crystals; some crystals with p-type and n-type regions were also obtained with tellurium doping. The

addition of sulfur and selenium to the growth ampules did not noticeably affect the electrical properties of the crystals. The best n-type dopant, however, was silicon, and only n-type boron phosphide was obtained from growth experiments with silicon as the intentionally added impurity. The limited success of the doping experiments is probably due to the use of an element which is not a constituent of the grown crystals in the solution and to the presence of impurities in the nickel phosphide solvent.

4. Summary and Conclusions

The accelerated container rotation technique has been shown to be useful for the growth of boron phosphide crystals from a nickel phosphide solution. Larger crystals, with dimensions up to 8 mm, were obtained from experiments which used an accelerated container than from experiments with a stationary container. These results were obtained even with tall, small diameter growth ampules, in which the effect of accelerated container rotation is probably not as pronounced as in large diameter containers. The results of the experiments described in this paper also indicate that Ni_2P may be the best nickel phosphide solvent for the recrystallization of boron phosphide. Neither Ni_7P_3 nor phase mixtures of Ni_2P with more phosphorus-rich nickel phosphides produced large crystals. More nickel-rich nickel phosphides may also not be suitable, since a certain minimum amount of excess phosphorus had to be added to the growth ampules. Without the intentional addition of impurities to the growth ampules, the solution grown boron phosphide crystals usually contained built-in

p-n junctions. Easily visible, red electroluminescence was observed in some of these crystals. Intentional doping was successfully accomplished: silicon added to the solution produced only n-type boron phosphide and beryllium produced mostly p-type material. The boron phosphide crystals described in this paper have been used as substrates for epitaxial growth and for electrolytic etching investigations.

Acknowledgment

The work discussed in this paper was supported by the Langley Research Center of the National Aeronautics and Space Administration under Grant NGL 44-007-042.

References

1. R. J. Archer, R. Y. Koyana, E. E. Loebner, and R. C. Lucas, Phys. Rev. Lett. 12 (1964) 538.

2. C. C. Wang, M. Cardona, and A. G. Fischer, RCA Rev. 25 (1964) 159.

3. F. V. Williams and R. A. Ruehrwein, J. Amer. Chem. Soc. 82 (1960) 1330.

4. T. Nishinaga, H. Ogawa, H. Watanabe, and T. Arizumi, J. Crystal Growth 13/14 (1972) 346.

5. T. L. Chu, J. M. Jackson, and R. K. Smeltzer, J. Crystal Growth 15 (1972) 254.

6. T. Niemyski, S. Mierzejewska-Appenheimer, and J. Majewski, in "Crystal Growth", ed. H. S. Peiser (Peragamon, Oxford, 1967) p. 585.

7. K. P. Ananthanarayanan, C. Mohanty, and P. J. Gielisse, J. Crystal Growth 20 (1973) 63.

8. T. Kobayshi, K. Susa, S. Taniguchi, Mat. Res. Bull. 9 (1974) 625.

9. B. V. Baranov, V. D. Prochukhan, and N. A. Goryunova, Izv. Akad. Nauk SSSR, Neorgan. Materialy 3 (1967) 1691 {English translation p. 1477}.

10. T. L. Chu, J. M. Jackson, and R. K. Smeltzer, J. Electrochem. Soc. 120 (1973) 802.

11. M. Iwani, N. Fujita, and K. Kawabe, Jap. J. Appl. Phys. 10 (1971) 1746.

12. H. J. Scheel and E. O. Schulz-DuBois, J. Crystal Growth 8 (1971) 304.

13. H. J. Scheel, J. Crystal Growth 13/14 (1972) 560.

14. W. Tolksdorf and F. Welz, J. Crystal Growth 13/14 (1972) 566.

15. Egon Larsson, Arkin för Kemi 23 (1965) 335.

16. J. W. Faust and H. F. John, J. Phys. Chem. Solids 25 (1964) 1407.

17. T. L. Chu, M. Gill, and R. K. Smeltzer, J. Electrochem. Soc. (to be submitted).

FIGURE CAPTIONS

Fig. 1. Boron phosphide crystals grown by recrystallization near 1200°C from Ni_2P with accelerated container rotation.

Fig. 2. Cross section from an electrolytically etched boron phosphide crystal. The p-type core has been removed due to the preferential nature of electrolytic etching.

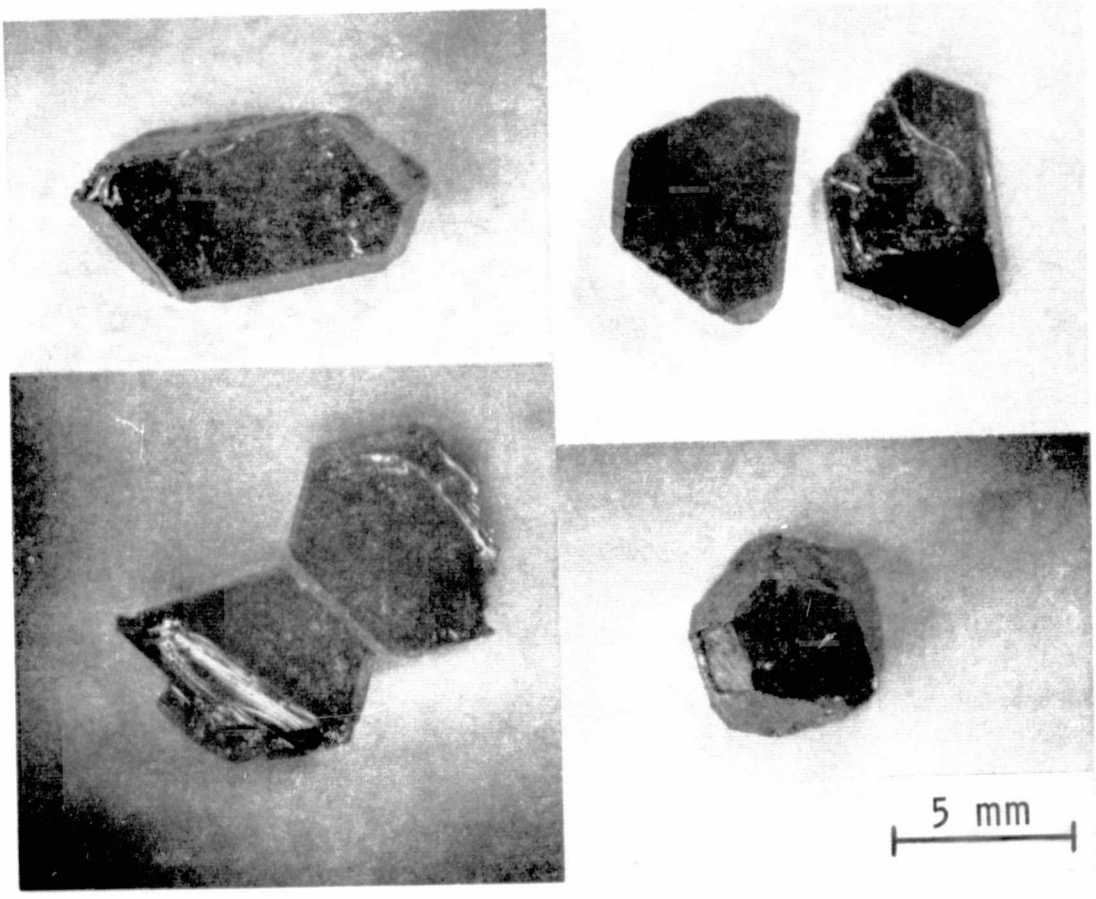

Fig. 1 Boron phosphide crystals grown by recrystallization near 1200°C from Ni_2P with accelerated container rotation.

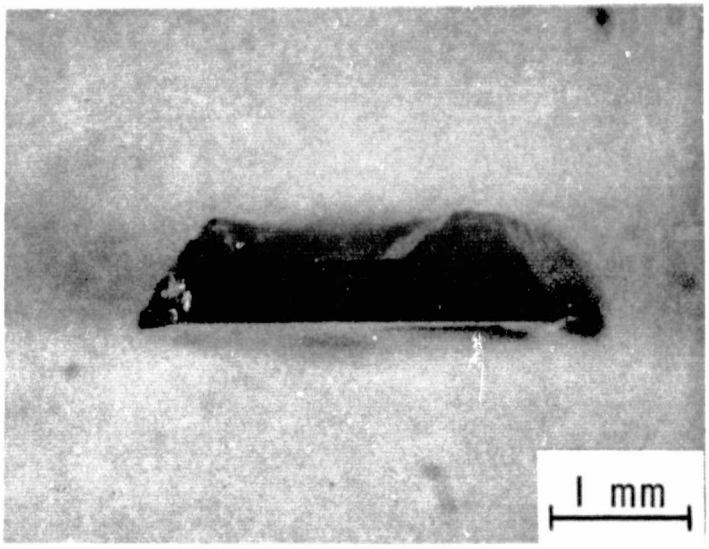

Fig. 2 Cross section from an electrolytically etched boron phosphide crystal. The p-type core has been removed due to the preferential nature of electrolytic etching.

APPENDIX I

"Boron Phosphide Crystals and Devices," Manzur Gill, Ph.D. Dissertation, Southern Methodist University, Dallas, Texas, 1975.

BORON PHOSPHIDE CRYSTALS AND DEVICES

A Dissertation

Presented through the

Department of Electrical Engineering

to

the Faculty of the

Institute of Technology

of

Southern Methodist University

in

Partial Fulfillment of the Requirements

for the Degree of

Doctor of Philosophy

by

MANZUR GILL

(B.Sc., The University of the Panjab, Lahore, Pakistan, 1962)
(M.Sc., The University of the Panjab, Lahore, Pakistan, 1965)
(M.S., Southern Methodist University, 1971)

August 20, 1975

ABSTRACT

This dissertation is concerned with the preparation of bulk single crystals and epitaxial layers of boron phosphide, the development of fabrication technology for boron phosphide devices, and the characterization of boron phosphide devices.

Bulk crystals of boron phosphide of both n-type and p-type conductivity were grown by recrystallization from nickel phosphide solutions near 1200°C using stationary and accelerated crucible rotation techniques. Both n-type and p-type epitaxial single crystalline layers of boron phosphide were grown on hexagonal silicon carbide and solution grown boron phosphide platelets by the thermal reduction of a boron tribromide-phosphorus trichloride mixture with hydrogen near 1075°C. The epitaxial layers were used for the fabrication of heterojunction and homojunction devices.

Because of the chemical inertness of boron phosphide, an electrolytic etching technique was developed for the controlled removal of boron phosphide at room temperature. This technique has been extremely useful for delineating p-n junctions in boron phosphide devices.

Metal-insulator-boron phosphide structures with silicon nitride (or silicon dioxide-silicon nitride) as the insulator have been fabricated; they are characterized by negative charges in the semiconductor-insulator interface. Silicon carbide-boron phosphide heterojunctions have been fabricated; they are characterized by high density of interface states. Mesa type boron phosphide p-n junctions were isolated from epitaxial layers and solution grown crystals. Easily visible red electroluminescence was observed from both epitaxial and solution grown p-n junctions as well as from point contact diodes.

ACKNOWLEDGMENT

The author is deeply grateful to Dr. T.L. Chu, for his guidance, encouragement, and patience during the course of this research.

Thanks are also due to the other members of his committee: Drs. J.K. Butler, J.P. Holman, W.F. Leonard, and R.K. Williams for their helpful suggestions. The author would also like to thank Drs. Shirley C. Chu and K.W. Heizer for their assistance.

The author is thankful to Mrs. Margaret C. Ingram for typing this dissertation.

The author would like to acknowledge the support of the National Aeronautics and Space Administration who funded this research under grant NGL 44-007-042.

This dissertation is dedicated to Susila, my loving wife.

TABLE OF CONTENTS

LIST OF TABLES

LIST OF ILLUSTRATIONS

C-3

C-3

CHAPTER I

INTRODUCTION

Boron monophosphide (BP, referred to as boron phosphide hereafter) is a III-V compound semiconductor which crystallizes in the zincblende structure with a lattice parameter a = 4.538 Å.[1] Boron phosphide has an indirect energy gap of approximately 2.0 eV.[2,3] Due to this relatively large band gap, boron phosphide has potential applications for high temperature devices and for optoelectronic devices for visible light emission. Gallium phosphide, another III-V compound with a similar band gap (2.2 eV), has been used extensively in the fabrication of light emitting diodes[4] and for high temperature rectifiers.[5] Gallium arsenide, also a III-V semiconductor of lower band gap (1.4 eV) has been used to fabricate infrared electroluminescent devices and high temperature diodes.[6,7] In contrast to gallium phosphide and gallium arsenide, boron phosphide is chemically inert and has a hardness almost equal to that of silicon carbide. Boron phosphide has recently been used as a component in the preparation of heat-resistant electrically insulating materials.[8] However, its high melting point ($>3000^{\circ}C$)[3], high dissociation

pressure (about 1 mm at 1100°C), and decomposition into a subphosphide (B_6P) at elevated temperatures[9] have posed difficulties in the crystal growth of boron phosphide of controlled purity suitable for device fabrication.

I.A Amorphous and Polycrystalline Boron Phosphide

Besson[10] and Moissan[11] first reported the preparation of boron phosphide powder by reacting boron halides with phosphorus or phosphine, but interest in boron phosphide increased only after Welker[12] showed that the compound has interesting semiconducting properties. Since then several investigators have used different methods to prepare boron phosphide. Amorphous and polycrystalline boron phosphide have been prepared by: (1) the direct combination of the elements in sealed tubes at 900° to 1100°C,[1,13-15] (2) the thermal decomposition of an addition compound of boron trichloride and phosphorus pentachloride[16] ($BCl_3 \cdot PCl_5 \xrightarrow{\Delta} BP + 4Cl_2$), (3) the reaction of boron and zinc phosphide[14] ($Zn_3P_2 + 2B \xrightarrow{1100°C} 2BP + 3Zn$), (4) the reaction of boron trichloride and phosphine[9] ($BCl_3 + PH_3 \xrightarrow{1100°C} BP + 3HCl$), (5) the reaction of aluminum phosphide with boron trichloride[9] ($BCl_3 + AlP \xrightarrow{1100°C} BP + AlCl_3$), and (6) the reaction of

phosphine with boron powder[17] ($2B + 2PH_3 \xrightarrow{1100^{\circ}C} 2BP + 3H_2$). Boron phosphide and boron subphosphide were found to be chemically inert to boiling mineral acids and aqueous alkali solutions, and only at elevated temperatures did molten sodium hydroxide attack boron phosphide slightly. Boron phosphide was also found to be resistant to oxidation in air up to about 800° to 1000°C, and at higher temperatures, the product of oxidation is boron phosphate (BPO_4).[9]

I.B Bulk Single Crystals of Boron Phosphide

The first single crystals of boron phosphide were grown in 1960 by Stone and Hill[18] by two different methods. In the first method, the vapor phase reaction of boron compounds with phosphorus compounds or phosphorus vapor was used to produce reddish brown boron phosphide crystals, 1 or 2 mm in length, and polycrystalline films on quartz. In the second method, the slow cooling of a melt containing boron and phosphorus resulted in boron phosphide crystals on the order of 1 mm in all dimensions. Hall measurements indicated that these boron phosphide crystals had a dopant concentration on the order of 10^{18} cm^{-3}. They estimated the index of refraction of boron phosphide from measurements of the displacement of an image to be between 3.0 and 3.5. An

abrupt decrease in the transmittance of polycrystalline films at 6 eV was interpreted to be the band gap of boron phosphide, and an absorption edge at 2 eV was assumed to account for the red color of boron phosphide.

Archer et al.[2] produced 1 mm x 1 mm x 0.1 mm boron phosphide single crystals by crystallization from a nickel phosphide solution. From their investigation of injection electroluminescence, optical absorption, and photoelectric response of gold-boron phosphide surface barrier diodes, they concluded that boron phosphide has an indirect energy gap of about 2 eV consistent with the red color of boron phosphide crystals. This was confirmed by Wang and co-workers[3] from optical transmission measurements on boron phosphide crystals. These crystals were grown by recrystallization from metal (nickel, iron, platinum, and germanium) solutions. Boron phosphide powder was dissolved in metal solvents which were heated by an rf generator to 1300° to 1500°C in closed quartz ampules under a phosphorus pressure of about 1 atm. Slow cooling of the saturated solution resulted in p-type, orange red, boron phosphide crystals which were several millimeter in size and polyhedral in shape. These crystals had a room temperature resistivity of 10^{-2} ohm-cm, a carrier concentration of

10^{18} cm^{-3}, and a hole mobility of 500 cm^2-$volt^{-1}$-sec^{-1} at room temperature. Red injection electroluminescence was observed at the anode when the crystals were contacted with metal probes. Yellow needle shaped boron phosphide crystallites, produced by the vapor phase reaction of boron oxide or boron oxysulfide with phosphorus, were also reported by Wang and co-workers.[3]

Grinberg and co-workers[19,20] used closed tube chemical transport to produce boron phosphide single crystals. The process was carried out at 900° to 1200°C with various temperature gradients between the source and the crystallization zone, and group VI elements were used as transport agents. It was found that the transport is diffusion limited and therefore proportional to the temperature gradient. The number of nuclei increased rapidly with the rise in temperature gradient. The temperature in the growth zone mainly affected the shape of the crystals; plate-like and dendritic crystals grew at high temperatures and isometric single crystals grew at low temperatures. The boron phosphide crystals grown in these experiments did not exceed 2 mm x 2 mm x 1 mm. The closed tube chemical vapor transport technique was also employed by Armington[21] to grow boron phosphide single crystals with

sulfur, selenium, and iodine as transport agents. Boron phosphide was transported from the high temperature zone (950° to 1000°C) to the low temperature zone (800°C) in evacuated quartz ampules. The reaction times varied from 30 to 90 days, but most of the transport appeared to occur during the first week. The yields in all the experiments were small and the largest crystals were 0.25 mm in diameter.

Baranov et al.[22,23] grew n-type boron phosphide single crystals by recrystallization from copper subphosphide (Cu_3P) with a vertically positioned ampule in a temperature gradient. A sintered pallet of boron phosphide, pressed mechanically into the lower portion of the ampule, was used as the source material. Since boron phosphide has a lower density than the solvent, the growth of boron phosphide crystals occurred in the upper, colder portion of the ampule. The experiment time of 1 month and the slow cooling at the end of the experiment resulted in transparent red boron phosphide single crystals with dimensions up to 4 mm x 3 mm x 2 mm.

Stearns and Greene[24] prepared boron phosphide and boron subphosphide ($B_{12}P_2$) from B-Ni-P systems in attempts to construct a phase diagram of the B-Ni-P system. They

reported that Ni_2P dissolves boron and Ni_3P does not, in agreement with the findings of Rundquist.[25] Boron phosphide single crystals were also prepared by Iwami and co-workers[26] from a B-Ni-P solution in a vacuum sealed silica tube, which was in a horizontal two zone furnace. In this work, a B-Ni alloy was heated to 1250°C in one end of the tube, and the temperature of the other end of the ampule was held at 430°C which corresponds to a phosphorus vapor pressure of 1 atm. Slow pulling of the ampule out of the furnace produced boron phosphide crystals up to 5 mm x 2 mm x 2 mm..

Chu et al.[27,28] have investigated the crystal growth of boron phosphide by both closed tube transport and recrystallization from metal phosphide solutions. In closed tube chemical transport experiments, polycrystalline boron phosphide was used as the source material. Phosphorus was introduced into the quartz ampule to suppress the decomposition of boron phosphide at high temperatures. Phosphorus trichloride, iodine and bromine were used as the transport agents. A source temperature of 1000° to 1290°C and temperature gradients in the range from 15° to 75°C were employed. The use of iodine as the transport agent with a source temperature of 1290°C, a temperature gradient of 15°

to 20°C and a flame worked fused silica tube yielded p-type boron phosphide single crystals in the form of polyhedrons measuring 1 to 2 mm on each side. In the recrystallization experiments two approaches were investigated: in the first, the addition of phosphorus to a boron-nickel or boron-copper melt at 1300°C followed by slow cooling resulted in boron phosphide single crystals up to 3 mm in size; secondly, the recrystallization of boron phosphide from a nickel phosphide or a copper phosphide solution in a temperature gradient at 1200°C produced low resistivity n-type crystals up to 4 mm in size.

I.C Epitaxial Layers of Boron Phosphide

In addition to the preparation of bulk crystals, the growth of epitaxial layers of boron phosphide has also been investigated. Takigawa and co-workers[29] grew 1 μm thick layers of single crystalline boron phosphide on silicon substrates of (100), (110) and (111) orientation by the thermal decomposition of a diborane-phosphine mixture in hydrogen in the temperature range of 950° to 1050°C. By adjusting the temperature and flow rates of the reactant gasses, both n-type and p-type, epitaxial boron phosphide layers of low resistivity were deposited. Nishinaga et al.[30] employed the thermal reduction of boron

tribromide-phosphorus trichloride mixtures to grow epitaxial single crystalline layers of boron phosphide, up to 30 μm in thickness, on the (111) face of silicon in the temperature range of 1000° to 1100°C. However, because of the lattice mismatch and the difference in the thermal expansion coefficients, grown samples were severely distorted into a concave shape with the boron phosphide layer inside. Chu et al.[31] have deposited boron phosphide layers on the basal plane of hexagonal silicon carbide by thermal reduction of boron tribromide-phosphorus trichloride mixtures with hydrogen. The grown boron phosphide layers were single crystalline and epitaxial with respect to the substrate and were of low resistivity p-type.

In addition to the work reviewed above, other researchers have determined several properties of boron phosphide. Ryan and Miller[32] studied the photoluminescence of boron phosphide at 1.8°, 5.0° and 77°K and reported a donor-acceptor pair spectrum at 1.8°K similar to that observed by Hopfield and co-workers[33] in gallium phosphide. The index of refraction from the measurement of the Brewster angle was reported to be 2.6 in contrast to a value of 3.1 from reflectivity measurements by Wang and co-workers.[3] Hemstreet and Fong[34] and others[3,35-37] have shown

theoretically and experimentally that boron phosphide has the most covalent character among the III-V compounds. In addition, boron phosphide is characterized by direct interband transitions of 5, 6.9 and 7.9 eV. The heat of formation of boron phosphide has been determined to be $-22.7 \pm .84$ Kcal/mole at 25°C.[38]

I.D Research Objectives

One may conclude from the above review that the fabrication of boron phosphide devices presents a number of extremely difficult problems. First, the crystal growth of boron phosphide is an extremely difficult task. Second, the impurity concentration in the vapor and solution grown crystals cannot be controlled to meet the requirements of device quality material. Third, its near inertness at ordinary temperatures and high dissociation pressures at elevated temperatures pose some formidable device fabrication difficulties. Thus, the objectives of this work were: (1) to grow reproducibly boron phosphide single crystals of reasonable size and perfection, (2) to grow epitaxially n-type and p-type boron phosphide layers of controlled impurity concentration, (3) to develop device fabrication techniques, and (4) to fabricate and to

characterize boron phosphide devices such as homojunction and heterojunction structures, and MIS devices.

CHAPTER II

CRYSTAL GROWTH OF BORON PHOSPHIDE FROM SOLUTIONS

This chapter is concerned with the growth of single crystalline boron phosphide by various solution growth techniques and the characterization of their properties. Single crystals of boron phosphide have been grown by recrystallization from metal phosphide solutions in a vertical temperature gradient with both stationary and accelerated crucible rotation techniques. The feasibility of using group III metals for the recrystallization of boron phosphide was also investigated. Doping of boron phosphide crystals was carried out and the characteristics of the solution grown crystals were determined.

II.A Introduction to Solution Growth

The growth of crystals from solutions is a useful technique for materials that have high melting point or decompose at high temperatures. Although the rate of crystal growth from solutions is only a small fraction of that from the melt, the melt growth technique is not suitable to grow materials that decompose at the melting point or undergo phase transformations between the melting point

and room temperature. Solution growth, which can often be achieved at temperatures considerably below the melting point, is appropriate for materials with these properties.

The solution growth method is based on the temperature dependence of solubility according to the relation:[39]

$$d(\ln S)/dT = \Delta H/RT^2$$

where S is solubility, ΔH is the heat of the solution, T is the absolute temperature, and R is the gas constant. In this method, the constituents of the desired crystal are dissolved in the solvent (the flux) to form a saturated solution at a high temperature and growth occurs by reducing the temperature of the solution to cause supersaturation. The growth process occurs in three steps: (1) transport of the solute to the crystal-solution interface, (2) the surface diffusion and deposition of the solute on the growing interface, and (3) the dissipation of the heat of crystallization. The transport of the solute involves diffusion and convection. For crystal growth to occur, a supersaturated solution must exist in the neighbourhood of the crystal. As the crystal grows, the solute concentration at the interface is reduced and

a concentration gradient normal to the interface is created. This leads to the diffusion of solute towards the crystal. From values of the appropriate diffusion coefficients, the process of solute diffusion can be analysed. Surface diffusion influences the growth behaviour of crystal faces and of steps on faces. The deposition of solute on the growing crystal is very structure sensitive. For example, in some materials, good quality crystals can be grown only in a particular direction, and the growth rate will be slow if a seed of another orientation is used. The solute diffusion and the surface reaction are invariably much slower than the dissipation of the heat of crystallization and they are usually the rate controlling steps in contrast to the melt growth technique, in which the rate determining step is the dissipation of the heat of fusion from the solid-liquid interface.[40]

The choice of a suitable solvent is the most important parameter in the solution growth process. Some of the desired characteristics of the solvent are:[41] (1) A high solubility of the solute at temperatures much lower than the melting point of the solute, (2) inertness towards the crucible material, (3) low viscosity to facilitate transport

of solute by diffusion and convection, (4) low vapor pressure at the growth temperature, (5) low melting point and high boiling point of the solvent, (6) possession of a common ion with the solute, or if not, then be composed of ions that are not readily incorporated in the crystallizing solute, and (7) low solubility in the solid solute so that the solvent does not influence the physical properties of the crystallized material. A complete phase diagram for the solvent-solute system, if available, is very useful.

Growth of large single crystals from high temperature solutions requires control of nucleation, maintenance of sufficiently fast solution flow at the crystal interface, and prevention of constitutional supercooling and dendritic growth after nucleation. These conditions are realized by the use of seed crystals and stirring in crystal growth from aqueous solutions. However, the use of seed crystals and stirring are extremely difficult to employ under the conditions of high temperature solution growth. In the absence of forced stirring, growth rates are very slow especially with very viscous solvents. In addition, small convection cells within the solution are easily set up due to localized small temperature gradients.[42] The uniform rotation of the container can only reduce temperature

differences due to a thermally asymmetric furnace, but does not lead to adequate mixing of the solution because the crucible and solution rotate at the same angular velocity.

In high temperature solution growth, a mechanism is required which agitates the solution in much the same way as conventional mechanical stirring in crystal growth from aqueous solutions. An accelerated rotation (e.g. bringing a container from rest to rotation) leads to effective stirring of the solution.[42-46] The solution close to the crucible wall follows any changes in the motion without delay. Solution further inside tends to continue in its previous motion due to inertia. The resulting pattern is one of slippage and shear around the rotation axis. Any local variations in solute concentration and temperature, although still located at the same radial distance from the axis, are distributed in the shape of a tightly coiled spiral. Therefore, parts of the solution with differing concentrations are in close contact, and local differences in the solute concentration or in temperature rapidly disappear. Besides radial mixing by accelerated rotation of the crucible, mixing in radial and vertical directions occurs by convection and by the motion of the solution caused by centrifugal forces. Additional mixing is caused

by the growing crystal itself. These considerations and results from the growth of gadolinium aluminate crystals point to the usefulness of the accelerated crucible rotation technique (ACRT) in the control of nucleation and the adverse effects of constitutional supercooling and convection.[43] Crystals grown by accelerated crucible rotation technique had fewer flux inclusions and cracks than crystals grown in a stationary crucible.[45]

As discussed above, the solution growth technique is most useful for the preparation of materials with high melting points and low dissociation temperatures. Materials grown from solution also tend to have a smaller concentration of electrically active or optically active point defects. Materials grown from solution often have few dislocations, since they grow in a strain-free and nearly isothermal environment. Some of the other possible advantages of the solution growth technique are that highly reactive substances may be greatly moderated by dilution with the solvent and by the lower temperatures employed, and the problem of finding a suitable crucible material may be greatly alleviated. Boron phosphide, which is the subject of this dissertation, has a high melting point and high dissociation pressure. The solution growth technique

is therefore well suited and was used for crystal growth of boron phosphide.

II.B Boron Phosphide Solvents

Single crystals of a number of III-V semiconductors have been prepared by recrystallization from an excess of the metallic component or from metals foreign to the growing substance. For example, single crystal gallium phosphide has been prepared from gallium and tin solutions.[47,48] In the case of boron phosphide, boron is not a suitable solvent because of its high melting point (2300°C). As discussed in chapter I, a number of other metals such as nickel, copper, iron, and platinum or their phosphides have been used by researchers as solvents for the crystal growth of boron phosphide. The use of nickel and copper appears to offer advantages over other metals for the following reasons:[49,50] (1) boron is soluble in nickel and copper over a wide temperature range, (2) nickel forms at least eight phosphides (Ni_3P, Ni_5P_2, $Ni_{12}P_5$, Ni_2P, Ni_5P_4, NiP, NiP_2, and NiP_3), and the first four phosphides have melting points below 1200°C, and (3) copper forms two phosphides (Cu_3P and CuP_2) and both have melting points below 1200°C. In addition, experiments carried out in this laboratory on the recrystallization of boron

phosphide from copper phosphides (Cu_3P and CuP_2) and nickel phosphides showed that boron phosphide was more soluble in nickel phosphides than in copper phosphides.[51] These considerations suggest that nickel phosphides are probably the most suitable solvent for boron phosphide and were therefore used in the preparation of boron phosphide crystals.

Polycrystalline nickel phosphides were synthesized from the elements under conditions similar to those used for the recrystallization of boron phosphide from nickel phosphide solutions. A schematic diagram of the apparatus is shown in Figure 2.1. An alumina boat with a 46 g nickel ingot was fitted into a cylinderical graphite sleeve of 25 mm ID and 31 mm OD which was used as a susceptor for rf heating. The susceptor was positioned in a fused silica spacer so that the graphite contacted the spacer only at eight points. This assembly and 23 g of red phosphorus were placed in a fused silica tube of 50 mm ID and 55 mm OD, which was evacuated to less than 10^{-5} Torr and sealed. The reaction tube was about 45 cm long after sealing. The end of the tube containing the susceptor and phosphorus was heated slowly to sublime all phosphorus to the other end of the tube. The susceptor was then heated at the desired

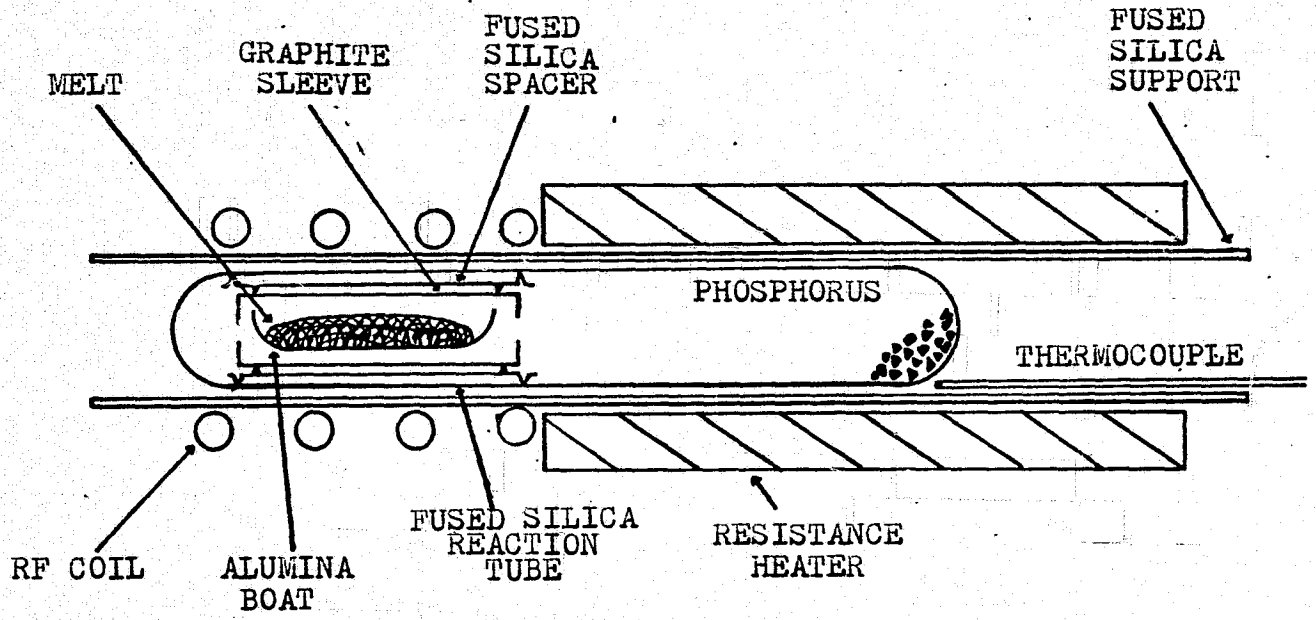

Figure 2.1 Schematic Diagram of the Apparatus for the Synthesis of Nickel Phosphides

temperature, 1250° to 1300°C, with an rf generator, and a resistance heater surrounding a major portion of the reaction tube was used to maintain the phosphorus pressure in the tube at about 2 to 3 atm. The reaction time was usually 24 hr or longer to assure saturation. The X-ray Debye-Scherrer pattern of the resulting product was identical with that of Ni_2P[52] (Figure 2.2). Several other varieties of nickel phosphide were also prepared by adjusting the temperature of nickel, the phosphorus pressure, and the reaction time. For example, nickel phosphide prepared from nickel held at 1350° to 1400°C with a phosphorus pressure of 3 to 4 atm for 32 hr produced an ingot with an average composition of Ni_3P_2 as deduced from the weight increase of the nickel ingot. This material was analysed by the X-ray Debye-Scherrer technique; however, the diffraction patterns were too complicated to identify its composition. It was probable that NiP was the most phosphorus rich compound formed. Since phosphorus is soluble in Ni_2P, it is also likely that there was an excess of phosphorus in the ingots.

Nickel phosphide was also synthesized by saturating nickel at about 1200°C with phosphorus at a pressure of 1 to 2 atm. About 12 g of red phosphorus was put into a

fused silica tube of 25 mm ID and 29 mm OD after a fused silica boat containing a 50 g nickel ingot was fitted in one side of the ampule. The tube was then sealed at a pressure of 10^{-5} Torr or lower. The tube was placed in a horizontal Kanthal resistance heater, and the phosphorus was sublimed to the other end of the tube. The temperature of the nickel ingot was about 1200°C and the temperature at the other end of the tube corresponded to 1 to 2 atm of phosphorus pressure. After 3 days the nickel was found to be saturated with phosphorus, and the X-ray Debye-Scherrer pattern of this variety of nickel phosphide was found to correspond to Ni_7P_3[52] (Figure 2.2).

Other materials investigated as solvents in the crystal growth of boron phosphide were copper phosphide (Cu_3P), indium, and aluminum. The use of aluminum and indium as solvents for the crystal growth of boron phosphide has not been investigated previously. Copper phosphide (Cu_3P) was prepared in the manner described for the preparation of nickel phosphide in a Kanthal furnace. The copper ingot was held in an alumina boat, since molten copper wets fused silica. The copper ingot was kept at a temperature of 1150° to 1200°C, and the phosphorus pressure was maintained at 1 atm. The reaction between copper and

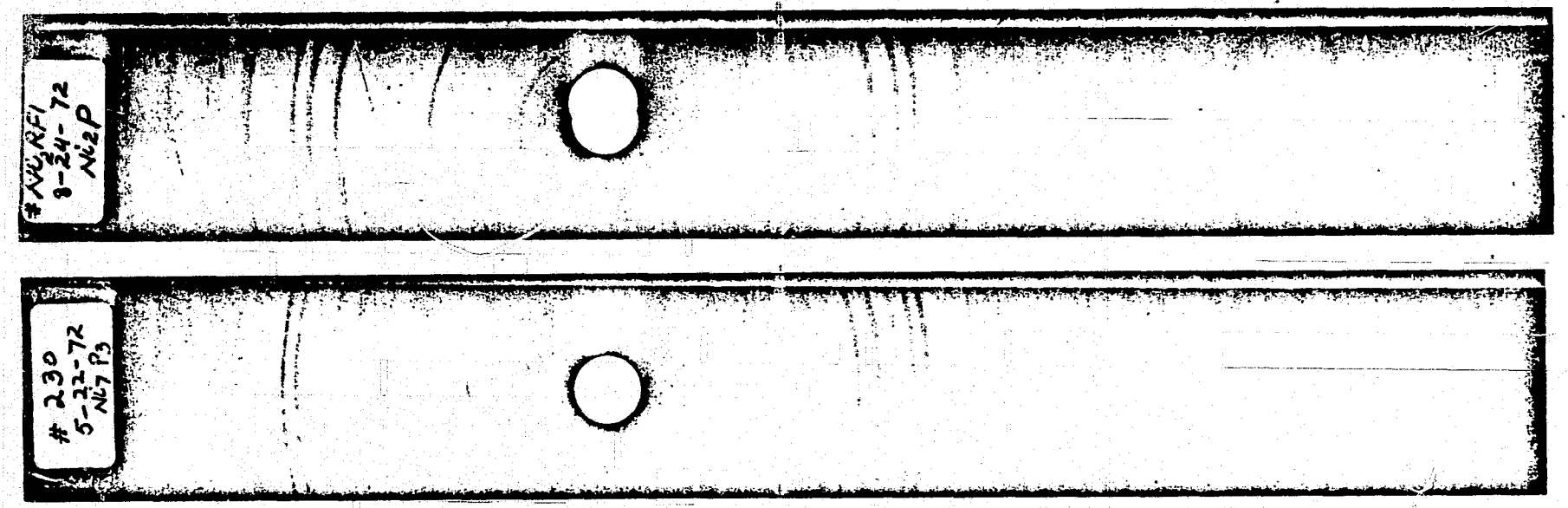

Figure 2.2 Debye-Scherrer Powder Patterns of Nickel Phosphides

phosphorus was complete in about 1 day.

II.C Growth of Boron Phosphide Crystals by Recrystallization in a Stationary Crucible

The temperature dependence of the solubility of boron phosphide in nickel phosphide was utilized for the crystal growth of boron phosphide by the temperature gradient recrystallization technique. In this technique, a small temperature gradient was maintained across a saturated solution of boron phosphide in nickel phosphide with polycrystalline boron phosphide in the higher temperature region. Due to the higher solubility of boron phosphide at high temperatures, a concentration gradient is set up across the solution, and consequently, transport of boron phosphide from the polycrystalline source to the lower temperature region occurs.

The recrystallization experiments were carried out in vertical fused silica tubes with a Kanthal resistance heated furnace. Since the density of boron phosphide is lower than that of the nickel phosphide solution, the temperature of the reaction tube decreased in the downward direction in the majority of the experiments. These experiments were carried out by sealing 15 g of nickel phosphide, 0.5 g of

polycrystalline boron phosphide, and varied amounts of phosphorus in a 13 cm long, 10 mm ID, and 16 mm OD fused silica ampule after evacuation to a pressure of 10^{-5} Torr or lower. The added phosphorus was used to suppress the decomposition of boron phosphide. Fused silica ampules of 15 mm ID and 20 mm OD were also used in these experiments to improve the size of the boron phosphide crystals. In these larger tubes, 25 to 35 g of nickel phosphide, 1.0 to 2.0 g of polycrystalline boron phosphide and varied amounts of phosphorus were sealed. The ampules were then held in a vertical furnace at temperatures between 1190° and 1240°C with temperature gradients from 10° to 30°C across the solution. A quartz rod, 3 to 8 cm long, was connected to the bottom of the ampule as a heat sink. After 3 to 4 weeks, boron phosphide crystals in the form of hexagonal platelets and polyhedrons were obtained. The main faces of the platelets were up to 20 mm^2 in area and the thickness of the platelets was up to 2 mm, and the polyhedrons were up to 5 mm x 4 mm x 3.5 mm in dimensions.

The composition of the nickel phosphide was found to be very important in the recrystallization process. All of the crystal growth experiments which produced large single crystals of boron phosphide used only Ni_2P as the solvent.

The use of Ni_7P_3 produced only small crystals, and the phase mixtures of Ni_2P with other nickel phosphides produced no crystals. It was therefore concluded that Ni_2P is the most suitable nickel phosphide as a solvent for the crystal growth of boron phosphide. In addition to nickel phosphide synthesized in this laboratory, commercial nickel phosphide, predominantly Ni_2P (purchased from Puratek, Norwood, Ohio), was also used in these experiments and was found to be satisfactory as a solvent in the solution growth of boron phosphide single crystals. However, the use of commercial nickel phosphide always required a larger amount of phosphorus than the laboratory grown nickel phosphide. For example, in a typical experiment with a 10 mm ID and 16 mm OD fused silica ampule described earlier, about 1 g of phosphorus was required with commercial nickel phosphide compared to about 0.2 g of phosphorus needed with the laboratory synthesized nickel phosphide. This indicates that the laboratory synthesized nickel phosphide (Ni_2P) contained an excess of dissolved phosphorus.

The effect of phosphorus concentration on the recrystallization of boron phosphide was also studied. It was found that a certain minimum amount of phosphorus was necessary to grow boron phosphide crystals. The upper limit

to the phosphorus concentration was imposed by the vapor pressure of undissolved phosphorus at the solution temperature. For example, when a 10 mm ID and 16 mm OD fused silica tube containing 0.7 g of phosphorus and 15 g of commercial nickel phosphide was kept at 1240°C for 18 days, the tube was found to be completely collapsed, and no boron phosphide crystals were recovered. On the other hand, a same size tube containing 1.2 g of phosphorus and 15 g of commercial nickel phosphide was found to have expanded slightly after 20 days under similar conditions. Boron phosphide crystals were also recovered in the latter experiment. About 1 g of phosphorus was found to be adequate for the growth of boron phosphide under the conditions described. The phosphorus concentration used in the larger ampules was extrapolated from these considerations and was found to be satisfactory.

A few recrystallization experiments were also carried out with copper phosphide (Cu_3P) as a solvent for boron phosphide. In a typical experiment, 15 g of copper phosphide and 1 g of polycrystalline boron phosphide were sealed in a 13 cm long, 10 mm ID, and 16 mm OD fused silica tube at 10^{-5} Torr or lower. The temperature gradient varied from 15° to 30°C across the solution. After 2 to 3 weeks,

recrystallized boron phosphide was found in the form of platelets 2 to 3 mm in size. Boron phosphide crystals obtained from nickel phosphide (Ni_2P) solution were larger than those from copper phosphide (Cu_3P) solution. The use of larger diameter fused silica ampules also produced larger boron phosphide crystals.

II.D Growth of Boron Phosphide Crystals by Recrystallization with the Accelerated Crucible Rotation Technique

The accelerated crucible rotation technique was applied to the crystal growth of boron phosphide with the same ampule size, ampule contents and solution temperature as described above. Figure 2.3 shows a schematic diagram of the apparatus. It consists of an electrical system driving a motor with a linear voltage-speed characteristic, and the motor rotates the container about its vertical axis. The circuit diagram of the wave generator and motor driver are shown in Figure 2.4. The maximum rotation rate is adjustable from zero to 120 rpm, the acceleration is adjustable to a maximum of 0.4π rad/sec^2, and the time period of the system can be varied from about 10 sec to 1 min. This system is therefore sufficiently flexible to permit a variety of accelerated rotation cycles. Figure 2.5 shows two such cycles of accelerated crucible

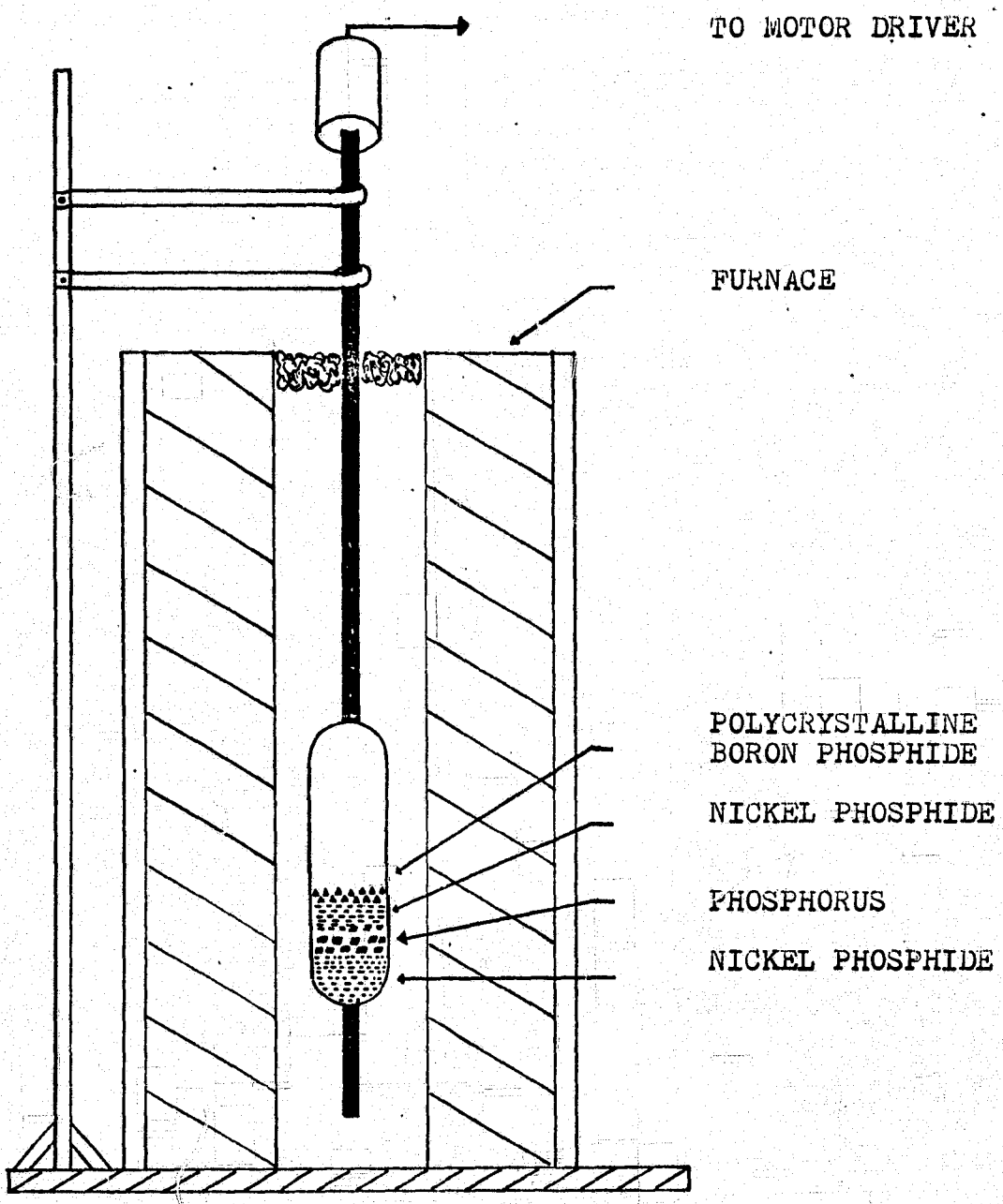

Figure 2.3 Schematic Diagram of the Apparatus for the Solution Growth of Boron Phosphide by Accelerated Crucible Rotation Technique

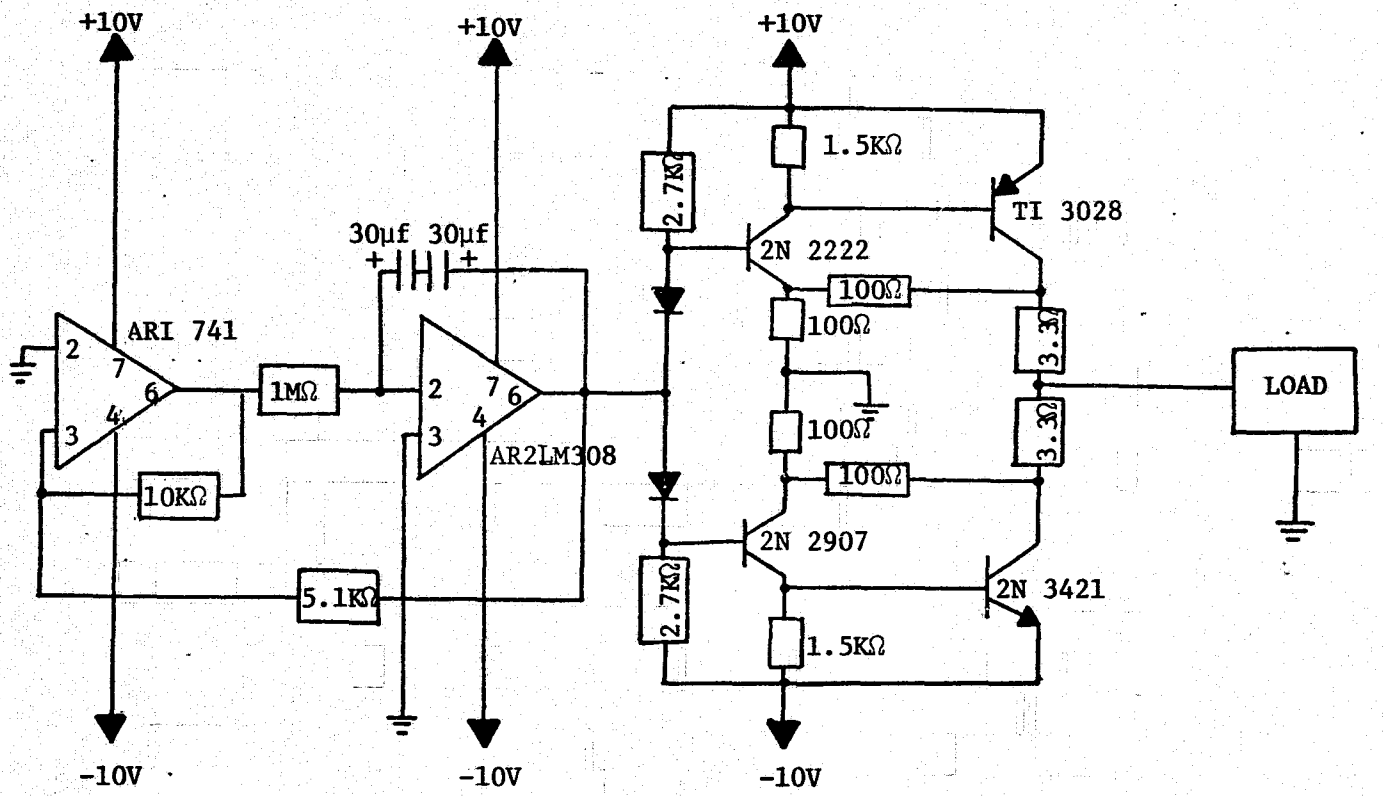

Figure 2.4 Circuit Diagram of the Wave Generator and the Motor Driver

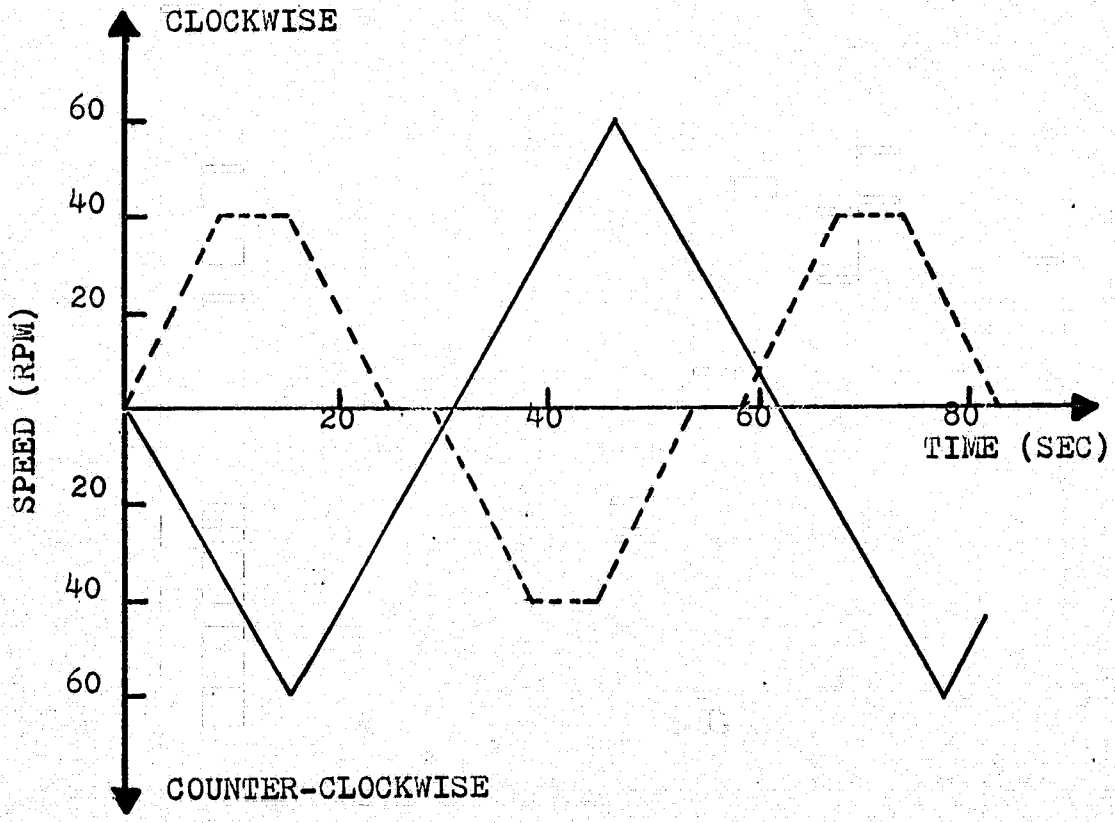

Figure 2.5 Speed-Time Graphs of the Accelerated Tube

rotation used.

Boron phosphide crystals grown with the accelerated crucible rotation technique were larger, had fewer voids, and had better developed faces than those obtained in a stationary crucible. The experiments with the accelerated crucible rotation technique produced boron phosphide crystals of up to 8 mm x 4 mm x 2.5 mm in dimensions as shown in Figure 2.6. The optimum conditions for the growth of boron phosphide crystals in the recrystallization experiments with 15 mm ID and 20 mm OD fused silica ampules with commercial nickel phosphide were:

Nickel phosphide	= 30 to 35 g
Boron phosphide	= 1.5 to 2.0 g
Phosphorus	= 2 g
Vertical temperature gradient	= 10° to 30°C
Run time	= 3 to 4 weeks
Rotation period of ampule	= 60 sec
ACRT maximum rotation rate	= 40 to 70 rpm

II.E Growth of Boron Phosphide Crystals by Recrystallization in a Vertical Two Zone Furnace

The general exponential dependence of solubility on temperature suggests that larger boron phosphide crystals

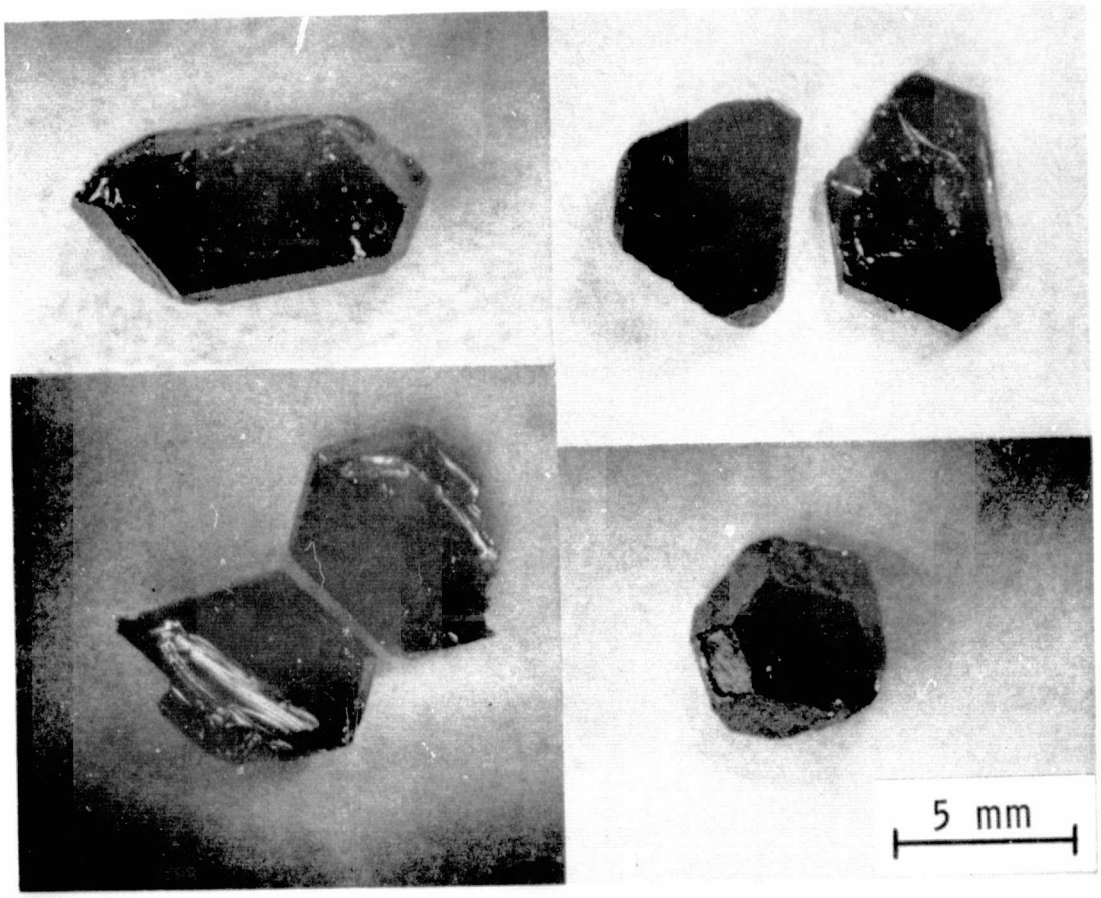

Figure 2.6 Boron Phosphide Crystals Grown by Recrystallization from a Nickel Phosphide (Ni_2P) Solution Using the Accelerated Crucible Rotation Technique

may be obtained by growth at temperatures higher than those obtainable in a resistance heated Kanthal furnace. To investigate this possibility, the apparatus shown schematically in Figure 2.7 was used. It is essentially a two zone arrangement with a 45 to 55 cm long, 30 mm ID, and 34 mm OD fused silica ampule. Within the tube is an excess of phosphorus and a "Boralloy" (Union Carbide Corporation) boron nitride crucible containing the solvent, and polycrystalline boron phosphide. The ampule was sealed at a pressure of 10^{-5} Torr or lower. The polycrystalline boron phosphide was on top of the solvent and the temperature decreased in a downward direction. The crucible (15 to 18 mm OD and about 7 cm long) was positioned on a quartz support such that a clearance of several millimeters between the crucible and the ampule wall existed. Since boron nitride has a low emissivity, the crucible could be heated to above 1500°C without softening the silica ampule. The ampule was positioned within a vertical tubular furnace on a platform which could be lowered. The charge was heated inductively to 1000°C while the temperature of the phosphorus was slowly increased. The ingot temperature was then gradually raised to 1350° to 1450°C (uncorrected readings with a Leeds and Northrup model 6831C optical pyrometer) while the pressure of the phosphorus was

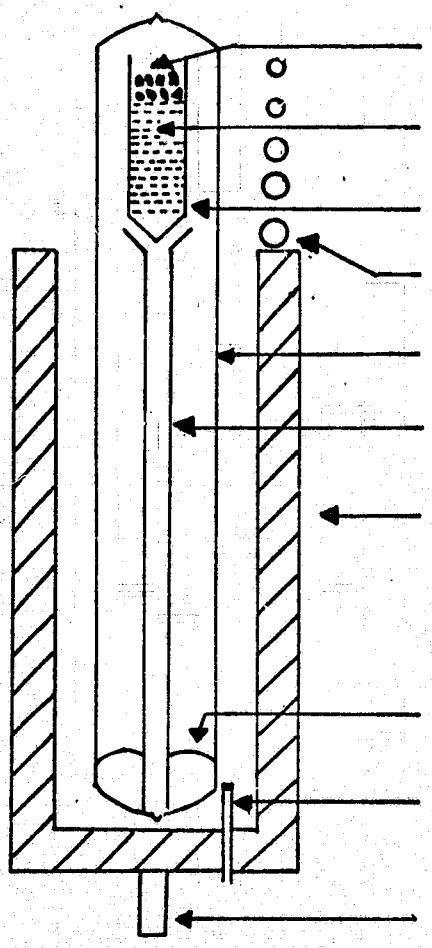

Figure 2.7 Schematic Diagram of the Vertical Two-Zone Furnace for the Growth of Boron Phosphide Crystals by Recrystallization

maintained at 1 atm. After 48 hr, the ampule was slowly lowered. The lowering rate was adjustable from 0.1 mm/hr to about 10 mm/hr.

The solvents investigated in this apparatus were: indium, aluminum, and nickel phosphide (Ni_2P). Boron phosphide was found to be insoluble in indium up to 1400°C. Aluminum has an appreciable vapor pressure (about 1 Torr at 1400°C) and attacked the quartz ampule in the vicinity of the crucible profusely. Aluminum also reacted slightly with the boron nitride crucible. As a consequence, no boron phosphide crystals were obtained and it was concluded that this set up is not suitable for the use of aluminum as a solvent in the crystal growth of boron phosphide. In a typical experiment with nickel phosphide as the solvent, 2.0 g of polycrystalline boron phosphide, 50 to 60 g of nickel phosphide, and 5 to 7 g of phosphorus were sealed in the ampule at a pressure of 10^{-5} Torr or lower. These experiments produced small crystallites, many of which stuck together, presumably due to the lack of control of the temperature gradient.

II.F Doping of Boron Phosphide Solution Grown Crystals

Boron phosphide crystals obtained by

recrystallization near 1200°C from both the stationary and accelerated crucible rotation techniques usually had built-in p-n junctions. Boron phosphide crystals of either n-type or p-type conductivity were grown by doping the charge in the recrystallization experiments. About 40 doping experiments were carried out, and the impurities investigated were: zinc, magnesium, beryllium, sulfur, selenium, tellurium, and silicon. Table 2.1 is a summary of the doping experiments carried out in the solution growth of boron phosphide crystals.

In efforts to grow p-type boron phosphide crystals, zinc was investigated extensively. In all of the recrystallization experiments in which zinc was used, however, the boron phosphide crystals produced were either n-type or had built-in p-n junctions, results similar to those obtained when no dopant was used. It was therefore concluded that zinc does not dope boron phosphide under the conditions described.

The use of beryllium and magnesium in the recrystallization experiments at 1200°C produced a few crystals that had p-type conductivity but majority of these crystals had built-in p-n junctions on their faces. Also both beryllium and magnesium reacted with the fused silica at 1200°C,

Table 2.1

Solution Growth of Doped Boron Phosphide Crystals

Size of fused silica ampule = 13 cm long, 10 mm ID, and 16 mm OD
Weight of nickel phosphide (Ni_2P) = 15 g
Weight of boron phosphide = 0.5 to 1 g
Solution temperature = 1190° to 1240°C

Run Number	Dopant and Weight (g)	Weight of Phosphorus (g)	Experiment Time (Days)	Result
BP43	Si (0.16)	0.6	25	n-type & Built-in p-n junctions
BP47	Si (0.8)	0.8	23	n-type
BP33	Te (0.14)	0.6	21	n-type & Built-in p-n junctions
BP38	Te (0.3)	1.0	18	n-type
BP44	Se (0.3)	0.67	16	Built-in p-n junctions
BP45	Se (0.39)	0.8	19	no crystals
BP55	NiS (0.4)	1.0	14	Built-in p-n junctions
BP36	Zn (0.14)	1.0	14	n-type
BP39	Zn (0.4)	1.0	25	n-type
BP63	Zn (1.5)	2.5	--	the tube exploded
BP65	ZnP (3.0)	---	19	no crystals
BP52	Be (0.3)	1.2	19	p-type & Built-in p-n junctions
BP53	Be (0.5)	0.7	16	p-type
BP57	Be (1.0)	1.0	14	p-type
BP69	Be_3P_2 (1.2)	---	20	p-type
BP49	Mg (0.6)	0.7	18	no crystals
BP58	Mg (0.1)	0.5	17	p-type

and this reaction may have had adverse effects on the recrystallization process since crystals were only 1 to 2 mm in size. The use of an alumina crucible as the container for the solution material was investigated. An alumina crucible, 12 mm ID and 16 mm OD, containing polycrystalline boron phosphide, nickel phosphide, phosphorus, and the dopant was sealed in a fused silica ampule at a pressure of 10^{-5} Torr or lower. After 20 days, the crucible was found to have reacted with quartz. The crucible material may also have reacted with beryllium. The boron phosphide crystals obtained in this experiment were up to 3.5 mm in size and had smooth well developed faces suitable for device work. Some of these crystals were p-type and their resistivity varied from one face to the other, characteristic of solution grown crystals. To further reduce contamination from the container material and the reaction between the container and beryllium phosphide, one experiment was carried out with the alumina crucible replaced by a boron nitride ("Boralloy") crucible. The crystals produced with the boron nitride crucible were not significantly different in conductivity type and resistivity profile compared with the crystals obtained from an alumina crucible. However, no visible signs of reaction between ampule wall and the ingot were observed. It was found in cases of beryllium,

magnesium, and zinc, that when phosphides of these metals were used as dopants, the ampules remained intact. On the other hand, when these metals and enough phosphorus to make the metal phosphide were used, tubes frequently exploded. No significant difference was observed between the crystals obtained from ampules with metal phosphide dopants and the crystals obtained from intact ampules which contained metal and excess phosphorus.

Among the expected n-type dopants, the use of sulfur, and selenium did not compensate the p-type impurities and boron phosphide crystals produced in these experiments had built-in p-n junctions. Tellurium, however, produced only n-type boron phosphide crystals in majority of the experiments. Also, silicon was found to be the most effective n-type dopant and has produced the best results. Thus, boron phosphide has been doped successfully for the first time to produce both n-type and p-type crystals. Silicon and beryllium were found to be the most suitable n-type and p-type dopants, respectively.

II.G Properties of Solution Grown Boron Phosphide Crystals

Boron phosphide crystals obtained from recrystallization experiments were usually in the form of platelets, but sometimes polyhedrons. The platelets were usually

hexagonal, and three alternate sides were always longer than the others. Figure 2.6 shows the typical forms of boron phosphide crystals obtained from the recrystallization experiments. The platelets usually had one face flat and smooth, and the other face relatively rough. The crystallographic orientation of the main faces of the platelets was determined by X-ray Laue back reflection studies. Figure 2.8 shows a three-fold symmetry, which indicates that the main faces are of (111) orientation. Chemical etching by a 3:1 molten mixture of sodium hydroxide and sodium peroxide was employed to distinguish the two (111) faces. The study of the etched faces showed that the face which was initially flat and smooth developed dislocation etch pits, but the other face remained relatively unaffected.

This difference in etching behavior is the result of some ionic character in the chemical bond in compound semiconductors. For example, (111)-type planes of III-V compound semiconductors (zincblende structure) exhibit polarity along the $\langle 111 \rangle$ directions.[53] A (111) plane of III-V compound semiconductors terminates with group III atoms (face A) and the inverse $(\bar{1}\bar{1}\bar{1})$ plane terminates with group V atoms (face B). Face B atoms are very reactive chemically since they are only triply bonded to the lattice, whereas their normal valence is five. Face A atoms, also triply bonded

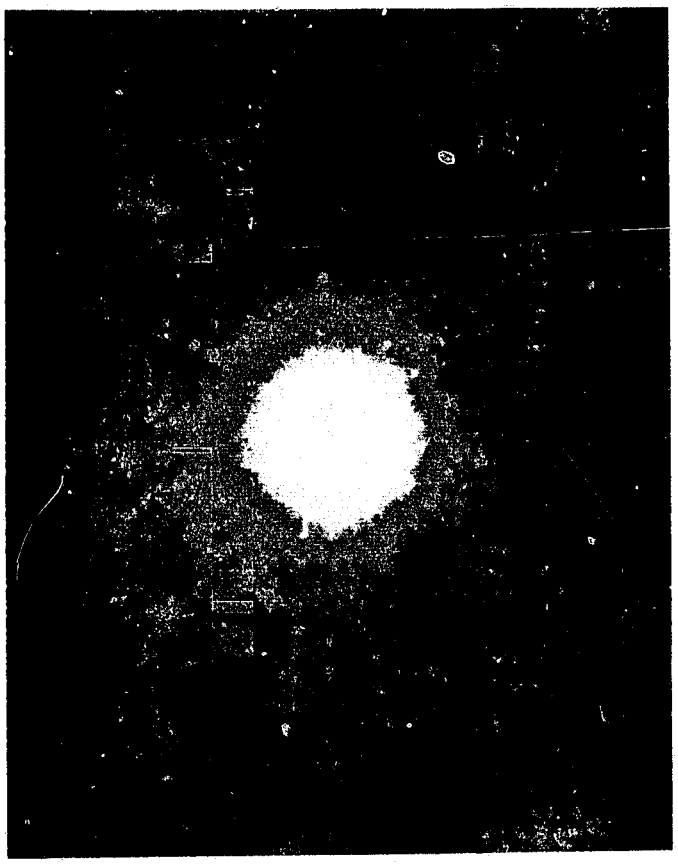

Figure 2.8 X- ray Laue Back Reflection Pattern of a Main Face of a Solution Grown Boron Phosphide Crystal

to the lattice, must be appreciably less reactive since they are normally trivalent. Thus, the (111) and ($\bar{1}\bar{1}\bar{1}$) planes show different etching characteristics under certain conditions. Based upon the etching characteristics of (111) faces of other III-V compound semiconductors,[53-59] it is suggestive that the flat and smooth face of the boron phosphide platelets is the boron face. Thermodynamic analysis of the solution growth process also indicates that the smooth face of a III-V compound semiconductor should be A (III) face.[48] The platelets are characterized by a twinned structure, with twinning taking place in the (111) planes. The twinned structure provides the means for the extension of the crystal,[47] and the growth of semiconductor crystals from solutions has been explained by the Twin-Plane Reentrant-Edge mechanism.[48]

The conductivity type and the relative local electrical resistivity of the solution grown boron phosphide crystals were determined by the thermoelectric probe and the spreading resistance technique, respectively. The spreading resistance technique is based on the resistance measurement of a small area pressure contact between a metal probe and a semiconductor surface.[60] This resistance is contained in a small volume of the semiconductor immediately below the probe and is directly related to the resistivity

of the semiconductor. The spreading resistance measurements are carried out at low voltages to maintain contributions from minority carrier injection, the electric field in the spreading resistance region, and joule heating in the contact region negligible. The spreading resistance R_s (contact resistance between a metal probe and the semiconductor) is given by

$$R_s = K \frac{\rho}{4a}$$

where ρ is the resistivity of the semiconductor, a is the radius of the circular contact spot, and K is the proportionality constant that accounts for the zero-bias barrier resistance due to the difference in the work function between the metal and the semiconductor. In practice, the parameter K is evaluated by caliberation. The apparatus used for the spreading resistance measurements consisted of two osmium tipped probes with a 25 μm radius of curvature. The probes were mounted on separate booms loaded with 25 g of weight. These were spaced 1 mm apart and could be lowered onto a preselected area of the specimen. The resistance between the two probes was measured with a Keithley 610B in its ohmmeter function. Since the parameter

K is not known for boron phosphide under the measurement conditions here, absolute resistivity values cannot be obtained. However, nearly all crystals showed relatively low spreading resistance, a few hundred ohms, indicating that these crystals are of low resistivity. Van der Pauw measurements on the solution grown crystals indicated resistivity values on the order of 0.1 ohm-cm and carrier concentration on the order of 10^{17} cm^{-3} or above. These results are in reasonable agreement with the carrier concentration values obtained from the measurements made on Schottky barrier diodes fabricated on solution grown crystals.

Among the boron phosphide crystals obtained without intentional doping, all polyhedrons and the majority of the platelets had built-in p-n junctions. Usually both the (111) faces were n-type and the core was p-type. These features were observed by delineating p-n junction interface in solution grown crystals using electrolytic etching technique (chapter III). The inhomogeneous distribution of impurities is probably a result of two factors: a higher segregation coefficient for p-type impurities than for n-type impurities so that p-type impurities are depleted from the solution and a continuous supply of silicon, an n-type impurity in boron phosphide, going into the solution from

the ampule.

Easily visible red electroluminescence was observed in crystals with built-in p-n junctions, and in some crystals with no built-in junctions when probed with a metal contact. The electroluminescence will be discussed in detail in chapter VII.

II.H Summary

The growth of boron phosphide crystals by recrystallization was investigated in a stationary crucible, in a crucible with an accelerated rotation, and in a vertical two zone furnace. Indium, aluminum, copper phosphide (Cu_3P), and nickel phosphide (Ni_2P) were investigated as solvents in the recrystallization process. Boron phosphide crystals in the form of platelets and polyhedrons were obtained in recrystallization experiments in a stationary crucible from a nickel phosphide solution. The accelerated crucible rotation technique yielded larger boron phosphide crystals and platelets with fewer voids and better developed faces suitable as substrates for the growth of epitaxial boron phosphide layers. The dimensions of these crystals are considerably larger than those reported heretofore. For the first time, boron phosphide crystals have been doped. N-type and

p-type boron phosphide crystals were obtained using silicon and beryllium as dopants, respectively. These crystals, although of low resistivity, have been used successfully as substrates for the epitaxial growth of boron phosphide and for the fabrication of boron phosphide devices.

CHAPTER III

ELECTROLYTIC ETCHING OF BORON PHOSPHIDE

This chapter is concerned with the electrolytic etching and polishing of boron phosphide. P-type boron phosphide was readily etched and polished; however, the etching of n-type boron phosphide is considerably more complicated. Electrolytic etching was used to isolate mesa structures in boron phosphide p-n junctions and in silicon carbide-boron phosphide heterojunctions, and to polish p-type boron phosphide.

III.A Introduction to Electrolytic Etching

Electrolytic etching is an electrochemical process for the removal of material by passing current through a substance at the anode of an electrolytic cell. Irregular regions and damaged material can be uniformly removed to produce a smooth surface in electrolytic polishing, which occurs within a certain range of current densities. In addition, electrolytic treatment can be used to locate the crystallographic directions, crystalline imperfections, doping inhomogeneities and p-n junctions.[61] Electrolytic treatment offers some advantages over mechanical and

chemical processes. In contrast to mechanical material removal process such as lapping and abrasive cutting, electrolytic etching does not leave a damaged layer on the surface that can adversely affect the electrical properties of devices. Electrolytic etching is often the only way to remove material without damage if no chemical etchant is available. Electrolytic treatment offers flexibility of control. Masking and localized carrier injection by optical or electrical means can be used to control the geometry of etching. The etch rate can be adjusted by changing the carrier concentration at the surface optically or by adjustment of the current density. The choice of chemical composition of the electrolyte is critical to successful electrolytic etching. The choice of electrolyte is based on the chemical behavior of the semiconductor; the products of oxidation should be soluble in the electrolyte or be continuously removed from the surface of the semiconductor, and the electrolyte should not react chemically with the semiconductor and the other materials in the electrolytic cell. In many cases, an empirical selection process is the only way to determine a suitable electrolyte.

An electrochemical cell with a semiconductor

electrode is represented schematically as shown below:

Metal Semiconductor Electrolyte [Reference Electrode] Metal

Both oxidation and reduction processes occur simultaneously in an electrochemical cell, oxidation taking place at the anode and reduction at the cathode. An electrical potential difference is formed as a result of the transfer of charges across the electrode-electrolyte interface and is referred to as the electrode potential. The electrical potential difference between the two terminal phases in the electrochemical cell is called the cell potential difference.

It is not possible to measure the potential difference between an electrode and the solution in contact with it, without another metallic electrode. But by arbitrarily assigning a potential to an electrode, which is not drawing current, it is possible to determine the potentials of other electrodes with respect to this standard. The calomel electrode is one of the standard electrodes used as a reference electrode. The calomel electrode consists of mercury in the bottom of a vessel with a paste of mercury and mercurous chloride (calomel) over it in contact with a solution of potassium chloride

saturated with mercurous chloride. A reference electrode such as the calomel electrode permits the measurement of changes in electrode potential under nonequilibrium conditions.

A small region on both sides of the semiconductor-electrolyte interface is called the electrical double layer.[62] At the semiconductor-electrolyte interface, the conductance mechanism changes from electronic to ionic. When the two phases are brought into contact, diffusion flow of charge takes place until the electrostatic field established across the interface balances the inherent tendency of charge transfer. Charge flows until the electrochemical potential of electrons (Fermi level) is the same on the two sides of the interface. The interface represents a barrier for the flow of electric current in the absence of an electrochemical reaction at the interface. The potential difference developed across the electrolyte-semiconductor interface under an open circuit condition is termed the rest potential.

When the electronic equilibrium at the surface of the semiconductor electrode is disturbed by an external source of electromotive force, two types of reactions can be initiated at the semiconductor electrode:[63] electron

transfer processes and electrolytic processes with chemical changes of the semiconductor. Electron transfer processes take place between the semiconductor electrode and electron donors or acceptors in the electrolyte without structural changes in the surface of the semiconductor.

Electrolytic processes, in which the chemical structure of the semiconductor surface is changed, take place when a semiconductor surface undergoes, for example, oxidation at an anode in the electrochemical cell. The oxidation process in semiconductors occurs normally in two steps.[64] In the first step, interruption of the chemical bond between two neighbouring atoms under the influence of electrical forces and the interaction with a reactant from the electrolyte solution takes place. This results in the formation of a new bond between one of the semiconductor atoms and a reactant. Simultaneously, an intermediate state of the other surface atom with a radical character is generated. In the second step, this radical intermediate on the semiconductor surface reacts with another reactant from the solution and forms a second covalent bond.

In the electrolytic oxidation process, the first step

is rate determining, because the reactivity of the radical intermediate is much higher than that of the fully bonded surface atoms. The rate of these processes is proportional to the concentration of the charge carriers at the surface. In addition, it is always observed that anodic currents through n-type materials tend to saturate whereas, current saturation is not found with p-type materials. Therefore, it is inferred that holes are the dominant charge carriers in anodic processes in semiconductors. Holes, which are necessary for anodic dissolution of semiconductors, can be supplied in n-type semiconductors by illumination. In the anodic process, the reactions involving holes have a greater probability of occurance than those involving electrons since, the bonding between the neighbouring atoms in the crystal is due to the interaction between electrons in bonding orbitals and the atomic nuclei. The presence of a hole near the surface of the semiconductor means that one of the bonding states in the crystal is unoccupied and the missing electron has been excited from a bonding state in the valence band to an antibonding state in the conduction band. This band is therefore weakened, and it can be attacked much more easily. The importance of holes becomes more pronounced for large band gap intrinsic and n-type materials because the

concentration of holes is extremely small.

The mechanism for the anodic oxidation of compound semiconductors (type AB) is essentially the same as the one for the elemental semiconductors with a slight modification. In the compound semiconductors, the first step of oxidation results in forming a new bond with the more electropositive component of the compound, while the more electronegative component remains in the radical state. If the latter component has an electronegative character and cannot be oxidized easily (or not at all), an association type of reaction between adjacent radicals can complete the bond breaking process.

III.B Experimental Procedure

Boron phosphide, which is a refractory material, is chemically inert and cannot be etched in aqueous solutions at room temperature. High temperature etchants, such as fused alkalis near 400°C or hydrogen chloride near 1100°C, are not suitable for the shaping of boron phosphide crystals for device fabrication. Therefore, electrolytic etching is probably the only room temperature etching process suitable for boron phosphide.

A series of experiments were performed on both n-type and p-type solution grown boron phosphide platelets to determine the conditions for etching and polishing. The platelets had main faces of (111) orientation, and both (111) and ($\bar{1}\bar{1}\bar{1}$) faces were evaluated. The platelets generally had one smooth face and one rough face. These faces were designated (111) and ($\bar{1}\bar{1}\bar{1}$) faces, respectively, on the basis of chemical etching described in chapter II. The room temperature carrier concentration determined by measurements on Schottky barrier diodes fabricated from these solution grown crystals was on the order of 10^{18} cm^{-3} or above.[65]

Prior to electrolytic etching, rough faces were polished with 0.3 μm alumina powder, and smooth faces were used without mechanical polishing. An ohmic contact was made to the back surface of the boron phosphide crystals by an electroless nickel plating process followed by annealing in hydrogen at 800° to 850°C for 1 hr to obtain reproducible values of electrode potential. The small size (a few mm^2 in area) of the crystals necessitated careful mounting and masking procedures. After the formation of back contact, the back side was bonded to a small metal sheet with silver epoxy and mounted on a teflon disc with

polyethylene screws. Apiezon W wax was used to mask the wire leads, metal sheet, and the boron phosphide platelet, so that only the region of the crystal surface under investigation was exposed to the electrolyte. Silicon monoxide and silicon dioxide were also used for masking boron phosphide platelets and were found to be more reliable than apiezon W wax for controlling small area geometries in the fabrication of mesa structures. Silicon monoxide was evaporated in a Veeco 775 vacuum system and silicon dioxide was deposited by the oxidation of silane in an hydrogen atmosphere in an open flow system. The oxide was masked with either apiezon W wax or with photoresist, and windows were opened in the oxide with buffered hydrofluoric acid (144 cc of 49% HF, 450 g of NH_4F, and 660 cc of H_2O).

The electrolytic cell for the etching and polishing of boron phosphide is shown schematically in Figure 3.1. Boron phosphide was the anode, and a graphite rod was the cathode. The crystal-electrolyte potential difference was measured by a calomel reference electrode. The solution was continuously agitated by bubbling nitrogen into the electrolyte. The electrolytes investigated were:
(I) aqueous solutions of potassium hydroxide, sodium

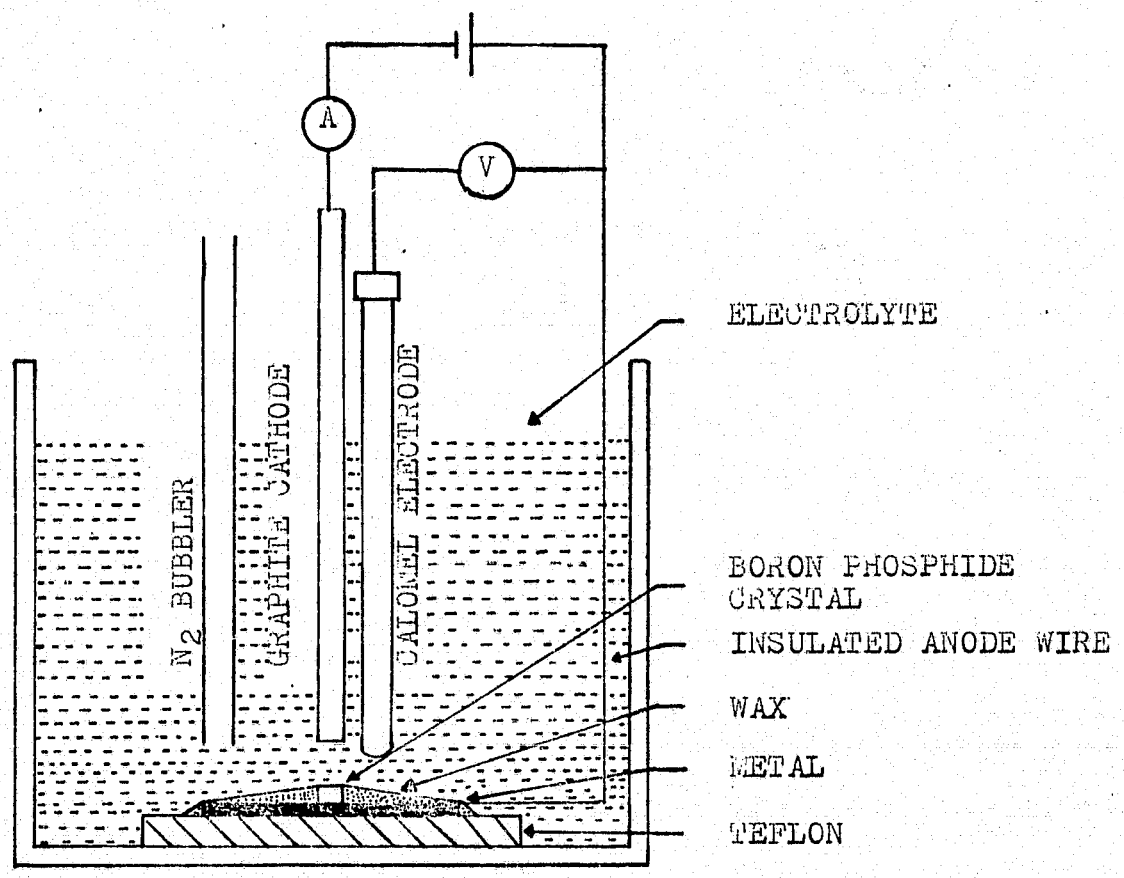

Figure 3.1 Schematic of the Electrolytic Cell for the Etching of Boron Phosphide with a Graphite Rod Cathode

hydroxide, hydrochloric acid, nitric acid, sulfuric acid, and hydrofluoric acid of various concentrations, (2) 5:1:1 H_2SO_4: 30% H_2O_2: H_2O, (3) 1:1 20% KOH: 30% H_2O_2, and (4) 1:1 1M $K_3Fe(CN)_6$: 0.5M KOH. The current-voltage characteristics were measured by slowly increasing the applied voltage and noting the anode voltage and the corresponding current.

In the fabrication of boron phosphide mesa type p-n junctions, the electrode geometry shown in Figure 3.1 produced an uneven etched surface and resulted in the undercutting of the mask. It was found that with the boron phosphide platelet near the axis of a cylinderical molybdenum cathode, whose diameter was 7 cm (Figure 3.2), the material was removed evenly. Another modification to the system is shown in Figure 3.3. This circuit produces a constant anode potential regardless of the contact resistance.[66] In this set up, low resistance ohmic contact to boron phosphide crystals was not necessary, and a single component silver epoxy was used between the boron phosphide and the metallic sheet. This improved apparatus was used to isolate mesa type silicon carbide-boron phosphide heterojunctions and boron phosphide p-n junction structures described in chapters VI and VIII, respectively.

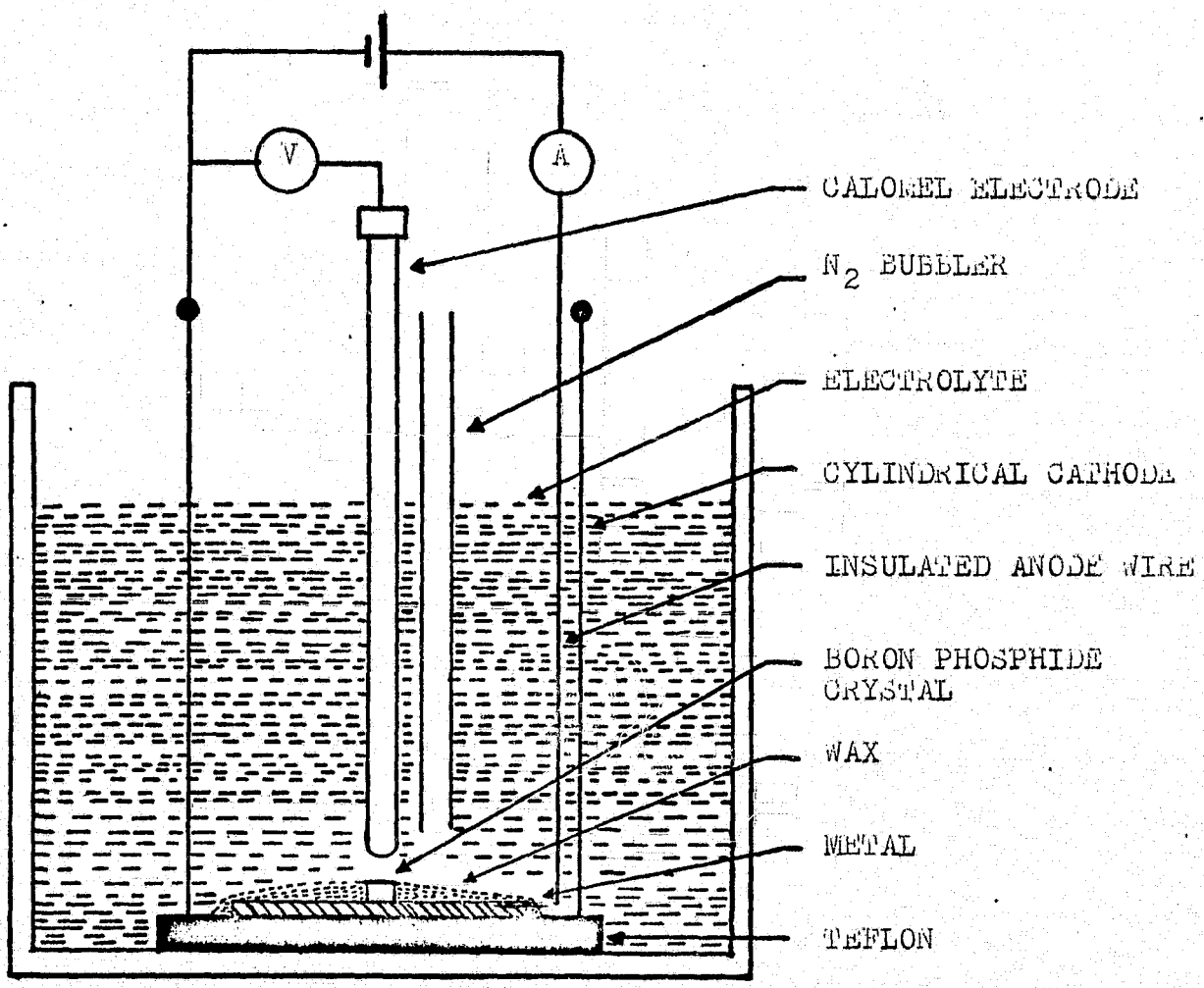

Figure 3.2 Schematic of the Electrolytic Cell for the Etching of Boron Phosphide with a Cylinderical Molybdenum Cathode

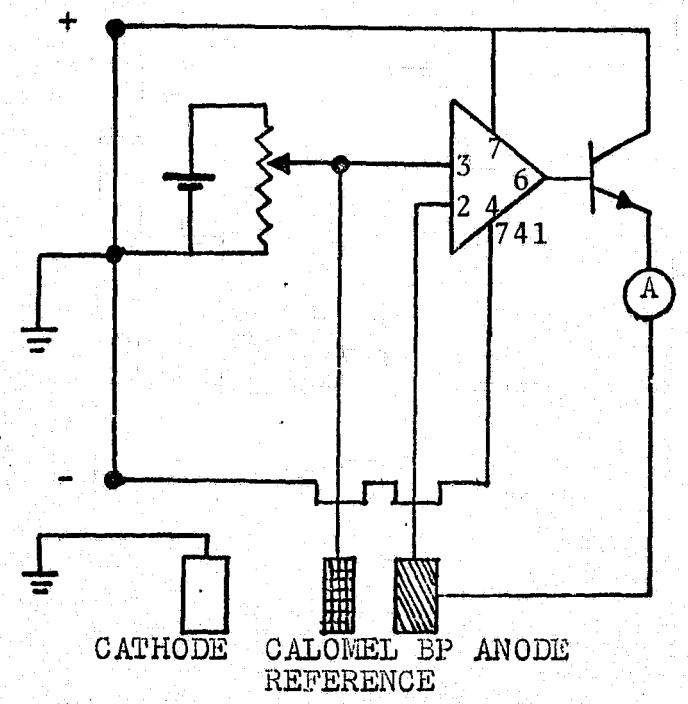

Figure 3.3 Circuit Diagram for a Constant Anode Potential in the Electrolytic Cell

The effect of illumination on the etching of n-type boron phosphide was investigated with a 50 W and a 300 W Sylvania reflector lamp. The light intensity was measured in an arbitrary unit equal to the light intensity of a 50 W lamp at a distance of 25 cm from the sample under investigation. The rest potential of a number of n-type boron phosphide crystals was determined as a function of light intensity. Different current densities were passed through n-type boron phosphide under strong illumination to investigate the conditions required for electrolytic polishing.

III.C Electrolytic Etching of Boron Phosphide

Figure 3.4 shows the typical current density-voltage relations for a p-type and an n-type boron phosphide crystal in a 10% sodium hydroxide solution at room temperature in the dark. Current saturation was observed in all n-type boron phosphide crystals investigated. The p-type material was readily dissolved and large currents were drawn. The rest potentials of both n-type and p-type boron phosphide were also measured in a number of electrolytes. The rest potential for n-type crystals was always more negative than for p-type crystals as, for example, shown

in Figure 3.4.

In the case of p-type boron phosphide, grain boundaries and twin planes were revealed at current densities of 0.01 A cm^{-2} or lower. At current densities between 0.01 A cm^{-2} and about 0.2 A cm^{-2}, etch pits were made visible. Figure 3.5 shows the etch pits formed when the p-type boron phosphide crystal was exposed to a current density of 0.05 A cm^{-2} for 1 hr. Polishing occurred at a current density of about 0.5 A cm^{-2}, and current densities of up to 10 A cm^{-2} have been used with good results. In general, mirror-like surface was readily obtained on ($\bar{1}\bar{1}\bar{1}$) faces; however, a spongy film developed on (111) faces at current densities on the order of 0.5 A cm^{-2}, and the resulting surface had a matte appearance (Figures 3.6A and 3.6B). P-type boron phosphide can also be etched in a potassium hydroxide solution and in the diluted acids listed above. If a film formed, it was readily rinsed off in water or removed by a soft brush.

Etching of n-type boron phosphide in all electrolytes under study was accompanied by the formation of an adherent orange red film on the surface at a current density of

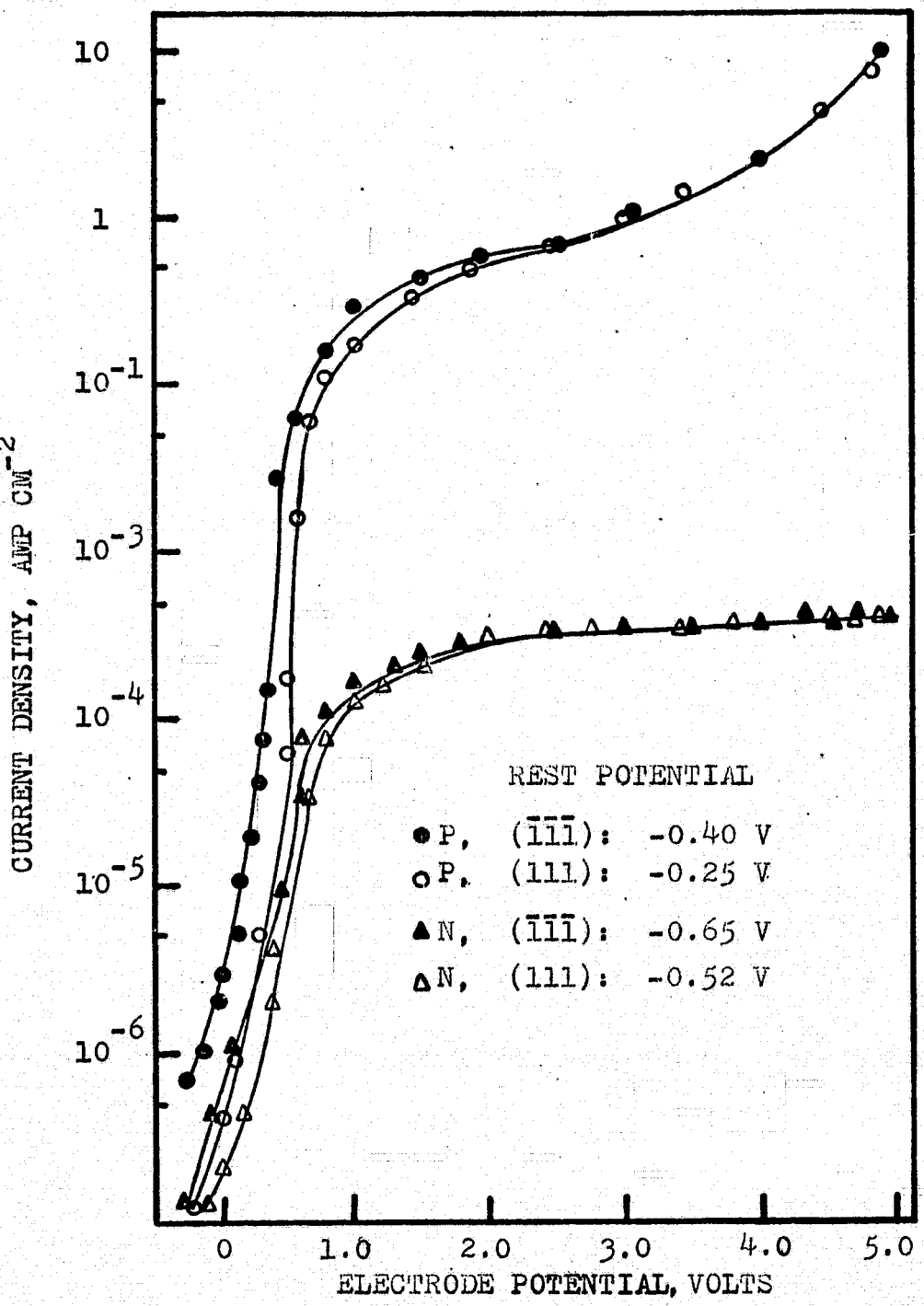

Figure 3.4 Current Density Vs. Electrode Potential for (111) and $(\bar{1}\bar{1}\bar{1})$ Faces of N-Type and P-Type Boron Phosphide in a 10% NaOH Solution in the Dark.

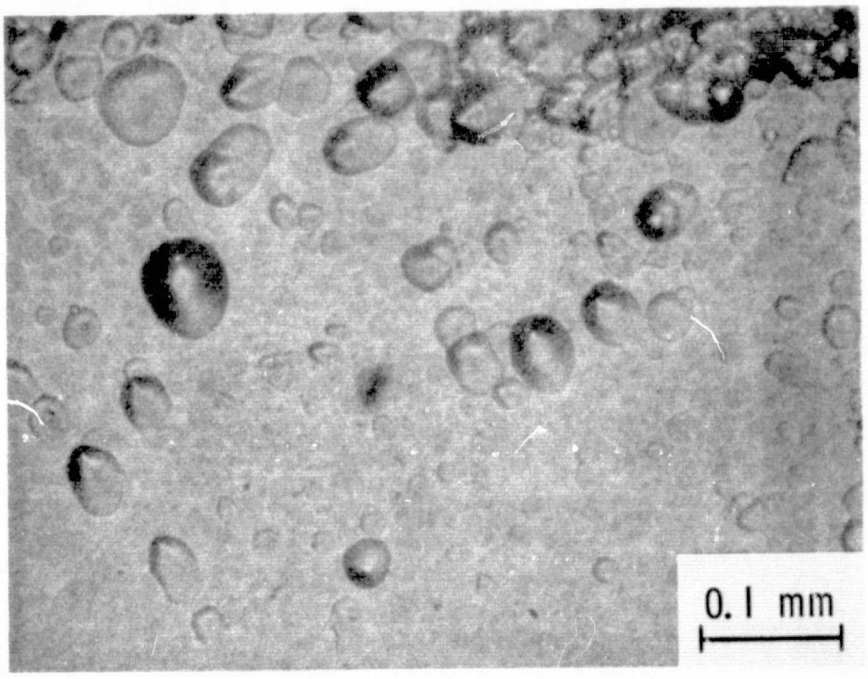

Figure 3.5 Electrolytic Etch Pits Developed on P-Type Boron Phosphide With a Current Density of 0.05 A cm^{-2} for 1 hr

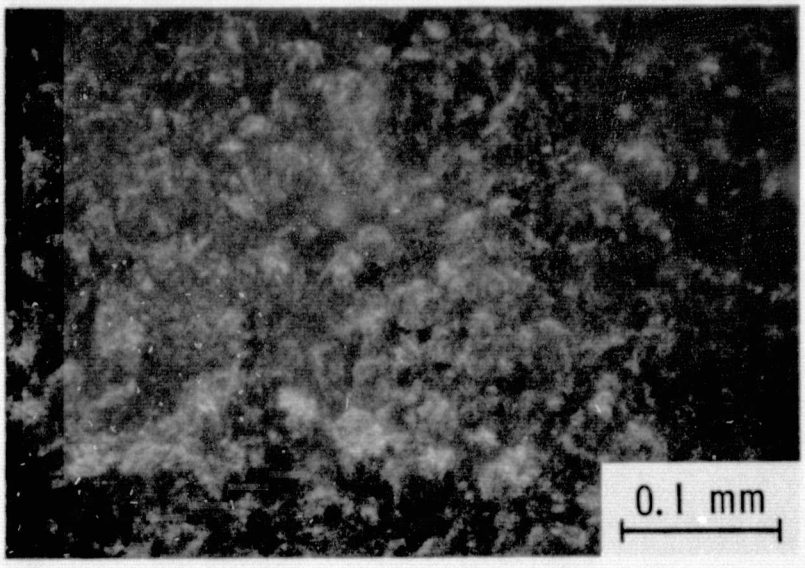

(A)

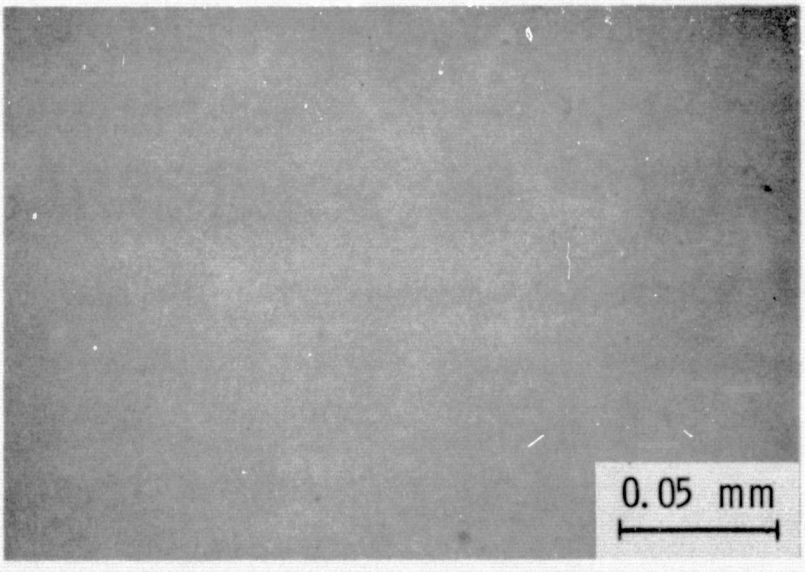

(B)

Figure 3.6 Electrolytically Etched Surfaces of P-Type Boron Phosphide With a Current Density of 0.5 A cm^{-2} for a Few min (A) (111) Face, (B) $(\bar{1}\bar{1}\bar{1})$ Face

about 0.001 A cm^{-2} or above. This film was found to be insoluble in boiling alkalis, boiling mineral acids, and a molten mixture of 3:1 sodium hydroxide and sodium peroxide at 500°C. The anodic film turned grey when heated to 950°C in hydrogen for a few minutes and, presumably, it was at least partly reduced.

The exact composition of the films formed on n-type material at low current densities was difficult to establish. Examinations by the X-ray diffraction technique using a General Electric Model XRD-6 diffractometer with Cu K_α radiation and by the reflection electron diffraction technique did not reveal any crystalline structure to these films. The X-ray Debye-Scherrer technique with Cu K_α radiation, however, indicated these films may be a mixture of boron oxide (B_2O_3) and boron phosphate.

At elevated current densities, a brittle fibre-like film was formed on n-type boron phosphide accompanied by the evolution of gas. The film could partly be removed from the substrate by a brush or by ultrasonic agitation, but it was insoluble in common acids and alkalis. Reflection electron diffraction examination of the fibrous film on n-type material showed it to be monocrystalline

boron phosphide of (111) orientation. It was therefore concluded that the fibrous film has the same crystallographic orientation as the substrate from which it originated. A similar fibre-like film was also obtained when gallium arsenide was exposed to large current densities.[67] At high current densities, as the process of film formation progresses, the current density decreases at a constant applied voltage. This decrease of current may be due to formation of an oxide film such as was found on gallium arsenide.[67] When the film separated from the substrate, the current density again increased.

The effect of illumination on the electrolytic etching of n-type boron phosphide crystals was also investigated. The rest potential of a number of n-type crystals was measured as a function of intensity of light. Figure 3.7 is a typical rest potential-light intensity relation for an n-type boron phosphide crystal. The rest potential became more negative upon illumination, and the linear relationship between the potential and the logarithm of light intensity was observed.[68] Illumination of n-type boron phosphide creates electron hole pairs and should enhance the etching process. But experimental results on a number of n-type crystals did not show any noticeable

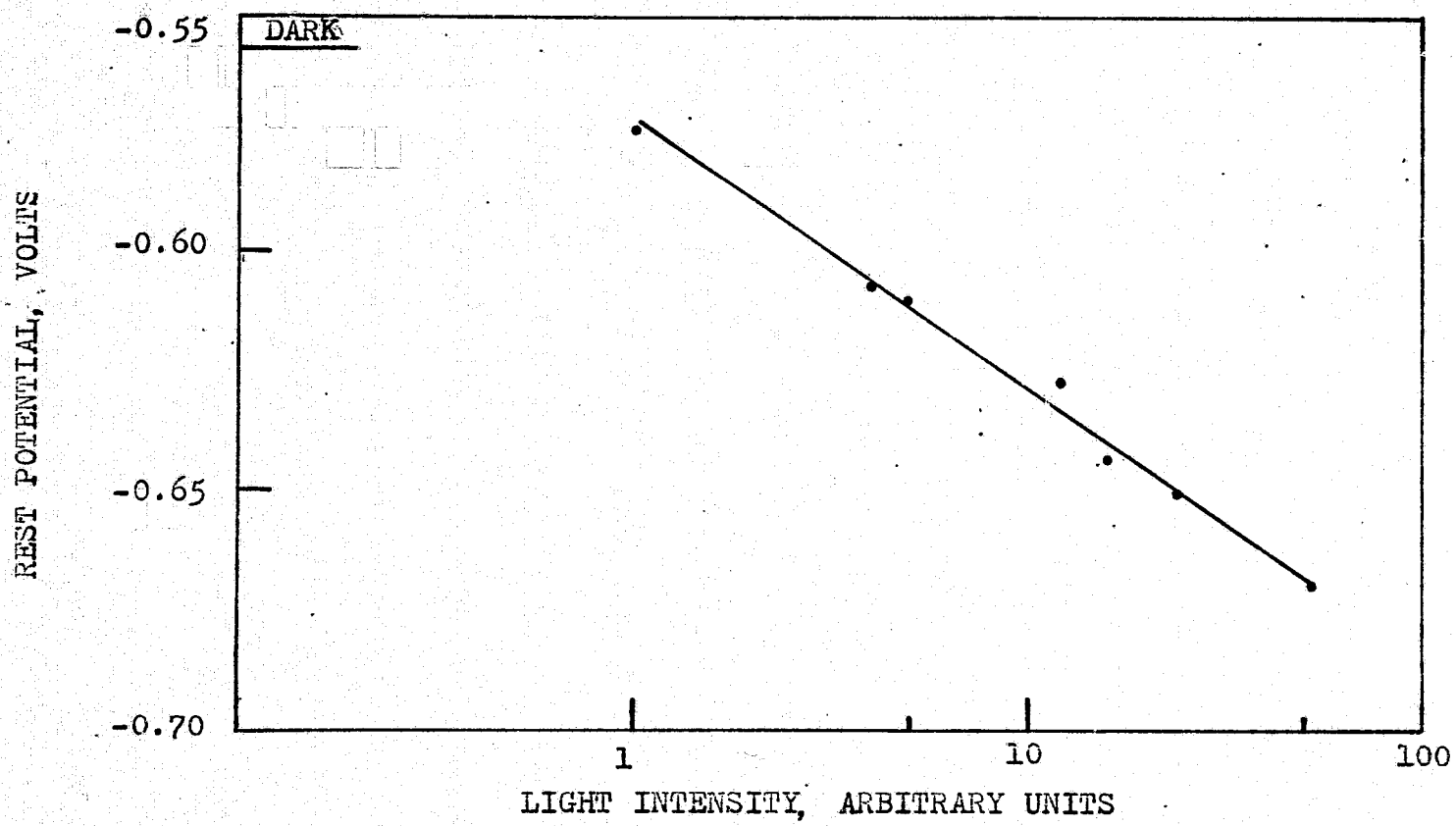

Figure 3.7 N-Type Boron Phosphide Rest Potential Vs. Light Intensity in a 10% Sodium Hydroxide Solution

etching without film formation. For a rather heavily doped n-type material, the short supply of holes and a short lifetime of holes could be responsible for the observed results.

When a voltage was applied to a crystal with a very shallow built-in p-n junction, such that the junction was forward biased and the n-side of the junction was exposed to the electrolyte, dissolution of n-type material did occur without film formation. In the case of deep junctions, film formation on n-type material was observed. In general, however, illumination of the substrate surface, bubbling of nitrogen gas through the electrolyte, or the use of various electrolytes did not reduce film formation noticeably in n-type boron phosphide.

For both n-type and p-type boron phosphide, the rest potential was more positive for the (111) face as shown in Figure 3.4. This shows that the potential drop across the interface, including both the semiconductor and electrolyte space charge potentials is different for the two surfaces. This polarity effect has been observed in a number of other III-V compound semiconductors and is in agreement with the observation of Gatos.[53] For both n-type and p-type material, the $(\bar{1}\bar{1}\bar{1})$ face draws a larger current density at a given

electrode potential than does the (111) face.

III.D Selective Etching, Junction Delineation, and Mesa Formation

It can be seen from Figure 3.4 that the current density at, for example, 3 V is about 300 times higher for p-type boron phosphide than for n-type material. This corresponds to the ratio of etch rates between p-type and n-type boron phosphide and presents the possibility of selectively removing p-type material from boron phosphide p-n junction structures. A solution grown boron phosphide crystal with a built-in p-n junction on one face was lapped with 5 μm silicon carbide abrasive and subjected to a current density of 10 A cm^{-2} for about 10 sec, although current densities below 0.5 A cm^{-2}, may be preferred to minimize the formation of anodic films in the n-region and to better control the dissolution of the p-region. The results are shown in Figures 3.8A and 3.8B where the p-type material was selectively removed and the p-n junction is delineated. The p-region developed a mirror-like surface in contrast to the n-region which was not etched. Thus, the preferential etching of p-type boron phosphide is extremely suited for the delineation of p-n junctions in boron phosphide, and is the only method available at present to remove p-type material selectively.

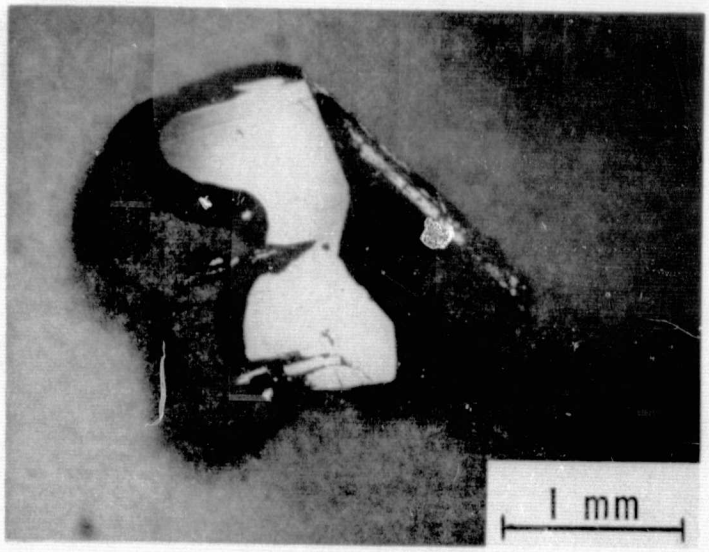

(A)

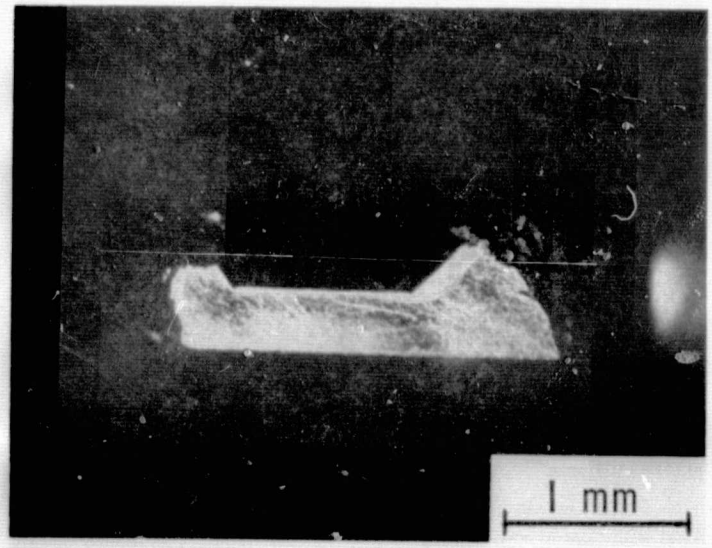

(B)

Figure 3.8 Boron Phosphide Crystal With a Built-in P-N Junction Electrolytically Etched at 10 A cm^{-2} for About 10 sec (A) Top View, (B) Cross Sectional View

Because of the inertness of boron phosphide towards ordinary chemical etchants, electrolytic etching is an attractive means of isolating the p-region in the fabrication of mesa type boron phosphide homoepitaxial and heteroepitaxial p-n junctions. Both n-type and p-type layers of boron phosphide were deposited on solution grown boron phosphide crystals and on hexagonal silicon carbide platelets by the thermal reduction of a boron tribromide-phosphorus trichloride mixture as described in chapter IV. Figure 3.9A shows a typical boron phosphide mesa type p-n junction fabricated by masking and electrolytic etching. In the case of silicon carbide-boron phosphide heterostructures, boron phosphide was exposed to the electrolyte. A sharp decrease in current density indicated the removal of all the boron phosphide layer exposed to the electrolyte. At that stage, the electrolyte was replaced by a dilute aqueous solution of hydrofluoric acid, generally 1N HF to remove a thin layer of silicon carbide, thus ensuring complete isolation of the boron phosphide from silicon carbide. Figure 3.9B shows a (n) silicon carbide-(p) boron phosphide mesa structure fabricated by the anodic dissolution of boron phosphide and silicon carbide. The fabricated mesa type homojunction and heterojunction structures have rectifying properties and easily visible, red, p-n junction electroluminescence has

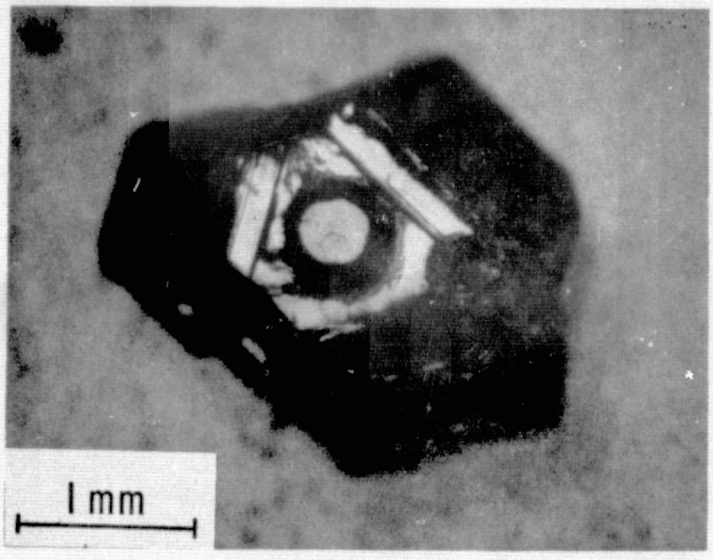

(A)

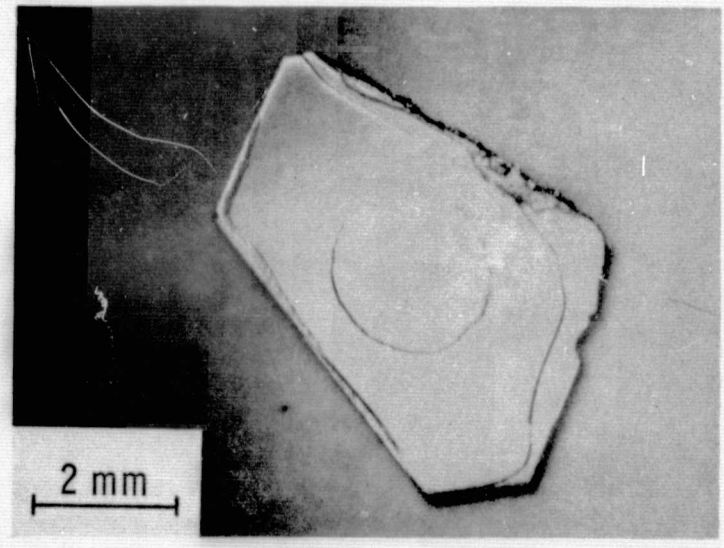

(B)

Figure 3.9 Two Mesa Structures Fabricated by Electrolytic Etching (A) Boron Phosphide P-N Homojunction, (B) Silicon Carbide-Boron Phosphide Hetero-Junction

been observed in homojunction structures. Measurements from these devices are described in chapters VI and VII respectively.

III.E Summary

Due to the chemical inertness of boron phosphide, room temperature chemical etching of boron phosphide is not possible, and electrolytic etching of boron phosphide was investigated for device applications. P-type boron phosphide could be etched or polished in several electrolytes; in contrast, n-type boron phosphide developed a film that was not soluble in common acids and alkalis. Due to a large difference in the etch rates of p-type and n-type boron phosphide, electrolytic etching was successfully applied to delineate boron phosphide p-n junction interfaces and to fabricate mesa type boron phosphide homostructures. Electrolytic etching was also used to prepare silicon carbide-boron phosphide mesa type structures. Electrolytic etching, therefore, is an attractive room temperature material shaping technique for the fabrication of boron phosphide devices.

CHAPTER IV

EPITAXIAL GROWTH OF BORON PHOSPHIDE

This chapter is concerned with the epitaxial growth of boron phosphide layers on silicon carbide and boron phosphide substrates. Boron phosphide was deposited by chemical vapor deposition using the hydrogen reduction of a mixture of boron and phosphorus halides in an open flow system. In nearly all cases, the deposited layers were epitaxial and single crystalline. In-situ doping of boron phosphide layers was carried out with hydrogen selenide.

IV.A Introduction to Epitaxial Growth

The word epitaxy is derived from two Greek words "επι" meaning upon, and "ταξι" meaning arrangement. The term now means oriented overgrowth of a single crystalline material upon a single crystal substrate. The grown material and the substrate may be the same-homoepitaxial or different-heteroepitaxial. Epitaxial growth has distinct advantages over other methods for the fabrication of semiconductor junctions, and it is in this area that epitaxial growth has been extensively applied. The dopant concentration and distribution are more readily controlled in the epitaxial layer than those in the diffusion technique. Also, in the

epitaxial growth process, impurity atoms are incorporated in the crystal lattice during the growth process; therefore, epitaxial junctions have better perfection than diffused junctions. Epitaxial growth is particularly suited for the formation of junctions in III-V compounds. Most III-V materials have appreciable dissociation pressures at temperatures required for the diffusion process but epitaxial growth can be achieved at considerably lower temperatures.

Epitaxial layers can be produced either by physical vapor deposition or by chemical vapor deposition. Physical vapor deposition process such as vacuum evaporation or sputtering have a very limited usefulness for the growth of compound semiconductors, because of the problems associated with the control of stoichimetry and doping levels. Chemical vapor growth, however, has been extensively used for the formation of layers of conductors, semiconductors, and insulators.[69,70] Chemical vapor deposition can be carried out in either a closed system or an open flow system. In general, only an open flow system provides the flexibility required for the growth of compound semiconductors with a well controlled dopant concentration and distribution.

Chemical vapor growth in a flow system, involves a substrate held at a suitable temperature in a reaction

chamber provided with a gas inlet and an exhaust. A gaseous mixture containing the constituents of the desired material is introduced into the reaction chamber, and a chemical reaction takes place on the substrate surface, depositing the desired material. Thermodynamics, kinetics, and nucleation effects involved in chemical vapor deposition have been discussed by several authors,[71-74] and the growth process is usually described with the following steps:

(1) Mass transfer of the reactants to the substrate surface,

(2) Adsorption of the reactants onto the substrate surface,

(3) The reaction or series of reactions on the surface,

(4) Desorption of the by-product molecules,

(5) Mass transfer of the by-product molecules from the surface.

Step (1) or (3) is often the rate determining step. At elevated temperatures, however, most chemical reactions proceed repidly, and step (1) is rate determining.[74]

The chemical reactions used for the vapor growth process are important factors which influence the chemical and structural perfection of the grown material. The reactants should be amenable to purification, and they should be chemically inert towards the wall of the reaction system. Furthermore, the experimental conditions should be adjusted

so that chemical reactions used for the vapor growth take place predominantly on the surface of the substrate. Gas phase reactions result in the formation of atomic or molecular clusters in the space surrounding the substrate, and the deposition of these clusters on the substrate produces polycrystalline material. The reaction products, except the desired material, should be gaseous to be effectively transported away from the substrate.

The morphology of deposits formed by chemical vapor deposition depends upon the deposition conditions, the condition of substrate surface, and the nature of the substrate. Substrate temperature is one of the most important factors that govern the crystallinity of the deposit. At very low temperatures, kinetics are not favourable for epitaxial growth. Therefore, very finely crystalline or amorphous deposits are formed. As the deposition temperature is increased, kinetic factors will tend to favor epitaxial growth. At still higher temperatures, growth rates may become too high and other reactions, such as decomposition of the deposit and volume reactions, may adversely affect the crystallinity and the composition of the deposit. Foreign impurities and structural defects on the substrate surface are the major causes for defects in epitaxial layers.

Therefore, an in-situ etching of the substrate in the reaction chamber just prior to deposition is desirable. Smooth layers are formed if the substrate surface is smooth and if there are no particles on the surface. If, however, there are asperities on the surface, growth irregularities are formed and transmitted to the surface of the deposit.[69] The smoothness of epitaxial films may also be influenced by the substrate orientation. Deposition onto different major crystallographic planes may produce very dissimilar results. Also, slight misorientations can be critical to the quality of the deposit. In contrast to homoepitaxial layers, heteroepitaxial layers usually exhibit defects due to the mismatch of lattice constants and the difference in thermal expansion coefficients of the two materials. Dislocations produced as a result of a strained lattice can extend not only into the deposit but also into the substrate.[75] The selection of a substrate for heteroepitaxial growth is determined primarily by the chemical stability, lattice parameters, and thermal expansion coefficient of the substrate.

The most important chemical reactions used for chemical vapor epitaxial growth are:

(1) Decomposition reactions,

(2) Hydrogen reduction of halides, and

(3) Transport reactions.

In decomposition reactions (or pyrolysis), the substrate is heated to a sufficiently high temperature to cause decomposition of the starting material. For example, the decomposition of silane can be used for the deposition of silicon:

$$SiH_4 \xrightarrow{800^\circ \text{ to } 1300^\circ C} Si + 2H_2$$

The hydrogen reduction process is the most common chemical vapor deposition technique in use for semiconducting materials. Halides of most of the common group III, IV, and V elements can be reduced at convenient temperatures. Hydrogen reduction will, of course, occur at a lower temperature than the pyrolysis of the same compound. An example of a reduction reaction is the deposition of silicon by the hydrogen reduction of trichlorosilane:

$$SiHCl_3 + H_2 \xrightarrow{1000^\circ \text{ to } 1300^\circ C} Si + 3HCl$$

Chemical transport process is based on the reversible reaction of the solid, A, with a gaseous transport agent, T, to form products C and D:

$$A(s) + T(g) \rightleftharpoons C(g) + D(g)$$

The equilibrium constant of the reaction is temperature

dependent and the temperatures of the source and the substrate are so arranged that the forward reaction takes place in the source region and the reverse reaction takes place in the substrate region. For example, silicon can be transported by silicon tetrachloride according to the reaction:

$$Si(s) + SiI_4(g) \underset{900^{\circ}C}{\overset{1100^{\circ}C}{\rightleftharpoons}} 2SiI_2(g)$$

In this work, the hydrogen reduction of a mixture of boron and phosphorus halides in a gas flow system was used for the epitaxial growth of boron phosphide:

$$BBr_3(g) + PCl_3(g) + 3H_2(g) \longrightarrow BP(s) + 3HCl(g) + 3HBr(g)$$

A basic constraint is that a phosphorus pressure equal to or greater than the vapor pressure of boron phosphide must be present over the substrate surface to maintain the stoichiometry of the deposit. The above mentioned considerations and the previous work[51] were used as guidelines to determine the optimum conditions for homoepitaxial and heteroepitaxial growth of boron phosphide.

IV.B Susceptor Preparation

In the chemical vapor deposition of boron phosphide, the substrates are supported on a suitable susceptor in a reaction tube, and the susceptor is heated externally by an rf generator. Thus, the surface preparation of the susceptor

is an important factor in epitaxial growth. A boron phosphide coated graphite block was used initially as the susceptor. The reproducible resistivity and structural features of boron phosphide layers obtained with this susceptor indicated that the coating was impervious and retarded the reaction of hydrogen with graphite and the out-diffusion of impurities from graphite to the substrate. However, the boron phosphide coating was always etched by the hydrogen chloride generated during the epitaxial growth process, and the susceptor had to be recoated after each deposition. To avoid this time consuming process new susceptor coatings were evaluated. The use of a silicon dioxide coating on the graphite susceptor was investigated; however, the chemically deposited silicon dioxide was apparently not as impervious as boron phosphide, and the electrical properties of epitaxial boron phosphide layers could not be accurately controlled. The use of a fused silica envelope around the graphite also did not yield reproducible results. The deposition of thin layers of silicon nitride or combinations of silicon dioxide and and silicon nitride on the graphite susceptor was found to be inadequate. Silicon nitride and silicon dioxide were also deposited on the boron phosphide coated graphite susceptor to prevent the etching of boron phosphide by hydrogen

chloride, but reactions with boron phosphide were observed in both cases at high temperatures. Finally, the surface of the graphite susceptor was converted into silicon carbide by the deposition of silicon onto the susceptor at about 850°C, and subsequent heating to about 1450°C. After the excess silicon was etched off with a hydrogen-hydrogen chloride mixture, thin layers of silicon dioxide and silicon nitride were deposited successively. The use of susceptors prepared in this manner yielded reproducible doping levels in the epitaxial layers, and the same susceptor could be used time and again to deposit boron phosphide layers.

IV.C Heteroepitaxial Growth of Boron Phosphide

Hexagonal silicon carbide was selected as a substrate for the deposition of boron phosphide. This selection was based on considerations of chemical inertness, crystal symmetry, and lattice parameters. The basal plane of hexagonal silicon carbide has a three-fold symmetry and a lattice parameter of 3.08 Å,[76] which is very similar to the interatomic distance in the (111) plane of boron phosphide, 3.12 Å. The coefficient of thermal expansion of silicon carbide is 4.68×10^{-6} per °C in the c-direction and 4.2×10^{-6} per °C in the a-direction,[77] but no data is available for boron phosphide.

The hexagonal silicon carbide platelets had their main faces parallel to the basal plane. The silicon and carbon atoms are arranged in alternate layers parallel to the basal plane. At one face, the silicon carbide structure terminates in silicon atoms triply bonded to the matrix, and at the opposite face this structure terminates in carbon atoms triply bonded to the matrix. The polarity of the substrate surface was distinguished by etching with a 1:1 molten mixture of sodium hydroxide and sodium peroxide at 800°C for 1 to 3 min; the silicon face remains smooth and the carbon face becomes rough in appearance due to hexagonal etch pits.[78] Generally the as-grown silicon carbide platelets had one face mirror smooth and the opposite face rough. In preliminary experiments it was found that boron phosphide layers on the silicon face of silicon carbide platelets had better structural perfection than layers on the carbon face. Therefore, silicon carbide platelets with a smooth silicon face were generally selected as substrates. In the case of a rough silicon face, the silicon carbide crystals were lapped with 5 μm boron carbide powder and polished with $\frac{1}{4}$ μm diamond paste on a polishing pad. The substrate was degreased with organic solvents and left overnight in a hydrofluoric acid-nitric acid mixture. The substrate was then heated for 30 min in a 1:1 mixture of

nitric acid and sulfuric acid, rinsed several times in hot deionized water, and blown dry with filtered dry nitrogen. After this thorough cleaning, the substrate was set on the susceptor and introduced into the reaction tube for boron phosphide deposition.

The epitaxial deposition of boron phosphide was carried out by the thermal reduction of a boron tribromide-phosphorus trichloride mixture in an apparatus shown schematically in Figure 4.1. The halides were kept at a temperature of 30°C in a constant temperature bath. The hydrogen gas was bubbled through the halides to carry their vapors into the 25 mm ID and 29 mm OD fused silica reaction tube. The silicon carbide substrates were located on a graphite susceptor that had been coated with silicon carbide, silicon dioxide and silicon nitride. The susceptor was inclined towards the incoming gases at an angle of 10° and was heated from outside by rf induction (Westinghouse 10 KW rf generator type 20K65). Before deposition of boron phosphide, the silicon carbide substrate was heated in hydrogen for 30 min at 1075°C. Phosphorus trichloride was introduced into the reaction tube first and the flow rate of boron tribromide was then slowly increased. A slow increase of boron tribromide was required to avoid random nucleation. The deposition time was usually 1 hr. At the conclusion of

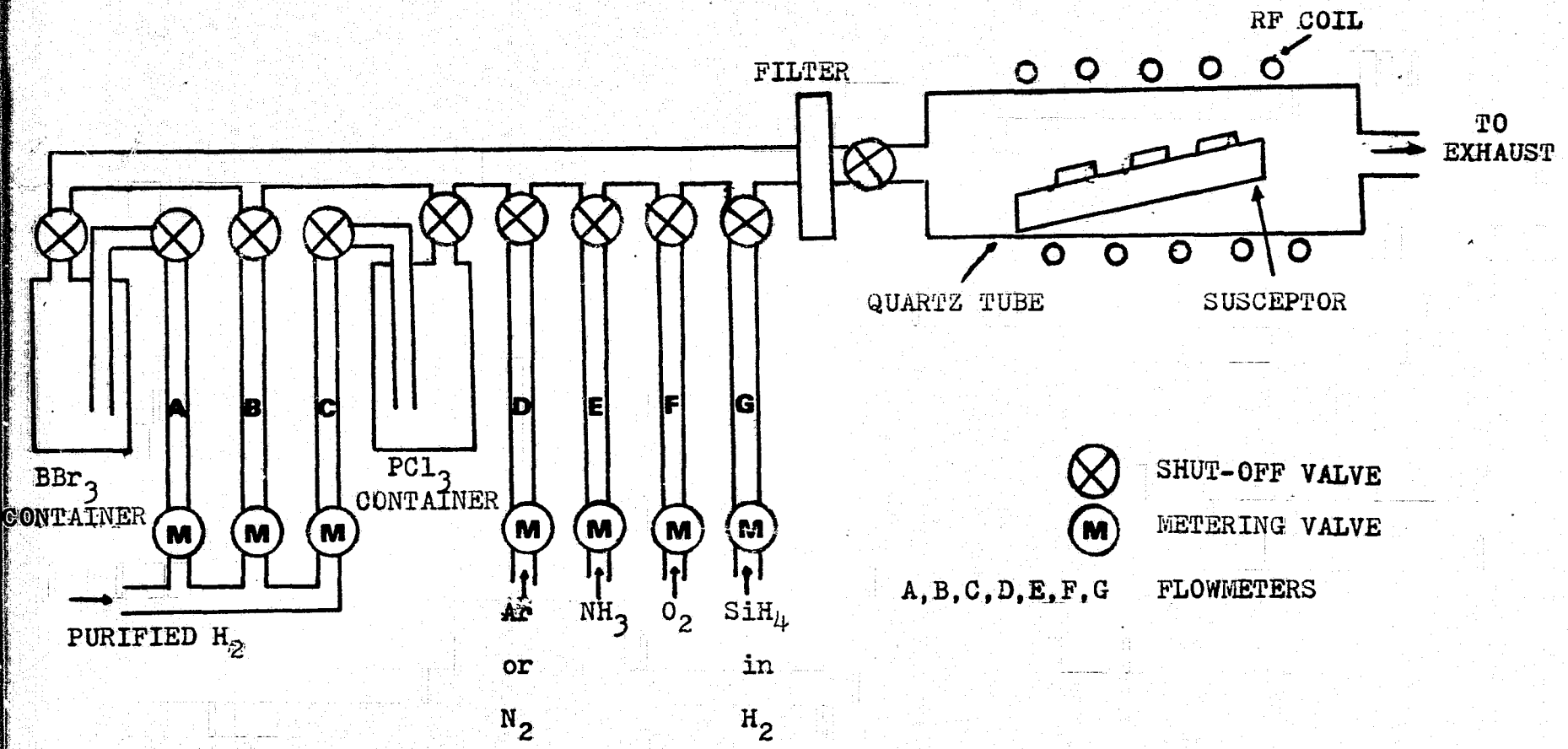

Figure 4.1 Schematic Diagram of the Apparatus for the Deposition of Boron Phosphide, Silicon Nitride and Silicon Dioxide

deposition, the flow of boron tribromide was stopped before the phosphorus trichloride flow. The growth rate and quality of the boron phosphide depended upon the substrate temperature, the polarity of the substrate, and the ratio of the concentrations of boron tribromide and phosphorus trichloride. The optimum conditions for the epitaxial growth of boron phosphide on silicon carbide were determined to be: flow rates of hydrogen, boron tribromide, and phosphorus trichloride of 0.125, 1.8×10^{-4}, and 2.4×10^{-3} moles/min, respectively; a substrate temperature of 1075° to 1100°C; and the use of the silicon face of the substrate. The deposition rate of boron phosphide on a polished face could be varied from about 20 μm/hr to 60 μm/hr by adjustment of the boron tribromide flow rate without affecting the quality of the boron phosphide layers. The deposition rate of boron phosphide on an as-grown mirror smooth silicon face was about 10 μm/hr. No warping of substrates as thin as 300 μm with boron phosphide layers up to 60 μm thick was observed.

The intentional doping of boron phosphide layers was carried out by the addition of hydrogen selenide to the reactor. A measured flow of a hydrogen-hydrogen selenide mixture containing 0.5% hydrogen selenide was introduced

into the reactant mixture while the remainder was discarded. Thus, the intentional doping of deposited boron phosphide could be reproducibly controlled.

The structural features of boron phosphide grown on hexagonal silicon carbide substrates were studied by optical microscopy and reflection electron diffraction. Figure 4.2 is a photomicrograph of a 30 μm thick boron phosphide layer deposited on the polished silicon face of a hexagonal silicon carbide platelet at 1075°C. The flow rates of hydrogen, boron tribromide, and phosphorus trichloride were 0.125, 1.6×10^{-4}, and 2.5×10^{-3} moles/min, respectively. The deposition time was 30 min. The thickness of this layer was determined by direct measurement of the fractured cross section of the specimen with an optical microscope. The surface shows a number of line defects at 60° or 120° to each other; some of these defects intersect to form triangles or partial triangles. These lines are presumably stacking faults resulting from the coalescence of initial crystallites. The geometry of the defects indicates that the grown layer is single crystalline and is of (111) orientation. Boron phosphide layers deposited on an as-grown mirror smooth silicon face did not show any structure under the optical microscope. The epitaxial relation as revealed by

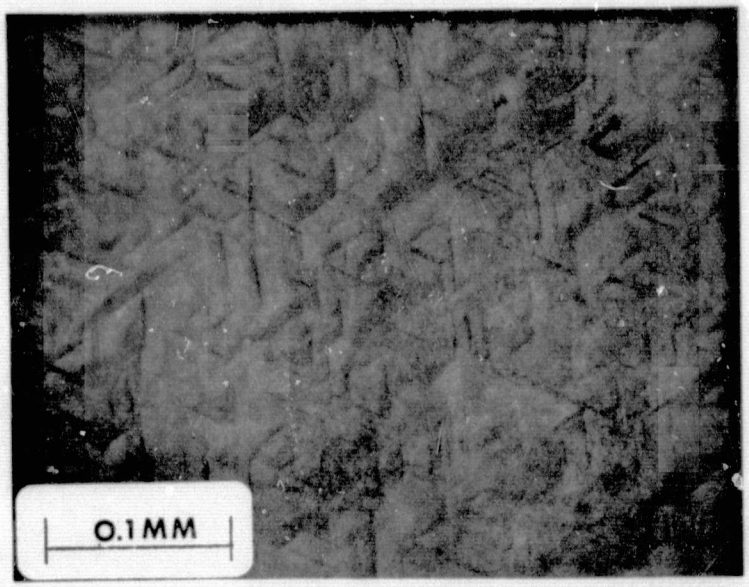

Figure 4.2 As-Grown Surface of a 30 μm Thick Boron Phosphide Layer on the Polished Silicon Face of a Hexagonal Silicon Carbide Platelet by the Thermal Reduction Technique at 1075°C

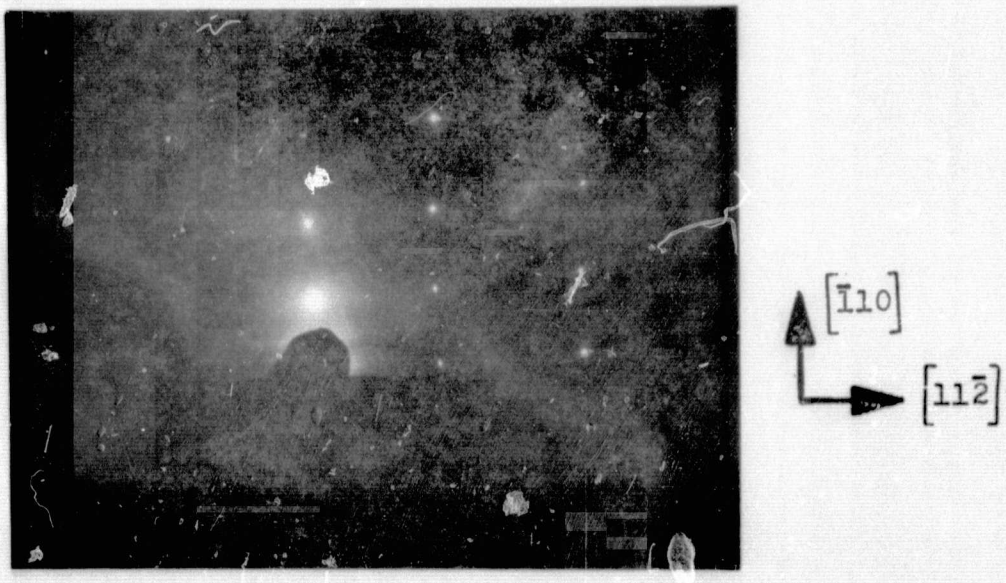

Figure 4.3 Reflection Electron Diffraction Pattern of an Epitaxial Boron Phosphide Layer Deposited on the Silicon Face of a Hexagonal Silicon Carbide Substrate by the Thermal Reduction Technique at 1075°C

the reflection electron diffraction pattern shown in Figure 4.3 is: BP(111)// SiC(001) and BP$\langle 1\bar{1}0\rangle$// SiC$\langle 010\rangle$.

The thermal reduction of the boron tribromide-phosphorus trichloride mixture without intentional doping yielded p-type boron phosphide layers. A number of doping experiments were carried out by using different flow rates of hydrogen selenide under otherwise similar conditions. Table 4.1 is a summary of the doping experiments. An average value from typically five readings of spreading resistance was used as a relative measure of the doping level in the grown layers.

IV.D Homoepitaxial Growth of Boron Phosphide

The epitaxial growth of boron phosphide on solution grown boron phosphide crystals was carried out by the thermal reduction of a boron tribromide-phosphorus trichloride mixture with hydrogen in the same manner as the deposition of boron phosphide on silicon carbide. Homoepitaxial boron phosphide layers had better structural perfection than the heteroepitaxial layers.

The flat and smooth face of boron phosphide platelets was preferred for the epitaxial growth of boron phosphide. In the case of a rough face, the boron phosphide crystals

TABLE 4.1

Doping of Epitaxial Boron Phosphide on Hexagonal Silicon Carbide

Flow rate of hydrogen gas = 0.125 moles/min

Flow rate of boron tribromide = 1.6×10^{-4} moles/min

Flow rate of phosphorus trichloride = $(1.8 \pm 0.2) \times 10^{-3}$ moles/min

Substrate temperature = $1075^{\circ}C$

Run Number	Flow Rate Of Hydrogen Selenide (cc/min)	Conductivity Type	Average Spreading Resistance(ohms)
153	0	P	7×10^{2}
157	5.8	P	4×10^{3}
156	11	P	1.9×10^{4}
155	21	P	2.5×10^{4}
159	22.5	N	1.3×10^{4}
158	25	N	2.8×10^{3}
154	35	N	2×10^{2}
152	45	N	3.5×10^{2}

were mechanically lapped and then polished with 0.3 μm alumina abrasive to yield two flat parallel faces. A few previously untried chemical etchants were also investigated as possible polishing etchants, but boron phosphide was found to be inert. Before deposition, the boron phosphide crystals were cleaned in the same manner as the silicon carbide platelets. The boron phosphide crystals were placed on the graphite susceptor, introduced into the reaction tube, and heated in hydrogen at 900°C for 30 min. The substrate temperature was then raised to 1075°C and the substrate was etched for 2 min with phosphorus trichloride. Phosphorus trichloride, instead of hydrogen chloride, was used as an etchant to suppress the dissociation of boron phosphide. Boron tribromide was then introduced and its flow rate slowly increased to its optimum value. At the end of the deposition, the flow of boron tribromide was first turned off, the temperature lowered, and the flow of phosphorus trichloride stopped. A number of experiments were carried out to determine the optimum conditions for the deposition of device quality boron phosphide on solution grown boron phosphide platelets. At flow rates of hydrogen, boron tribromide, and phosphorus trichloride of 0.125, 1.44×10^{-4}, and 1.95×10^{-3} moles/min, respectively, the growth rate of boron phosphide was approximately 30 μm/hr at a substrate

temperature of 1075°C. There was no noticeable difference in the quality of boron phosphide layers deposited on the opposite faces of solution grown boron phosphide platelets. The thickness of epitaxial layers was measured by lapping the specimen at an angle of 3° followed by etching with a 3:1 molten mixture of sodium hydroxide and sodium peroxide. The substrate-deposit interface was visible due to the presence of some defects.

Epitaxial layers deposited on as-grown mirror smooth faces of boron phosphide platelets showed no structural features when examined through an optical microscope. Figure 4.4 is a photomicrograph of a boron phosphide layer on the smooth face of a solution grown boron phosphide platelet by the thermal reduction of boron tribromide (1.44×10^{-4} moles/min) and phosphorus trichloride (1.95×10^{-3} moles/min) with hydrogen (0.125 moles/min) at 1075°C. The deposition time was 1 hr. The grown layers were single crystalline and epitaxial with respect to the substrate.

Boron phosphide layers deposited on low resistivity n-type solution grown boron phosphide platelets were n-type in contrast to the undoped p-type boron phosphide layers grown on hexagonal silicon carbide. This suggests that the

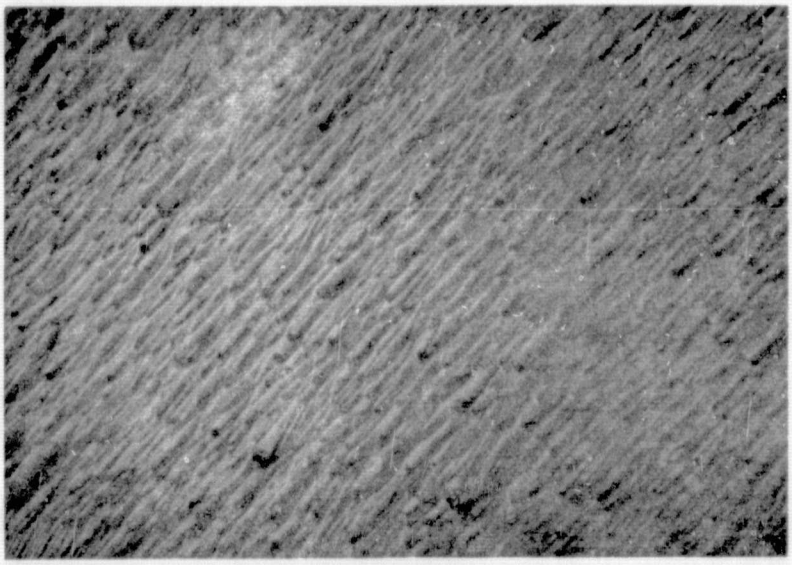

Figure 4.4 As-Grown Boron Phosphide Layer of 30 μm Thickness Deposited on the Mirror Smooth Face of a Solution Grown Boron Phosphide Platelet by the Thermal Reduction Technique at 1075°C (Magnification 500)

autodoping of boron phosphide homoepitaxial layers from the low resistivity n-type solution grown boron phosphide crystals was responsible for the conductivity type of the grown layers. Homoepitaxial layers of boron phosphide grown on n-type or high resistivity n-type solution grown boron phosphide substrates had p-type conductivity. With hydrogen selsenide as a dopant, p-type impurities were compensated and either n-type or p-type layers were produced. The relative local resistivity of epitaxial boron phosphide was compared with the spreading resistance technique. The spreading resistance of lightly doped layers was on the order of 10^6 ohms and that of highly doped layers was on the order of 10 ohms. In contrast, the resistivity of the heteroepitaxial boron phosphide films on silicon carbide could only be varied by about two orders of magnitude. This suggests that there may be fewer lattice defects or a lower concentration of unwanted impurities in the boron phosphide homoepitaxial layers.

IV.E Summary

It has been shown that heteroepitaxial layers of boron phosphide of reasonably good structural perfections can be deposited on silicon carbide. Optimum results were obtained when boron phosphide was deposited onto as-grown silicon faces of hexagonal silicon carbide platelets. Both

n-type and p-type boron phosphide layers with reproducible doping levels were grown. The boron phosphide layers deposited on solution grown boron phosphide platelets had better structural perfection than those grown on silicon carbide substrates. The heteroepitaxial and homoepitaxial boron phosphide layers were used for the fabrication of heterojunction and homojunction devices discussed in the following chapters.

CHAPTER V

METAL-INSULATOR-BORON PHOSPHIDE STRUCTURES

This chapter is concerned with metal-insulator-semiconductor (MIS) devices. Devices were made with solution-grown crystals or with epitaxial layers of boron phosphide on solution grown crystals. The insulating layer was a deposited silicon nitride or a silicon dioxide-silicon nitride double layer. The devices were characterized by capacitance-voltage measurements.

V.A Introduction to Metal-Insulator-Semiconductor Structures

The metal-insulator-semiconductor structure has become increasingly important since the development of the charge-coupled device concept in 1970.[79] An MIS structure consists of an n-type or p-type semiconductor covered by a thin film (typically between 100 Å and 2000 Å thick) of an insulating material upon which a metal electrode is deposited. The investigation of MIS structures is useful for the study of insulator-semiconductor interfaces.

The characteristics of MIS structures can be interpreted on the basis of physical models discussed by

Grove,[80] Sze,[81] and others. In an ideal MIS structure there is no metal-semiconductor work function difference and no surface states. At zero bias, the Fermi levels in metal and semiconductor are equal and no band bending is observed (flat-band condition). The capacitance-voltage behavior of an ideal MIS structure with an n-type semiconductor is shown in Figure 5.1. When the gate voltage is positive, the electrons from the semiconductor bulk are attracted towards the semiconductor-insulator interface, and the surface of the semiconductor is accumulated. The measured capacitance for a positive gate voltage is then simply the insulator capacitance. With a small negative bias, some of the majority carriers are repelled from the surface, forming a depletion layer and the total capacitance decreases. As the negative voltage is reduced sufficiently, the total capacitance goes through a minimum and then increases again as the inversion layer of holes forms at the surface. The increase in the total capacitance depends upon the ability of the minority carriers to follow the applied ac signal. This is only possible at low frequencies where the minority carriers are supplied by the generation-recombination process in the surface depletion layer in sufficient quantity to the inversion layer so that they can adequately follow the small-signal ac voltage. As

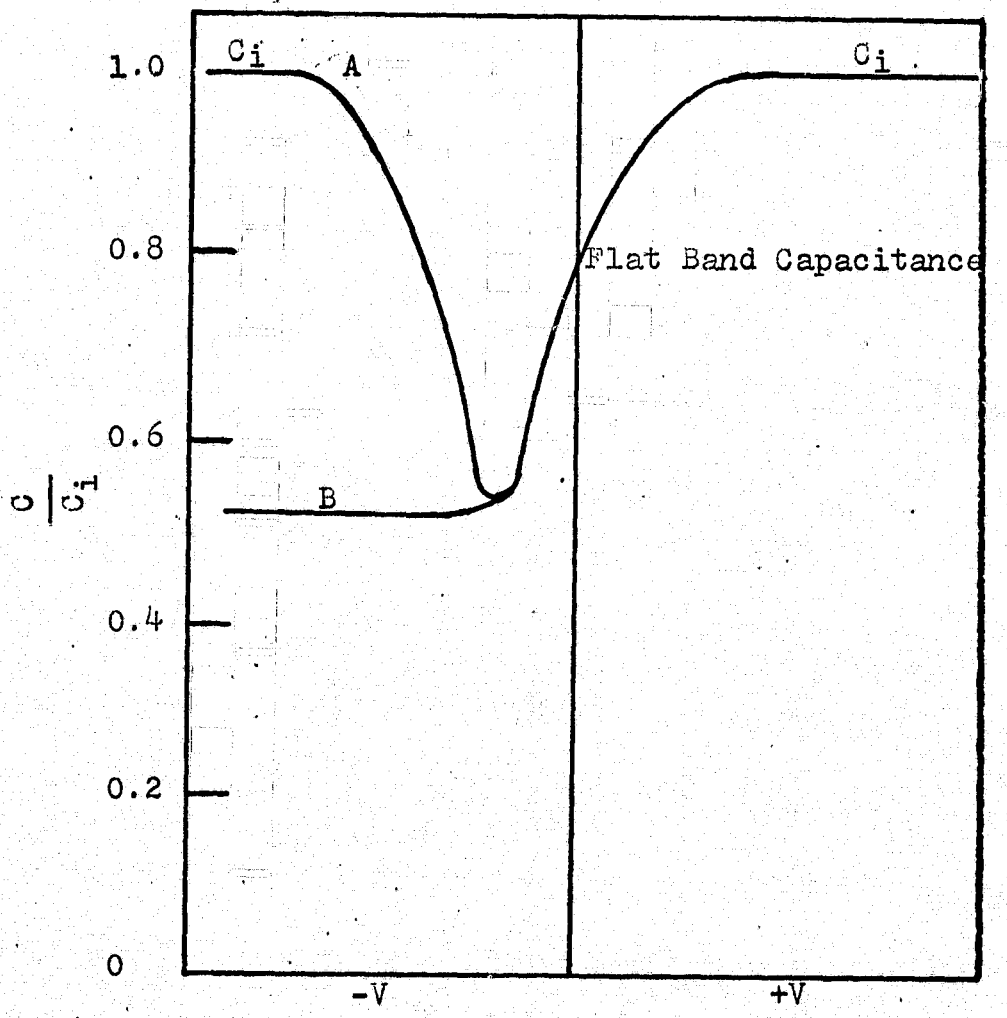

Figure 5.1 MIS Capacitance-Voltage Curves for an N-Type Semiconductor (A) Low Frequency, (B) High Frequency

a result, the capacitance measured will approach that of the insulator alone. If the frequency used for the small-signal capacitance-voltage measurement is too high, the generation mechanism cannot supply holes to the inversion layer instantaneously, and the total capacitance remains at a constant minimum.

In a practical MIS diode, the presence of interface states and charges affects the capacitance-voltage characteristics. The interface states and charges can be due to (1) energy levels within the forbidden band gap at the insulator-semiconductor interface which can exchange charges with the semiconductor in a short time, (2) fixed surface charges located near or at the semiconductor surface, and (3) mobile ions such as sodium ions which are mobile within the insulator under temperature-bias stress.

V.B Dielectrics by Oxidation and Nitridation of Boron Phosphide

One of the important aspects of the technology of any new semiconductor material is the development of a process which can be used to form a dielectric on the semiconductor surface, both for surface passivation and as the insulator for metal-insulator-semiconductor structures. In silicon technology, thermally grown silicon dioxide is superior to

deposited oxide in interface properties. Attempts were made to produce a similar dielectric on boron phosphide.

The oxidation and nitridation of boron phosphide were studied. Boron phosphide was found to be readily oxidized in an oxygen atmosphere at 800°C or higher. However, the resulting product was not adherent to the boron phosphide substrate. The X-ray Debye-Scherrer analysis showed that the oxidation product was a mixture of tetragonal boron phosphate (BPO_4) and boron oxide (B_2O_3). Oxidation at lower temperatures, which in general tends to produce more adherent films, produced boron phosphate films with pinholes. It was concluded, therefore, that thermal oxidation of boron phosphide does not produce a suitable dielectric for device purposes. The nitridation of boron phosphide was investigated by heating the crystals in ammonia for several hours. At temperature below 925°C, no appreciable reaction was observed. As the temperature was increased to about 1000°C, a discontinuous film of boron nitride was produced. Since neither film produced by the oxidation or nitridation technique appeared to be suitable as dielectric on boron phosphide, deposited layers described in the next section were used.

Towards the end of this research, the electrolytic

oxidation of boron phosphide in various electrolytes was investigated to determine the feasibility of growing oxide film on boron phosphide. P-type boron phosphide was readily dissolved in all the electrolytes investigated. Anodic oxidation of n-type boron phosphide in 5% to 30% hydrogen peroxide produced adherent and insulating film at low current densities. More work is recommended to characterize this oxide.

V.C Silicon Dioxide and Silicon Nitride Films

Silicon nitride and silicon nitride-silicon dioxide double layers were used as dielectrics in the fabrication of boron phosphide MIS structures. The oxide and nitride were deposited by the oxidation and ammonolysis of silane, respectively. A number of experiments were carried out to determine the conditions and the rate of deposition of silicon dioxide and silicon nitride on boron phosphide substrates. The boron phosphide crystals to be used as substrates were lapped and polished mechanically to yield two smooth parallel and flat faces. The substrates were supported on a graphite susceptor (prepared as described in Chapter IV) in the 25 mm ID and 29 mm OD water cooled fused silica tube. The susceptor was heated externally by rf induction. The substrate was heated in hydrogen for 30 min

before deposition. The deposition of silicon dioxide was carried out at temperatures near 550°C, since silicon dioxide was found to react with boron phosphide when the oxidation of silane was carried out at temperatures above 900°C. Oxygen was introduced into the reaction tube first and the flow rate of silane was then slowly increased. At the conclusion of deposition, the supply of silane was turned off followed by that of oxygen. The deposition time varied from 15 to 30 min. Silicon nitride was deposited at a substrate temperature of 850°C, since there were indications of reactions between silicon nitride and boron phosphide at temperatures above 1000°C. A deposition rate of 190 Å/min was determined for silicon nitride at a substrate temperature of 850°C with the flow rates of hydrogen, silane, and ammonia of 5, 0.003, and 0.13 l/min, respectively. Silicon dioxide was deposited at a rate of 233 Å/min at a substrate temperature of 850°C with the flow rates of hydrogen, silane, and oxygen of 5, 0.003, and 0.1 l/min, respectively. When the substrate temperature was lowered to 550°C, the deposition rate of silicon dioxide increased to about 360 Å/min. The thickness of these films on boron phosphide substrates was determined as follows: a part of the film was masked by Apiezon W wax and the exposed film was etched with buffered hydrofluoric acid (for silicon

dioxide) or with hydrofluoric acid (for silicon nitride). The height of the step generated by etching was measured with a Sloan Dektek.

The silicon dioxide and silicon nitride films were transparent and were adherent to boron phosphide. When observed through the high power metallurgical microscope, the films showed no pinholes. The electrical resistivity of a typical 1500 Å thick silicon nitride film was on the order of 10^{10} ohm-cm compared to 10^{15} ohm-cm[82] for silicon nitride films deposited on silicon. The break down strength was on the order of 10^{6} V-cm^{-1} compared to 10^{7} V-cm^{-1}.[82] Thus the silicon nitride films deposited on boron phosphide are inferior to those reported elsewhere due presumably to the relatively low temperatures used in the deposition process.

V.D Fabrication and Characterization of Boron Phosphide MIS Structures

Several approaches were investigated for the fabrication of boron phosphide MIS structures. In one approach silicon nitride films from 1000 to 2000 Å in thickness were deposited on a mechanically polished face of either n-type solution grown crystals or homoepitaxial boron phosphide at

850°C. After the deposition of silicon nitride, the back side of the boron phosphide substrate was lapped to remove unwanted silicon nitride. Electroless nickel was then plated onto the back of the boron phosphide crystal at 80° to 90°C. During electroless nickel plating, the silicon nitride face was covered with Apiezon W wax to protect it from plating. The crystal with the plated nickel was annealed in either an argon or a hydrogen atmosphere at 850°C for 1 hr to form ohmic contact. Aluminum gate electrodes of 0.25 mm diameter were then deposited onto the silicon nitride by vacuum evaporation. The evaporator was a diffusion-oil pumped Varian PS-10E system with a liquid nitrogen trap. The capacitance-voltage measurements on the fabricated metal-insulator-boron phosphide structures were made with a Tektronix type 130 L-C meter, operated at 0.2 MHz, in conjunction with a Hewlett-Packard 7034A X-Y recorder, or with a Boonton 75C Direct Capacitance bridge, operated at a frequency of 0.4 MHz. These measurements were made under a dc bias upon which was superimposed a small ac signal. The capacitance-voltage characteristics of a typical (n) boron phosphide MIS structure are shown in Figure 5.2 The positive flat-band voltage indicates the existence of a negative charge in silicon nitride near the silicon nitride-boron phosphide interface. Because of

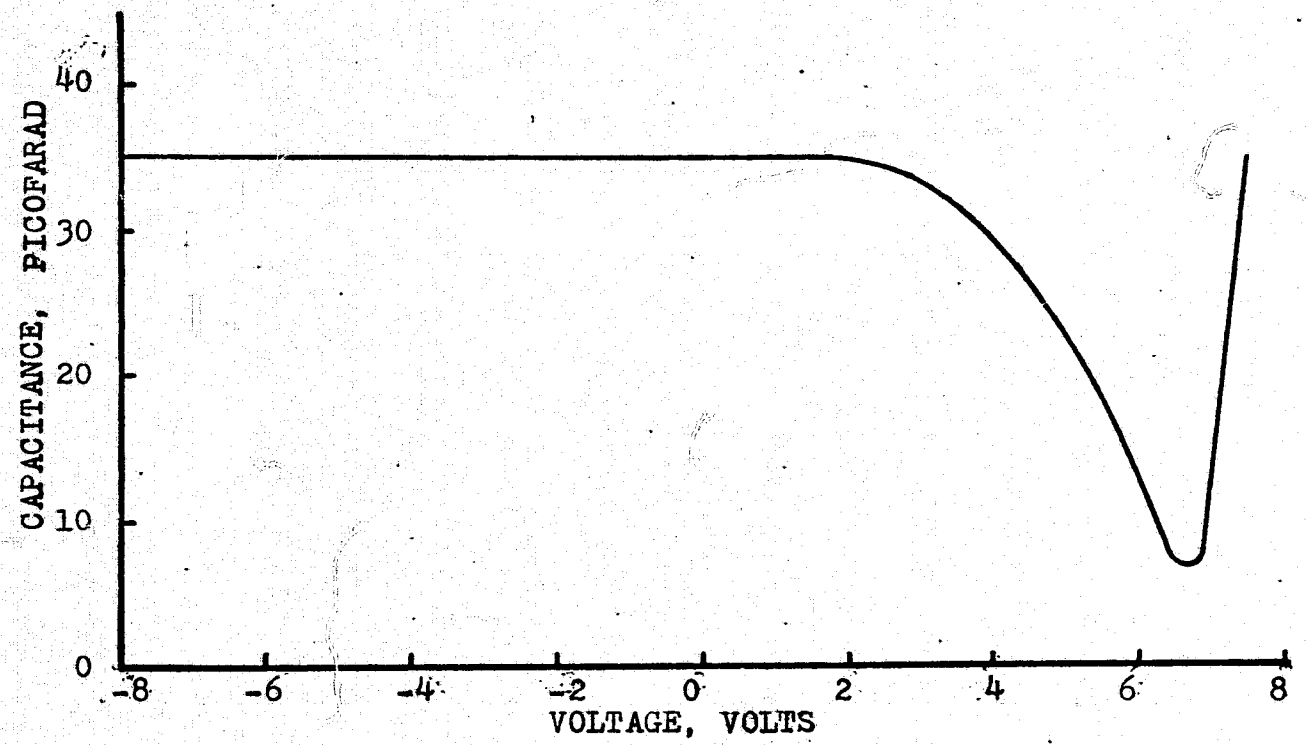

Figure 5.2 Capacitance-Voltage Relation of an Aluminum-Silicon Nitride-(N) Boron Phosphide Structure at 400 KHZ

the negative charge in the nitride, an inversion layer is formed at the entire n-type boron phosphide surface for positive gate voltage. Since the insulator layer extends over an area greater than the metal electrode the device has two parts of inversion layer:[5] an intrinsic portion directly beneath the metal region and an extrinsic portion in the area covered only by the insulator. The two parts are coupled to form a distributive R-C network, made up of the lateral resistance of the inversion region and the depletion capacitance. The distributed R-C network beyond the gate can be considered a low pass filter. Therefore, as frequency increases, the ac propagates a shorter distance down the line away from the gate before dying out. Both the external conductance and external capacitance will then be smaller, and measured capacitance will become bias independent at a value less than insulator capacitance. At high enough frequency, depending upon lateral resistance and boron phosphide resistivity, hardly any ac propagates into the distributed network. At this cut off frequency, the overall capacitance of the insulator is in series with the depletion capacitance for all values of bias at which the boron phosphide under the gate is inverted. Similar observations have been made by a number of workers on silicon MOS structures,[83-85] and low frequency regime extends up to

a few MHz.

Another procedure used for the fabrication of boron phosphide MIS structure was to deposit epitaxial boron phosphide and silicon nitride consecutively to minimize the possibility of introducing impurities at the boron phosphide-silicon nitride interface. A low resistivity n-type epitaxial boron phosphide layer was deposited on the back side of the substrate at 1075°C to facilitate the formation of the ohmic contact. After thoroughly flushing the gas flow lines, a silicon nitride layer of 1000 to 2000 Å in thickness was deposited on the n^+ layer to minimize the auto doping effect in the subsequent epitaxial growth process. The front side of the substrate was lapped and polished mechanically to remove any silicon nitride and n^+ boron phosphide. A high resistivity n-type epitaxial boron phosphide layer was then deposited on the polished face of the substrate, followed by the deposition of a 2000 Å thick silicon nitride layer. The back face of the boron phosphide substrate was then lapped with 600 grit silicon carbide abrasive powder to expose the n^+ boron phosphide epitaxial layer. The electroless nickel plating and annealing on the lapped back face of the substrate was performed as described before. Aluminum gate electrodes of

0.25 mm diameter were then deposited onto the silicon nitride by vacuum evaporation. It is important that the silicon nitride-boron phosphide structure is not subjected to temperatures above 850°C because of dissociation of boron phosphide at temperatures above 900°C and the reaction between boron phosphide and silicon nitride at high temperatures. The capacitance-voltage relations of a typical boron phosphide MIS structure described above are shown in Figure 5.3. The positive flat-band voltage indicates the existence of negative charge in the silicon nitride near the silicon nitride-boron phosphide interface. This result supports the analysis of the previous device and indicates that the one-step process would influence the density of interface charges.

Double layers of silicon dioxide deposited at 600°C and silicon nitride deposited at 850°C were also used as the insulator in boron phosphide MIS structures. The capacitance-voltage measurements of these boron phosphide MIS structures are similar to those shown in Figure 5.3 and again indicate the presence of negative charges in the insulator.

V.E Summary

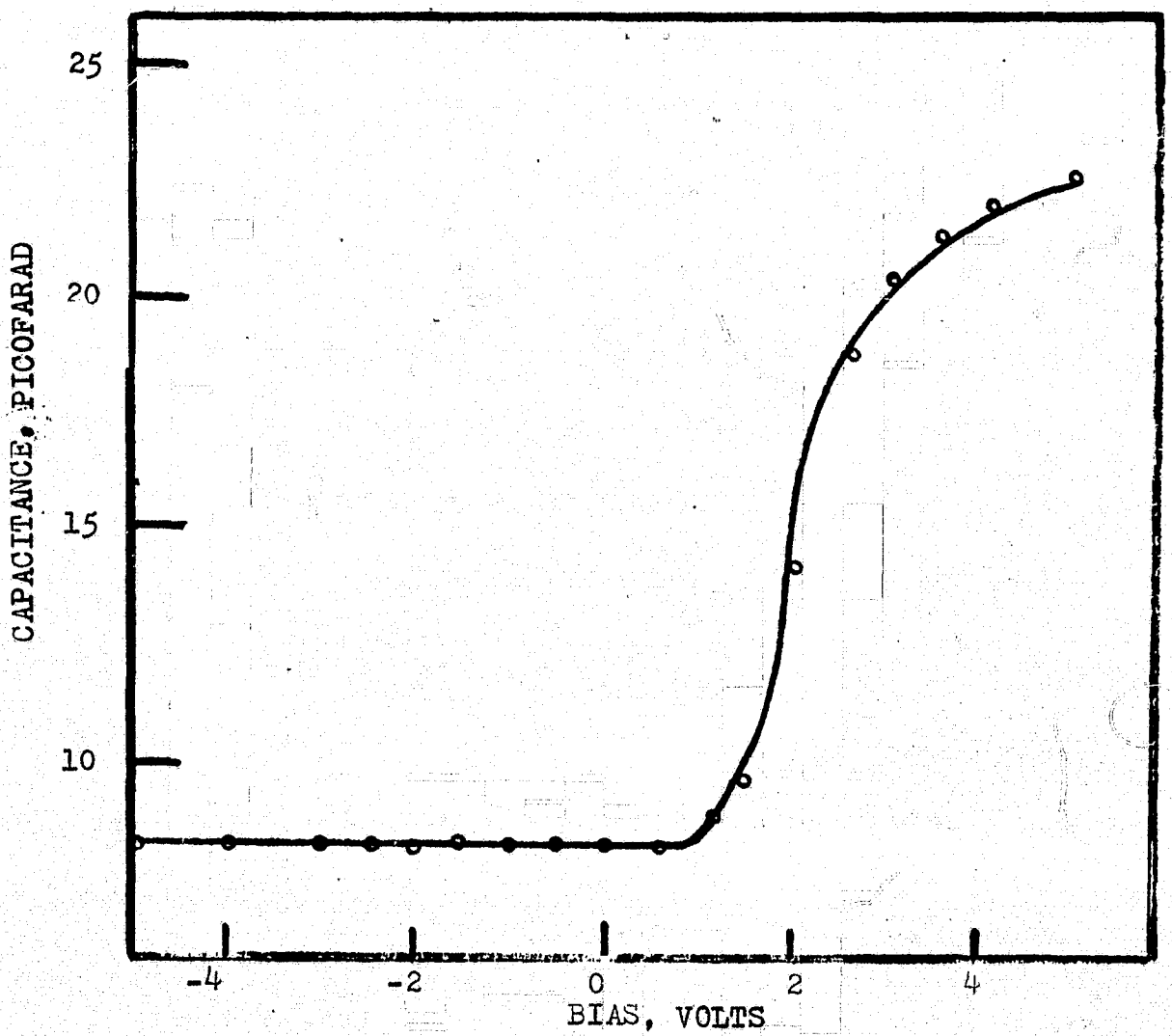

Figure 5.3 Capacitance-Voltage Relation of an Aluminum-Silicon Nitride-(N) Boron Phosphide Structure at 400 KHZ

The silicon nitride-boron phosphide structures have been prepared for the first time and the interface is characterized by high density of interface states. Oxidation and nitridation products of boron phosphide have been found to be unsuitable as dielectrics for boron phosphide devices. The use of other dielectrics such as aluminum nitride[86] and anodic oxide of boron phosphide should therefore be investigated in the passivation of boron phosphide devices and in the fabrication of boron phosphide MIS structures.

CHAPTER VI

SILICON CARBIDE-BORON PHOSPHIDE JUNCTIONS

This chapter is concerned with the fabrication and characterization of silicon carbide-boron phosphide heterojunctions. Both n-type and p-type epitaxial layers of boron phosphide were deposited on hexagonal silicon carbide platelets using the chemical vapor deposition technique. Ohmic contacts were applied to both boron phosphide and silicon carbide faces. Mesa junctions were isolated by electrolytic etching and current-voltage and capacitance-voltage characteristics of these mesa junctions were determined.

VI.A Introduction to Heterojunctions

A semiconductor heterojunction is a junction between two different semiconductor materials. A p-p or n-n heterojunction is called an isotype heterojunction and a p-n heterojunction, an anisotype heterojunction. The two sides of a heterojunction will, in general have different gaps, dielectric constants, work functions, and electron affinities. As a consequence, the energy band diagram of a heterojunction is not as simple as the diagram for a homojunction, and there are energy steps at the junction in

both the valence and conduction bands. The device characteristics, are therefore, more complicated than those of a homojunction.

In 1951, Shockley[87] suggested that an abrupt heterojunction would be an efficient emitter-base junction in a transistor. Kroemer[88] analysed a graded heterojunction as a wide-gap emitter. Since then, many other applications of heterojunctions have been proposed, such as the majority carrier rectifier, the high-speed band-pass photodetector, and the indirect-gap injection laser.[89] A heterojunction transistor with a large band gap semiconductor emitter (n-type) and a smaller band gap base and collector can have higher gains and better frequency response than is possible in homojunction transistors.[90] This is possible because the difference in band gaps appears as an energy barrier in the valence band, which prevents reverse hole injection from a p-type base into an n-type emitter and thereby increases the electron injection efficiency of the emitter. In p-n heterojunctions, the large-gap material is usually transparent to radiation generated in the small-gap material, and therefore, is sometimes used as a "window" for transmitting the radiation.[91] This "window effect" can be used to fabricate photovoltaic p-n heterojunctions with a higher conversion efficiency than photovoltaic p-n homojunctions,[92] because incident photons with

energies between the two forbidden gap energies are transmitted with little or no attenuation across the interface from the large band gap side and are absorbed in the narrow band gap material.

In practice, heterojunction devices suffer from one major limitation: a high density of states within the band gap at the junction interface. These interface states can act as trapping centers and they severely limit the device potential.[93] These interface states are due, in large part, to the lattice parameter and thermal expansion coefficient mismatch between the two materials of the device. Both types of mismatch will produce a strained lattice and dislocations. In addition, interface states can result from autodoping of the grown layer from the substrates and from other unwanted impurities in the growth system.

VI.B Preparation of Silicon Carbide-Boron Phosphide Heterojunctions

P-type boron phosphide layers were deposited on low resistivity n-type hexagonal silicon carbide substrates at 1075°C, as described in chapter IV. After removal of the deposit on the back side of the substrate, mesa structures were fabricated by electrolytic etching. Selective etching of boron phosphide was done as described in chapter III.

Ohmic contacts were applied to silicon carbide and boron phosphide by using successive layers of palladium and nickel applied from plating solutions. The contact resistance was reduced by annealing at 800° to 850°C for 1 hr in a hydrogen or argon atmosphere.

VI.C Characteristics of (n) Silicon Carbide-(p) Boron Phosphide Heterojunctions

The spreading resistance technique was used to compare the relative local resistivity and to determine the junction depth in heteroepitaxial p-n junctions. Measurements of spreading resistance were made on angle-polished specimens and an average of those taken at each step was used for the spreading resistance profile of the heterojunction. Figure 6.1 shows a profile of a typical (n) silicon carbide-(p) boron phosphide epitaxial junction. The junction depth determined from this profile was about 37 μm from the grown surface.

A preliminary evaluation of the current-voltage characteristics of (n) silicon carbide-(p) boron phosphide junctions was made with a diode curve tracer. Figure 6.2 shows a typical trace. Diodes with poor reverse characteristics were often improved by additional electrolytic etching. When additional etching did not improve the diode

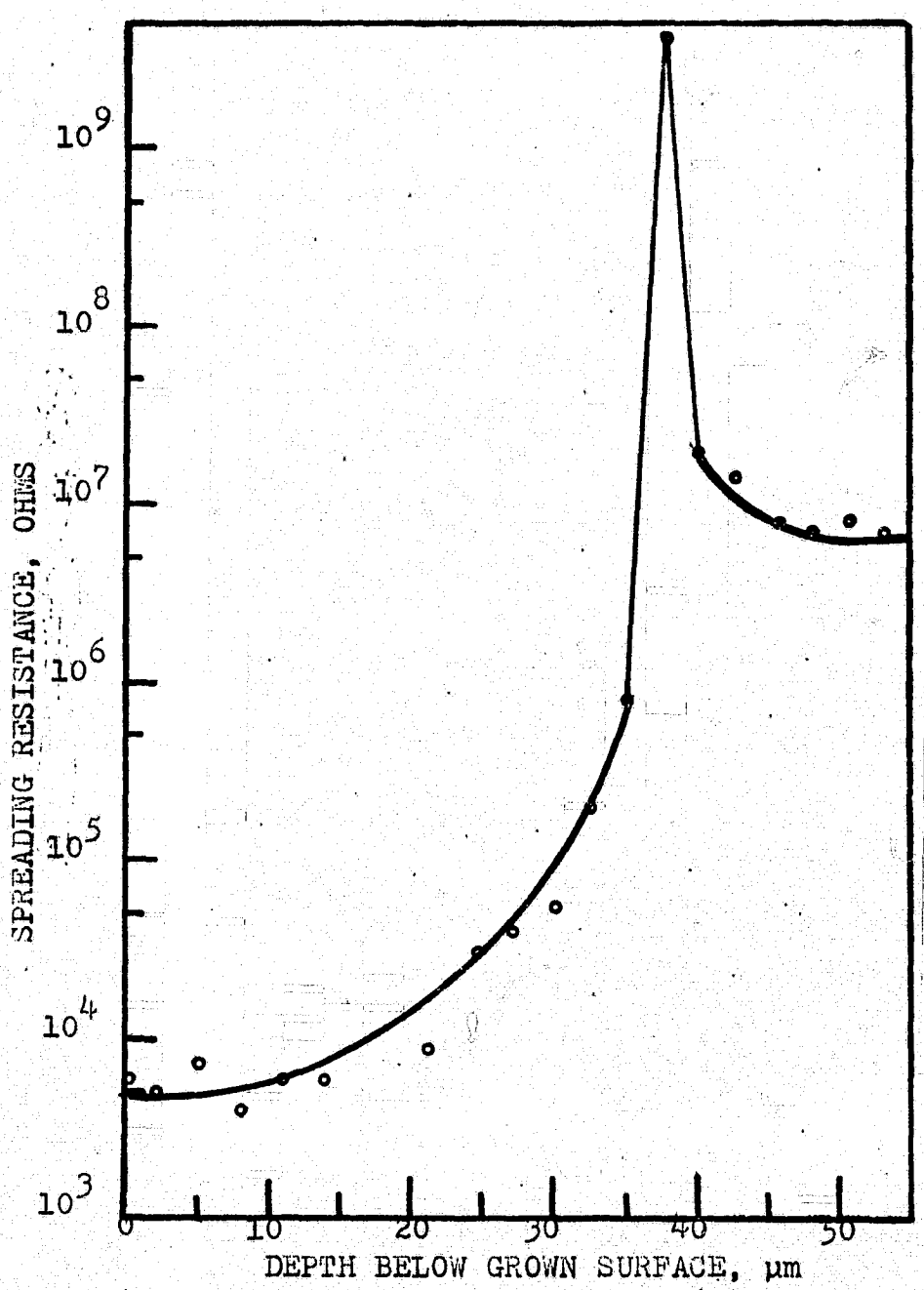

Figure 6.1 Spreading Resistance Profile of an (N) Silicon Carbide-(P) boron Phosphide Heterojunction

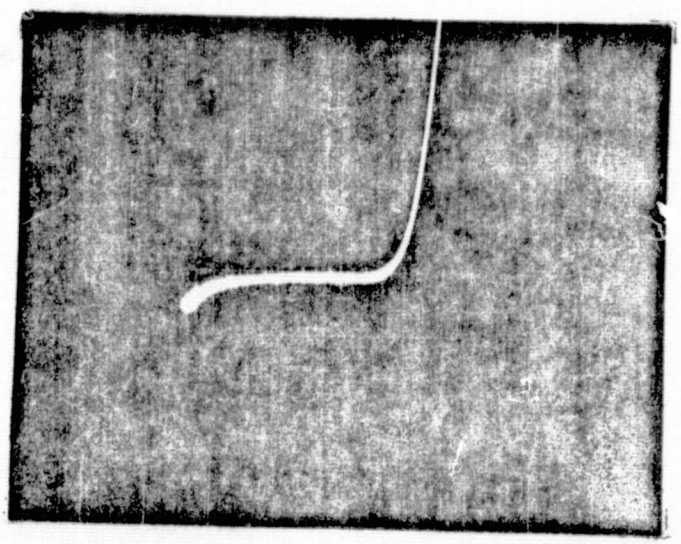

Figure 6.2 Current-Voltage Characteristics of an (N) Silicon Carbide-(P) Boron Phosphide Diode (Horizontal 10 V/Div, Vertical 1 mA/Div)

reverse characteristics, the diode was cleaned thoroughly, dried and transported to a probe station for point by point measurements at room temperature. Figures 6.3 and 6.4 show, respectively, the forward and reverse current-voltage characteristics of the (n) silicon carbide-(p) boron phosphide junction whose spreading resistance profile is shown in Figure 6.1. The forward current is proportional to $\exp(\frac{qV}{\eta KT})$, where η is 1.9. At voltages higher than 0.7 V, the series resistance of the device limited the forward characteristics. The reverse current increases exponentially with voltage up to -4 V. Below -4 V, the current increases slowly with voltage. These characteristics are to be expected in accordance with the Dolega model.[94] In this model, the presence of a thin layer with an extremely small carrier life time at the interface between the two semiconductors is considered to be typical of p-n heterojunctions. The p-n heterojunction corresponds to two metal-semiconductor contacts in series. When the impurity concentrations in the two sides of the junction are widely different, practically all the voltage drop occurs on the side with lower impurity concentration. This corresponds to a single Schottky barrier diode and η reaches 1. On the other hand, when impurity concentrations on the two sides are comparable, voltage drop occurs on both sides of the junction, and η reaches 2.

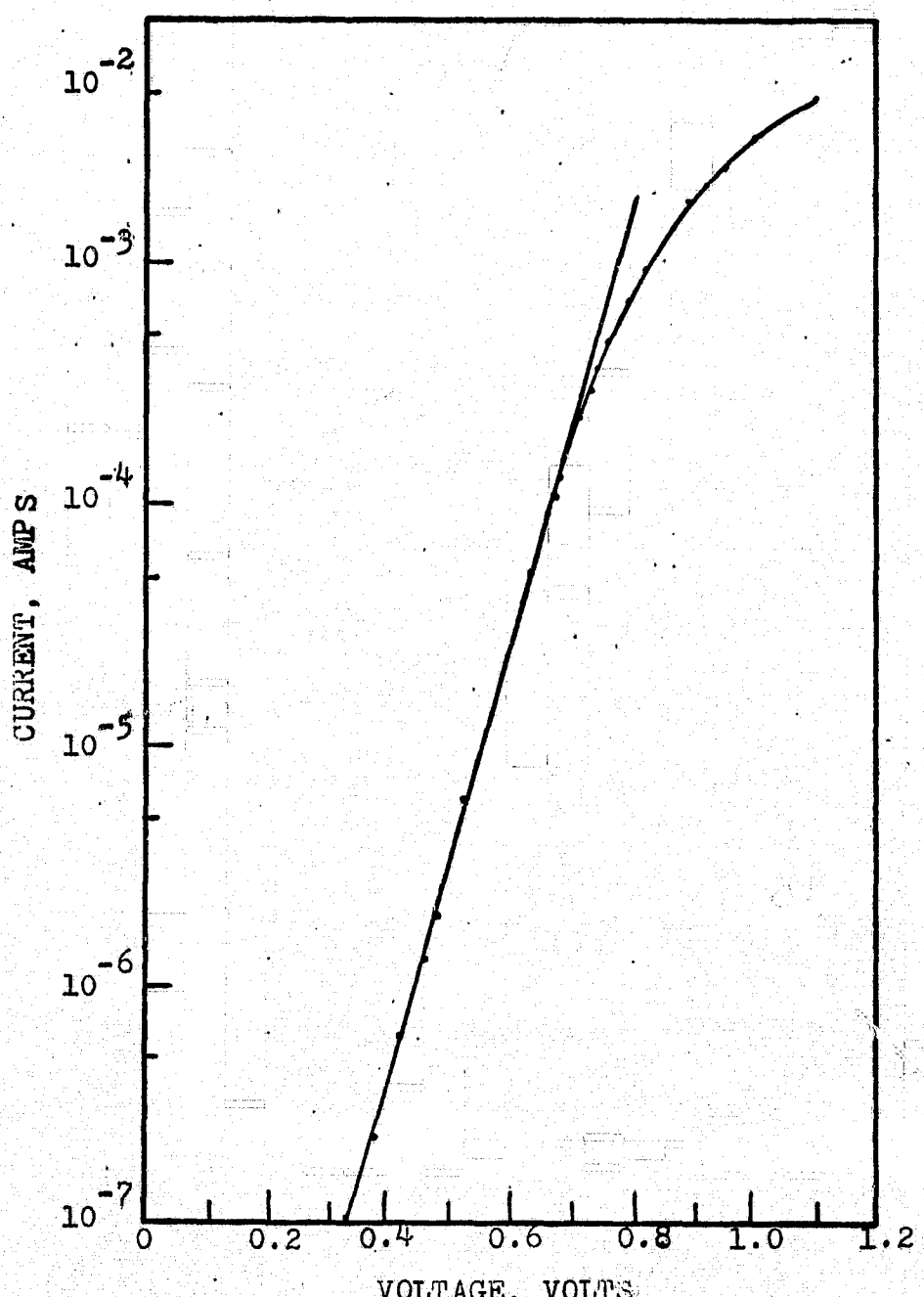

Figure 6.3 Forward Characteristics of the (N) Silicon Carbide-(P) Boron Phosphide Heterojunction

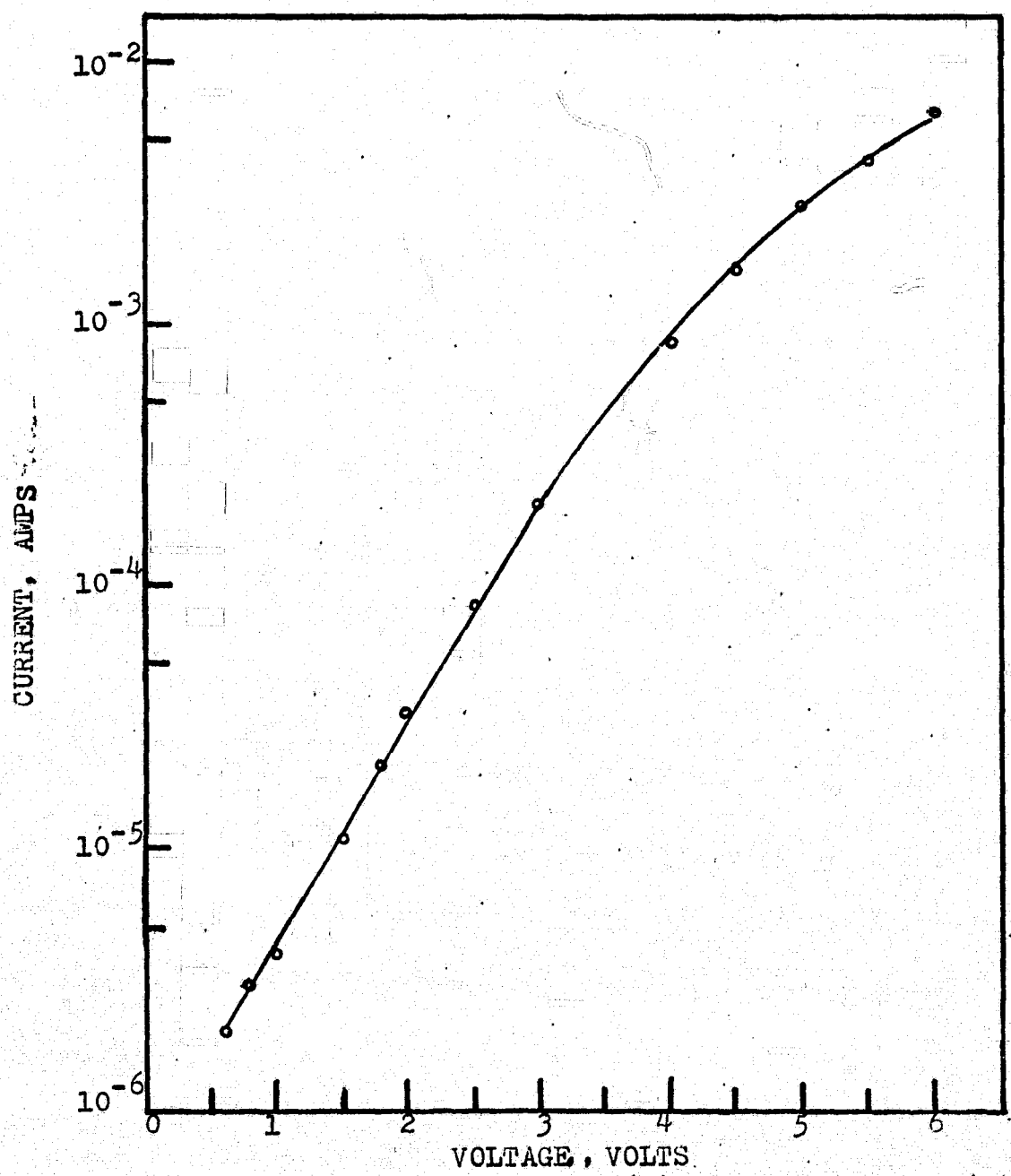

Figure 6.4 Reverse Characteristics of the (N) Silicon Carbide-(P) Boron Phosphide Heterojunction

According to this model, an initial exponential rise followed by a linear increase in the reverse current occurs as the reverse bias is increased.

Capacitance-voltage measurements were also carried out on (n) silicon carbide-(p) boron phosphide heterojunction diodes. Figure 6.5 shows the relationship between the inverse capacitance squared and voltage for the diode described above. The linear relation between C^{-2} versus V indicates the abrupt nature of the junction. The voltage intercept of about 2.6 V is the diffusion potential resulting from two Schottky diodes in series according to Dolega model. The slope of C^{-2} versus V gives $\frac{1}{q}\left(\frac{1}{\epsilon_n N_d} + \frac{1}{\epsilon_p N_a}\right)$, where ϵ_n and N_d are the permitivity and the net impurity concentration in n-type material. N_a and ϵ_p correspond to p-type semiconductor. The slope of Figure 6.5 indicates that $\left(\frac{1}{N_d} + \frac{1}{N_a}\right)^{-1}$ is on the order of 10^{18} cm^{-3}.

VI.D Summary

Silicon carbide-boron phosphide heterojunction diodes have been fabricated and characterized for the first time. Boron phosphide layers were deposited on hexagonal silicon carbide platelets by hydrogen reduction of a mixture of boron tribromide-phosphorus trichloride at 1075°C. Mesa

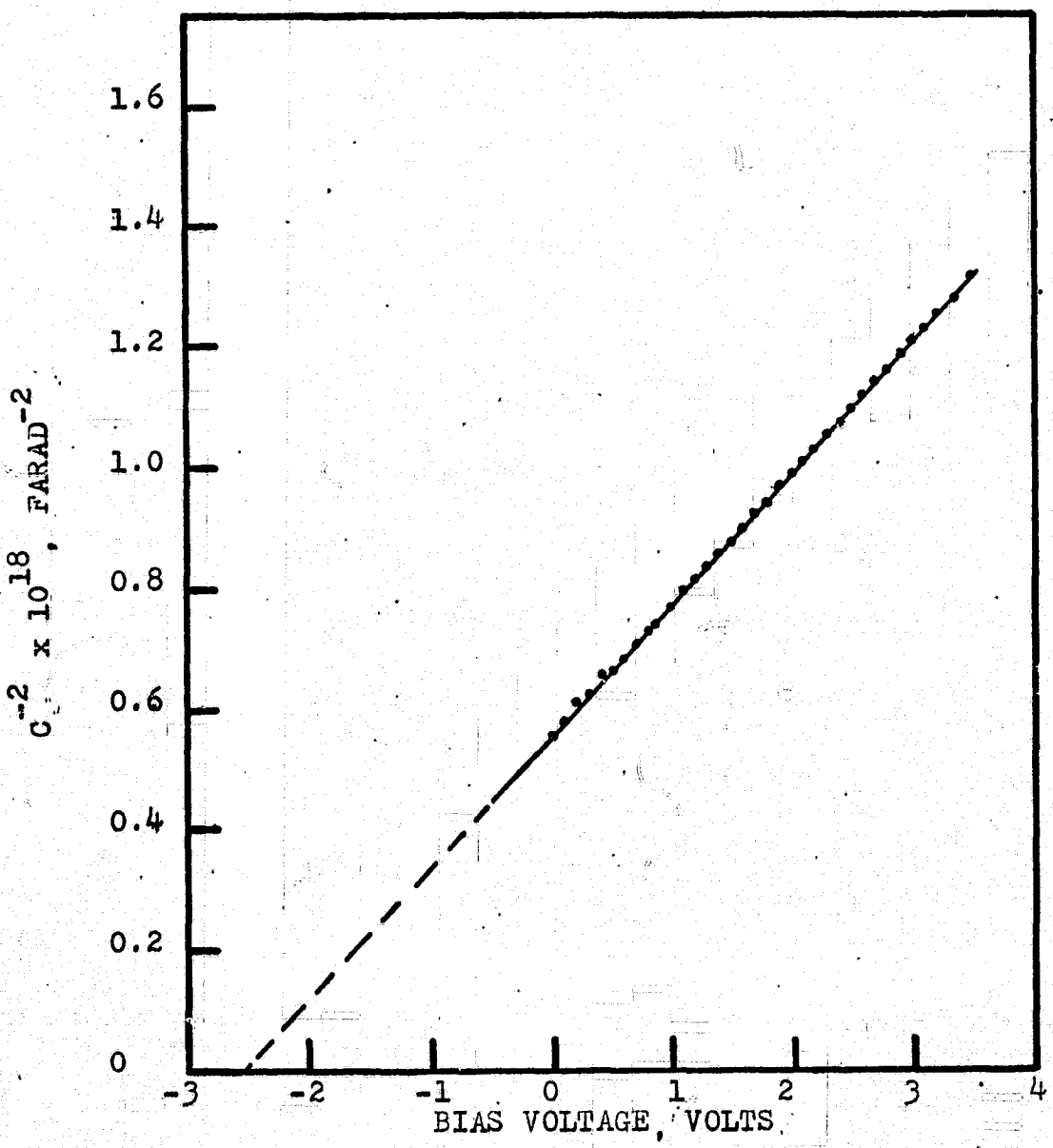

Figure 6.5 Capacitance-Voltage Characteristics of (N) Silicon Carbide-(P) Boron Phosphide Heterojunction

structures were fabricated by electrolytic etching of boron phosphide and silicon carbide. Ohmic contacts to both boron phosphide and silicon carbide were applied by electroless nickel plating followed by annealing. The current-voltage and capacitance-voltage characteristics of the fabricated (n) silicon carbide-(p) boron phosphide mesa type diodes were determined.

CHAPTER VII

BORON PHOSPHIDE P-N JUNCTIONS AND LIGHT EMITTING DIODES

This chapter is concerned with the fabrication and characterization of boron phosphide p-n junctions and electroluminescent diodes. Boron phosphide p-n junctions were fabricated by the epitaxial growth, electrolytic etching and contacting techniques discussed in the preceeding chapters. Current-voltage and capacitance-voltage, and electroluminescent characteristics of the epitaxial and solution grown boron phosphide p-n junctions were determined. Electroluminescence from point-contact diodes was also investigated.

VII.A Introduction to P-N Junction Theory

A p-n junction may be formed by joining an n-type to a p-type semiconductor in any manner that allows the crystal lattice to be continuous across the junction. The interface between the two regions is called a p-n junction. A p-n junction can perform various functions depending upon its biasing conditions as well as its doping profile and device geometry. The more important of these functions are rectifier, voltage regulator, varister, varactor, fast recovery diode, charge storage diode, p-i-n diode, impatt

diode, tunnel diode, and light-emitting diodes. Light emitting diodes have been fabricated from a number of III-V and other compound semiconductors.

The electrical characteristics of a p-n junction are well known. If there is no external voltage applied between the two sides, the Fermi level exists at a single energy value throughout the crystal. At the p-n junction, conduction and valance bands are warped in such a way that the two majority carrier distributions are confined to their own areas, the warping being just sufficient to establish that no net current flows across the junction. In equilibrium, the current flow across the junction is composed of two equal components of opposite sign; one component is due to carrier diffusion and the other is due to carrier drift as a result of the built-in electric field.

If an external voltage is applied to a p-n junction, this equilibrium is disturbed. If a forward bias is applied, the Fermi levels on both sides of the junction are different by an amount qV. The barrier to the flow of majority carriers is thus lowered, and a current can flow which increases exponentially with voltage. Holes flow through the p-type region and either recombine with electrons which have crossed the junction or move over into the n-type region and

recombine there. The behavior of electrons is analogous.

If a reverse voltage is applied, the barrier is raised so that fewer majority carriers can cross the barrier, and current is only carried by minority carriers which are easily swept across the region of the accelerating field. The magnitude of this current is ideally independent of the applied voltage and is only determined by the abundance of minority carriers in the two regions. It results from the thermal generation of carriers and is, therefore, a function of temperature. At a high reverse voltage, avalanche breakdown sets in.

The current-voltage characteristics of a p-n junction are given by

$$I = I_s \left(\exp \frac{qV}{nkT} - 1 \right) \qquad (7.1)$$

where I_s is the saturation current, V is the voltage across the junction, k is Boltzman's constant, T is absolute temperature, and n is a parameter whose value is 1 or larger. The value of n is unity when the diffusion current dominates, and is higher when the recombination current dominates. The saturation current of an ideal junction is given by

$$I_s = q \left(\frac{P_n \ D_p}{L_p} + \frac{n_p \ D_n}{L_n} \right) \qquad (7.2)$$

where P_n is the concentration of holes in the region, D_p is the diffusion constant for holes, and L_p is the diffusion length of holes. Other symbols have similar meanings.

In the transition region a charge dipole region or depletion layer is created by the carriers diffusing out of the regions leaving on either side the immobile ionized impurity atoms. The voltage across the junction repels more majority carriers away from the junction and exposes more impurity ions on both sides. Thus the depletion layer widens with voltage and behaves like a voltage dependent capacitance.

The total capacitance C of a p-n junction is composed of the depletion layer capacitance C_{dep} and the diffusion capacitance C_d:

$$C = C_{dep} + C_d \qquad (7.3)$$

Both of these contributions are voltage dependent. The total electrostatic potential variation across the junction is given by

$$V = V_{bi} \pm V_a \qquad (7.4)$$

where V_{bi} and V_a are the applied voltage and the built-in voltage, respectively. The positive sign is for reverse bias and negative sign for forward bias.

Since the depletion layer is essentially free of carriers, it acts as a dielectric and is associated with a corresponding capacitance C_{dep}. The depletion layer capacitance accounts for most of the junction capacitance if the junction is reversed biased. For a planar one sided step junction

$$C_{dep} = \sqrt{\frac{q\ \epsilon_s\ N_b}{2V}} \qquad pf/cm^2 \qquad (7.5)$$

where q is electronic charge, ϵ_s is the dielectric constant of the semiconductor, and N_b is impurity concentration at the edges of the depletion layer and is equal to N_D or N_A depending upon whether $N_A \gg N_D$ or vice versa. It follows from equation (7.5) that

$$\frac{d}{dV}\left(C^{-2}_{dep}\right) = \frac{2}{q\ \epsilon_s\ N_b} \qquad (7.6)$$

It is clear from equations (7.5) and (7.6) that a plot of C^{-2} versus V will be a straight line for a one sided abrupt junction. The slope would give the impurity concentration N_b, and the intercept (at $C^{-2}=0$) gives the built-in potential V_{bi} (more accurate consideration gives $V_{bi}-\frac{2kT}{q}$).

VII.B Ohmic Contacts to Boron Phosphide

One of the important parameters in developing device technology for new semiconductor materials is the formation of low resistance ohmic contacts, which are essential for efficient and reliable operation of junction devices. The general guidelines for obtaining ohmic contacts to semiconductors are (1) to use contacting materials of high work function on p-type and of low work function on n-type semiconductors, and (2) to create a region of high carrier concentration under the contact through alloying or in-diffusion of a suitable dopant provided by the contacting material. In practice, it is difficult to satisfy these guidelines. For example, at temperatures high enough to affect alloying or impurity in-diffusion, boron phosphide decomposes. In this work, a number of materials were investigated under various heat treatment conditions to yield low resistance ohmic contacts to boron phosphide. The results are summarized in Table 7.1. The carrier concentration of boron

Table 7.1

Contact Resistance of Different Materials to Boron Phosphide

Conductivity Type of	Contact Material	Contact Resistance (ohm-cm^2) After Different Heating Temperatures				
		As Deposited	600°C	750°C	850°C	950°C
N	Al	N-O	N-O	N-O	--	--
N	In	N-O	N-O	--	--	--
N	Ag	N-O	N-O	N-O	N-O	N-O
N	Ag-Ge	N-O	N-O	N-O	N-O	--
N	Ag-Sn	N-O	N-O	N-O	N-O	--
N	Ag-Si	N-O	N-O	N-O	N-O	--
N	Au	N-O	--	--	Ohmic	--
N	Au-Si(1-5%)	N-O	--	--	$\sim 10^{-2}$	--
N	Au-Sn	N-O	--	--	$\sim 10^{-2}$	--
N	Au-Ge-Ni	N-O	--	--	--	--
N	Au-Ge	N-O	--	--	Ohmic	--
N	Electroless Ni	N-O	--	--	$\sim 10^{-2}$	--
P	Au-Be(1%)	N-O	--	--	$\sim 10^{-2}$	--
P	In	N-O	--	--	Ohmic	--
P	Al	N-O	--	--	Ohmic	--

N-O = Non-Ohmic

phosphide crystals was approximately 10^{18} cm^{-3}. All the metals or their alloys were deposited on boron phosphide by evaporation under a pressure of 10^{-6} Torr or lower with the exception of nickel. The electroless plating was used for the deposition of nickel, and indium was also applied by soldering in addition to evaporation. Annealing was carried out in a hydrogen atmosphere from 600° to 850°C for 5 min to 1 hr, though occasionally annealing temperature was raised to 950°C for a few minutes. The current-voltage characteristics of these contacts were determined on a curve tracer.

For n-type solution grown crystals, aluminum and indium contacts remained non-Ohmic even after annealing up to 750°C for 1 hr. Electroless nickel was found to form low resistance, ohmic contacts to all but lightly doped n-type boron phosphide crystals. The plating was carried out at 90° to 100°C using Nicklex (Transene Company, Inc., Danvers, Mass.) plating solution. Lapping of boron phosphide crystals with 600 grit silicon carbide abrasive facilitated the plating process and improved the adhesion of nickel deposit to the crystal. The electroless plating of lightly doped boron phosphide with nickel was very difficult and was facilitated considerably by rinsing boron phosphide platlets in palladium chloride solution, deionized water, stannous chloride solution,

and deionized water successively before plating. Annealing temperatures of 850° to 900°C produced ohmic contacts of specific contact resistance on the order of 10^{-2} ohm-cm^2.

In the fabrication of small area devices, evaporated contacts are preferred, and gold, silver, and a number of their alloys were investigated. Gold-germanium-nickel and gold-silicon have produced low resistance ohmic contacts to n-type boron phosphide, and gold-beryllium has formed low resistance ohmic contacts to p-type material. On heavily doped boron phosphide crystals, evaporated gold contacts were found to be ohmic after annealing.

VII.C Preparation and Characterization of P-N Junctions and Point-Contact Diodes

Boron phosphide p-n junction structures were prepared by the epitaxial growth of boron phosphide using thermal reduction of a boron tribromide-phosphorus trichloride mixture with hydrogen on solution grown boron phosphide platelets as described in chapter IV. The procedure had to be modified, however, in case of low resistivity n-type boron phosphide substrates. Silicon nitride or a boron phosphide layer without intentional doping was deposited on the back side of the boron phosphide platelet. The front side of platelet was then lapped and polished mechanically, and the boron phosphide epitaxial layers grown on the polished front

face were sometimes n-type and sometimes p-type in conductivity.

After preparing boron phosphide layers containing a p-n junction, mesa diodes were isolated by electrolytic etching (chapter III) or by laser scribing. Figures 7.1A and 7.1B show, respectively, an array of laser scribed boron phosphide diodes and the typical current-voltage characteristics. Built-in p-n junctions in solution grown boron phosphide crystals were also isolated by electrolytic etching. Gold or gold-silicon contacts were evaporated onto the n-type region and gold-beryllium contacts were evaporated on the p-type region. After evaporation, the contacts were annealed in hydrogen at 850^{o}C to reduce the contact resistance. The fabricated boron phosphide diodes were mounted on a TO-18 header with a single component silver epoxy. The mounted diodes were generally encapsulated in Hysol LED epoxy before making measurements.

Figure 7.2 shows the current-voltage characteristics of an unpassivated epitaxial boron phosphide diode fabricated on an n-type solution grown substrate. The n value in the diode equation is approximately 29 due to high series resistance of the device. The reverse breakdown voltage was higher than 20 volts. The excessive leakage current was reduced by passivation.

The current-voltage and capacitance-voltage characteristics

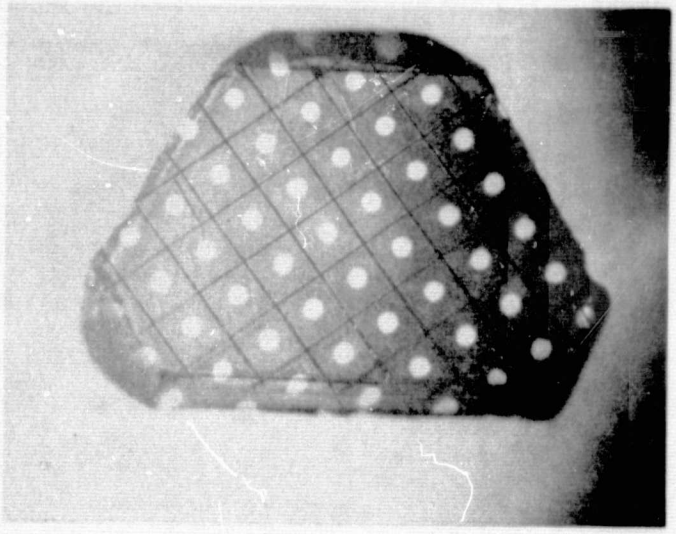

(A)

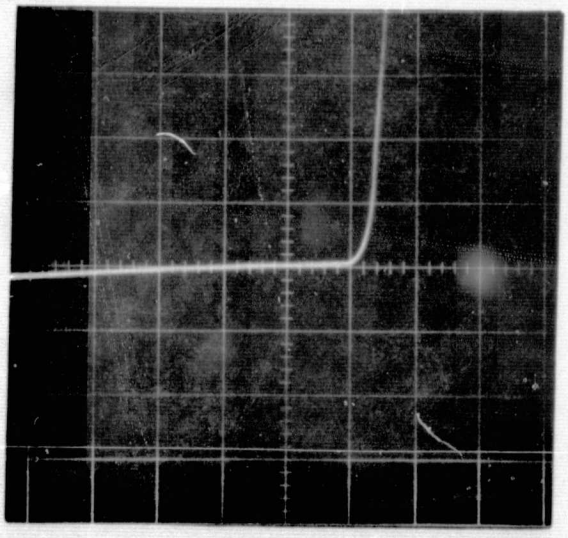

(B)

Figure 7.1 (A) An Array of Laser Scribed Boron Phosphide P-N Junction Diodes (B) Current-Voltage Trace of a Laser Scribed Boron Phosphide P-N Junction Diode (Horizontal 2 V/Div, Vertical 1 mA/Div)

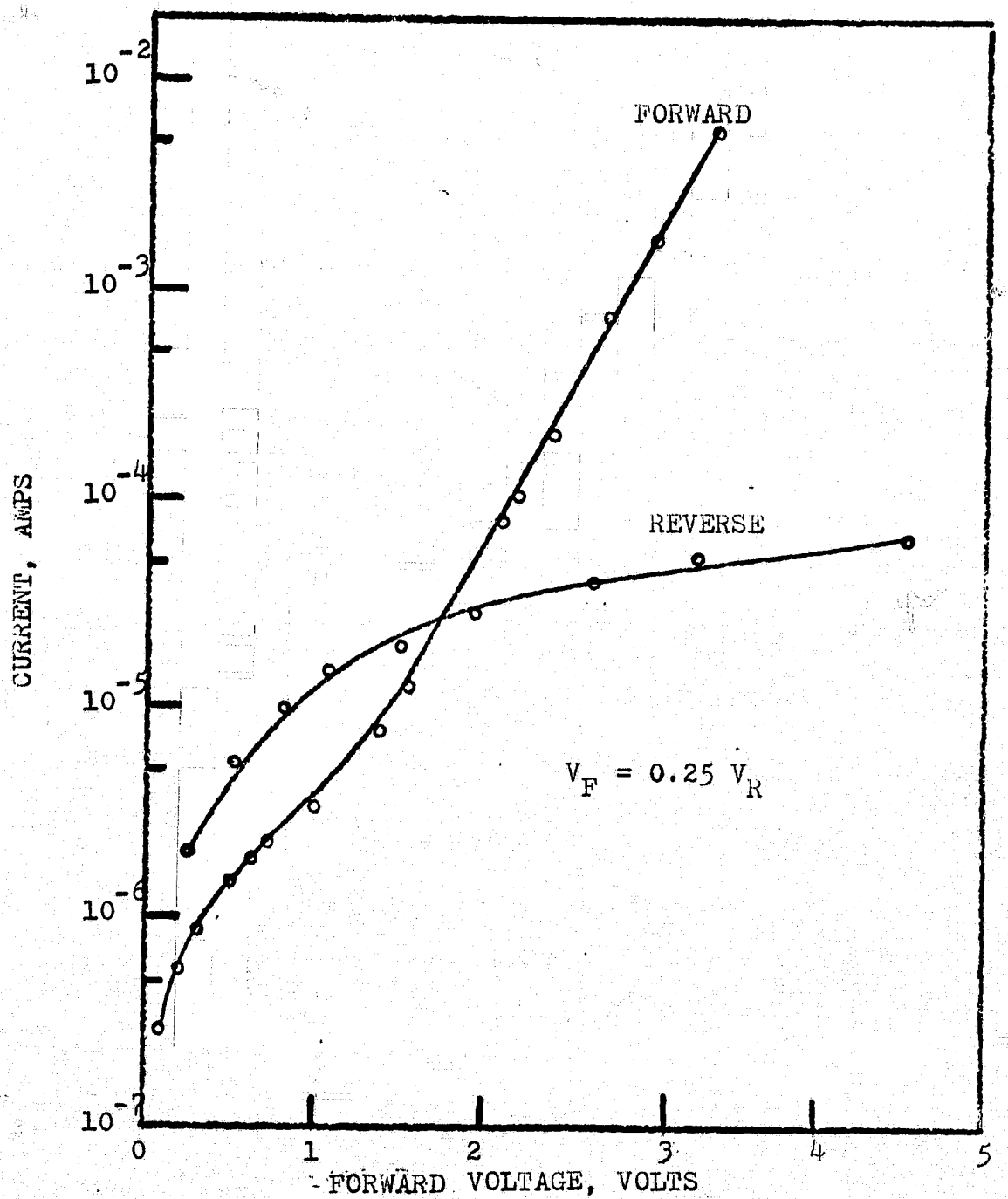

Figure 7.2 Current-Voltage Characteristics of a Boron Phosphide P-N Junction Fabricated on N-Type Substrate

of a built-in p-n junction in a solution grown boron phosphide crystal are shown in Figures 7.3 and 7.4 respectively. Over a small range of voltage the n value is approximately 2 at 300°K and 3.4 at 77°K. This is due to the recombination of carriers in the space charge region. A linear relationship between C^{-2} and V indicates an abrupt nature of the junction. The voltage intercept is about 2.1 V, slightly greater than the band gap of boron phosphide. This is attributed to the presence of p-i-n structure in place of a simple p-n junction. The carrier concentration calculated from the slope of C^{-2} versus V relation is approximately 10^{18} cm^{-3}.

On probing doped and undoped boron phosphide crystals with a metal point, strong rectification was observed. The crystal was placed on a metal sheet, and a metal point-contact, gold or tungsten tip was applied to the surface of the crystal. Figure 7.5A and 7.5B show typical rectification curves obtained when an n-type boron phosphide crystal was probed with a gold probe.

VII.D Electroluminescence from P-N Junctions and Point-Contact Diodes

Electroluminescence is the emission of optical radiation as a result of electronic excitation in a material under the application of an electric field. The electronic

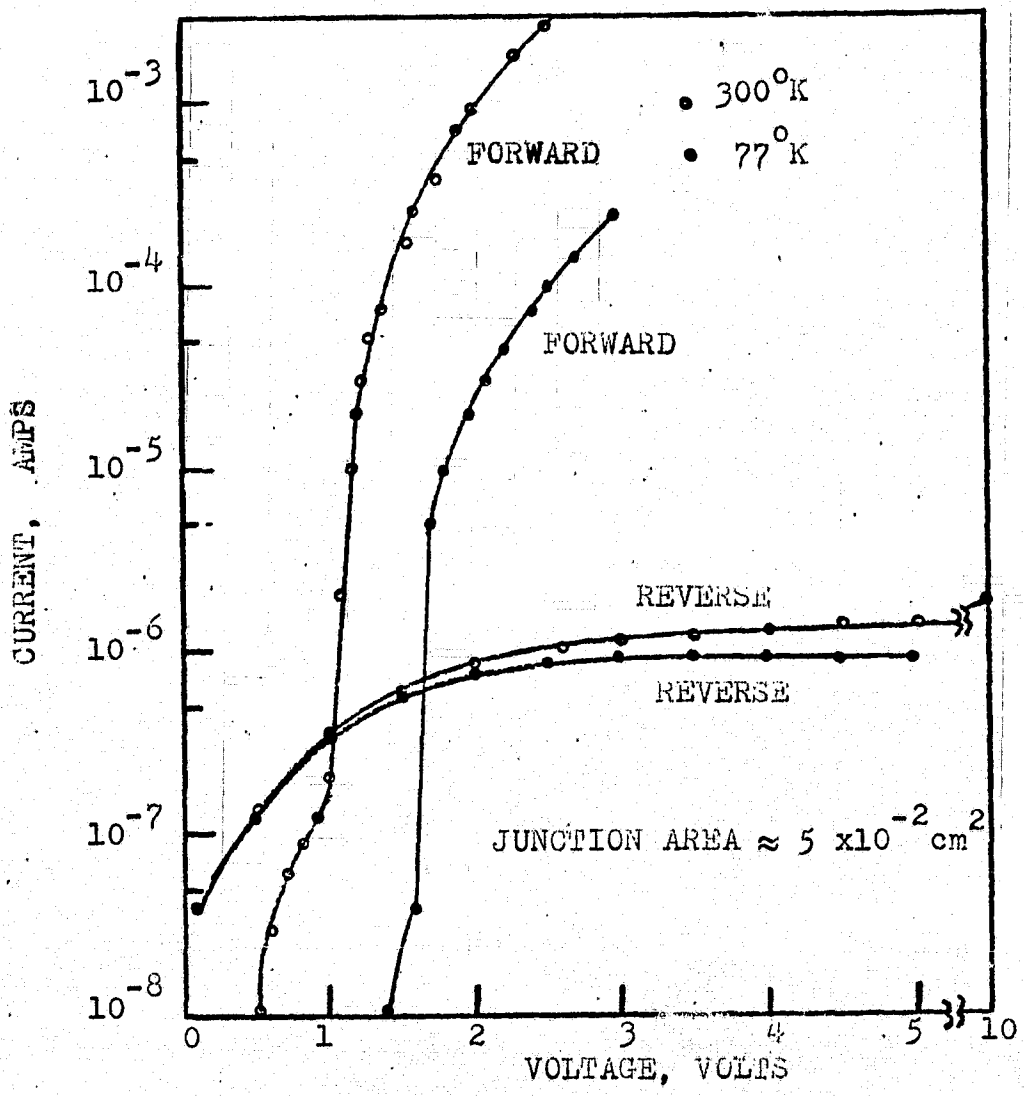

Figure 7.3 Current-Voltage Characteristics of a Solution Grown Boron Phosphide Diode.

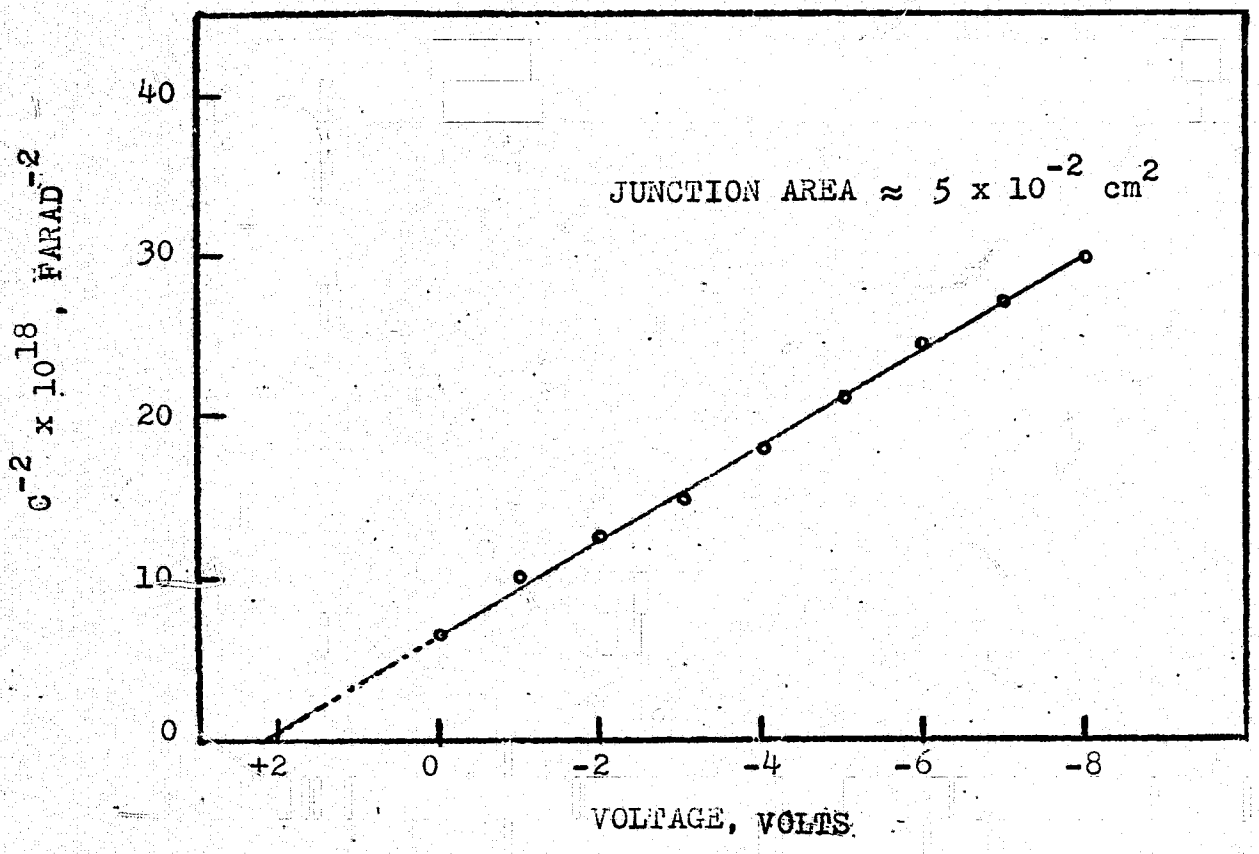

Figure 7.4 Capacitance-Voltage Characteristics of the Solution Grown Boron Phosphide Diode

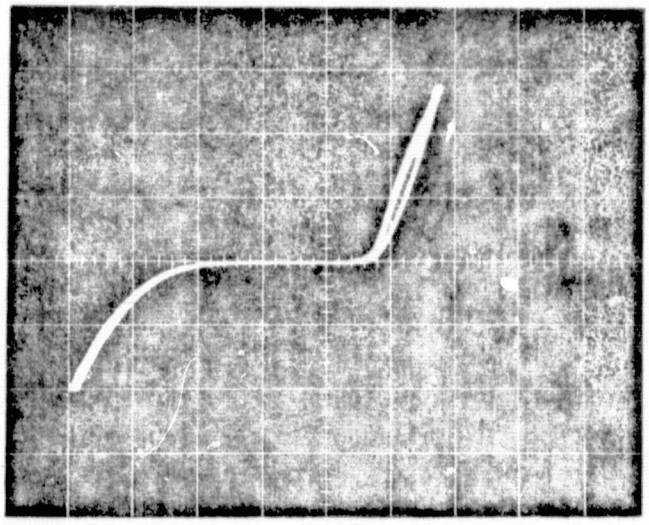

(A)

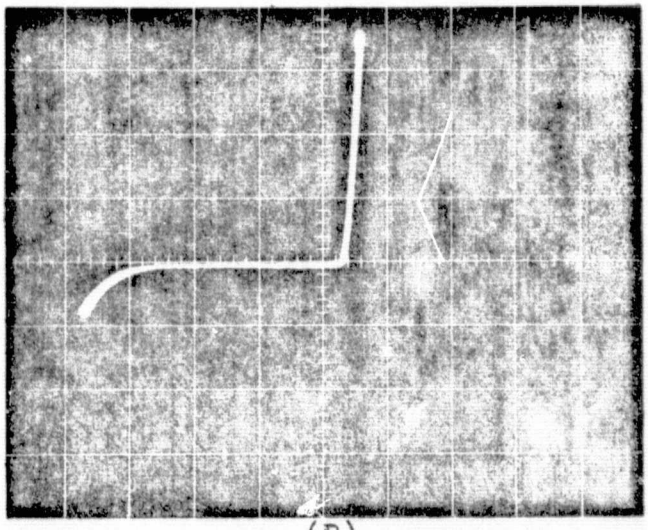

(B)

Figure 7.5 Typical Rectification Characteristics of Phosphide Point-Contact Diodes (Horizontal 5 V/Div, Vertical 1 mA/Div)

transitions that follow the excitation in a semiconductor or an insulator are shown schematically in Figure 7.6.[95] In a semiconductor, injection of minority current carriers is sufficient to lead to recombinations of the type shown in Figure 7.6 as transitions (1a) to (1c) and (2a). This can occur by injection at point-contacts, over forward-biased p-n junctions, or by tunnel injection. Transitions of the type (2b) and (3) can occur at reverse biased p-n junctions, by impact ionization, or by "avalanche injection" (microplasma formation). A given semiconductor may, therefore, emit in different spectral regions, and by different mechanisms, depending on the magnitude and direction of the applied voltage, the nature of the contacts, etc. Figure 7.7 shows schematically the injection-electroluminescence mechanism in a p-n junction.

The electroluminescence from boron phosphide p-n junction diodes and point-contact diodes was studied under dc and pulsed conditions. For spectral measurements, the diode emission was focused on the entrance slit of a Perkin-Elmer model E-1 monochromator. The detector was a RCA 7102 photomultiplier tube (with S-1 characteristics).

The emission in solution grown diodes appeared to originate from n-type region. Also, electroluminescence was observed when the diodes was under forward or reverse bias, although the brightness level was much higher under reverse

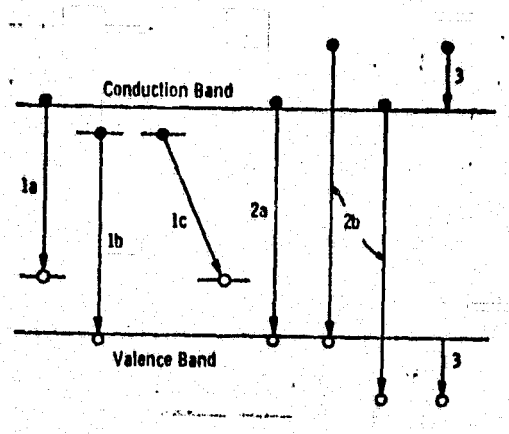

Figure 7.6 Basic Transitions in a Semiconductor

1) Transitions Involving Chemical Impurities or Physical Defects (Lattice Vacancies, etc.)
   (a) Conduction Band to Acceptor
   (b) Donor to Valence Band
   (c) Donor to Acceptor ("Pair Emission").
2) Interband Transitions
   (a) Intrinsic or "Edge Emission" Corresponding **Very** Closely in Energy to the Band Gap; Phonons and/or Excitons May be Involved
   (b) Higher Energy Emission Involving Energetic or "Hot" Carriers; Sometimes Called "Avalanche Emission".
3) Intraband Transitions Involving "Hot" Carriers; Sometimes Called "Deceleration Emission".

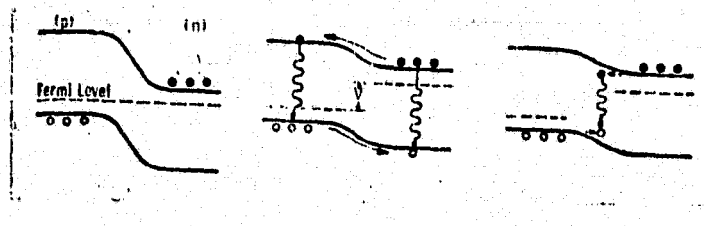

Figure 7.7 Energy Band Diagrams for (A) Unbiased P-N Junction, (B) Junction Biased in Forward Direction Showing Thermal Injection of Minority Carriers and Radiative Recombination on Each Side of the Junction (Drawn for Band-to-Band Recombination), and (C) Junction Biased in Forward Direction Showing Tunneling of Electron and Hole with Radiative Recombination in Junction

bias. Figure 7.8 shows the spectral emission of a solution grown boron phosphide p-n junction under reverse bias. The spectrum consists of bands associated with transitions between impurity states. The spectrum extends into near infra red (about 1.5 eV).

The electroluminescence from epitaxial p-n junctions was of less intensity than the solution grown diodes.

Electroluminescence from point-contact diode and built-in junction diodes was visible in room light. Figure 7.9 shows the spectral emission from a point-contact diode. In addition to broad band emission, there are strong peaks at 6200, 6500, and 8200 Å. These correspond to near band gap and relatively deep impurity transitions.

VII.E Summary

Boron phosphide epitaxial p-n junctions and solution grown p-n junctions have been fabricated. The electrical characteristics and electroluminescent properties of the boron phosphide p-n junction diodes and point-contact diodes were studied. Electroluminescence from these diodes is characterized by near band gap, shallow, and relatively deep impurity transitions.

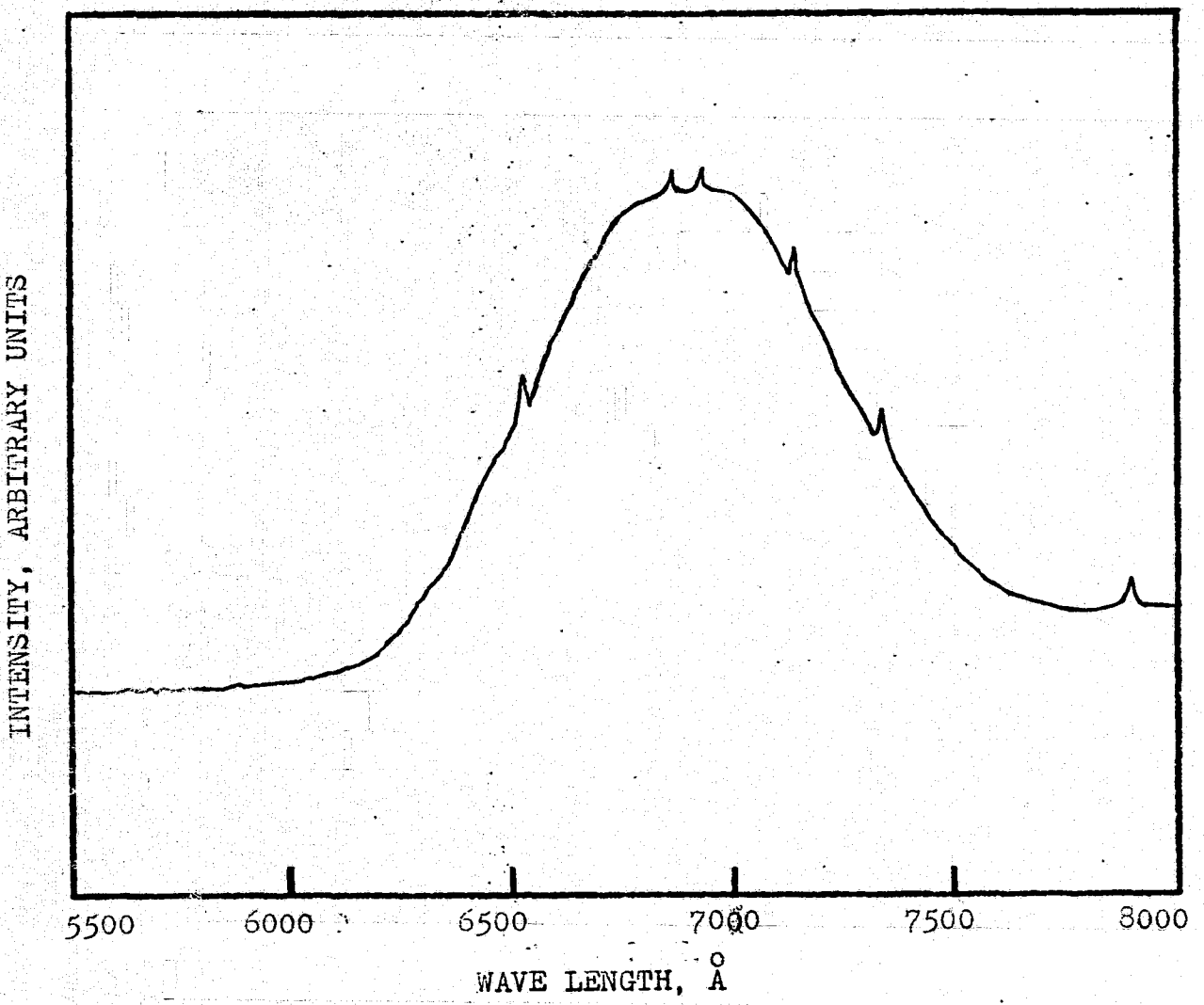

Figure 7.8 Emission Spectra from a Solution Grown Boron Phosphide P-N Junction

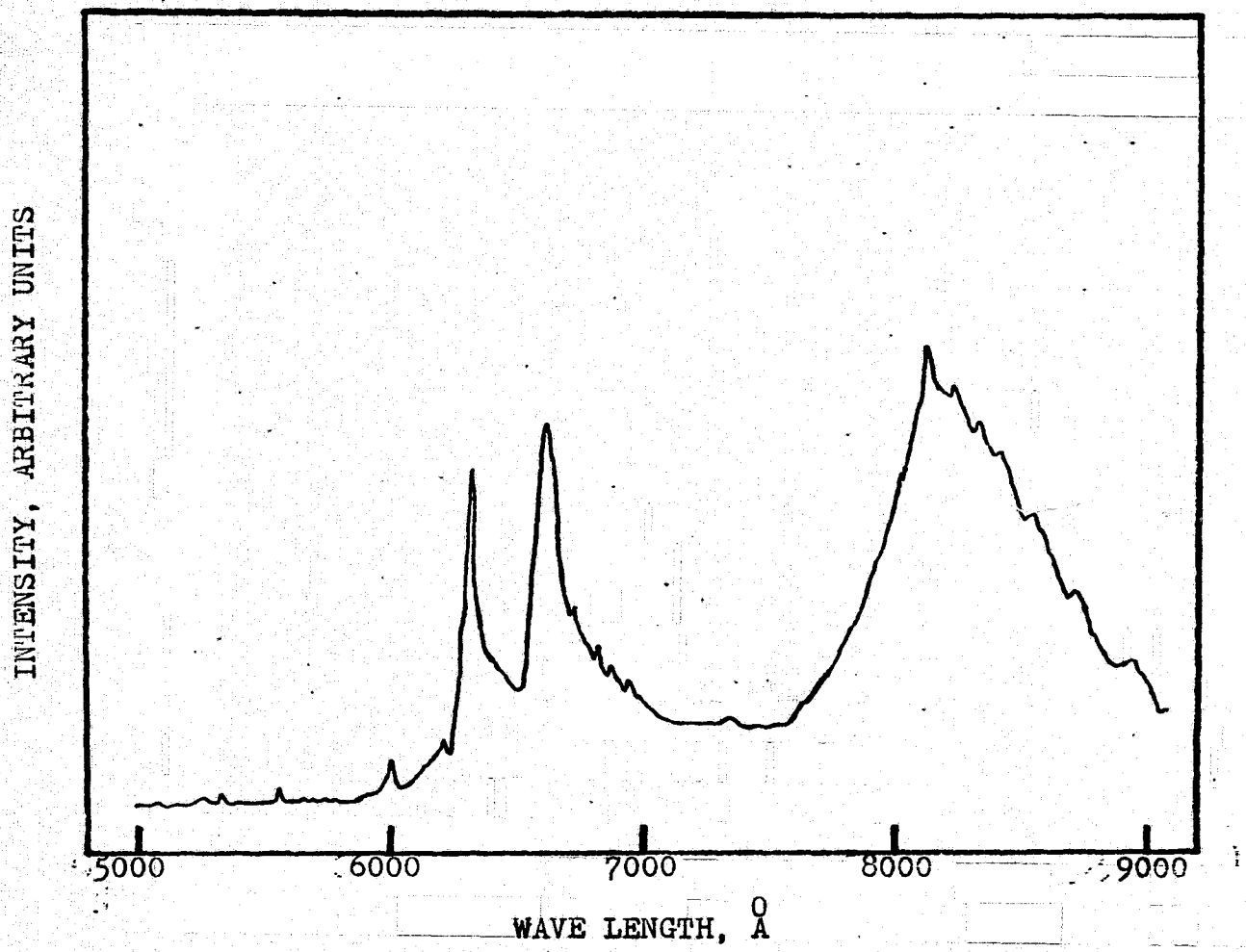

Figure 7.9 Emission Spectra from a Boron Phosphide Point-Contact Diode

CHAPTER VIII

SUMMARY AND CONCLUSION

A review of the literature indicated that essentially no device work on boron phosphide had been carried out. This is attributed to several factors: (1) the crystal growth of boron phosphide of reasonable size and perfection and of controlled impurity suitable for device is an extremely difficult task, (2) boron phosphide is refractory and is chemically inert at room temperature, rendering the device fabrication an extremely difficult process, (3) the appreciable dissociation pressure of boron phosphide at 1200°C or above poses a serious problem to the formation of p-n junctions. Thus, the objective of this research was to prepare device quality boron phosphide single crystals and epitaxial layers, to develope device fabrication techniques, and to characterize boron phosphide homojunction and heterojunction devices.

(1) The growth of single crystals of boron phosphide by recrystallization has been carried out using stationary and accelerated crucible rotation technique. The boron phosphide crystals grown here are considerably larger than those reported heretofore. These boron phosphide crystals

have well developed faces and are ideal as substrates for the epitaxial growth of boron phosphide. For the first time, the intentional doping of single crystals of boron phosphide has been carried out, and both n-type and p-type boron phosphide single crystals have been obtained by the recrystallization technique. The room temperature carrier concentration of these solution grown crystals was approximately 10^{18} cm^{-3}.

(2) The electrolytic etching of boron phosphide has been investigated for the first time, and has been used in device fabrication. A technique has been developed to etch and polish p-type boron phosphide. In contrast, an insoluble film tended to form on n-type boron phosphide, and the removal of material was very slow. Due to a large difference in etch rates between p-type and n-type materials, boron phosphide p-n junction interface has been delineated by electrolytic etching. Electrolytic etching has been also applied to the fabrication of mesa type boron phosphide p-n junction and boron phosphide-silicon carbide heterojunction structures. Because of the inert nature of boron phosphide, electrolytic etching is the most suitable means available to remove p-type material and to isolate mesa type junctions.

(3) Epitaxial layers of boron phosphide have been deposited on hexagonal silicon carbide platelets and solution grown boron phosphide platelets by the hydrogen reduction of a boron tribromide-phosphorus trichloride mixture at 1075° to 1100°C. The optical microscopy and reflection electron diffraction examinations showed the grown boron phosphide layers to be single crystalline and epitaxial with respect to the substrates. The boron phosphide layers grown on silicon carbide substrates and on p-type or n-type boron phosphide platelets were p-type, and p-type or n-type boron phosphide layers were obtained by doping with hydrogen selenide. The boron phosphide layers deposited on n^+-boron phosphide crystals were n-type presumably due to autodoping effect during the deposition process. P-type layers could, however, be grown on n^+-boron phosphide crystals by coating the back face of the substrate with boron phosphide or silicon nitride. For the first time, the epitaxial boron phosphide layers have been used for the fabrication of heterojunction and homojunction devices.

(4) In search for a suitable dielectric for the surface passivation of boron phosphide devices and as the insulator in MIS structures, thermal oxidation, thermal nitridation, and electrolytic oxidation of boron phosphide have been investigated. Of the three processes, electrolytic

oxidation appears to produce the best results. Silicon dioxide and silicon nitride films were also deposited on boron phosphide; however, they are inferior to those deposited on silicon at higher temperatures. The boron phosphide-insulator-metal structures with silicon nitride (or silicon dioxide-silicon nitride) layer as the insulator are characterized by the presence of negative charges in the semiconductor-insulator interface.

(5) Silicon carbide-boron phosphide heterojunction structures have been fabricated and characterized. Mesa diodes were fabricated by electrolytic etching. The current-voltage characteristics of (n) silicon carbide-(p) boron phosphide heterojunction structures have been found to deviate considerably from p-n homojunction structures and indicate a high recombination rate at the interface.

(6) Boron phosphide p-n junction diodes have been fabricated and characterized. Epitaxial boron phosphide p-n junction structures deposited on solution grown substrates were isolated into mesas by electrolytic etching or laser scribing. Built-in p-n junctions in solution grown boron phosphide crystals were isolated by electrolytic etching. The current-voltage and capacitance-voltage characteristics of these diodes have been investigated.

Easily visible electroluminescence has been observed from both epitaxial and built-in p-n junctions as well as from point contact diodes. Electroluminescence from these diodes was characterized by near band gap, shallow and relatively deep impurity transitions.

REFERENCES

1. J.A. Perri, S. LaPlaca, and B. Post, Acta Cryst., 11, 310(1958).

2. R.J. Archer et al., Phys. Rev. Letters, 12, 538(1964).

3. C.C. Wang, M. Cardona, and A.G. Fischer, RCA Rev., 25, 159(1964).

4. C.H. Henry, P.J. Dean, and J.D. Cuthbert, Phys. Rev., 166, 754(1968).

5. Y. Nannichi and G.L. Pearson, Solid-State Electron., 12, 341(1969).

6. A.C. Stickland, "Gallium Arsenide, 1966 Symposium Proceedings" (Institute of Physics and Physical Society Conferences Series No. 3), The Institute of Physics and the Physical Society, London(1967).

7. C.I. Pedersen, "Gallium Arsenide, 1968 Symposium Proceedings" (Institute of Physics and Physical Society Conferences Series No. 7), The Institute of Physics and the Physical Society, London(1969).

8. S. Funakisako and T. Adachi, Chem. Abst., No. 163310a, 78, 235(1973).

9. F.V. Williams and R.A. Ruehrwein, J. Am. Chem. Soc., 82, 1330(1960).

10. H. Besson, Compt. Rend., 113, 78(1891).

11. H. Moissan, Compt. Rend., 113, 726(1891).

12. H. Welker, Z. Naturforsch., 7a, 744(1952).

13. P. Popper and T.A. Ingles, Nature, 179, 1075(1957).

14. J.L. Peret, J. Amer. Cer. Soc., 47, 44(1964).

15. P.E. Grayson, J.T. Buford, and A.F. Armington, Electrochem. Tech., 3, 338(1965).

16. K. Vickery, Nature, 184, 268(1959).

17. G.V. Samsonov and Y.B. Tithov, J. Appl. Chem. of USSR, 36, 669(1963).

18. B.D. Stone and D. Hill, Phys. Rev. Letters, 4, 282 (1960).

19. Ya. Kh. Grinberg, E.G. Zhukov, and Z.S. Medvedeva, Zh. Neorgan. Materialy, 1, 478(1965).

20. Ya. Kh. Grinberg et al., Sov. Phys. Dokl., 10, 6(1965).

21. A.F. Armington, J. Crystal Growth, 1, 47(1967).

22. B.V. Baranov et al., Opt. I Spectroskopiya, 19, 553 (1965).

23. B.V. Baranov, V.D. Prochukhan, and N.A. Goryunova, I. A. N. SSSR, Neorgan. Materialy, 3, 1691(1967).

24. R.I. Stearns and P.E. Greene, J. Electrochem. Soc., 112, 1239(1965).

25. S. Rundquist, Acta Chem. Scand., 16, 1(1962).

26. M. Iwami, N. Fujita, and K. Kawabe, Japan. J. Appl. Phys., 10, 1746(1971).

27. T.L. Chu, J.M. Jackson, and R.K. Smeltzer, J. Crystal Growth, 15, 254(1972).

28. T.L. Chu, J.M. Jackson, and R.K. Smeltzer, J. Electrochem. Soc., 120, 802(1973).

29. M. Takigawa, M. Hirayama, and K. Shohno Japan. J. Appl. Phys., 13, 411(1974).

30. T. Nishinaga et al., J. Crystal Growth, 13/14, 346 (1972).

31. T.L. Chu et al., J. Appl. Phys., 42, 420(1971).

32. F.M. Ryan and R.C. Miller, Phys. Rev., 148, 858(1966).

33. J.J. Hopfield, D.G. Thomas, and M. Gershenzon, Phys. Rev. Letters, 10, 162(1963).

34. L.A. Hemstreet Jr. and C.Y. Fong, Phys. Rev., B6, 1464(1972).

35. J.C. Phillips, Rev. Mod. Phys., 42, 317(1970).

36. J.A. Van Vechten, Phys. Rev., 182, 891(1969); 187, 1007(1969).

37. V.A. Fomichev.,I.I. Zhukova, and I.K. Polushina, J. Phys. Chem. Solids, 29, 1025(1968).

38. G.L. Gal'Chenko, B.I. Timofeev, and Ya. Kh. Grinberg, I.A.N. SSSR, Neorgan. Materialy, 8, 634(1972).

39. R.A. Laudise, "The Growth of Single Crystals", Prentice Hall, Inc., Englewood Cliffs, New Jersey(1970).

40. N.B. Hannay, "Semiconductors", Reinhold, New York(1959).

41. N.P. Luzhnaya, J. Crystal Growth, 3/4, 97(1968).

42. H.J. Scheel, J. Crystal Growth, 13/14, 560(1972).

43. H.J. Scheel and E.O. Schulz-DuBois, J. Crystal Growth, 8, 304(1971).

44. E.O. Schulz-DuBois, J. Crystal Growth, 12, 81(1972).

45. W. Tolksdorf and F. Welz, J. Crystal Growth, 13/14, 566(1972).

46. D.Elwell and B.W. Neate, J. Mater. Sci., 6, 1499 (1971).

47. J.W. Faust Jr. and H.F. John, J. Phys. Chem. Solids, 25, 1407(1964).

48. L.M. Foster, T.S. Plaskett and J.E. Scardefield, I.B.M. Journal, 10, 114(1966).

49. F.A. Shunk, "Constitution of Binary Alloys", Second Supplement, McGraw-Hill, New York(1969).

50. M. Hansen, "Constitution of Binary Alloys", McGraw-Hill, New York(1958).

51. J.M. Jackson III, Ph.D. Dissertation, Southern Methodist University, Dallas, Texas(1972).

52. H. Nowotny and E. Henglein, Z. Physik. Chem., B40, 281(1938).

53. H.C. Gatos and M.C. Lavine, J. Electrochem. Soc., 107, 427, 433(1960).

54. H. Gerischer, Z. Elektrochem., 69, 578(1965).

55. R.L. Meek and N.E. Schumaker, J. Electrochem. Soc., 119, 1148(1972).

56. E.P. Warekois and P.H. Metzger, J. Appl. Phys., 30, 960(1959).

57. J.G. White and W.C. Roth, J. Appl. Phys., 30, 946 (1959).

58. R.W. Haisty, J. Electrochem. Soc., 108, 790(1961).

59. M.E. Straumanis and L. Hu, J. Electrochem. Soc., 118, 433(1971).

60. R.G. Mazur and D.H. Dickey, J. Electrochem. Soc., 113, 255(1966).

61. P.J. Holmes, "The Electrochemistry of Semiconductors", Academic Press, London(1962).

62. V.A. Myamlin and Y.V. Pleskov, "Electrochemistry of Semiconductors", Plenum Press, New York(1967).

63. H. Gerischer, "Physical Chemistry" An Advanced Treatise Volume IXA/Electrochemistry (H. Eyring ed.), 463, Academic Press, New York(1970).

64. H. Gerischer and W. Mindt, Electrochimic. Acta., 13, 1329(1968).

65. H.B. Morris, M.S. Thesis, Southern Methodist University, Dallas, Texas(1973).

66. R.L. Meek, J. Electrochem. Soc., 118, 1240(1971).

67. J.P. Krumme and M.E. Straumanis, Trans. Met. Soc. AIME, 239, 395(1967).

68. H. Gerischer, J. Electrochem. Soc., 113, 1174(1966).

69. W.M. Fiest, S.R. Steele, and D.W. Readey, "Physics of Thin Films" (G. Hass and R.E. Thun eds.), 5, 237, Academic Press, New York(1969).

70. T.L. Chu and R.K. Smeltzer, J. Vac. Sci. Technol., 10, 1(1973).

71. B.A. Joyee, "The Use of Thin Films in Physical Investigations" (J.C. Anderson, ed.), 87, Academic Press, London(1966).

72. T.J. LaChapelle, A. Miller and F.L. Morritz, "Progress in Solid State Chemistry" (H. Reiss ed.), 3, 1, Pergamon Press, New York(1967).

73. H. Lydtin, "Chemical Vapor Deposition" (J.M. Blocher, Jr. and J.C. Withers eds.), Second International Conference, 71, Electrochem. Soc., Inc., New York (1970).

74. P.E. Gruber, "Chemical Vapor Deposition" (J.M. Blocher, Jr. and J.C. Withers eds.), Second International Conference, 25, Electrochem. Soc., Inc., New York (1970).

75. J.A. Amick, RCA Rev., 24, 555(1963).

76. A. Taylor et al., Brit. J. Appl. Phys., 1, 174(1950).

77. A. Taylor and R.M. Jones, "Silicon Carbide" (H.K. O'Conner and J. Smiltens eds.), 147, Pergamon Press, Inc., New York(1960).

78. K. Brack, J. Appl. Phys., 36, 3560(1965).

79. W.S. Boyle and G.E. Smith, Bell System Tech. J., 49, 487(1970).

80. A.S. Grove, "Physics and Technology of Semiconductor Devices", John Wiley and Sons, Inc., New York(1967).

81. S.M. Sze, "Physics of Semiconductor Devices", John Wiley and Sons, Inc., New York(1969).

82. S.M. Hu, J. Electrochem. Soc., 113, 693(1966).

83. E.H. Nicollian and A. Goetzberger, IEEE Transactions on Electron Devices, ED-12, 108(1965).

84. S.R. Hofstein and G. Warfield, Solid-State Electron., 8, 321(1965).

85. S.R. Hofstein, K.H. Zainiger, and G. Warfield, Proc. IEEE (corres.) 52, 971(1964).

86. R.W. Kelm, Ph.D. Dissertation, Southern Methodist University, Dallas, Texas (1973).

87. W. Shockley, U.S. Patent 2,569,347(1951).

88. H. Kroemer, Proc. IRE, 45, 1535(1957).

89. R.H. Rediker, S. Stopek, and J.H.R. Ward, Solid-State Electron., 7, 621(1964).

90. K.J. Sleger, A.G. Milnes, and D.L. Feucht, "Proceedings of the International Conference on the Physics and Chemistry of Semiconductor Heterojunctions and Layer Structures", (G.Szigeti et al. eds.), 1, 73, Akademiai Kiado, Budapest(1971).

91. J.I. Pankove, "Optical Processes in Semiconductors", Prentice-Hall, Inc., Englewood Cliffs, New Jersey (1971).

92. A.K. Sreedhar, B.L. Sharma, and R.K. Purohit, IEEE Trans. Electron Devices, ED-16, 309(1969).

93. J. Bardeen, Phys. Rev., 71, 717(1947).

94. U. Dolega, Z. Naturforsch., 18, 653(1963).

95. H.F. Ivey, IEEE J. of Quantum Electronics, QE-2, 713(1966).